Regulation Mechanisms of Peptide Hormones in Neuroendocrine Cancers

A thesis submitted in fulfilment of the requirements for admission to the degree

of

Doctor of Philosophy (Chemistry)

By

Jeremy A. M. Morgan

December 2016

THE AUSTRALIAN NATIONAL UNIVERSITY

RESEARCH SCHOOL OF CHEMISTRY

INSTITUTE OF ADVANCED STUDIES

Australian National University

Declaration

This is to declare that the research presented in this thesis represents original work that I carried out during my PhD candidature, with the exception of the following:

The work described in Chapter 2 has subsequently been published in ACS Analytical Chemistry in June 2017 (F. Cao, A. B. Gamble, H. Onagi, J. Howes, J. E. Hennessy, C. Gu, J. A. M. Morgan and C. J. Easton, Analytical Chemistry 2017, 89, 6992-6999). My contributions to that work are clearly specified in Chapter 2.

To the best of my knowledge the work presented in this thesis does not contain material that has been submitted for a degree or diploma in any university or any other tertiary institution. Established results and methodologies published or written by another person have been acknowledged by citation of the original work throughout the text.

I give permission for this copy of my thesis when deposited at the University library to be made available for loan and photocopying.

Jeremy Morgan

December 2016 / August 2017

Acknowledgements

I would like to thank Prof. Chris Easton for welcoming me into his research group, for allowing me to pursue the questions I found most interesting even if they were outside his comfort zone, and for providing opportunities not afforded to most PhD students. Chris's grasp of the scientific method and ability to analyse an argument is absolute, and I have been very fortunate to learn under this framework. Just as importantly, Chris is happy to go above and beyond his role as supervisor for his group members, for which I am equally grateful.

I would like to thank the trio of women who have dominated my PhD experience: Dr. Lucy Cao and Dr. Hye-Kyung Kim, and Dr. Kate Hannan of JCSMR. As a postdoc during my first 2½ years, Lucy guided me through learning to be a successful PhD candidate; without her knowledge, expertise, kindness and support I would be far poorer. H.K painstakingly taught a chemistry student about biology and how cell culture, biological assays, and protocols are performed. I am very grateful for her patience, humour and skill. Kate has been incredibility generous with her time and resources in helping with molecular biology experiments, writing and proof reading. Her opinions and experience have been invaluable and I cannot thank her enough.

I would like to thank Hideki Onagi, for his endless expertise in HPLC and MS, as well as his patience in dealing with every problem I put before him, and Lee Alissandratos for his analysis and advice whenever I was stuck. Thank you the PAM group for your support and for making research enjoyable, and to the entire Easton group for making our lab a welcoming and friendly place to work. Thank you to the Research School of Chemistry for their support and the AS Sargeson and Supplementary scholarships, and thank you to the Australian National University for the Australia Postgraduate Award.

On a personal note, I would like to thank Louis Moran and Jason Whitfield for the hundreds of coffee breaks, the new research ideas and interpretations, the board games, the commiserations and celebrations, and the support over the last 4 years. It was much easier with friends like you. Also to my friends in other research groups, in Lyneham, in Aranda and in Turner, thanks for making Canberra a great place to live. Thank you to my family for their love and support, and for reminding me of what is important.

Finally, I would like to thank Aude Février for her unending patience in listening to my ideas, plans and complaints, her input into my problems, her emotional, physical and financial support, and the sacrifices she has made to stay close by. I could not have done it without you.

Abstract

In the work described in this thesis, analytical methods for the detection and quantification of peptide hormones featuring on-line analyte concentration, post-separation tagging and HPLC-fluorescence detection were presented. These methods were used to detect and quantify calcitonin (CT) and its prohormones glycyllysyllysine-extended CT (CTGKK), glycyllysine-extended CT (CTGK) and glycine-extended CT (CT-G) for the first time, in DMS53 small cell lung carcinoma (SCLC) cell culture medium and lysate. Additionally, novel glycosylated versions of each species were also identified, suggesting the presence of a parallel biosynthetic pathway in DMS53. Extracellular but not intracellular levels of CT were reduced as a result of treatment with biosynthesis inhibitors, and it was suggested CT precursor flux through the glycosylated pathway acts as a bypass mechanism to maintain intracellular CT levels. Moreover, the up-regulation of extracellular levels of CT-related species in response to increased medium volume provided evidence of a homeostatic feedback loop maintaining extracellular CT concentrations.

To interrogate the mechanism of this feedback, DMS53 cultures were treated with a specific human calcitonin receptor (hCTR) agonist, SUNB8155, to determine if the hCTR is involved in the regulation of CT. It was observed that the relative levels of extracellular CT increased with SUNB8155 treatment, but that the relative levels of the intracellular CT-related species were unchanged. This suggested that hCTR is expressed in DMS53, and that activation of the receptor influences the expression and biosynthetic processing of CT-related species. To investigate this hypothesis, hCTR was identified in DMS53 cells using reverse transcription PCR and Western blot analyses. Specifically, transcriptional and translational evidence of the isoform hCTR2 was identified. Thus, for the first time,

hCTR activation was implicated in the up-regulation of CT. This suggested that a positive autocrine feedback loop was operating in DMS53, and based on the hCTR2 isoform, may be mediated by signal transduction through the cAMP- and Ca^{2+}-dependent signalling pathways.

To assess which signalling enzymes are activated by hCTR, signal transduction pathways were investigated using small molecule enzymes inhibitors, and their effects on the levels of CT-related species observed. It was observed that treatment of DMS53 cultures with the protein kinase C inhibitor, GF109203X had an effect on the levels of CT-related species in the medium. Again, the relative levels of the intracellular CT-related species were not changed by treatment with this inhibitor. This implicated PKC as a component of the hCTR signal transduction pathway.

It was concluded that DMS53 cultures have mechanisms to maintain the intracellular and extracellular concentrations of CT-related species. The concentration of extracellular CT is regulated by a positive feedback mechanism, mediated by hCTR activation, and subsequent signalling involving PKC and AC. Treatment with biosynthetic and signalling inhibitors had no significant effect on the intracellular levels of CT-related species, demonstrating that DMS53 cultures prioritise tight control of intracellular concentrations over extracellular concentrations. With the methodology to detect and quantify peptide hormones in cell culture medium and lysate in hand, the generality of CT glycosylation was explored. Preliminary experiments successfully characterised the presence of glycosylated CT and CT-G in the medullary thyroid carcinoma cell line, TT. To broaden the range of detected hormones, HPLC-fluorescence methodology was developed to detect and quantify oxytocin (OT) and its precursors, and this methodology was used to investigate the presence of OT in the DMS79 SCLC cell line.

Table of Contents

Abbreviations

7TM	seven transmembrane
aa	amino acid
AC	adenylate cyclase
Ac	acetyl
ACTH	adrenocorticotropic hormone
AM	adrenomedullin
AMY / IAPP	amylin
ATCC	American type culture collection
BPB	bromophenol blue
cAMP	cyclic adenosine monophosphate
CCPI	calcitonin carboxyterminus peptide 1 OR katacalcin
cDNA	complimentary DNA
CDS	coding DNA sequence
CGRP	calcitonin gene-related peptide
CKK	cholecystokinin
CPE	carboxypeptidase E
CRE	cAMP responsive region
CT / hCT / sCT	calcitonin / human calcitonin / salmon calcitonin
CT-G	glycine-extended calcitonin
CTGK	glycyllysine-extended calcitonin
CTGKK	glycyllysyllysine-extended calcitonin
DAG	diacylglycerol
DMEM	Dulbecco's modified Eagle's medium
DRE	downstream regulatory element
ECL	extracellular domain
ECL	enhanced chemiluminescence
EDTA	ethylenediaminetetraacetic acid
EIA	enzyme immunoassay
ER	endoplasmic reticulum
ERK	extracellular-regulated kinase
G protein	guanine nucleotide-binding protein
G / Gly	glycine
Gal	galactosamine
gCT	glycosylated calcitonin
gCT-G	glycosylated glycine-extended calcitonin
gCTGK	glycosylated glycyllysine-extended calcitonin
gCTGKK	glycosylated glycyllysyllysine-extended calcitonin
GEMSA	guanidinoethylmercaptosuccinic acid
GFI09203X	2-[1-(3-Dimethylaminopropyl)-1H-indol-3-yl]-3-(1H-indol-3-yl) maleimide
GHRH	growth hormone- releasing hormone
GLP-1	glucagon-like peptide 1

GnRH	gonadotropin-releasing hormone
GPCR	G protein coupled receptor
GRP	gastrin-releasing peptide
GTP	guanosine triphosphate
H89	N-[2-[[3-(4-Bromophenyl)-2-propenyl]amino]ethyl]-5-isoquinolinesulfonamide
hCTR	human calcitonin receptor
HGH	human growth hormone
HO-CT	hydroxylated calcitonin
HPLC	high performance liquid chromatography
HRP	horseradish peroxidase
ICD	Intracellular domain
ICL	intracellular loop
IP3	inositol 1,4,5-trisphosphate
K / Lys	lysine
LCMS	liquid chromatography - mass spectrometry
M1	method 1
MAPK	mitogen-activated protein kinase
MRM	multiple reaction monitoring
mRNA	messenger RNA
MTC	medullary thyroid carcinoma
NCBI	national centre for biotechnology information
NET	neuroendocrine tumour
Neu	neuraminic acid
NMU	neuromedin U
NPY	neuropeptide y
OT	oxytocin
P1	primer 1
PAM	peptidylglycine α-amidating monooxygenase
PBA	*E*-4-phenyl-3-butenoic acid
PC	prohormone convertase
PIP2	phosphatidylinositol 4,5-bisphosphate
PKA	protein kinase A
PKC	protein kinase C
PLC	phospholipase C
PTH	parathyroid hormone
PTHr / hPTHr	parathyroid hormone receptor / human parathyroid hormone receptor
PTM	post-translational modification
PVDF	polyvinyldene fluoride
R / Arg	arginine
RAMP	receptor-activity modifying protein
RIA	radioimmunoassay
RIPA	radioimmunoprecipitation assay
RPMI	Roswell Park memorial institute
RT-PCR	reverse transcription PCR

SEM	standard error of the mean
SCLC	small cell lung carcinoma
SDS	sodium dodecyl sulfate
SP	substance P
SQ22536	9-(Tetrahydro-2-furanyl)-9H-purin-6-amine
SUNB8155	5-[1-[(2-Aminophenyl)imino]ethyl]-1,6-dihydroxy-4-methyl-2(1H)-pyridone
Thr	threonine
TRH	thyrotropin-releasing hormone
Tris	tris(hydroxymethyl)aminomethane
U73122	1-[6-[[(17β)-3-Methoxyestra-1,3,5(10)-trien-17-yl]amino]hexyl]-1H-pyrrole-2,5-dione
UTR	untranslated region
VIP	vasoactive intestinal peptide

Chapter One

Introduction

1.1 Hormones, the endocrine system and cancer

As multicellular organisms evolved, the need arose to coordinate functions between cells. As outlined by Griffin and Ojeda,[1] two systems developed to fulfill this role: the nervous system and the endocrine system. The nervous system is characterised by the use of electrochemical signals to send and receive messages from periphery organs, while the endocrine system accomplishes a similar and complementary role by utilising chemical agents transported through the blood stream. These chemical agents are known as hormones. While the systems differ in their mechanistic agents, they are closely linked, thus these distinctions can be blurred. In the pituitary gland, neuronal cells send signals to the hypothalamus, which in turn dictates secretion of hormones as part of the endocrine system. Conversely, hormones such as gastrin and ghrelin, initially discovered in the gastrointestinal tract, were later identified in neuronal cells of the peripheral and central nervous system acting as neurotransmitters. As a consequence, interplay between the nervous and endocrine networks forms what is collectively known as the neuroendocrine system.[1]

Hormone Structure and Function

Hormones are categorised by their structure and manner of action, of which there is a large diversity, providing a range of chemical properties and nuance of function.[2, 3] After the discovery of the first hormone, the peptide hormone secretin in 1902,[4] Starling

proposed that hormones are produced by an organ and transported via the bloodstream to a distant organ where they exert their effects, thus defining "classical" hormone action.[5] Subsequently, it has been discovered that classical hormones can act on cells near their site of production, and also on the cell producing the hormone, in mechanisms known as paracrine and autocrine signalling, respectively (**Figure 1.1**).[2] This has complicated the definition of a hormone somewhat, as other paracrine factors share features with some hormones. For example, cytokines are peptidic and can effect systemic changes in a similar manner to some peptide hormones.[6, 7] The modern definition of a hormones[7] requires that they are produced in large amounts relative to other signalling molecules to maintain effective concentrations in blood, that their specificity does not vary with distance from the site of production to the target cell or organ, and that they are not reliant on binding proteins to control diffusion.

All hormones exert their actions through high affinity receptors specific to one or several hormones.[3] Most peptide and amine hormones act at the cell surface through membrane-bound receptors belonging to two super families: G protein-coupled receptors and tyrosine kinase-activated receptors. Regardless of the receptor family, upon hormone binding the receptors transmit signals via the generation of secondary messenger chemicals or through protein phosphorylation, providing a connection between the cell nucleus and the extracellular environment. In contrast, most steroid hormones diffuse into cells and bind to nuclear receptors. These interact directly with hormone-response proteins to affect transcription of specific genes.

As described by Melmed and coworkers,[7] each class of hormone has inherent chemical and structural properties that define its function. Amine hormones are derived from amino acids, and are small water-soluble compounds. Tyrosine is a common precursor; derivatives include catecholamines, thyroid hormones and dopamine. Catecholamines are a good example of the interlinked nature of the endocrine and nervous system, as

members of this family, for example epinephrine, are also sympathetic neurotransmitters. Steroid hormones are lipid-soluble hormones synthesised from cholesterol and often control sex and reproductive signalling. Due to their insolubility, steroid hormones are transported through the bloodstream bound to carrier proteins. Peptidic hormones are diverse, in terms of both structure and function. Examples range in size from the thyrotropin-releasing hormone (TRH) tripeptide at 362 Da, to the human growth hormone (HGH) protein at 22 kDA.[8] Generally, peptidic hormones with a molecular weight less than 10 kDa are considered peptides, whilst larger species are proteins.[9] The work described in this thesis focuses on peptide hormones.
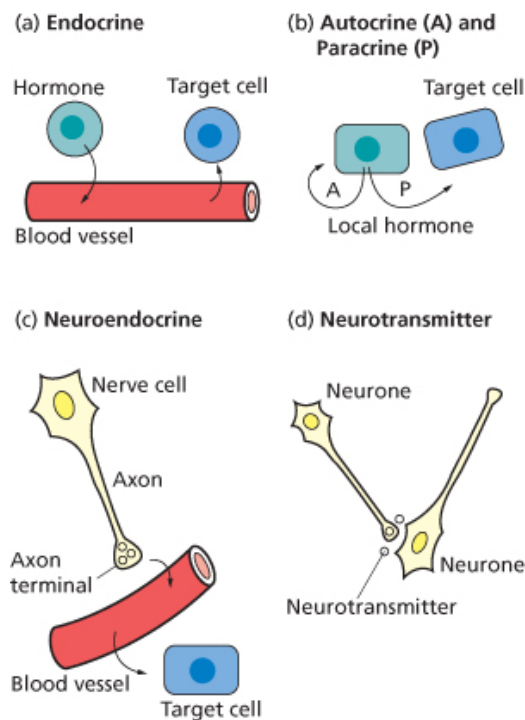
Figure 1.1: *Mechanisms of hormone and neurotransmitter action.*[2] Used with permission from Wiley-Blackwell.

Peptide Hormone Biosynthesis

Peptide hormones are responsible for the regulation of numerous physiological processes, including digestion,[10] serum glucose[11] and calcium levels,[12] lactation and

social bonding responses.[3] The biosynthesis of peptide hormones is shown in **Figure 1.2**. Beginning in the ribosome, mRNA is translated into a large peptide chain called a preprohormone. The preprohormone is directed through the endoplasmic reticulum (ER) lumen, where it is cleaved to form the prohormone.[7] The prohormone leaves the ER packaged into transport vesicles for the Golgi complex, to be exposed to enzymes mediating post-translational modifications (PTMs). The modified prohormone is then packaged in secretory granules derived from the Golgi membrane, along with maturation enzymes that convert the prohormone to the mature hormone via further cleavages and additional PTMs.[2] The mature hormone is then transported to the cell membrane for secretion. Secretion can also occur earlier in the biosynthesis, either by transport of vesicles or by transport of immature secretory granules.
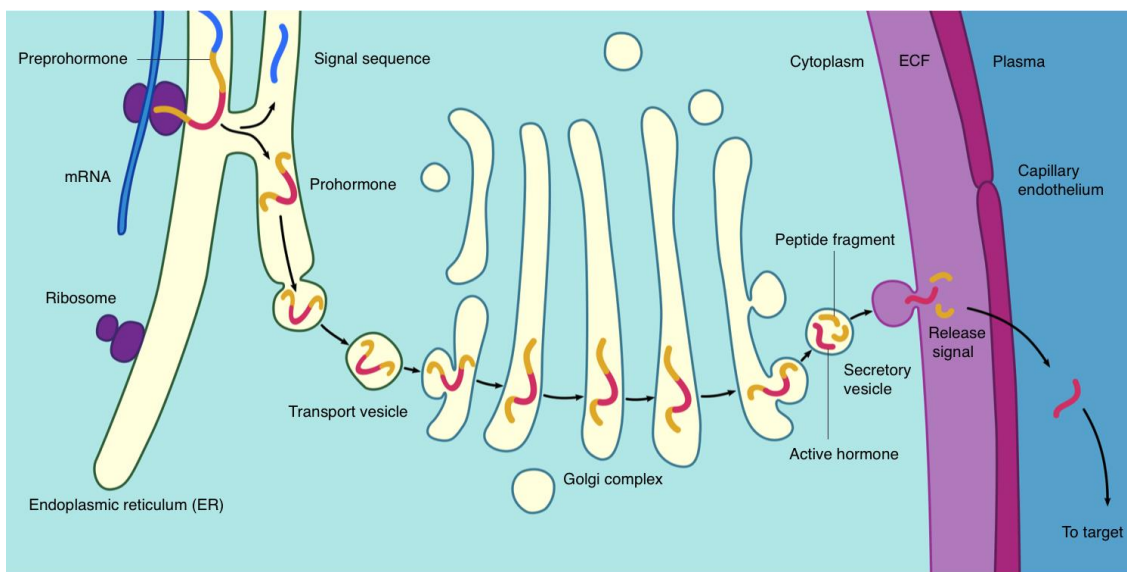
Figure 1.2: *Outline of the biosynthetic route of a peptide hormone from preprohormone to secretion of the mature hormone.* Used with permission from Aleksis Kavalieris.

Enzymes involved in the maturation of the hormone include prohormone convertases (PCs), exopeptidases such as carboxypeptidase E (CPE), aminopeptidases, and specific PTM enzymes such as glycosidases, carboxylases and hydroxylases (**Figure 1.3**). Prohormones typically contain basic residues (K-K, R-R, K-R, R-K) that act as markers

for where PCs should cleave. The extraneous basic residues are then removed by exo-
and aminopeptidases. Certain hormones require PTMs to achieve full biological activity,
typically for specific receptor recognition. Modifications include acetylation,
phosphorylation, glycosylation and C-terminal amidation.[14] Of these, one of the most
prevalent is C-terminal amidation, which occurs for around 50% of all mammalian
hormones and 80% of insect hormones. C-terminal amidation is processed by
peptidylglycine α-amidating monooxygenase (PAM), which converts a C-terminal
glycine into an amide.[15] It has been suggested that processing by PAM is the rate-
limiting step in the biosynthesis of α-amidated neuropeptides *in vivo.*[16]
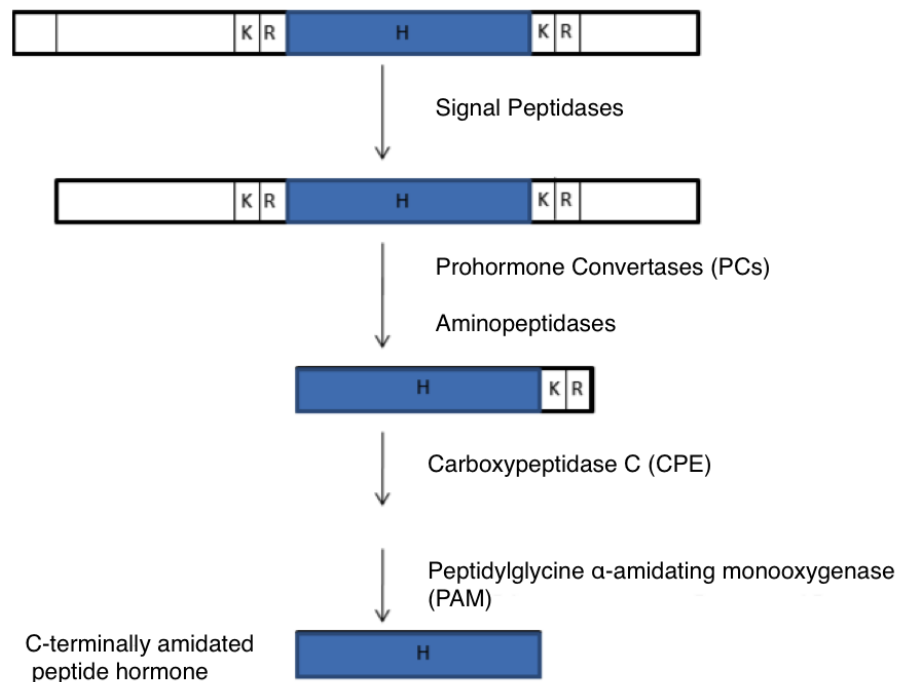
Figure 1.3: *Outline of enzymatic conversion of the preprohormone to a mature C-terminally amidated hormone.*[14, 17] Used with permission from Feihua Cao.

Peptide Hormone Regulation and Disease

Errors in the regulation of the biosynthesis or the secretion of a hormone can result in
the development of disease states, due to a dearth or an excess of the hormone. For

example, Cushing's disease is caused by excess production of adrenocorticotropic hormone (ACTH) in the thyroid. Typically, this results in obesity, as well as wide-ranging health issues with the skin, bone and reproductive systems.[7] In contrast, pathology associated with type 2 diabetes mellitus[11] and hypopituitarism[18] are the result of reduced production of insulin or growth hormone, respectively. Overproduction of peptide hormones is also associated with specific forms of cancer. Neoplasia in hormone producing organs may develop into cancers referred to as neuroendocrine tumours (NETs), as these secrete hormones into the tumour microenvironment that interact with both the endocrine and nervous systems, and can support the growth of the tumour.[19] Such tumours are often characterised by the hormones they produce, for example insulinomas, gastrinomas and VIPomas (vasoactive intestinal peptide).[19] Given that the majority of peptide hormones are C-terminally amidated, hormones with this modification are commonly produced by NETs and have been associated with the growth and development of the cancer.[20] Examples of NET-related C-terminally amidated hormones are summarised in **Table 1.1**

This work focuses on calcitonin (CT) as a case study for the pathological regulation of amidated peptide hormones in cancer, and as a model for the exogenous control of this regulation. The link between CT and cancer is well established in the literature; its oncogenic action on prostate cancer has been investigated in depth, and it is routinely used as a marker for medullary thyroid carcinoma.[12, 21, 22] Thus understanding the regulation of CT is not only biochemically but also medically important. The remainder of this Introduction will outline the structure and biosynthesis of CT; discuss the structure, function and signalling of the human calcitonin receptor (hCTR); and outline and contrast the physiological and pathological actions of CT.

Table 1.1: Example of C-terminally amidated peptide hormones known to be involved in cancer.

Peptide Hormone	Associated Cancer(s)	Action(s)	Reference
Adrenomedullin (AM)	Lung, breast, brain, skin	Increases growth, angiogenesis, bone metastasis	[23]
Amylin (AMY)/ islet amyloid polypeptide (IAPP)	Pancreatic	Overproduced, thought to lead to diabetes	[24]
Bombesin	Prostate, small cell lung, pancreatic, gastric, breast	Increases angiogenesis, cell division and growth	[25]
Calcitonin (CT)	Lung, prostate, thyroid, breast	Increases growth, tumour marker. Decreases growth in certain systems	[26, 27, 28]
Calcitonin gene-related peptide (CGRP)	Breast, prostate	Increases bone metastases, angiogenesis, and invasion	[29]
Cholecystokinin (CKK)	Lung, pancreatic, colon	Increases growth and survival	[30, 31]
Gastrin	Pancreatic, lung, gastric, colon	Increases growth, migration and proliferation	[10, 32]
Gastrin-regulating peptide (GRP)	Head and neck, lung, pancreatic, prostate, gastric, breast, colorectal	Increases growth, cell division, survival and migration	[30, 33]
Glucagon-like peptide 1 (GLP-1)	Breast, colon, pancreatic	Inhibits growth and augments apoptosis in breast and colon. May increase growth of pancreatic cancer	[34]
Gonadotropin-releasing hormone 1 &	Endometrial, ovarian,	Antiproliferative effects, increases	[35]

2 (GnRH-1, -2)	prostate	apoptosis	
Growth Hormone-Releasing Hormone (GHRH)	Breast, endometrial, ovarian	Increases proliferation and growth	[36]
Neuromedin U (NMU)	Bladder, pancreas	Increases tumourigenicity, invasiveness and metastatic potential	[37]
Neuropeptide Y (NPY)	Prostate, breast, ovarian, brain, pancreas, bone, bile duct	Increases growth and angiogenesis in prostate, brain, breast, ovarian and pancreas. Decreases in bile duct and bone	[38]
Oxytocin (OT)	Lung, bone, endometrial, prostate	Increases growth, invasion and migration. Decreases growth in some bone cancers	[39, 40]
Secretin	Bile duct	Inhibits growth in bile duct	[41]
Substance P (SP)	Brain, breast, colon, gastric	Increases growth, cell division, and drug resistance	[42]
Vasoactive intestinal peptide (VIP)	Prostate, breast	Increases growth and angiogenesis	[43]

1.2   Calcitonin

Structure and Chemistry

Originally known as thyrocalcitonin, the hormone was identified by Copp and coworkers[44] during experiments to determine whether parathyroid hormone cooperated with other molecules to maintain tight control of serum calcium levels. Perfusion of the thyroid-parathyroid glands of dogs with high calcium blood resulted in a rapid drop in blood calcium. This was attributed to the secretion of an unknown factor, later named calcitonin (CT).

Cys-Gly-Asn-Leu-Ser-Thr-Cys-Met-Leu-Gly-Thr-Tyr-Thr-Gln-Asp-Phe-
 1   2   3   4   5   6   7   8   9   10   11   12   13   14   15   16

Asn-Lys-Phe-His-Thr-Phe-Pro-Gln-Thr-Ala-Ile-Gly-Val-Gly-Ala-Pro-NH$_2$
17   18   19   20   21   22   23   24   25   26   27   28   29   30   31   32
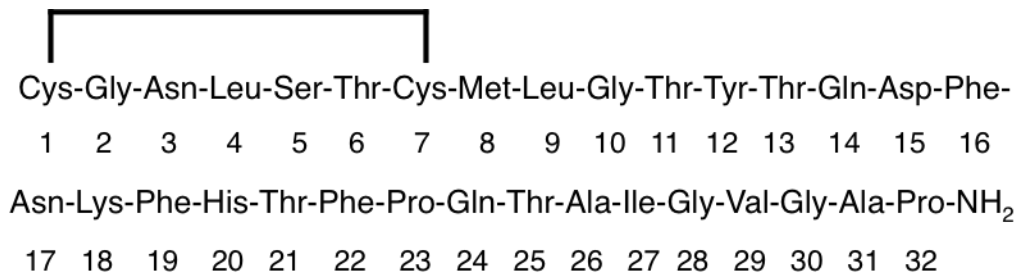
Figure 1.4: *Amino acid sequence of human CT (hCT).* A disulphide bridge is formed between Cys1 and Cys7, with Pro32 C-terminally amidated.

The peptide sequence of CT has been elucidated for many species (human CT is illustrated in **Figure 1.4**) and highly conserved in the N-terminal region (1-7) but with variation through residues 8 to 32. Categorised by structure, CT variants fall into three families: artiodacyl (including porcine, bovine and ovine, differing by four amino acids), primate/rodent (including human and rat, differing by two amino acids) and televost/avian (including salmon, eel, goldfish and chicken, differing by four amino acids).[21] Common to all variants is the 32 amino acid length containing the C-terminal proline amide and a disulphide bridge between residues 1 and 7. Divergence in the structure occurs at the α-helix motif, typically spanning residues 8 to 22, where amino

acid variations have profound effects on biological activity. In general, CT potency follows the trend televost≥artiodacyl≥human.[21] For example, the binding preference of salmon CT (sCT) to the most common isoform of human calcitonin receptor (hCTR2) is more than ten times that of human CT (hCT), attributed to an increased α-helicity. [45, 46]

hCTR is the main physiological target of hCT and this interaction is well explored in the literature.[46, 47] It is generally accepted that the N-terminal disulphide ring sits within the seven-transmembrane (7TM) region of the receptor and is responsible for receptor activation,[48] while the α-helix determines binding to the extracellular domain (ECD) of the receptor.[49] The C-terminal amide is also reported to be important for binding as the glycine-extended precursor exhibits a weaker binding.[50] This model was elegantly supported in a study by Bergwitz and coworkers,[51] where chimeric peptides comprising the C-terminus of PTH (a hormone thought to oppose CT physiological action) and the N-terminus of CT, failed to activate wildtype receptors but successfully activated chimeric receptors consisting of the PTH receptor (PTHr) ECD and the hCTR 7TM region.

CT is known to possess unusual physical properties for a peptide. It has exhibited cell penetrating ability; specifically it was shown to cross the nasal epithelium allowing it to be used in nasal sprays.[52] Through structure-activity relationship analysis, this property was attributed to the C-terminal sequence of the peptide[53] which was isolated as the hCT(9-32) peptide. This fragment has subsequently been used to transport both fluorescent proteins[54] and drugs[55] across cell membranes. CT can also form amyloid fibrils when present in high concentration.[56, 57] There has been some suggestion that CT is secreted from secretory granules in fibril-form, both in pathological (particularly medullary thyroid carcinoma) and non-pathological conditions.[57] The role of these fibrils in physiology or disease is not clear.

Biosynthesis

CT is produced primarily in the thyroid, by parafollicular cells (C cells) although its production has also been detected in the human prostate,[58] lungs,[59] seminal fluid[60] and brain.[61] The biosynthesis of CT begins with a complicated transcription process.
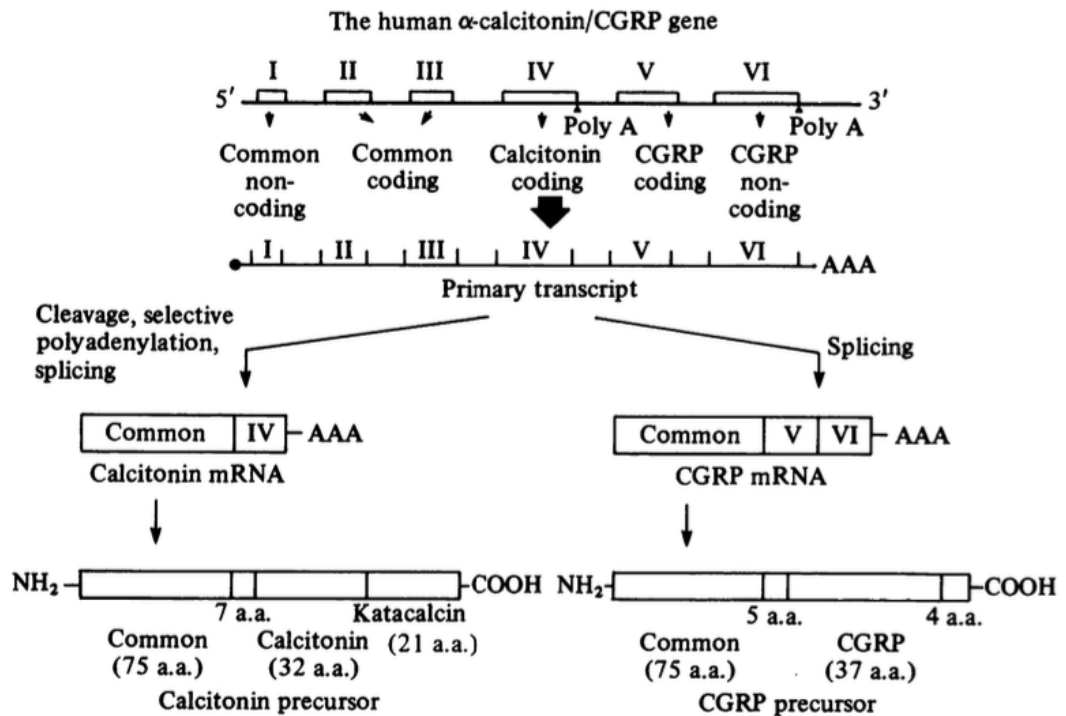
Figure 1.5: *Summary of the mRNA transcripts generated from alternate splicing of the CT/CGRP (CALCA) gene.* When translated, these transcripts produce either the CT or CGRP precursor polypeptide.[62, 63] Used with permission from Wiley-Blackwell.

The CT gene (CALCA) can encode two possible mRNA transcripts depending on the splicing; CT or calcitonin gene-related peptide (CGRP) are the two possible products.[21] The splicing is cell and tissue specific, with one product favoured over the other depending on the cell type. The production of a CT mRNA transcript from premessenger RNA uses exons 1-4, with exon 4 as the 3' terminal and polyadenylation site. In contrast, the CGRP transcript excludes exon 4 and involves the direct ligation of exon 3 to exon 5 with polyadenylation occurring at the end of exon 6 (**Figure 1.5**).[8, 64]
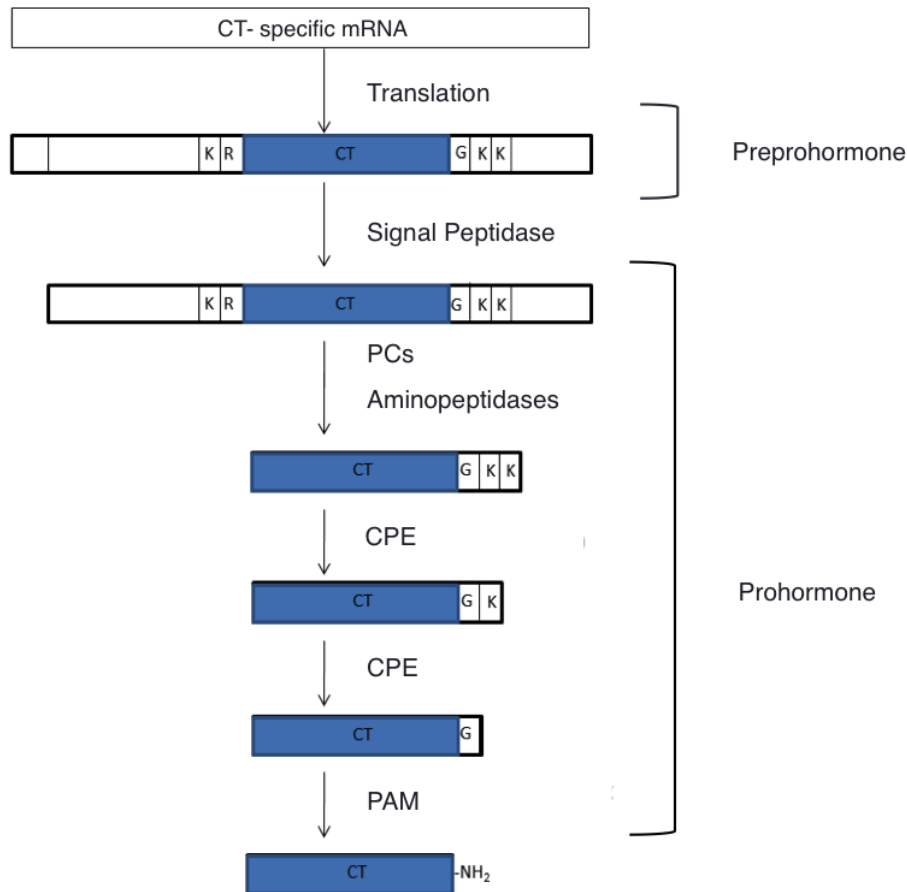
Figure 1.6: *Proposed enzymatic processing of CT precursor to mature CT by analogy to other hormones.* [14, 17] Used with permission from Feihua Cao.

The large molecular weight protein (or preprohormone) translated from CT-specific mRNA contains two peptide hormone sequences: CT and calcitonin carboxyterminus peptide 1 (CCP1, also known as katacalcin). CCP1 was originally thought to oppose the biological action of CT,[65] however this has been called into question[66] and as a result the function of this peptide is not known. There is evidence that the preprohormone is *N*-glycosylated, but this glycosylation has not been observed in mature CT.[67] Based on analogy to other peptide hormones, the enzymatic maturation of the CT preprohormone is outlined in **Figure 1.6**. CT and CCP1 are preceded by a large signal peptide sequence that is involved in directing the preprohormone through the cell. This is removed by signal peptidases in the ER. CT is thought to be packaged between basic amino acid cleavage sites, which guide cleavage by PCs.[68] If correct, this generates glycyllysyllysine-

extended CT (CTGKK), which is cleaved sequentially by CPE[68-70] to glycyllysine-extended CT (CTGK) and then glycine-extended CT (CT-G) following transport of the prohormone from the Golgi apparatus into the secretory vesicles.[69] Finally, the C-terminal glycine is cleaved by PAM to produce C-terminally amidated mature CT.[50, 71]

Detection

CT is measured diagnostically in plasma as a marker for medullary thyroid carcinoma,[28] as well as in tissue, serum and medium samples for medical and biological studies. The most common assay is an immunoassay, which uses a specific antibody to recognise CT and generates a measurable signal, often using luminescence or radiation. The first antibody was developed in 1968 for use in a radioimmunoassay,[72] however as the understanding of CT improved, it became apparent that this antibody was not specific for the mature form of CT, but rather, it recognised many biosynthetic CT precursors as well. In 1988 an antibody specific for mature CT (that is, the 32 amino acid peptide with an amidated C-terminal proline) was reported.[73] The main issues with current immunoassay detection of CT are that quantification of the hormone is poor, that there are no antibodies that can distinguish CT-G from any other CT precursor, and that the specificity of the mature CT antibody has been questioned.[74]

Other analytical detection methods have been developed, often in aid of the pharmaceutical production of sCT, such as HPLC separation with antibody quantification,[75] HPLC separation with UV detection,[76] electrochemical[77] or fluorescence tagging pre- and post-separation,[78] and LCMS detection.[79] However, few attempts have been made to apply these techniques to biological samples and they suffer either from a lack of sensitivity or the inability to accurately quantify the peptide.

1.3 The Calcitonin Receptor

General Structure and Function

Ten years after the discovery of CT, Marx and coworkers[80] discovered its primary physiological target, CTR, in isolated rat bone and kidney samples. The CTR falls into a superfamily of proteins known as G-protein coupled receptors (GCPRs), due to their activation of guanyl-nucleotide regulatory proteins (G proteins) upon the binding of an agonist. As the most common membrane receptors, GPCRs are ubiquitous across biology and are the cellular targets of a variety of effectors including light, ions, small molecules, peptides and proteins.[81] It is estimated that over 40% of pharmaceuticals target GPCRs.[82]

As described by Melmed and coworkers,[7] GPCRs have characteristic hydrophobic helical sequences that span the plasma membrane of the cell seven times and are joined by three intracellular and three extracellular loops. They are also known as seven-transmembrane domain (7TM) receptors for this reason. Ligands bind to GPCRs through interactions with the cavities between the transmembrane helices, the extracellular loops and the N-terminal extracellular domain (ECD), with the importance of each interaction dependent on the receptor class and type. Ligand binding activates the receptor and causes a conformational change that affects receptor structure across the cell membrane. A receptor in an active conformation can then bind G proteins through interactions with the intracellular transmembrane domains, intracellular loops and the C-terminal intracellular domain (ICD). When bound and activated by the GPCR, G proteins generate a cascade of secondary messengers such as cyclic adenosine monophosphate (cAMP) and inositol 1,4,5-trisphosphate (IP3) inside the cell. This allows the cell to respond to extracellular stimuli without allowing foreign species inside the cell membrane.[7] A characteristic GPCR-G protein complex, and thus the activation model,

was characterised in its entirety for the first time in 2011, when Rasmunssen and coworkers[83] reported a crystal structure of the β2 adrenergic receptor bound to the corresponding G protein, $G_{\alpha s}$. This work contributed to the Nobel prize won by the corresponding author Brian Kobilka.[84]

CTR is a member of the class B/secretin GPCR family, which encompasses the majority peptide hormone receptors such as the glucagon and parathyroid hormone receptors, and was originally characterised from porcine cDNA in 1991.[85] The general structure of these of receptors is represented in **Figure 1.7**.[86] Class B receptors are characterised by ECDs of around 120 amino acids extending from the 7TM domain, which dictates peptide binding affinity and specificity (although the role of the ECD in peptide binding varies between receptors). [87] Glycosylation in this region is also common.[86]
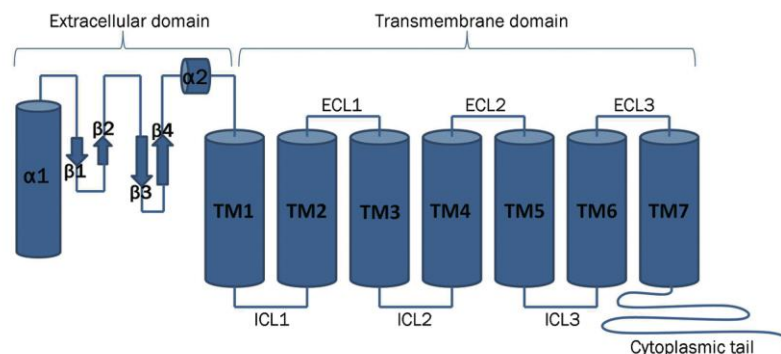
Figure 1.7: *The general architecture of Class B GCPRs.*[86] Used with permission from Nature Publishing Group.

Peptide binding to CTR is outlined pictorially in **Figure 1.8**. The N-terminal ECD governs the binding of peptide substrates to the receptor, initially guiding the C-terminus of the peptide into a binding orientation. Structurally, the ECD is dominated by an α-helix and two anti-parallel β-sheets. In turn, this helix forces binding peptides to adopt an α-helical conformation, generating electrostatic and hydrophobic stabilizing interactions, favouring a bound state.[88] The ECLs and the outer 7TM structures are

collectively known as the juxtamembrane region, which governs the binding of the N-terminal residues of the peptide to the cavity among the helices. This interaction is known to be responsible for the agonist mediated-activation of the receptor, as the binding induces a conformational change in the 7TM and cytoplasmic domain of the receptor, which mediates the interaction between the intracellular GPCR loops and a heterotrimeric G protein.[89]
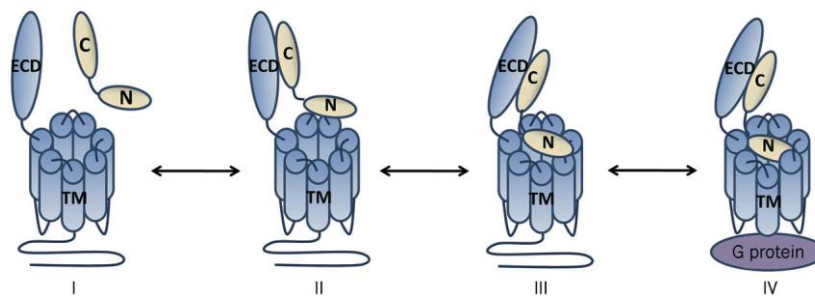
Figure 1.8: *Binding of peptide hormone to a class B GPCR.* Used with permission from Nature Publishing Group.

In humans, receptors for the CT family of peptides (CT, CGRPα, CGRPβ, AM, Intermedin and AMY) differ from other class B receptors in that they are further functionalized by RAMPs (Receptor Activity Modifying Proteins). RAMPs are a unique class of transmembrane proteins comprising of RAMP1, RAMP2 and RAMP3.[89] These proteins can associate with either CTR or the calcitonin-like receptor (CLR) to alter their specificity to members of the CT peptide family. When RAMPs are coexpressed with CTR, specific Amylin receptors are generated. Each protein dimerises with CTR to form a distinct receptor with a unique phenotype, surface level expression and binding characteristics, designated AMY_1, AMY_2 and AMY_3.[90] Receptors AMY_1 and AMY_3 have been shown to bind AMY selectively over CT, but the selectivity is not high (pEC_{50} 9.12 vs. 8.93 for AMY_1 respectively).[89] Receptors AMY1 and AMY3 have been shown to bind AMY selectively over CT, however this selectivity is hard to investigate due to the difficulties in generating a homogenous RAMP-modified CTR population.

Ligands

hCT is the primary physiological ligand for the unmodified hCTR. However, it has been reported that an orphan peptide (PHM-27) identified in neuroblastoma and neuroendocrine tumours, is able to stimulate a cAMP response with high efficacy upon binding to hCTR.[91] This suggests biological roles for hCTR that have not previously been identified. Several synthetic ligands have been generated in order to probe receptor biology and to aid in the development of new drugs. The most commonly studied ligand is sCT residues 8-32 (sCT(8-32)).[92] Interestingly, the truncation of the N-terminus of sCT produced a range of hCTR antagonists with sCT(8-32) the most effective (IC_{50} 1 x 10^{-9} M against competitive binding of sCT to hCTR2).[46, 93] This was attributed to the α-helix of sCT(8-32) binding to the ECD and preventing other ligands from binding; sCT(8-32) could not activate the receptor due to the lack of the disulphide ring at the N-terminus.

Katayama and coworkers[94] developed a small molecule agonist, SUNB8155, in 2001 as an orally available alternative to sCT for pharmaceutical applications. It bound to the hCTR selectively over hPTHr, stimulated a cAMP response (EC_{50} 21μM) and was antagonized by sCT(8-32). However, it did not displace radiolabelled sCT, which implied that SUNB8155 has an alternative mode of binding to CT. Its mode of binding has not been investigated further.[95] Further studies with other small molecule hCTR agonist candidates suggest that small molecule binding to the hCTR is dependent on the juxtamembrane region rather than the ECD, a finding which may shed light on the binding mode of SUNB8155.[96]

Isoforms

hCTR is reportedly expressed as multiple isoforms or splice variants depending on the mRNA splicing of the CALCR gene transcripts. At least five regions of difference in the receptor protein structure and six isoforms or splice variants have been reported resulting in protein varying in mass from 34 kDa to 59 kDa.[97, 98] Nomenclature for the isoforms varies in the literature. In this work, in accordance with the isoform assignments reported by Beaudreuil and coworkers,[97] the longest transcript first reported by Gorn and coworkers[99] is the canonical transcript and referred to as hCTR1. Subsequently reported transcripts considered by Beaudreuil and coworkers are labeled isoforms hCTR2 to hCTR6. Transcripts reported in the literature but not considered in the analysis by Beaudreuil and coworkers have not been assigned an isoform number. It should be noted that almost all characterisation of hCTR isoforms has been performed at the mRNA level rather than protein level.

The sequences of hCTR1-6 are outlined in **Figure 1.9** and the remaining reported variants in **Figure 1.10**. In 1992, Gorn and coworkers[99] first isolated hCTR cDNA 3588 bp in length, with the CDS (coding DNA sequence) corresponding to a 508 amino acid protein, from an ovarian small cell carcinoma line BIN-67. This cDNA was transfected into COS-M6 cells and the resulting receptor expression was verified through the competitive binding between radiolabelled and unlabeled hCT and sCT, and the stimulated production of the secondary messenger cAMP. Initially, the CDS region of hCTR cDNA was reported to begin at position 247, however later this was revised to be at position 192.[100] In 1994, a second isoform (hCTR2) was reported independently by two groups, Kuestner and co-workers,[101] and Frendo and coworkers.[63] Kuestner and coworkers isolated hCTR2 from T47D, a breast cancer cell line, while Frendo and coworkers used TT, a medullary thyroid carcinoma cell line. The specific cDNA sequence reported by Kuestner is described in **Figure 1.9**, and starts at position 221 of hCTR1. Both

groups reported a deletion of 48 bp (16 amino acids) relative to hCTR1 in the region coding for the putative first intracellular loop joining the transmembrane helices. It was later reported that this loop alters the binding of G proteins to the ICD of the hCTR.[102] hCTR2 activation led to the stimulation of IP3 production, unlike the activation of hCTR1, which suggests it is able to bind different G protein complexes and activate different signalling pathways. It was subsequently recognised that hCTR2 is the most commonly expressed form of hCTR, and that the 48 bp excision is the defining structural variation in terms of hCTR activity and pharmacology.[103]

hCTR3 and 4 were both discovered in 1995, by Albrandt and coworkers[104] in MCF-7 breast cancer cells, and by Moore and coworkers in baby hamster kidney cells transfected with hCTR2,[105] respectively. hCTR3 has the same 48 bp excision as hCTR2, but also exhibits a truncated ECD due to the loss of 125 bp at the start of the CDS corresponding to 47 amino acids. Surprisingly, it was found that this truncation still allowed the binding of sCT and the stimulation of cAMP production. hCTR4 was identified while assessing the binding characteristics of hCTR2. Rather than the previously reported 48 bp excision, a 35 bp alternative sequence at the same location was identified. This new sequence coded six amino acids of the first intracellular loop, and a stop codon, prematurely ending synthesis of the protein. It was suggested that this isoform could act as a soluble binding protein to modulate hormone activity, based on observations regarding thyrotropin.[106]

In 2004, Beaudreuil and coworkers[97] summarised the hCTR isoforms outlined above and presented two new isoforms isolated from T47D breast cancer cells; hCTR5 and hCTR6. Both isoforms are missing 218 amino acids from the 2nd intracellular loop, due to a 50 bp insertion after 850 base pairs that terminates protein translation 23 base pairs later. hCTR5 has the 48 bp excision in the first intracellular loop common to hCTR2 and 3, while hCTR6 does not. hCTR6 was transfected into HEK293 cells, and radiolabeled

sCT was unable to bind thus cAMP production was not stimulated. The inability to bind sCT raised the question as to whether the protein was expressed on the cell surface, as the ECD of the isoform remained unchanged. '

The analysis of the literature by Beaudreuil and coworkers[97] did not take into account the work reported in 1995 by Gorn and coworkers,[100] Nishikawa and coworkers[107] or by Nakamura and coworkers.[108] In 1995, Gorn and coworkers demonstrated the presence of two additional variants exhibiting N-terminal truncation isolated from giant cell tumour of the bone. In this case, the 71 bp excision from the cDNA overlapped with the 5′-UTR (5′-untranslated region) and CDS region, resulting in an 18 amino acid truncation of the putative ECD. This variation was observed both in the presence and the absence of the 48 bp excision reported for hCTR2. It was noted that the variant with the 48 bp excision exhibited reduced binding of sCT, but a stronger cAMP stimulation response. This suggests that the ECD is important not only for binding, but also for G protein signal transduction. In 1999, two more possible variations in the translation of hCTR were reported. Nishikawa and coworkers[107] reported two splice variations to the 5′-UTR in samples isolated from osteoclasts. It was suggested that these variations might be the result of multiple promoters splicing alternative exons, which is the case for other class B GPCRs.[107, 109] In contrast to the previous examples, Nakamura and coworkers[108] reported an allelic polymorphism in the Japanese population, with a base pair change of cytosine to thymidine at the 1377th position resulting in the substitution of leucine for proline. It was proposed that this change may effect signal transduction and later suggested that the leucine substitution is more common in sufferers of osteoporosis.[110]
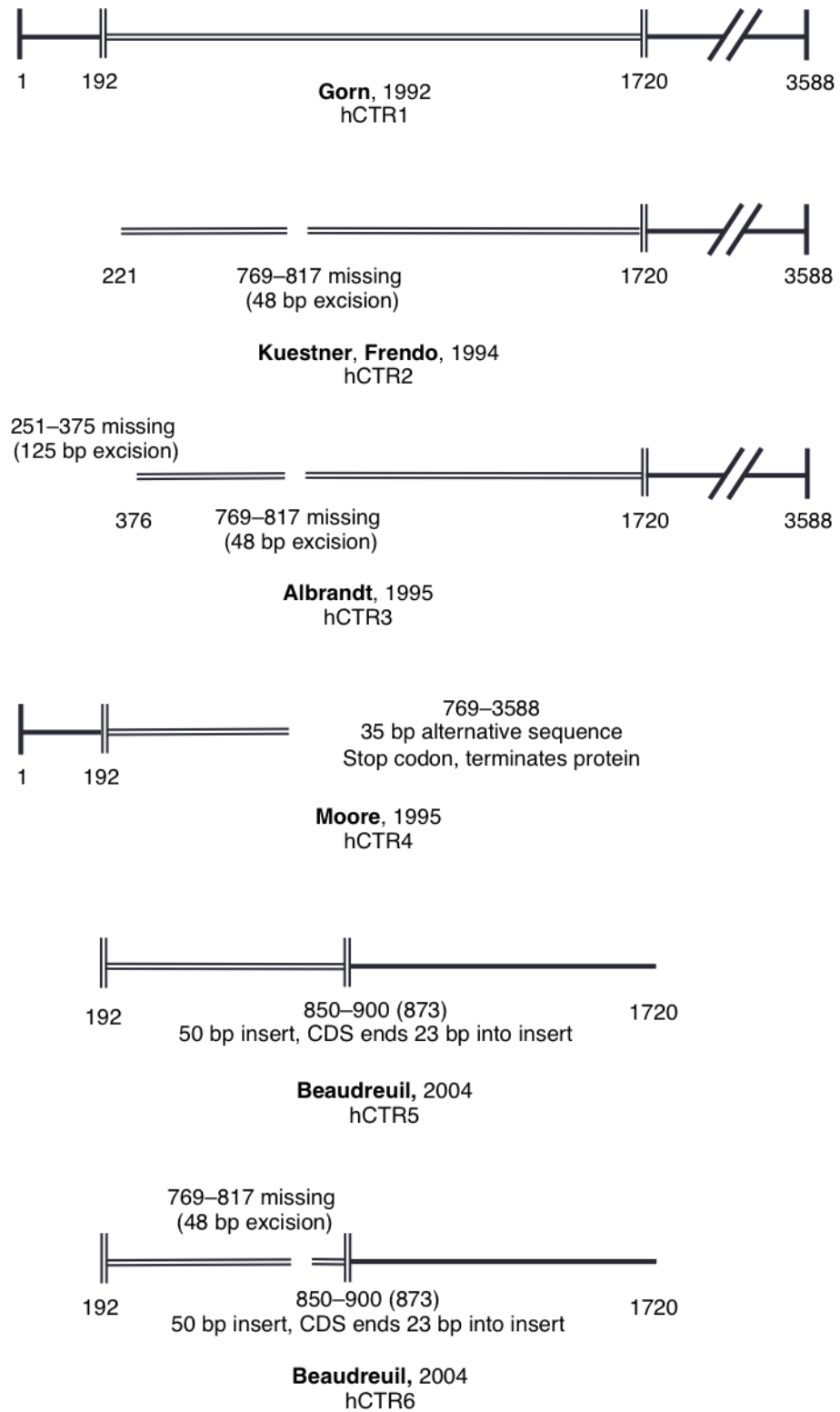
Figure 1.9: *The reported cDNA sequences corresponding to hCTR isoforms 1-6 assigned by Beaudreuil and coworkers.*[97] The sequence reported by Gorn and coworkers[99] has been taken as canonical (hCTR1) and subsequent sequence variants are aligned to it.[63, 99, 101, 105]
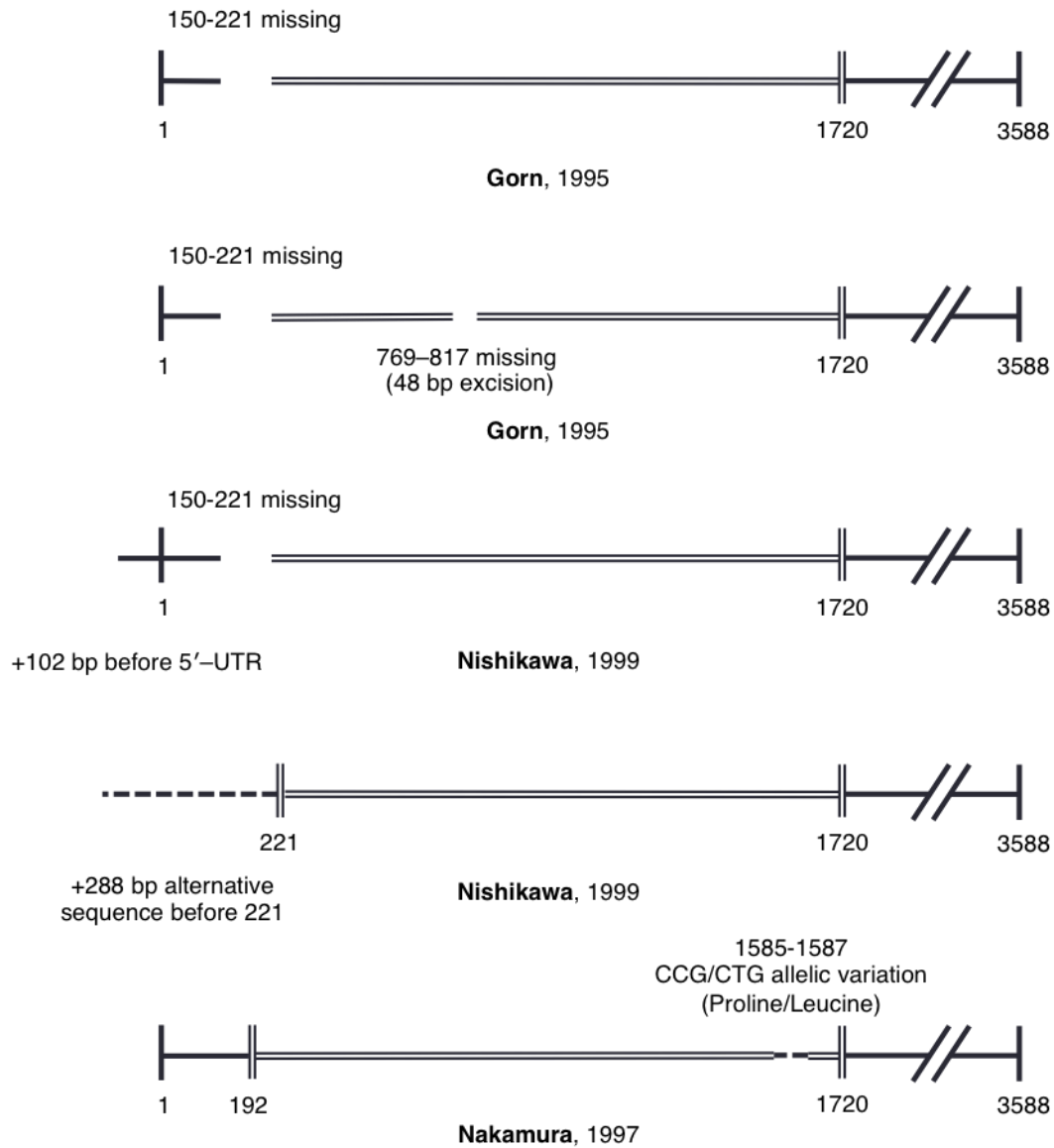
Figure 1.10: *Reported CTR cDNA sequences not considered in the 2004 analysis of Beaudreuil and coworkers.*
[100, 107, 108]

Signalling

The understanding of hCTR signalling has progressed alongside the general understanding of GPCRs. In the past, it had been recognised that the activation of hCTR increased the intracellular concentrations of the secondary messengers cAMP and Ca^{2+},[103, 111, 112] and that in CT-secreting cells these messengers impacted CT regulation; for example, by up regulating CT gene transcription.[113] However, it was not clear how the

activation of hCTR stimulated the production of secondary messengers. The discovery of G proteins in the 1980s provided understanding of the mechanistic link between the receptor and secondary messengers.[114]

It is now understood that binding of an agonist to the hCTR mediates a change in the conformation of the transmembrane cytoplasmic segments, enabling the intracellular binding of a G protein.[83] The receptor activation process is illustrated for a GPCR binding a $G_{\alpha s}$ protein in **Figure 1.11**. Upon binding to the ICD of the activated receptor, the α-subunit of the G protein heterotrimer releases GDP in favour of binding GTP. This results in the release of the heterotrimer from the receptor, and dissociation of the trimer into α- and βγ-subunits, with the α-subunit primarily dictating which secondary messenger pathway is activated.[30] In this example, the α- and βγ-subunits activate the adenylyl cyclase protein and the Ca^{2+} channel respectively, before reforming the heterotrimer following the hydrolysis of GTP to GDP by the α-subunit.[83]
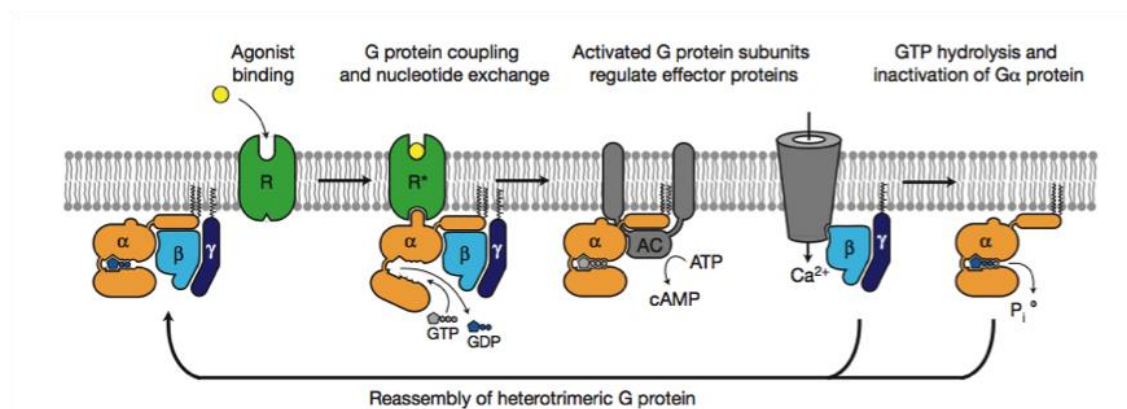
Figure 1.11: *G protein activation and dissociation cycle for the GPCR-$G_{\alpha s}$ complex.*[83] Used with permission from Nature Publishing Group.

Classical G protein signalling pathways are outlined in **Figure 1.12**. After the disassociation of the G protein heterotrimer, the α-subunit can affect a variety of secondary messaging enzymes.[115] Four main subclasses are known: $G_{\alpha s}$, $G_{\alpha i}$, $G_{\alpha q}$ and $G_{\alpha 12/13}$.[116] Both $G_{\alpha s}$ and $G_{\alpha i}$ interact with adenylate cyclase (AC); $G_{\alpha s}$ activates cAMP

production, while $G_{\alpha i}$ inhibits formation. This in turn affects protein kinase A (PKA), up-regulating or down-regulating phosphorylation respectively. $G_{\alpha q}$ activates phospholipase C (PLC), increasing generation of diacylglyerol (DAG) and IP3, which in turn activates protein kinase C (PKC), and increases intracellular Ca^{2+}, respectively. $G_{\alpha 12/13}$ activates the GTPase activating protein RhoGEF, which in turn activates RhoA. Those signalling components displayed in green then activate further signalling mechanisms, such as the MAPK pathway, which transduce towards the cell nucleus.[63, 117]
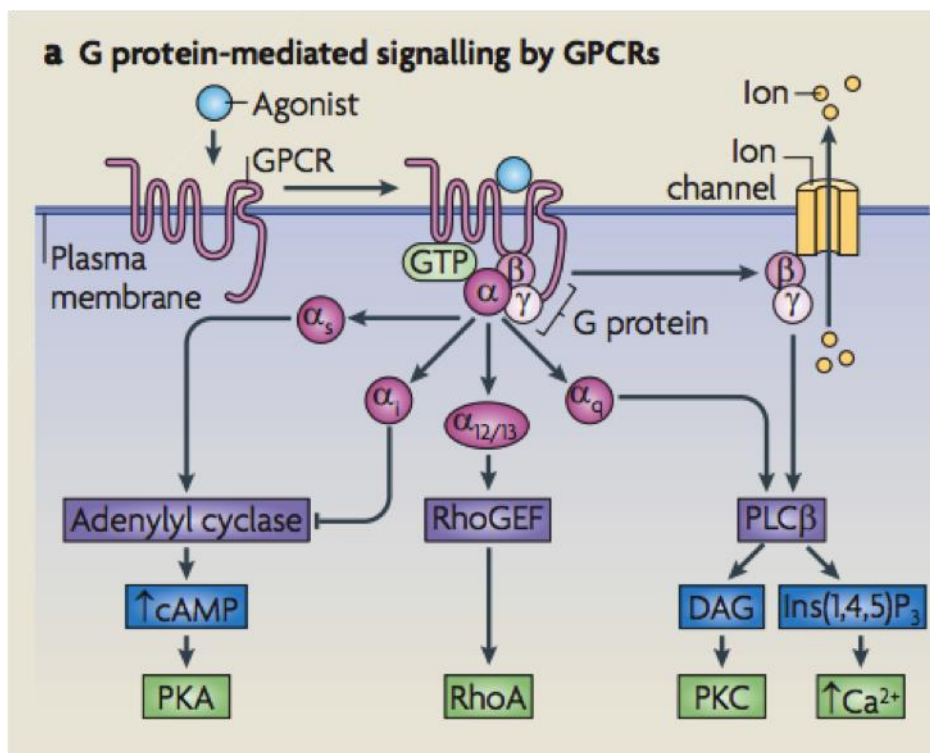
Figure 1.12: *Classical GCPR G protein α-subunit signalling pathways.*[117] Used with permission from Nature Publishing Group.

hCTR is thought to bind $G_{\alpha s}$,[112, 118] $G_{\alpha q}$,[119] and $G_{\alpha i}$.[120, 121] These assignments are based on studies of the secondary messengers generated by activation of hCTR, and the typical corresponding G protein, rather than direct evidence of G proteins binding to hCTR.[21, 103] Signalling through these pathways is thought to be responsible for the majority of the biological effects CT exerts.   hCTR is also thought to interact with β-arrestin as part of

the receptor internalisation pathway,[122] and activate MAPK pathways, potentially by binding the GTPase, Ras.[123] Interestingly it has been reported for hCTR1 and 2 that uncontrolled, agonist-independent signalling can occur.[124] Specifically, stimulation of cAMP production occurs in the absence of an agonist, and this may provide a mechanism for uncontrolled cell growth in cancer.

1.4 Roles of Calcitonin in Physiology

The well-established role CT plays in physiology involves the inhibition of bone resorption through binding to the CTR on osteoclasts, the cells that break down bone and transfer the mineral content to the serum.[125] Specifically CT action on osteoclasts decreases motility, induces contraction and causes the loss of the morphologically characteristic ruffled border required for bone resorption.[126] CT also interferes with osteoclast differentiation, and thus osteoblast generation, from precursor cells.[127] Because of these effects sCT has been approved for the treatment of osteoporosis and Paget's disease, diseases which involve unregulated bone loss.[21] CT is often associated with calcium regulation, however this is not entirely accurate regarding its action on bone. While the ability of CT to alter calcium levels is pronounced in young organisms or those under calcium stress (such as pregnant or lactating mammals),[128] its effectiveness decreases with age. In healthy adults CT has little direct impact on calcium regulation.[21, 129] The rate of bone resorption greatly decreases with age unless under stress, implying that the influence of CT is proportional to the rate of bone resorption. Therefore, CT should more accurately be thought of as a regulator of bone resorption rather than the calcium regulator as its name might suggest.[21]

The relationship between CT and bone density was confounded by studies demonstrating an increase in bone density in calcitonin-negative knockout mice,[130] and

the lack of osteoporosis pathology (low bone density) in patients who had undergone thyroidectomy.[131] It was not until 30 years after the initial hormone characterization that the mechanism of the hCTR-osteoclast axis was unraveled. Keller and coworkers[132] discovered that the activation of osteoclast hCTR by CT reduced the secretion of a key bone resorption compound, sphingosine 1-phosphate, by inhibiting the expression of the transporter gene *Spns 2*. The non-linear relationship between CT and the effector species provides an explanation as to why calcium-unstressed organisms do not experience a sharp decrease in bone density in the absence of CT.

CT is also active in the renal system, where its main reported action is to increase calcium excretion via inhibiting renal tubular resorption in the kidney, again through the CTR.[133] This is of particular importance for the treatment of cancer-derived hypercalcemia, which is thought to be due to the breakdown of bone. Administration of CT to hypercalcemic patients results in a rapid decrease in serum calcium levels, and in part, this action is distinct from the action of CT on osteoclasts.[134] As previously mentioned, CT has the properties of a cell penetrating peptide. A recent study reported that calcium ions could bind to CT, encouraging membrane pore formation and discouraging aggregation, indicating that pore formation may represent another method of calcium control by CT.[135]

CT has been implicated in both the implantation of the embryo to the uterus, and the development of the foetus.[103] In a study by Dacquin and coworkers,[136] it has been shown that a full CTR knockout through the deletion of exons 6 and 7 is embryonically lethal in mice. This has been challenged by the study of Keller and coworkers,[132] where CTR was successfully knocked down through the deletion of exons 13 and 14. The reason for this contradiction is not yet clear although differences in editing strategy may have had an influence In the rat uterus, it was found that the silencing of the CT gene and the subsequent abrogation of CT expression resulted in the severe impairment of embryo

implantation.[137] Recently, it was proposed that this impairment was mediated through the up-regulation of integrin β3, which is known to increase endometrial receptivity.[138] It has also been demonstrated that CT is involved in the development of blastocysts, particularly with regard to intracellular Ca^{2+} regulation. Upon implantation trophoblast cells, which make up the exterior of the blastocyst, begin to grow outwards. There is a relationship between trophoblast growth, differentiation and increases in intracellular Ca^{2+}. Wang and coworkers[139] demonstrated that hCTR2 is expressed in unfertilized eggs and zygotes, and that after fertilization, hCTR expression increases. They further showed that exposing blastocysts to calcitonin increased growth and intracellular Ca^{2+}.

There is evidence that CT can also exert an analgesic effect.[140] CTRs are expressed on serotonergic neurons in the regions of the mouse brain involved in processing pain.[141] Moreover, interruption of the serotonergic pathway decreases the analgesic potency of CT,[142] suggesting they interact. The analgesic effect is less well-established in humans,[143] with the most convincing evidence provided by a meta-study assessing the reduction of pain specifically during the treatment of osteoporotic vertebral fractures with sCT. In this context, 13 of the 14 studies reported a statistically significant improvement in pain or function in sCT-treated patients.[144] However, it is not clear if this effect is relevant for general analgesia, as opposed to bone-specific conditions.

1.5 Roles of Calcitonin in Cancer

CT has been associated with cancer since its discovery; many neuroendocrine cancer cell lines are reported to secrete CT and much of the characterisation has been undertaken in neuroendocrine cancer systems. Up-regulation of CT in certain cancers occurs to such an extent that it is used as a diagnostic marker in plasma, such as in the case of medullary thyroid carcinoma (MTC).[145] Despite this relationship, there has been little direct mechanistic evidence linking CT and the growth or development of cancer. In MTC,

Frendo and coworkers demonstrated that hCTR2 is expressed in TT cells derived from MTC tumours, and suggested that autocrine regulation of CT may be operating.[63] More recently, inhibition of the GPCR signalling enzyme PKC reduced cell proliferation and prevented the stimulation of CT secretion by Insulin-like Growth Factor 1 (IGF-1).[146] These reports suggest a link between CT and tumour growth, however there remains a lack of direct mechanistic evidence to implicate CT as an oncogenic peptide in MTC.

CT has only been mechanistically linked to growth and proliferation in prostate cancer, due in a large part to the work of Girish Shah and coworkers. In 1994, it was reported by Shah and coworkers[147] that exposure of LnCaP prostate cancer cells to CT mediated CT-hCTR binding and increased intracellular Ca^{2+} and cAMP. Downstream, this also mediated an increase in the incorporation of radiolabeled [³H]thymidine, implying elevated DNA synthesis and therefore growth. This was the first mechanistic evidence for the oncogenic activity of CT in prostate cancer. Furthermore in the same model the elevated cAMP activated the MAPK signalling pathways, also stimulating growth.[148]

Over the next decade in a series of papers,[27, 149-152] Shah and coworkers elucidated the role of hCTR signalling in PC-3 and PC-3M (a hCTR-transfected cell line) cells. They implicated the $G_{\alpha s}$ protein as responsible for the growth effects CT enacts on cells,[149] and demonstrated that the resultant PKA signalling promoted invasiveness[150] and tumourgenicity.[151] Moreover transcriptional knockdown of hCTR mediated growth arrest and apoptosis in *in vitro* and *in vivo* prostate cancer models,[27] and silencing CT expression *in vivo* decreased tumour size and frequency.[152] Most recently, Zonula Occludens-1 (ZO-1) was suggested as a possible effector protein required for increased prostate cancer metastatic potential upon stimulation with CT.[153]

While the presence of CT in high concentrations in neuroendocrine tumours and cells suggests a role in the cancer development, for the majority of cancers this role remains

unclear. It is well documented that neuroendocrine tumours of the lung, specifically small cell lung carcinoma (SCLC), produce higher concentrations of calcitonin compared to non-cancerous tissue,[154, 155] although this trait has not been adopted as a diagnostic marker.[155] Not surprisingly cell lines derived from SCLCs,[156] such as DMS53 secrete orders of magnitude greater (43 ng/ml/10^6 cells) CT,[157] than healthy lung tissue. It has been reported that BEN bronchial carcinoma cells respond to CT exposure by activating intracellular cAMP[158] and PKA,[159] and more CT is secreted when the external concentration of CT decreases.[160] However, there have been no reports that these mechanisms influence growth, invasion or tumourgenicity. Interestingly in 1988, for both humans and rodents, increased CT in the lung correlated with the nicotine levels of cigarettes.[59] This was later reinforced in a larger cohort study of smokers.[161] This relationship provides a tantalizing link between high precancerous levels of CT in the lung and the onset of smoking-induced lung cancer.

In contrast to the reported effects on prostate cancer, CT appears to have an anti-proliferative effect in breast cancer. Like the prostate cancer cell lines discussed above, the breast cancer cell line T47D expresses hCTR, along with a CT-responsive adenylate cyclase.[158] However, a PKC-dependent signalling pathway that down-regulates hCTR expression in response to CT stimulus was also observed.[162] As a consequence, CT exposure decreases the proliferation of T47D cells.[163] This suggests that CT has the ability to act as a growth or anti-proliferative agent, depending on the cell line. Based on the action of CT in T47D cells, this appears to be dependent on the activation of specific signalling pathways by hCTR, rather than on hCTR expression.

Taken as a whole, these findings suggest a complicated and nuanced relationship between CT and cancer that varies with cell type, tumour location and CT concentration. Given that the same receptor and signalling pathways mediate the apparently contradictory effects of CT in different cell lines, it can be assumed that the factors

responsible for differentiating the actions of CT have not yet been elucidated. In part, this is due to a lack of incisive tools that allow quantification of CT and its precursors *in vitro,* as described earlier in the discussion of CT detection techniques. The ability to compare the relative amounts of CT and its precursors secreted by cancer cells over different periods of growth is the first step towards discerning its role, and how this may vary in different systems.

1.6 Summary and Aims

It is clear that new analytical tools need to be developed to quantify CT and its precursors in order to explore its multifaceted relationship with cancer. It is also clear, based on the roles of CT in normal physiology and the result of its dysregulation in diseases such as cancer, that the ability to externally regulate CT production *in vitro* and *in vivo* is of medical and biochemical interest. Previous attempts to regulate CT production in order to elucidate its proliferative effect in cancer involved complicated techniques, such as antibody neutralization[150] and genetic silencing,[152] which are not suitable for broader applications. However, the biosynthesis of other hormones has been targeted through the inhibition of the hormone biosynthesis apparatus using small molecule inhibitors.

PAM, which mediates the C-terminal amidation essential for complete bioactivity in over 50% of human hormones, has been implicated as the rate-limiting enzyme in the production of neuropeptides.[16] This makes it a potential target for the generic disruption of hormone biosynthesis.[164] In a study by Iwai and coworkers,[165] production of the hormone GRP was targeted through the inhibition of the PAM enzyme with *E*-4-phenyl-3-butenoic acid (PBA) in SCLC cells. PBA reduced cell viability and growth in the treated cultures, while treatment with synthetic GRP overcame the growth inhibition. Growth inhibition was also observed when cell lines were transfected with antisense

PAM RNA to silence expression. It was suggested that PAM inhibition disrupted the GRP autocrine growth loop operating in the cell. However, because many hormones are C-terminally amidated, and changes in endogenous GRP concentration were not quantified, the reduction of GRP was not directly linked to the growth abrogation observed. The effect of CPE inhibition on neuroendocrine cancer survival and proliferation has also been investigated,[166] using guanidinoethylmercaptosuccinic acid (GEMSA) to inhibit CPE activity. It was found that the presence of CPE increased the survival of cells in hypoxic conditions, and that GEMSA inhibition did not reduce this effect. Again, effects on peptide hormone production in these conditions were not assessed. In order to link the disruption of hormone biosynthesis with changes in cancer cell growth and proliferation, it must first be demonstrated that biosynthesis inhibition decreases peptide hormone production.

As CT is C-terminally amidated, these findings suggest that CT may be regulated through the inhibition of PAM. CT precursors are also processed by CPE, so it is of interest to compare the effects of PAM and CPE inhibition on CT and CT precursor production. In order to thoroughly assess the effectiveness of CT biosynthesis inhibition, an assay method that can measure the relative proportions of the substrates and products of the inhibited enzymes is required. Specifically, this requires the detection and quantification of CT, CT-G and the two hypothesised base-residue extended CT precursors, CTGK and CTGKK. Such an analysis will provide insight as to whether inhibition of the biosynthetic enzymes is an effective strategy to abrogate CT production. As noted previously, immunological methods are not specific for the individual biosynthetic precursors of CT, and quantification is also difficult.

In the work performed in Chapter 2, an HPLC-fluorescence based protocol with online concentration and post-separation fluorescence tagging was developed to detect and quantify the relative amounts of CT, CT-G, CTGK and CTGKK for the first time, in

DMS53 SCLC cell medium and lysate. Novel glycosylated versions of each species were also detected, where they formed a parallel biosynthetic pathway. The effect of PAM inhibition, CPE inhibition and growth medium dilution on the glycosylated and non-glycosylated CT species produced by DMS53 SCLC cells was then assessed. Inhibition of the biosynthetic enzymes was shown to be ineffective in controlling CT production, raising the possibility that the parallel glycosylation pathway was involved in maintaining CT homeostasis. Additionally, DMS53 cells responded to dilution of the cell medium with the up-regulation of CT production. Together, these observations suggested that a feedback mechanism was operating in DMS53 cells to maintain intracellular and extracellular CT. It was hypothesised this mechanism might be mediated by the hCTR. In the work performed in Chapter 3, the relationship between the hCTR and CT feedback in DMS53 cells was explored through the application of a specific hCTR agonist, SUNB8155. Expression of hCTR mRNA and protein was determined in DMS53 (Chapter 4), and the impact of hCTR signalling pathway inhibition on CT production was investigated in Chapter 5. In Chapter 6, conclusions from the work in this thesis are drawn, and preliminary experiments screening the MTC TT cell line for CT-related species are outlined, as well as the development of methodology to detect and quantify another peptide hormone, OT.

This work aims to demonstrate that the ability to quantify CT and its related species *in vitro* would unlock an understanding of its regulation, and provide clues to its generic mechanisms of action in cancer.

Chapter Two

Results and Discussion: Detection of Biosynthetic Precursors, Discovery of a Glycosylation Pathway and Homeostasis of Calcitonin in Human Cancer Cells

2.1 Introduction

In the previous Chapter, the need for a quantitative detection method for CT and its biosynthetic precursors was outlined, as this would provide a platform to understand the regulation and role of CT in neuroendocrine cancers. While the speculative biosynthesis of CT had been proposed by analogy to other hormones,[167] the key precursors (CT-G, CTGK and CTGKK) had not been detected or quantified (**Figure 1a** in the following manuscript, denoted as Cao and coworkers). By extension, there had been no way to examine the impact of inhibitors of CT biosynthetic enzymes such as CPE or PAM even though such inhibitors may have significant therapeutic utility.[165, 168] In order to identify these species and investigate the effects of enzyme inhibition on CT, an HPLC-fluorescence detection technique featuring on-line analyte concentration and post-separation fluorescence labeling was developed. Using this system, an *in vitro* analysis method for CT-related species in the medium and lysate of the SCLC cell line DMS53 was designed. This was used to screen cell-derived samples for CT and its related species, and assess the effect of PBA, GEMSA, and changes in growth medium volume and incubation time on the production of these species. This work has been published in ACS Analytical Chemistry,[169] and is copied on the following pages. The work outlined in

the manuscript was undertaken in parallel to the work described in this thesis. As such, the manuscript is the first report of our methodology in the literature, and serves as an introduction to my independent studies. To delineate my contribution to this multiauthored paper: Drs. Onagi, Gamble and Hennessy developed the original analytical methods. Dr. Cao, Ms. Howes and Mr. Gu characterised CT and its precursors. Dr. Cao and Ms. Howes developed analytical methods to detect glycosylated CT-related species using HPLC-fluorescence, and to detect CT-related species in the lysate. Drs. Cao and Onagi and Ms. Howes characterised the glycosylated CT-related species using MS. Dr. Cao and Ms. Howes performed the PBA and GEMSA assays. Prof. Easton designed the research and wrote the manuscript. My contributions were to aid in the development of analytical methods for detecting glycosylated CT-related species and CT-related species in the lysate using HPLC-fluorescence, to perform the incubation time and medium volume variation assays in DMS53, and with Dr. Onagi, to perform the experiments with TT cells. Due to the limited space in the manuscript, the results from the incubation time and medium volume variation experiments will be discussed in detail after the manuscript in this Chapter, and the experiments with TT cells are discussed in Chapter 6.

The analysis of DMS53 medium and lysate revealed the presence of CT, CT-G, CTGK and CTGKK and their relative concentrations. Of these, CT and CT-G were shown to be the major species in the medium, while CT predominated in the lysate. The hydroxylated intermediate HO-CT-G, generated in the PAM-mediated conversion of CT-G to CT, was identified for the first time using MS. The buildup of CT-G and CT indicates that PAM processing is the limiting step in the post-translational CT biosynthetic pathway. Specifically, the lack of HO-CT-G in the HPLC chromatogram indicates that the first subunit of PAM (peptidylglycine α-hydroxylating monooxygenase (PHM), responsible for the formation of HO-CT-G) is the product-limiting component of PAM. Glycosylated

forms of CT and its precursors were identified by HPLC and characterised using LCMS. It was found that they were present in approximately equal amounts to the non-glycosylated species in the medium, but at much lower concentrations in the lysate. This suggested a bypass mechanism for the maintenance of cellular CT, where CT is selectively retained in the cell and excess CT precursor is shuttled towards the glycosylation pathway for subsequent secretion.

The effects of inhibitors of the biosynthetic enzymes supported this hypothesis, as a PAM inhibitor had moderate effect on the CT and gCT concentrations in the medium, but little effect in the lysate. CPE inhibition did not decrease CT concentration at all. A decrease in the amidated to glycine-extended CT ratio was observed with increased growth medium volume (and thus, endogenous CT dilution), suggesting a response in CT production to decreased extracellular CT occurred. Together, these studies suggest that complex interplay between regulatory mechanisms occurs to regulate CT production, and that understanding these mechanisms is required to effectively perturb CT biosynthesis. The following pages are the copied manuscript:

Detection of Biosynthetic Precursors, Discovery of Glycosylated Forms, and Homeostasis of Calcitonin in Human Cancer Cells

Feihua Cao, Allan B. Gamble, Hideki Onagi, Joanna Howes, James E. Hennessy, Chen Gu, Jeremy A. M. Morgan, and Christopher J. Easton*

Research School of Chemistry, Australian National University, Canberra, ACT 2601, Australia

Ⓢ *Supporting Information*

ABSTRACT: The peptide hormone calcitonin is intimately connected with human cancer development and proliferation. Its biosynthesis is reasoned to proceed via glycine-, α-hydroxyglycine-, glycyllysine-, and glycyllysyllysine-extended precursors; however, as a result of the limitations of current analytical methods, until now, there has been no procedure capable of detecting these individual species in cell or tissue samples. Therefore, their presence and dynamics in cancer had not been established. Here, we report the first methodology for the separation, detection, and quantification of calcitonin and each of its precursors in human cancer cells. We also report the discovery and characterization of *O*-glycosylated calcitonin and its analogous biosynthetic precursors. Through direct and simultaneous analysis of the glycosylated and nonglycosylated species, we interrogate the hormone biosynthesis. This shows that the cellular calcitonin level is maintained to mitigate effects of biosynthetic enzyme inhibitors that substantially change the proportions of calcitonin-related species released into the culture medium.
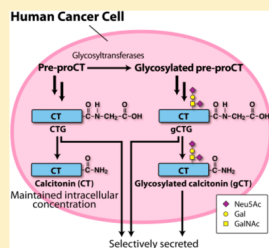
Calcitonin (CT), which normally functions to regulate physiological calcium levels,[1] is closely associated with various forms of human cancer. It is used as a marker for medullary thyroid carcinoma,[2−4] and elevated levels are seen with lung, pancreatic, and other tumors.[5−8] It has also been correlated with cancer cell proliferation and tumor growth, as well as disease recurrence following medical treatment.[9−13] Given the pathological relevance of CT, an improved understanding of its biological chemistry and a connection with disease progression are of considerable interest.[14,15]

The biosynthesis of CT is thought to occur as shown in Figure 1a, proposed based on transcribed nucleotide sequence analysis for preprocalcitonin (prepro-CT)[16] and by analogy with the formation of other amidated peptide hormones from their corresponding prohormones.[17] However, until now, none of the glycine-, α-hydroxyglycine-, glycyllysine-, and glycyllysyllysine-extended peptides (CTG, HO-CTG, CTGK, and CTGKK), which are the proposed precursors of CT, has been directly detected in cells. Analyses with immunoassays have detected only CT, or they have been incapable of distinguishing the individual precursors from CT and each other, because of their very similar overall chemical and physical characteristics.[18,19] Peptide hormone immunoassays are also subject to interference from other species.[20−22]

Therefore, it has not been possible to interrogate CT biosynthesis, examine the effects of inhibitors of the biosynthetic enzymes, peptidylglycine α-amidating monooxygenase (PAM), and carboxypeptidase E (CPE), and investigate the relationship between increased CT levels and carcinogenesis and metastasis. It has previously been reported that CPE is upregulated in many cancer cell lines and tumor tissues, and directly implicated in their tumorogenesis.[23−25] Potent PAM inhibitors including *E*-4-phenyl-3-butenoic acid (PBA, Figure 2) are also known to inhibit growth of some cancer cell types,[26−28] while other cell lines display a curious resistance to high concentrations of PBA and other very effective inhibitors of PAM, even though they are readily taken up by the cells.[29]

Here, we present the development of analytical methods that enable close analysis of the biosynthetic behavior of CT. For the first time, they allow the separation, detection, and quantification of CT, HO-CTG, CTG, CTGK, and CTGKK, produced by human cancer cells. Application of the methods directly establishes the biosynthetic relationships between these species, and the effects of PAM and CPE inhibitors. Through this study, we also discovered *O*-glycosylated calcitonin (gCT) and its parallel biosynthetic precursors gCTG, gCTGK, and gCTGKK (Figure 1). In addition, we developed procedures for direct analyses of the levels of the glycosylated and non-glycosylated species in both the culture medium and within the corresponding cells, requiring little or no sample pretreatment. These show that the cellular level and proportion of fully processed nonglycosylated CT is largely unresponsive to PAM and CPE inhibitors, even though they change the ratios of CT-related species secreted from the cells.
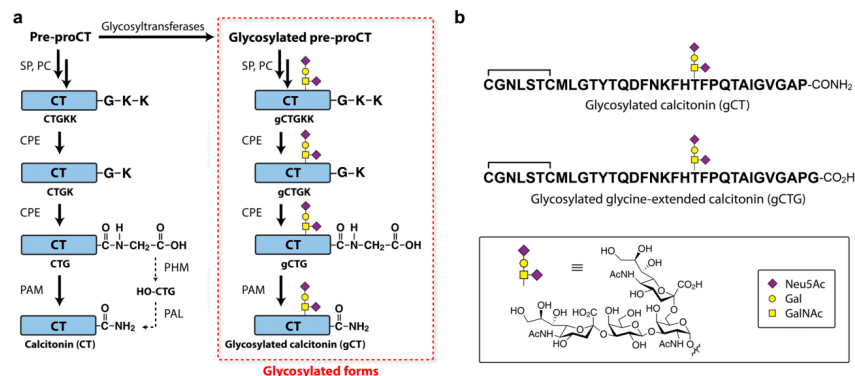
Figure 1. (a) Calcitonin (CT) biosynthesis pathway (shown on left) and parallel biosynthesis of *O*-glycosylated calcitonin (gCT) (shown on right) discovered during the course of this work. (b) Structures of gCT and the glycine-extended form (gCTG). [Legend: SP, signal peptidase; PC, prohormone convertase; CPE, carboxypeptidase E; PAM, peptidylglycine α-amidating monooxygenase; PHM, peptidylglycine α-hydroxylating monooxygenase; and PAL, peptidylamidoglycolate lyase.]
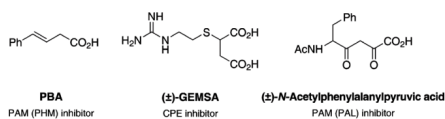
Figure 2. Enzyme inhibitors used in this study.

■ EXPERIMENTAL SECTION

General. The DMS53 human small cell lung cancer cell line was obtained from the American Type Culture Collection (Manassas, VA, USA). Cells were cultured in Gibco RPMI 1640 medium supplemented with 10% fetal bovine serum and 1% penicillin-streptomycin (10,000 U mL^{-1}), incubated under 5% CO$_2$ in air, at 37 °C. They were counted using a Bio-Rad TC20 automated cell counter with Trypan Blue stain.

Analysis for CT, CTG, CTGK, and CTGKK. Samples of CT, CTG, CTGK, and CTGKK were purchased from GL Biochem (Shanghai, China) and used to develop the analytical method that is illustrated in Figure 3. The method employs a Waters Alliance 2695 separation module fitted with a large volume sample loop and is fully automated using Waters Empower 3 software. The analyte is injected onto an online solid-phase extraction cartridge column (Waters Oasis HLB, 25 μm, 2.1 ×
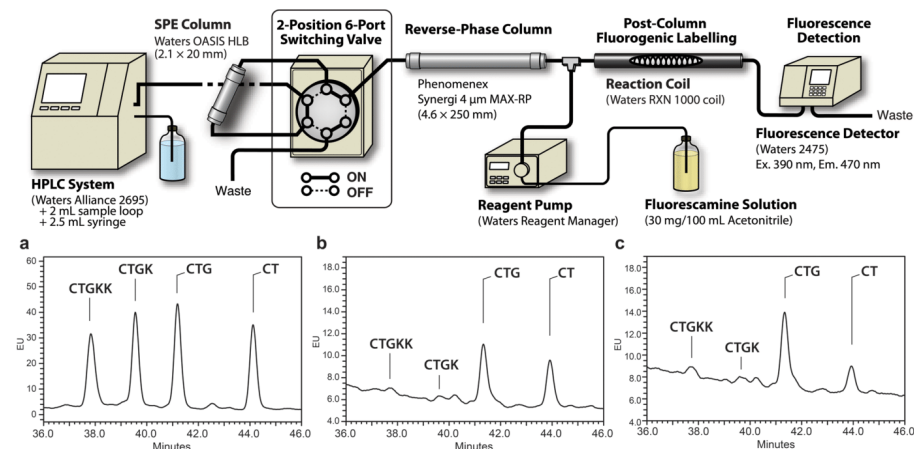
Figure 3. HPLC system overview and traces: (a) of calcitonin (CT) and precursor standards, (b) of culture medium from incubation of DMS53 cells without PBA, and (c) of medium from incubation of the cells with 400 μM PBA.

20 mm) maintained at 40 °C, which is then flushed with water at 3 mL min^{-1} for 4 min and 20% MeCN in buffer for 1 min; before the flow rate is reduced to 1.2 mL min^{-1}, the two-position, six-port valve is switched to divert the flow from waste to a reverse-phase column (Phenomenex Synergi MAX-RP, 4 μm, 4.6 × 250 mm) also maintained at 40 °C, and the mobile phase is adjusted with a solvent gradient over 35 min to 30% MeCN in buffer. Buffer refers to 2.5% Waters AccQ.Tag eluent A in water. Material eluting from the reverse-phase column is mixed with a solution of fluorescamine (Sigma–Aldrich, 30 mg) in acetonitrile (100 mL) delivered at 0.2 mL min^{-1} by a Waters Reagent Manager, before passing through a Waters RXN 1000 reaction coil maintained at 25 °C, then detection with a Waters 2475 fluorescence detector (excitation 390 nm, emission 470 nm).

DMS53 cell-culture medium was analyzed directly after centrifugation at 4 °C and 10 000 g for 5 min. In addition to fluorescence detection, samples of CT, CTG, CTGK, and CTGKK produced by the cells were isolated by manually collecting fractions eluting from the reverse-phase column without treatment with fluorescamine. The separated fractions were then concentrated and desalted, by loading onto a solid-phase extraction cartridge column (Waters Oasis HLB), followed by elution with 50% aqueous acetonitrile. The isolated samples were analyzed using electrospray ionization–mass spectrometry (ESI-MS).

Analysis for HO-CTG. PAM extracted from DMS53 cells[29] was used to prepare HO-CTG from CTG, in order to develop the analytical method. A mixture of CTG (0.1 mg) and PAM solution (5 μL) in MES buffer (100 μL, 150 mM, pH 5.8) containing 1.25 mM ascorbic acid, 10 μM copper sulfate, 0.2 mg mL^{-1} bovine liver catalase, 1% ethanol, and 1% dimethylsulfoxide (DMSO) was incubated at 37 °C for 2 h, before being filtered using an Amicon Ultra-0.5 mL centrifugal filter fitted with an Ultracel-3 membrane (Merck Millipore), at 12 000 g for 30 min. HPLC of the filtrate was used to isolate HO-CTG.

The method used for the analysis of CT, CTG, CTGK, and CTGKK in a cell-culture medium was also used for analysis for HO-CTG, except that tandem separation columns were employed (column 1: YMC ODS-AQ, 3 μm, 4.6 × 100 mm; column 2: Phenomenex Phenosphere SCX, 5 μm, 4.6 × 250 mm) (see Figure S1 in the Supporting Information), and the solvent gradient was introduced over 95 min instead of 35 min. A sample of HO-CTG produced by the cells was isolated, by manually collecting fractions eluting from the separation columns before treatment with fluorescamine, and was characterized using ESI-MS.

Identification and Characterization of gCT, gCTG, gCTGK, and gCTGKK. Samples of the compounds corresponding to two unidentified peaks in HPLC traces from analyses of DMS53 cell-culture medium were isolated using the protocol described above for analysis for HO-CTG, but with the solvent gradient introduced over 65 min instead of 95 min, and without fluorescent derivatization. The isolation was performed using 120 mL of medium from cells grown to 50%–90% confluency, after it had been concentrated by lyophilization, reconstituted in Milli-Q water to 10% of its original volume and centrifuged at RT and 10 000 g for 5 min.

Each of the isolated compounds was analyzed by MS using an Agilent 6530 Accurate-Mass Q-TOF LC/MS system, treated systematically with deglycosylation enzymes using the CarboR-elease Kit from QA-Bio (Palm Desert, CA, USA), as per the manufacturer's instructions, treated with trypsin in Tris-HCl buffer (100 mM, pH 7.8) at 37 °C for 6 h, and analyzed using electron transfer dissociation–tandem mass spectrometry (ETD-MS/MS). ETD-MS/MS data were matched using the Mascot program (Matrix Sciences). The results of these analyses, detailed below, established the species to be glycosylated CT and CTG (gCT and gCTG).

Direct MS analysis (LC-MS/MS-MRM) of the culture medium was used to confirm the presence of glycosylated CTGK and CTGKK (gCTGK and gCTGKK). gCTGK was identified on the basis of analyzing for the parent molecular ions, e.g., at calculated m/z 1138.2584 ([M+4H]$^{4+}$), as well as daughter ions at m/z 70.0107, 86.1058, 86.5681, and 136.0684. The daughter ions were expected based on the structure as well as the observation of identical fragmentations with CTGK. Similarly, gCTGKK was identified on the basis of analyzing for the parent molecular ions, e.g., at calculated m/z 936.4273 ([M+5H]$^{5+}$), as well as daughter ions at m/z 70.0107, 86.1058, 86.5681, and 129.1146. Again, the daughter ions were expected on the basis of the structure and the observation of identical fragmentations with CTGKK.

Analysis for CT, CTG, gCT, and gCTG in Cell Lysate and Culture Medium in the Presence and Absence of PBA and GEMSA. Cells were grown to confluency and then lifted with trypsin-EDTA (0.05%), before being suspended in RPMI 1640 medium supplemented with 10% fetal bovine serum and 1% penicillin–streptomycin (10 000 U mL^{-1}), and counted. This suspension was used to initiate subcultures with ~10^6 cells mL^{-1} in 10 mL of the medium in 75 cm^2 flasks. To examine the effect of PBA, these subcultures were prepared in quadruplicate, then incubated for 72 h to reach confluency (~25 × 10^6 cells per flask). The medium in each flask was then replaced, in two with the standard medium (10 mL) containing 0.1% DMSO as the control, and in the other two with a medium containing PBA (Sigma–Aldrich, 400 μM) added as a solution in the DMSO, and the flasks were incubated for 48 h. The cell-culture medium was then collected, and centrifuged at 4 °C and 10 000 g for 5 min, before being analyzed by HPLC. For analysis of the cell lysate, cells were trypsinized from the culture flask, pelleted by centrifugation at 2500 g for 5 min, washed with DPBS, and re-pelleted, before being re-suspended in 400 μL of the medium. The suspension was snap-frozen in liquid nitrogen then quickly thawed in hot water for 7 min. Lysates prepared in this manner were filtered using an Amicon Ultra-0.5 mL centrifugal filter fitted with an Ultracel-50 membrane (Merck Millipore) that had been deactivated by presoaking in 50% fetal bovine serum for 48 h. Filtration was carried out at 12 000 g for 30 min. The membrane was washed with additional medium (3 × 200 μL) and the combined filtrates were analyzed by HPLC. The same procedure was used to examine the effect of GEMSA (Santa Cruz Biotechnology, Inc., 100 μM) except that DMSO was not used. A similar protocol was also used to examine the effect of incubation time and volume of medium used, except that, for the final cultures, either 10 or 30 mL of fresh medium was used, and incubation was carried out for either 24 or 72 h.

■ RESULTS

Separation, Detection, and Quantification of CT and Biosynthetic Precursors. The DMS53 small cell lung cancer cell line was chosen for use in this investigation, because (i) it was established from an untreated biopsy, (ii) it shows excellent correlation in hormone production between cell cultures and in

vivo transplants, and (iii) it exhibits unusually stable hormone production characteristics and high expression of the CT-producing gene.[9,30] The protocol developed for the separation, detection, and quantification of CT, CTG, CTGK, and CTGKK, in a cell-culture medium (Figure 3) involves direct analysis of the medium through HPLC, using online solid-phase extraction to preclean and preconcentrate the analytes, before their passage onto a reverse-phase column, with online post-column fluorogenic derivatization to detect the separated species and determine the amounts present. The solid-phase extraction enables the direct injection of up to 10 mL of complex culture medium, without any pretreatment. The retention times of CT, CTG, CTGK, and CTGKK were determined using authentic commercial samples of the peptides (Figure 3a), which were also used to measure calibration curves and determine that all four compounds show very similar fluorescence detection response ratios. The detector response of each peptide was found to be due to reaction of the N-terminal primary amino group with fluorescamine. Side-chain amino groups of lysine residues present in peptides do not generate a measurable response under the assay conditions. This was established by analysis of free and N-acetylated peptides, both with and without lysine residues, and is attributable to the lysine amines being more extensively protonated and, therefore, several orders of magnitude less reactive. The method was shown to provide reliable quantification with a lower limit of 1 ng mL^{-1} for analysis of 1 mL of medium. Even greater sensitivity is achieved with larger injection volumes, by concentration of the medium prior to injection, and/or by detection using MS in place of fluorescent derivatization.

A representative chromatogram of 1 mL of medium sampled after 48 h from ∼10 × 10^6 DMS53 cells cultured in 10 mL is shown in Figure 3b. The quality of the chromatogram is remarkably good given such low concentrations of the analytes in the complex culture mixture. CT, CTG, CTGK, and CTGKK were all detected, and the identity of each of these species was confirmed by collecting fractions eluting from the separation column, then analyzing them without fluorescent labeling using ESI-MS (see Figures S2−S5 in the Supporting Information). CT and CTG were also identified by direct HPLC-MS analysis of the medium. The concentrations of the individual species CT, CTG, CTGK, and CTGKK in the medium were measured through HPLC with fluorescence detection and determined to be ∼10, 13, 1, and 1 ng mL^{-1}, respectively, under these conditions.

Having separately detected CT, CTG, CTGK, and CTGKK, we then probed their biosynthetic relationships using inhibitors of the enzymes that are understood to catalyze their interconversion. As would be anticipated, culturing the DMS53 cells in the presence of the PAM inhibitor PBA (400 μM) resulted in a decrease in the CT to CTG ratio in the medium, from 1:1.3 to 1:3 (Figure 3c). Use of the CPE inhibitor GEMSA[23] (Figure 2) (100 μM) increased the CTGK and CTGKK concentrations, and decreased that of CTG, as is discussed in more detail below.

PAM is a two-component enzyme comprising peptidylglycine α-hydroxylating monooxygenase (PHM), which catalyzes hydroxylation of glycine-extended peptide hormone precursors, and peptidylamidoglycolate lyase (PAL), which facilitates lysis of the hydroxylated materials, to give the physiologically active, amidated peptide hormones (Figure 4). The PAM inhibitor PBA, referred to above, interacts with PHM. The procedures
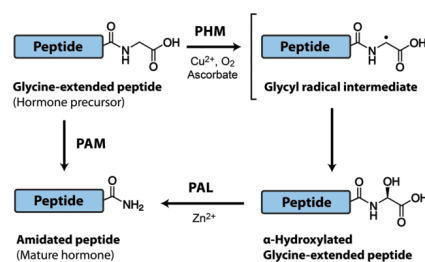

Figure 4. Production of amidated peptides from glycine-extended precursors, catalyzed by peptidylglycine α-amidating monooxygenase (PAM). [Legend: PHM, peptidylglycine α-hydroxylating monooxygenase; PAL, peptidylamidoglycolate lyase.]

used to detect CT, CTG, CTGK, and CTGKK were adapted to also analyze for the corresponding hydroxylated glycine-extended calcitonin (HO-CTG) in the cell-culture medium. Initially, an authentic sample of HO-CTG was prepared by treatment of CTG with isolated PAM,[29] purified through HPLC and analyzed by MS. This material was then utilized to develop the analytical method, which mainly involved introduction of an additional online ion-exchange column to the protocol used for CT, CTG, CTGK, and CTGKK, in a similar manner to two-dimensional (2D) liquid chromatography, for adequate resolution of the components in the medium (Figure S1 in the Supporting Information). Analysis of the medium sampled from cells cultured in the presence or absence of the PAL inhibitor N-acetylphenylalanylpyruvate[31] (up to 2 mM) (Figure 2), which would be expected to increase the amount of HO-CTG, then established that, in both cases, its concentration was below the fluorescence detection limit of <0.1 ng mL^{-1} (see Figure S6 in the Supporting Information). Even so, blind fractionation of medium by HPLC provided a sample that was unambiguously identified using ESI-MS (Figure S7 in the Supporting Information).

Identification and Characterization of gCT and gCTG. HPLC analyses of DMS53 cell-culture medium indicated the presence of two unidentified major components. Using a protocol adapted from the analysis for HO-CTG resulted in improved resolution of these species, marked with asterisks in Figure 5a. The addition of PBA changed their ratio, as it did with CT and CTG (Figure 5b), suggesting them to also be an amidated peptide and its biosynthetically related, glycine-extended precursor. HPLC enabled isolation of pure samples for structure determination.

MS analysis of the separated materials (see Figures S8 and S9 in the Supporting Information) showed ions with m/z 1092.2 and 1456.0 in one case, and 1106.7 and 1475.3 in the other, corresponding to [M+4H]$^{4+}$ and [M+3H]$^{3+}$ ions of species with molecular weights of 4365 and 4423 Da, respectively. The molecular weight difference of 58 Da confirmed the relationship between the two species of amidated peptide and its glycine-extended precursor. MS/MS analysis performed on the parent ions (see Figures S10 and S11 in the Supporting Information) provided the first indication that these species are the glycosylated derivatives of CT and CTG: gCT and gCTG. This was corroborated by enzymatic deglycosylation and MS of the product peptides, together with considerations of biosynthetic pathways. In particular, treatment with PNGase
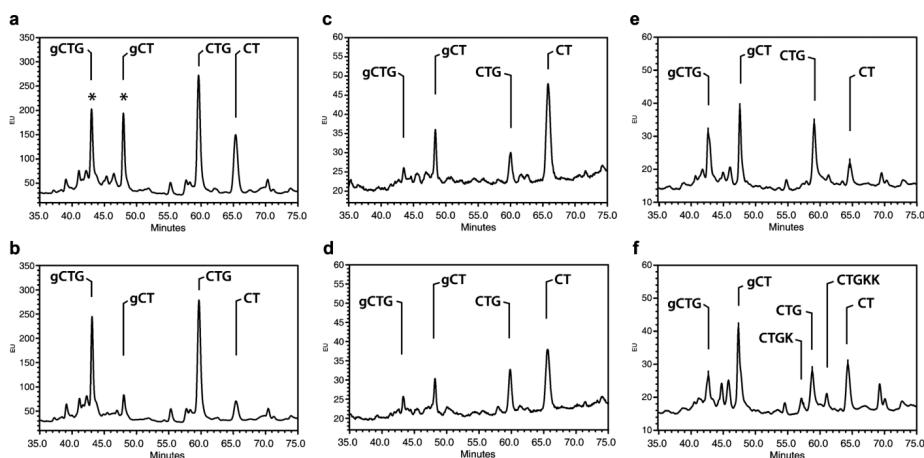
Article

Figure 5. HPLC traces of culture medium and cell lysate from incubation of DMS53 cells: (a) medium (5 mL) without PBA, (b) medium (5 mL) with 400 μM PBA, (c) lysate (entire sample) without PBA, (d) lysate (entire sample) with 400 μM PBA, (e) medium (1 mL) without GEMSA, and (f) medium (1 mL) with 100 μM GEMSA. (Retention times of CT, CTG, CTGK, and CTGKK were recalibrated with standards under these conditions.)

Table 1. Proportions of Calcitonin (CT), Glycine-Extended Calcitonin (CTG) and the Glycosylated Forms (gCT and gCTG) in a Cell-Culture Medium and Lysate

	entry	CT (%)[a,b]	CTG (%)[a,b]	gCT (%)[a,b]	gCTG (%)[a,b]	glycosylated (%)[a,c]	amidated (%)[a,d]
	Experiment 1: Effect of PBA (400 μM) with DMS53 Cells Grown in 10 mL of Medium for 48 h						
(i)	medium (− PBA)	25	38	18	19	37	43
(ii)	medium (+ PBA)	11	51	8	30	38	19
(iii)	lysate (− PBA)	63	16	16	5	21	79
(iv)	lysate (+ PBA)	53	28	13	6	19	66
	Experiment 2: Effect of GEMSA (100 μM) with DMS53 Cells Grown in 10 mL of Medium for 48 h						
(v)	medium (− GEMSA)	22	36	23	19	42	45
(vi)	medium (+ GEMSA)	32	25	31	11	42	63
(vii)	lysate (− GEMSA)	69	9	17	6	23	86
(viii)	lysate (+ GEMSA)	72	7	16	6	22	88
	Experiment 3: Effects of Volume of Culture Medium and Incubation Time with DMS53 Cells						
(ix)	24 h, 10 mL medium	31	30	29	10	39	60
(x)	24 h, 30 mL medium	24	41	23	12	35	47
(xi)	72 h, 10 mL medium	18	25	29	28	57	47
(xii)	72 h, 30 mL medium	14	31	16	39	55	30

[a]Average of incubations carried out at least in duplicate and HPLC analyses performed at least in duplicate. [b]Proportion as a percentage of the total quantities of CT, CTG, gCT, and gCTG. [c]Proportion of gCT and gCTG as a percentage of the total quantities of CT, CTG, gCT, and gCTG. [d]Proportion of CT and gCT as a percentage of the total quantities of CT, CTG, and gCTG.

F, sialidase, β-galactosidase, glucosaminidase, and O-glycosidase, to remove all N- and O-linked oligosaccharides, afforded product peptides that were shown by MS to be identical to CT and CTG. Alone, PNGase F failed to catalyze the deglycosylation, when it would have removed any N-linked glycan, while O-glycosidase and sialidase did so, in a stepwise manner, showing that the glycopeptides have the disialylated core 1 O-glycan, NeuAc(α2−3)Gal(β1−3)[NeuAc(α2−6)]-GalNAc.[32,33]

Having identified the tetrasaccharide, enzyme-catalyzed peptide digestion and ETD-MS/MS were then employed to ascertain the site of peptide glycosylation. Treatment of each

species with trypsin gave products identified through LC/MS analysis as nonglycosylated CT(1−18) and glycosylated CT(19−32), and nonglycosylated CTG(1−18) and glycosylated CTG(19−33). This corresponds to peptide cleavage between Lys18 and Phe19. CT and CTG each have one Ser and five Thr residues that are possible O-glycosylation sites but the retention of the glycan on the C-terminal fragments limits these to either Thr21 or Thr25. Finally, ETD-MS/MS was used in each case to determine Thr21 as the O-glycosylation site and confirm the identities of both gCT and gCTG. Data matched using the Mascot program showed, for example, peaks for the series of c ions. In particular, for both gCT and gCTG, peaks at

m/z 1147.0 and 1671.2 correspond to c_{20}^{++} and c_{21}^{++}, with the difference being the mass of Thr plus the glycan, whereas peaks at m/z 1857.3 and 1907.8 correspond to c_{24}^{++} and c_{25}^{++}, differing only by the mass of Thr. The complete analysis was carried out separately on gCT and gCTG, and their structures were therefore independently determined to be those illustrated in Figure 1b.

Having identified gCT and gCTG, by analogy with the biosynthesis of CT from CTG, CTGK, and CTGKK, it seemed logical that gCT and gCTG would be derived via a parallel route from the corresponding glycosylated lysine-extended precursors: gCTGK and gCTGKK (Figure 1). MS analysis (LC-MS/MS-MRM) of a cell-culture medium confirmed the presence of both species, in concentrations much lower than those of gCT and gCTG (see the Supporting Information for details).

Direct Comparative Analyses of CT, CTG, gCT, and gCTG, and Homeostasis of Cellular Calcitonin Levels. As described above, among CT, gCT and their biosynthetic precursors, CT, gCT, CTG, and gCTG are predominant in the cell-culture medium. Therefore, we monitored the relative proportions of these four compounds in the medium under a variety of conditions. The HPLC method used in these analyses, and particularly the online solid-phase extraction process, is sufficiently robust that it was also possible to monitor the intracellular proportions of these species by direct injection of the entire lysate of ~30 million cells, following simple filtration to remove cellular debris. The results of typical duplicate experiments are illustrated in Figure 5, and the relative proportions of CT, CTG, gCT, and gCTG are summarized in Table 1.

The concentrations of CT, CTG, gCT, and gCTG are dependent on several factors, such as the number of cells, the passage of the cells used for inoculation, the volume of the culture medium, and the time of incubation. Within each experiment, a common inoculate of cells was used but, because of practical limitations, it was necessary to use different inoculates for Experiments 1 and 2 in Table 1. This accounts for the differences between the outcomes of the corresponding controls (see entries (i) and (v), and entries (iii) and (vii) in the table). HPLC-MS analysis showed that (^{2}H$_{10}$-Leu)$_2$-CTG was not converted to (^{2}H$_{10}$-Leu)$_2$-CT in the medium, either during or after incubation with cells. When both (^{2}H$_{10}$-Leu)$_2$-CTG and (^{2}H$_{10}$-Leu)$_2$-CT were added, they remained in the same ratio. These experiments show that there is no turnover of CT and CTG in the medium, so the results in Table 1 correspond to materials produced in the cells then released. Further control experiments established that there was no change in the proportions of CT, CTG, gCT, and gCTG in cells after they were harvested.

With reference to Table 1 and the proportions of CT, CTG, gCT, and gCTG, with cells cultured in the absence of any enzyme inhibitor, the intracellular species are ~20% glycosylated (gCT and gCTG) and ~80%−90% amidated or processed by PAM (CT and gCT), and CT is dominant (63 and 69%, entries (iii) and (vii) in the table). By comparison, in the corresponding culture media (entries (i) and (v) in the table), the amount glycosylated is approximately doubled (to ~40%) and the amount processed by PAM is halved (to ~45%). Neither PBA nor GEMSA affects the proportion of glycosylated species, which remains at ~20% in the cells (see entries (iv) and (viii) in the table) and ~40% in the medium (entries (ii) and (vi) in the table). PBA only reduces the

cellular proportion of CT from 63% to 53%, which is a small reduction for the high concentration of PAM inhibitor used (400 μM). The same concentration of PBA more than halves the fraction of CT in the medium, reducing its proportion from 25% to 11% (entries (i) and (ii) in the table). Maintenance of the cellular CT level is also seen with GEMSA (69% and 72%, entries (vii) and (viii) in the table). In the medium, GEMSA increases the proportion of CT by ~1.5-fold (entries (v) and (vi) in the table, from 22% to 32%). This increase is a consequence of the CPE inhibitor increasing the CTGK and CTGKK concentrations, and decreasing that of CTG (and gCTG), as would be predicted, but without a corresponding decrease in CT (Figures 5e and 5f). In all experiments with GEMSA, the concentration of CT in the medium was the same or higher than with the corresponding controls. When results from experiments with different incubation times and volumes of culture medium are compared (entries (ix)−(xii) in the table), the proportion of the amidated species in the medium varies from 60% to 30%. The proportion of the glycosylated species increases, from 35%−40% to 55%−60%, with time but is not significantly affected by the change in the volume of the medium.

■ DISCUSSION

Despite the close association that links CT with cancer, before now, no method had been reported to separate, detect, and quantify CT and the peptides understood to be its biosynthetic precursors, CTG, CTGK, and CTGKK. The HPLC analysis illustrated in Figure 3 provided the original tool for this purpose and established that all four species are present in DMS53 cell-culture medium, this being the first direct observation of CTG, CTGK, or CTGKK in a cell or tissue sample. Adaptation of the analytical method also enabled the detection of HO-CTG, the intermediate between CTG and CT, using HPLC-MS. There has been no previous report of the detection of HO-CTG produced by cells and, indeed, the only other account of any hydroxylated, glycine-extended precursor of any amidated peptide in a biological specimen was the finding of the hydroxylated precursor of joining peptide in pituitary lysates from mice.[34]

The discovery of the O-glycosylated gCT, gCTG, gCTGK, and gCTGKK was unexpected. Not only were these glycopeptides previously unknown, as a group or individually, a much earlier investigation looking for the production of any N- or O-linked glycosylated form of CT by DMS53 cells yielded negative results.[35] The core 1 O-glycan of gCT has been found attached to many other glycopeptides produced by both normal and cancer cells, including the gonadotropin hormone family,[36] MUC-1,[37] and von Willebrand factor,[38] but it has not been associated before now with CT. The production of gCT, gCTG, gCTGK, and gCTGKK most logically proceeds through a biosynthetic pathway parallel to that for production of CT from CTG, CTGK, and CTGKK, that branches from the known pathway through glycosylation of prepro-CT in the Golgi apparatus, before CTGKK is excised (Figure 1a). We have used our analytical methods (HPLC fractionation; LC/MS - MRM) to discover identically glycosylated gCT and gCTG, in addition to CT and its precursors, produced by TT cells, so it is apparent that this glycosylation also occurs with the human medullary thyroid cancer cell line.

The studies summarized in Table 1 show selective intracellular retention of CT, compared to its biosynthetic precursor CTG, and the corresponding glycosylated forms gCT and

gCTG. They also show selective maintenance of CT levels in the cells in response to the PAM and CPE inhibitors, PBA and GEMSA, which, at the same time, bring about relatively large variations in the proportions of CT and gCT that are released into the medium. The accumulation of CTG and gCTG demonstrates that catalytic turnover by PAM limits the production of CT and gCT. More specifically, it is the limiting activity of the PHM component of PAM, since there is no buildup of HO-CTG. The anomalous effect of the CPE inhibitor GEMSA, already discussed above, to reduce the concentration of CTG, as expected, but without a corresponding decrease in CT, further shows that catalytic turnover by PAM is not proportional to substrate concentration in a typical manner.

CONCLUSION

In summary, the protocols reported here constitute sophisticated and sensitive, yet straightforward methods, that enable direct analysis of CT and its biosynthetic processes in biological samples. We expect that the techniques will be generally applicable for screening inhibitors of the associated biosynthetic enzymes, as well as for analysis of other amidated peptide hormones. Already, we have developed closely analogous procedures to analyze for oxytocin (OT) and its precursors (OTG, OTGK, and OTGKK).

The identification and full characterization of gCT, gCTG, gCTGK, and gCTGKK provides the platform for further studies to understand the function of the glycosylation pathway for CT. Glycopeptides are generally recognized as playing important and various roles in cancer.[39,40] O-Glycans control cellular trafficking and the metabolism of hormones, in particular, through affecting their processing by prohormone convertase.[41−43] They are also known to regulate hormone serum levels, confer peptides with resistance to degradation, and direct them to cell surface receptors,[33,44] as well as affect the cellular passaging of PAM.[45] In any event, already the studies described above and summarized in Table 1 establish that CT is selectively retained in the cells, while larger fractions of CTG and the glycosylated species gCT and gCTG are released. It is clear that there is a complex interplay of regulatory processes that maintain the intracellular concentration of CT, even when cells are challenged with the PAM and CPE inhibitors, PBA and GEMSA. Understanding them will be key to delineating the correlation between CT and cancer, and a prerequisite to developing therapies that seek to regulate the production of CT or other amidated peptide hormones associated with disease.

ASSOCIATED CONTENT

Ⓢ Supporting Information

The Supporting Information is available free of charge on the ACS Publications website at DOI: 10.1021/acs.analchem.7b00457.

Supplementary mass spectra, the HPLC separation and detection method for HO-CTG, gCT, gCTG, CT, CTG, CTGK, and CTGKK and details of LC-MS/MS-MRM analysis for gCTGK and gCTGKK (PDF)

AUTHOR INFORMATION

Corresponding Author

*E-mail: Chris.Easton@anu.edu.au.

ORCID ●

Allan B. Gamble: 0000-0001-5440-8771

Hideki Onagi: 0000-0003-0085-7349

Christopher J. Easton: 0000-0002-2263-1204

Notes

The authors declare no competing financial interest.

REFERENCES

(1) Findlay, D. M.; Sexton, P. M.; Martin, T. J. In *Endocrinology: Adult & Pediatric*, 7th Edition; Jameson, J. L., De Groot, L. J., de Kretser, D. M., Giudice, L. C., Grossman, A. B., Melmed, S., Potts, J. T., Weir, G. C., Eds.; Elsevier: Philadelphia, PA, 2016; pp 1004−1017.

(2) Williams, G. A.; Hargis, G. K.; Galloway, W. B.; Henderson, W. J. *Exp. Biol. Med.* **1966**, *122*, 1273−1276.

(3) Trimboli, P.; Giovanella, L.; Crescenzi, A.; Romanelli, F.; Valabrega, S.; Spriano, G.; Cremonini, N.; Guglielmi, R.; Papini, E. *Head Neck* **2014**, *36*, 1216−1223.

(4) Jung, K. Y.; Kim, S. M.; Yoo, W. S.; Kim, B. W.; Lee, Y. S.; Kim, K. W.; Lee, K. E.; Jeong, J. J.; Nam, K. H.; Lee, S. H.; Hah, J. H.; Chung, W. Y.; Yi, K. H.; Park, D. J.; Youn, Y. K.; Sung, M. W.; Cho, B. Y.; Park, C. S.; Park, Y. J.; Chang, H. S. *Clin. Endocrinol.* **2016**, *84*, 587−597.

(5) Baylin, S. B.; Weisburger, W. R.; Eggleston, J. C.; Mendelsohn, G.; Beaven, M. A.; Abeloff, M. D.; Ettinger, D. S. *N. Engl. J. Med.* **1978**, *299*, 105−110.

(6) Schneider, R.; Waldmann, J.; Swaid, Z.; Ramaswamy, A.; Fendrich, V.; Bartsch, D. K.; Schlosser, K. *Pancreas* **2011**, *40*, 213−221.

(7) Kovacova, M.; Filkova, M.; Potocarova, M.; Kinova, S.; Pajvani, U. *Endocr. Pract.* **2014**, *20*, e140−e144.

(8) Nozieres, C.; Chardon, L.; Goichot, B.; Borson-Chazot, F.; Hervieu, V.; Chikh, K.; Lombard-Bohas, C.; Walter, T. *Eur. J. Endocrinol.* **2016**, *174*, 335−341.

(9) Cate, C. C.; Douple, E. B.; Andrews, K. M.; Pettengill, O. S.; Curphey, T. J.; Sorenson, G. D.; Maurer, L. H. *Cancer Res.* **1984**, *44*, 949−954.

(10) Chigurupati, S.; Kulkarni, T.; Thomas, S.; Shah, G. *Cancer Res.* **2005**, *65*, 8519−8529.

(11) Sabbisetti, V. S.; Chirugupati, S.; Thomas, S.; Vaidya, K. S.; Reardon, D.; Chiriva-Internati, M.; Iczkowski, K. A.; Shah, G. V. *Int. J. Cancer* **2005**, *117*, 551−560.

(12) Shah, G. V.; Thomas, S.; Muralidharan, A.; Liu, Y.; Hermonat, P. L.; Williams, J.; Chaudhary, J. *Endocr.-Relat. Cancer* **2008**, *15*, 953−964.

(13) Hadoux, J.; Pacini, F.; Tuttle, R. M.; Schlumberger, M. *Lancet Diabetes Endocrinol.* **2016**, *4*, 64−71.

(14) Lee, S. M.; Hay, D. L.; Pioszak, A. A. *J. Biol. Chem.* **2016**, *291*, 8686−8700.

(15) Opsahl, E. M.; Brauckhoff, M.; Schlichting, E.; Helset, K.; Svartberg, J.; Brauckhoff, K.; Maehle, L.; Engebretsen, L. F.; Sigstad, E.; Groholt, K. K.; Akslen, L. A.; Jorgensen, L. H.; Varhaug, J. E.; Bjoro, T. *Thyroid* **2016**, *26*, 1225−1238.

(16) Le Moullec, J. M.; Jullienne, A.; Chenais, J.; Lasmoles, F.; Guliana, J. M.; Milhaud, G.; Moukhtar, M. S. *FEBS Lett.* **1984**, *167*, 93−97.

(17) Douglass, J.; Civelli, O.; Herbert, E. *Annu. Rev. Biochem.* **1984**, *53*, 665−715.

(18) Kratzsch, J.; Petzold, A.; Raue, F.; Reinhardt, W.; Brocker-Preuss, M.; Gorges, R.; Mann, K.; Karges, W.; Morgenthaler, N.;

Luster, M.; Reiners, C.; Thiery, J.; Dralle, H.; Fuhrer, D. *Clin. Chem.* **2011**, *57*, 467−474.

(19) Alves, T. G.; Kasamatsu, T. S.; Yang, J. H.; Meneghetti, M. C. Z.; Mendes, A.; Kunii, I. S.; Lindsey, S. C.; Camacho, C. P.; Dias da Silva, M. R.; Maciel, R. M. B.; Vieira, J. G. H.; Martins, J. R. M. J. *J. Clin. Endocrinol. Metab.* **2016**, *101*, 653−658.

(20) Gulbahar, O.; Konca Degertekin, C.; Akturk, M.; Yalcin, M. M.; Kalan, I.; Atikeler, G. F.; Altinova, A. E.; Yetkin, I.; Arslan, M.; Toruner, F. *J. Clin. Endocrinol. Metab.* **2015**, *100*, 2147−2153.

(21) Schiettecatte, J.; Strasser, O.; Anckaert, E.; Smitz, J. *Clin. Biochem.* **2016**, *49*, 929−931.

(22) Kwon, H.; Kim, W. G.; Choi, Y. M.; Jang, E. K.; Jeon, M. J.; Song, D. E.; Baek, J. H.; Ryu, J. S.; Hong, S. J.; Kim, T. Y.; Kim, W. B.; Shong, Y. K. *Clin. Endocrinol.* **2015**, *82*, 598−603.

(23) Murthy, S. R. K.; Dupart, E.; Al-Sweel, N.; Chen, A.; Cawley, N. X.; Loh, Y. P. *Cancer Lett.* **2013**, *341*, 204−213.

(24) Liu, A.; Shao, C. H.; Jin, G.; Liu, R.; Hao, J.; Shao, Z.; Liu, Q. Y.; Hu, X. G. *Tumor Biol.* **2014**, *35*, 12459−12465.

(25) Huang, S. F.; Wu, H. D. I.; Chen, Y. T.; Murthy, S. R. K.; Chiu, Y. T.; Chang, Y.; Chang, I. C.; Yang, X. Y.; Loh, Y. P. *Tumor Biol.* **2016**, *37*, 9745−9753.

(26) Iwai, N.; Martinez, A.; Miller, M. J.; Vos, M.; Mulshine, J. L.; Treston, A. M. *Lung Cancer-J. Iaslc* **1999**, *23*, 209−222.

(27) Sunman, J. A.; Foster, M. S.; Folse, S. L.; May, S. W.; Matesic, D. F. *Mol. Carcinog.* **2004**, *41*, 231−246.

(28) Ali, A.; Burns, T. J.; Lucrezi, J. D.; May, S. W.; Green, G. R.; Matesic, D. F. *Invest. New Drugs* **2015**, *33*, 827−834.

(29) Cao, F. H.; Gamble, A. B.; Kim, H. K.; Onagi, H.; Gresser, M. J.; Kerr, J.; Easton, C. J. *MedChemComm* **2011**, *2*, 760−763.

(30) Sorenson, G. D.; Pettengill, O. S.; Brinck-Johnsen, T.; Cate, C. C.; Maurer, L. H. *Cancer* **1981**, *47*, 1289−1296.

(31) Mounier, C. E.; Shi, J.; Sirimanne, S. R.; Chen, B. H.; Moore, A. B.; GillWoznichak, M. M.; Ping, D. S.; May, S. W. *J. Biol. Chem.* **1997**, *272*, 5016−5023.

(32) Capon, C.; Laboisse, C. L.; Wieruszeski, J. M.; Maoret, J. J.; Augeron, C.; Fournet, B. *J. Biol. Chem.* **1992**, *267*, 19248−19257.

(33) Hang, H. C.; Bertozzi, C. R. *Bioorg. Med. Chem.* **2005**, *13*, 5021−5034.

(34) Yin, P.; Bousquet-Moore, D.; Annangudi, S. P.; Southey, B. R.; Mains, R. E.; Eipper, B. A.; Sweedler, J. V. *PLoS One* **2011**, *6*, e28679.

(35) Cate, C. C.; Pettengill, O. S.; Sorenson, G. D. *Cancer Res.* **1986**, *46*, 812−818.

(36) Harrd, K.; Damm, J. B. L.; Spruijt, M. P. N.; Bergwerff, A. A.; Kamerling, J. P.; Van Dedem, G. W. K.; Vliegenthart, J. F. G. *Eur. J. Biochem.* **1992**, *205*, 785−798.

(37) Lloyd, K. O.; Burchell, J.; Kudryashov, V.; Yin, B. W. T.; Taylor-Papadimitriou, J. *J. Biol. Chem.* **1996**, *271*, 33325−33334.

(38) van Schooten, C. J. M.; Denis, C. V.; Lisman, T.; Eikenboom, J. C. J.; Leebeek, F. W.; Goudemand, J.; Fressinaud, E.; van den Berg, H. M.; de Groot, P. G.; Lenting, P. J. *Blood* **2007**, *109*, 2430−2437.

(39) Chia, J.; Goh, G.; Bard, F. *Biochim. Biophys. Acta, Gen. Subj.* **2016**, *1860*, 1623−1629.

(40) Zeng, Q. H.; Zhao, R. X.; Chen, J. F.; Li, Y. N.; Li, X. D.; Liu, X. L.; Zhang, W. M.; Quan, C. S.; Wang, Y. S.; Zhai, Y. X.; Wang, J. W.; Youssef, M.; Cui, R. T.; Liang, J. Y.; Genovese, N.; Chow, L. T.; Li, Y. L.; Xu, Z. X. *Proc. Natl. Acad. Sci. U. S. A.* **2016**, *113*, 9333−9338.

(41) Gram Schjoldager, K. T.-B.; Vester-Christensen, M. B.; Goth, C. K.; Petersen, T. N.; Brunak, S.; Bennett, E. P.; Levery, S. B.; Clausen, H. *J. Biol. Chem.* **2011**, *286*, 40122−40132.

(42) Zhang, L. P.; Syed, Z. A.; van Dijk Hard, I.; Lim, J. M.; Wells, L.; Ten Hagen, K. G. *Proc. Natl. Acad. Sci. U. S. A.* **2014**, *111*, 7296−7301.

(43) Tagliabracci, V. S.; Engel, J. L.; Wiley, S. E.; Xiao, J. Y.; Gonzalez, D. J.; Nidumanda Appaiah, H.; Koller, A.; Nizet, V.; White, K. E.; Dixon, J. E. *Proc. Natl. Acad. Sci. U. S. A.* **2014**, *111*, 5520−5525.

(44) Ellies, L. G.; Ditto, D.; Levy, G. G.; Wahrenbrock, M.; Ginsburg, D.; Varki, A.; Le, D. T.; Marth, J. D. *Proc. Natl. Acad. Sci. U. S. A.* **2002**, *99*, 10042−10047.

(45) Vishwanatha, K. S.; Bäck, N.; Lam, T. T.; Mains, R. E.; Eipper, B. A. *J. Biol. Chem.* **2016**, *291*, 9835−9850.

Supporting Information

Detection of Biosynthetic Precursors, Discovery of Glycosylated Forms and Homeostasis of Calcitonin in Human Cancer Cells

Feihua Cao, Allan B. Gamble, Hideki Onagi, Joanna Howes, James E. Hennessy, Chen Gu, Jeremy A. M. Morgan and Christopher J. Easton*

Research School of Chemistry, Australian National University

Canberra, ACT 2601, Australia.

*email: Chris.Easton@anu.edu.au

ABSTRACT: The peptide hormone calcitonin is intimately connected with human cancer development and proliferation. Its biosynthesis is reasoned to proceed via glycine-, α-hydroxyglycine-, glycyllysine- and glycyllysyllysine-extended precursors though, as a result of limitations of current analytical methods, until now there has been no procedure capable of detecting these individual species in cell or tissue samples. Therefore their presence and dynamics in cancer had not been established. Here we report the first methodology for the separation, detection and quantification of calcitonin and each of these precursors in human cancer cells. We also report the discovery and characterization of O-glycosylated calcitonin and its analogous biosynthetic precursors. Through direct and simultaneous analysis of the glycosylated and non-glycosylated species, we interrogate the hormone biosynthesis, to observe that the cellular calcitonin level is maintained to mitigate effects of biosynthetic enzyme inhibitors that substantially change the proportions of calcitonin-related species released into the culture medium.
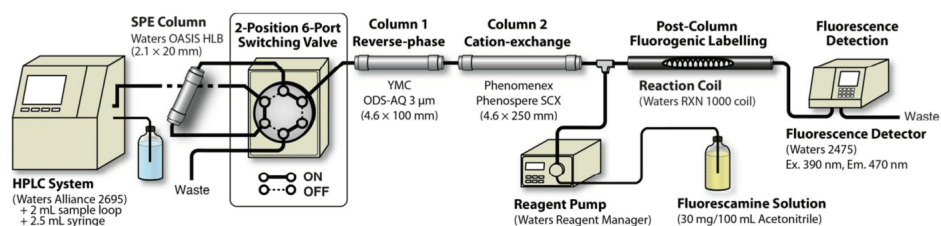
Figure S1. Hardware configuration of the HPLC separation and detection method for HO-CTG, gCT, gCTG, CT, CTG, CTGK and CTGKK.
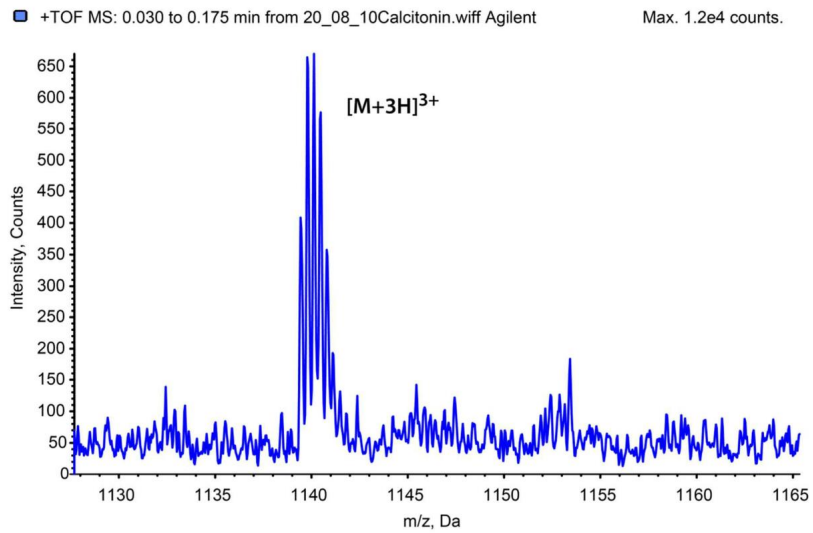
Figure S2. ESI-Mass spectrum of CT (mass 3418 Daltons) produced by DMS53 cells.
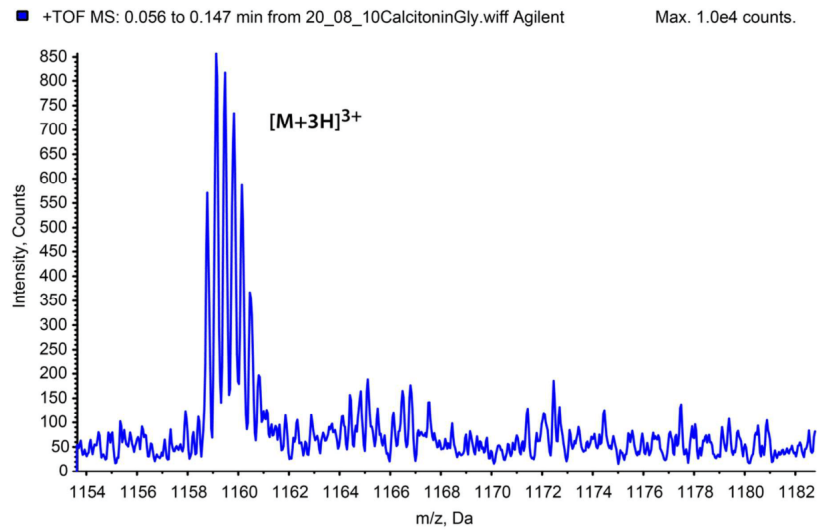
Figure S3. ESI-Mass spectrum of CTG (mass 3476 Daltons) produced by DMS53 cells.
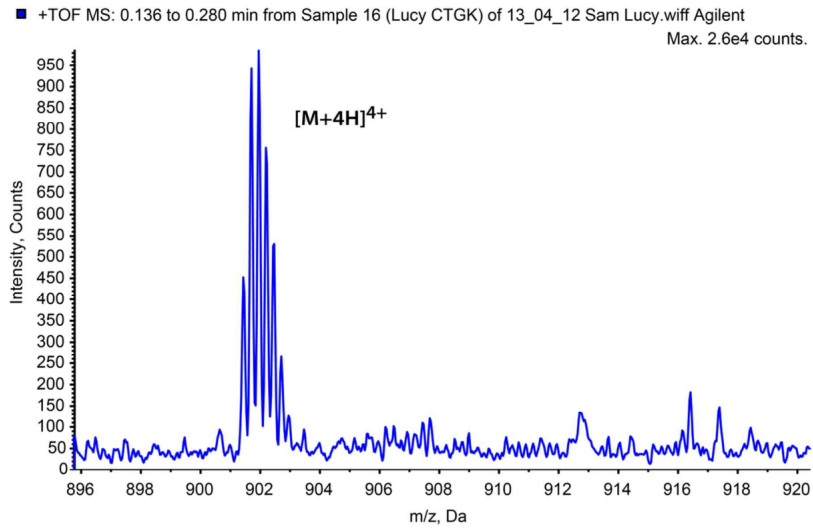
Figure S4. ESI-Mass spectrum of CTGK (mass 3604 Daltons) produced by DMS53 cells.
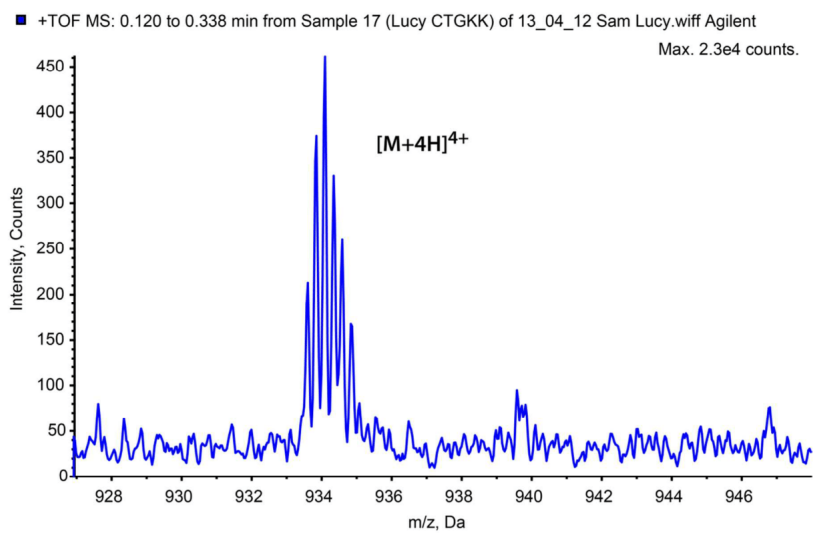
Figure S5. ESI-Mass spectrum of CTGKK (mass 3732 Daltons) produced by DMS53 cells.
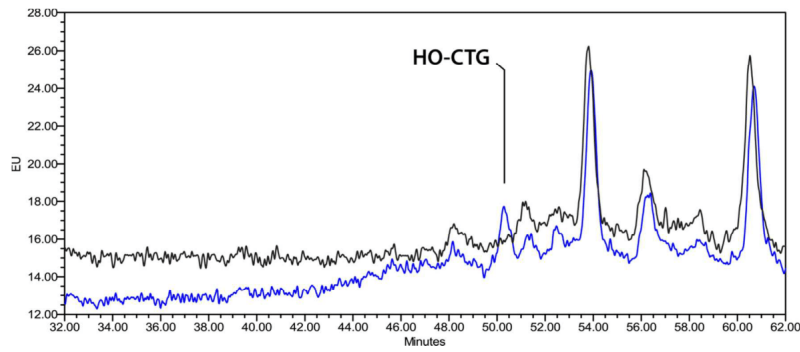
Figure S6. HPLC trace of DMS53 cell culture medium (black) overlaid with trace of medium to which HO-CTG standard has been added (blue).
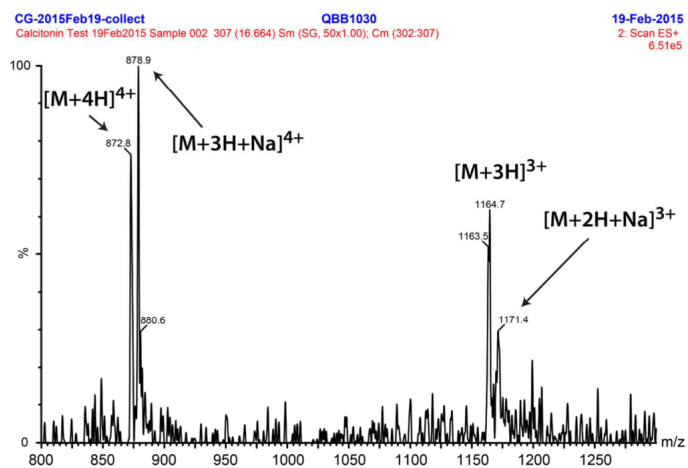
Figure S7. ESI mass spectrum (Waters Alliance 2695 separation module coupled to Waters TQD detector) of HO-CTG produced by DMS53 cells.
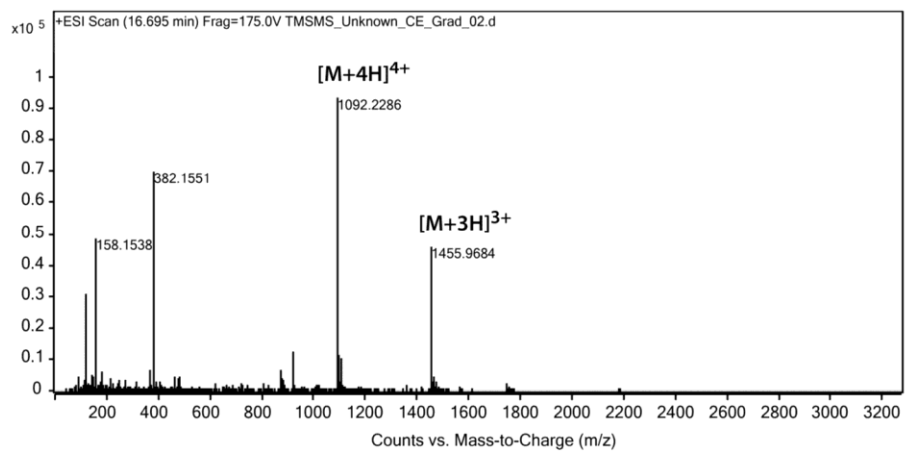
Figure S8. ESI mass spectrum (Agilent 6530 Accurate-Mass Q-TOF LC/MS) of gCT produced by DMS53 cells.
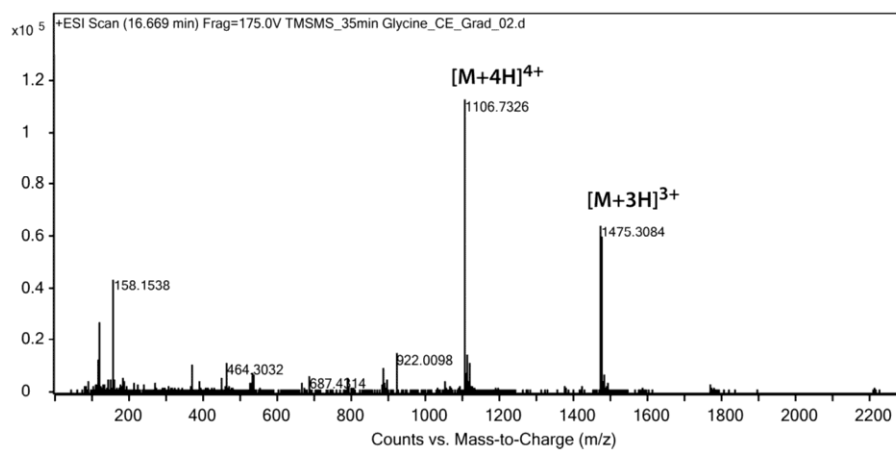
Figure S9. ESI mass spectrum (Agilent 6530 Accurate-Mass Q-TOF LC/MS) of gCTG produced by DMS53 cells.
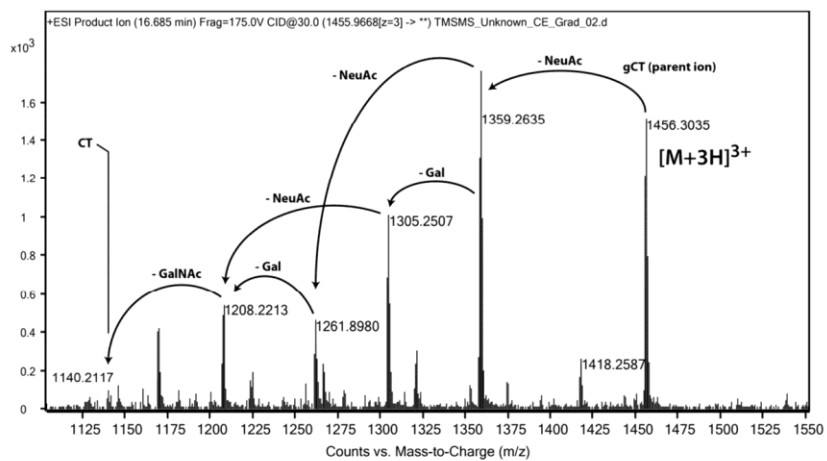
Figure S10. Q-TOF MS/MS spectrum (Agilent 6530 Accurate-Mass Q-TOF LC/MS) of gCT.
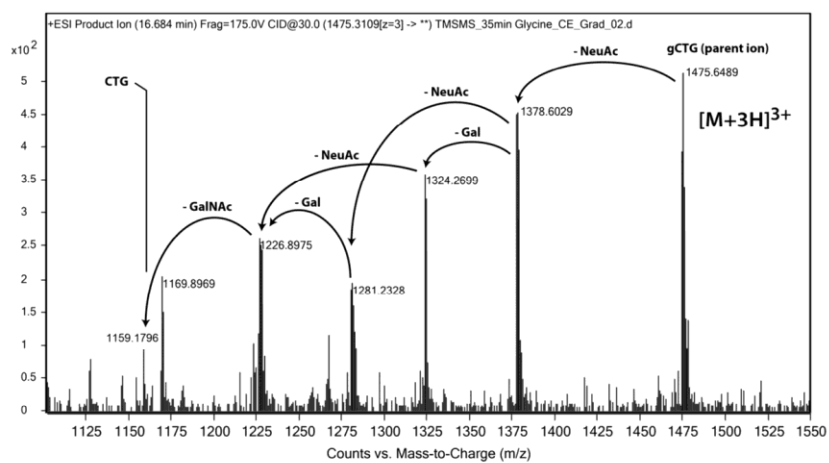
Figure S11. Q-TOF MS/MS spectrum (Agilent 6530 Accurate-Mass Q-TOF LC/MS) of gCTG.

LC-MS/MS MRM Analysis for gCTGK and gCTGKK

Analysis was performed using a Waters Alliance 2695 separation module coupled to a Waters TQD detector. HPLC Column: Waters Sunfire C18, 5 μm, 4.6 × 150 mm, heated at 30˚C. Flow: 0.7 mL/min (15:1 flow splitter). Eluent: acetonitrile/water 5/95 (0-1 min), acetonitrile/water 30/70 (1-30 min, linear), both eluents contain 0.1% formic acid.

gCTGK

Channel 1: Parent (m/z): 1138.2584, Daughter (m/z): 70.0107, Dwell (s): 0.025, Cone (V): 40, Collision (V): 80; Channel 2: Parent (m/z): 1138.2584, Daughter (m/z): 86.1058, Dwell (s): 0.025, Cone (V): 40, Collision (V): 78; Channel 3: Parent (m/z): 1138.2584, Daughter (m/z): 86.5681, Dwell (s): 0.025, Cone (V): 40, Collision (V): 80; Channel 4: Parent (m/z): 1138.2584, Daughter (m/z): 136.0684, Dwell (s): 0.025, Cone (V): 40, Collision (V): 80.

gCTGKK

Channel 1: Parent (m/z): 936.4273, Daughter (m/z): 70.0107, Dwell (s): 0.025, Cone (V): 50, Collision (V): 74; Channel 2: Parent (m/z): 936.4273, Daughter (m/z): 86.1159, Dwell (s): 0.025, Cone (V): 50, Collision (V): 74; Channel 3: Parent (m/z): 936.4273, Daughter (m/z): 86.698, Dwell (s): 0.025, Cone (V): 50, Collision (V): 78; Channel 4: Parent (m/z): 936.4273, Daughter (m/z): 129.1146, Dwell (s): 0.025, Cone (V): 50, Collision (V): 76.

2.2 Investigating the Effect of Medium Volume and Incubation Time on the Production of Calcitonin and Calcitonin-Related Species by DMS53 Cells.

In **Table 1** of the work described by Cao and coworkers, it was demonstrated that PBA more than halved the proportion of CT in the medium (11% of the total peak area, decreased from 25% in the control), and that it had less effect on CT in the lysate (53% of the total peak area, decreased from 63%). It was proposed that a by-pass mechanism is operating in DMS53 cells to maintain intracellular CT levels, where CT's biosynthetic precursors are transcribed in excess, and the flux through the non-glycosylated pathway is adjusted by diversion to the glycosylation pathway. This leads to an accumulation of CT-G, with the conversion to CT determined by PAM (specifically, PHM) expression and activity. Excess CT-G, and glycosylated species gCT and gCT-G, are then selectively secreted from the cells.

As outlined in the manuscript, the treatment of DMS53 cells with PAM and GEMSA inhibitors was undertaken over a incubation time of 48 h, and in a growth medium volume of 10 ml. Given the potential importance of the cellular efflux of CT-related species in the homeostasis of intracellular CT, it was of interest to compare the levels of the CT-related species present in the medium and lysate after different incubation times and with incubation in different volumes of growth medium. After a series of preliminary experiments to develop the methodology, experiments were devised comprising equally seeded cell cultures incubated in two different volumes of medium. Duplicate DMS53 cultures were seeded with 10 million cells and incubated in either 10 or 30 ml of medium. The medium and lysate was analysed after incubation for either 24 or 72 h (full protocol outlined in experimental section 7.6 of this thesis, HPLC analysis method outlined in experimental section 7.3).
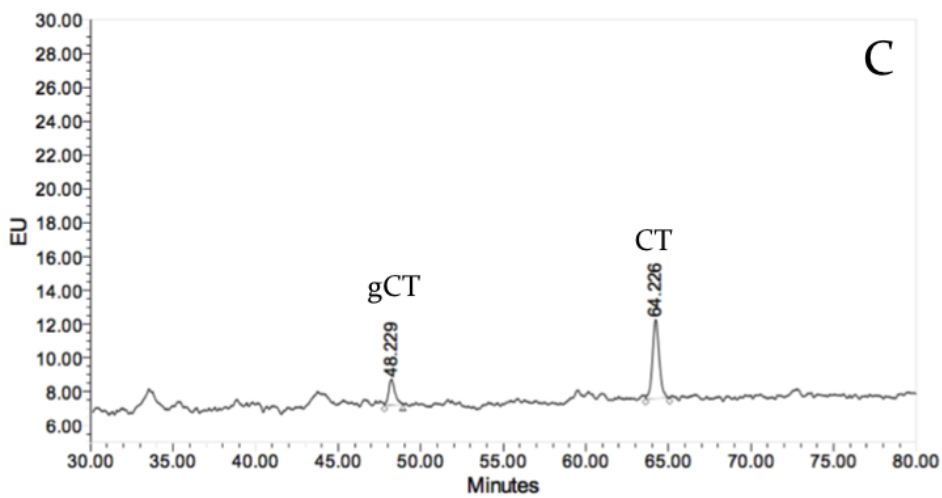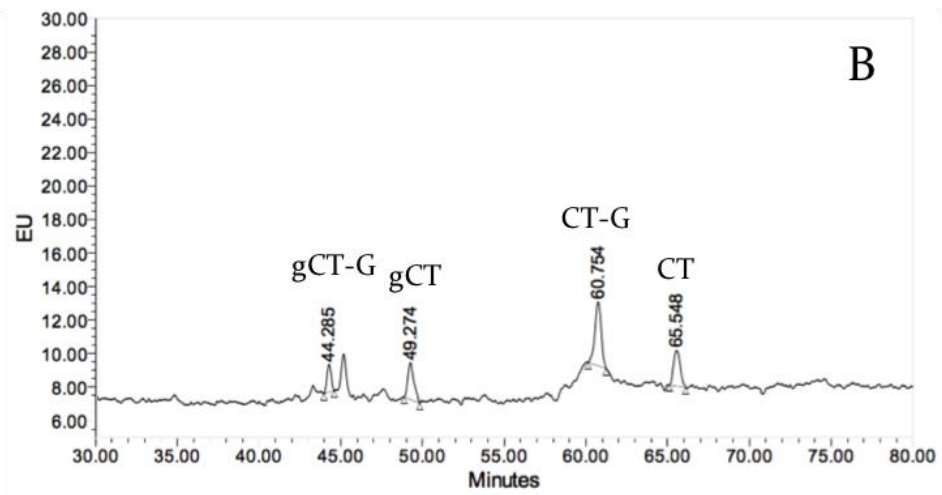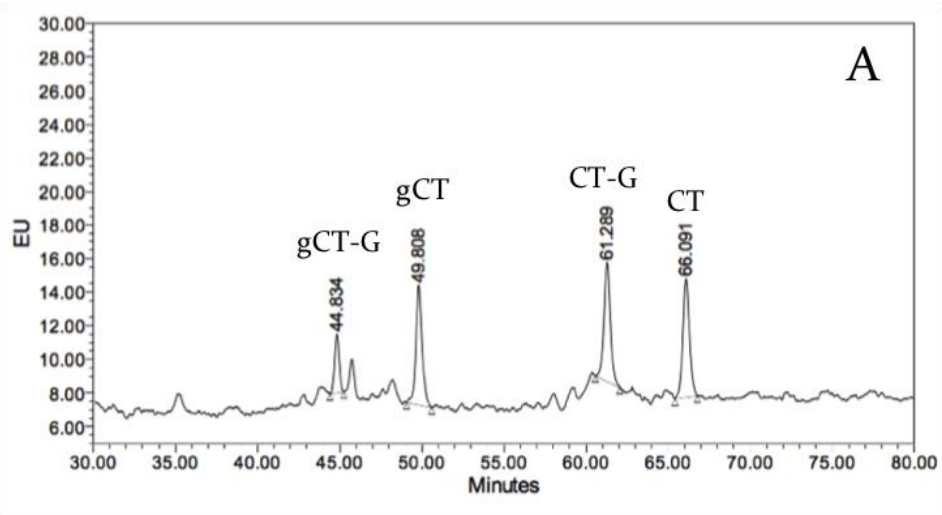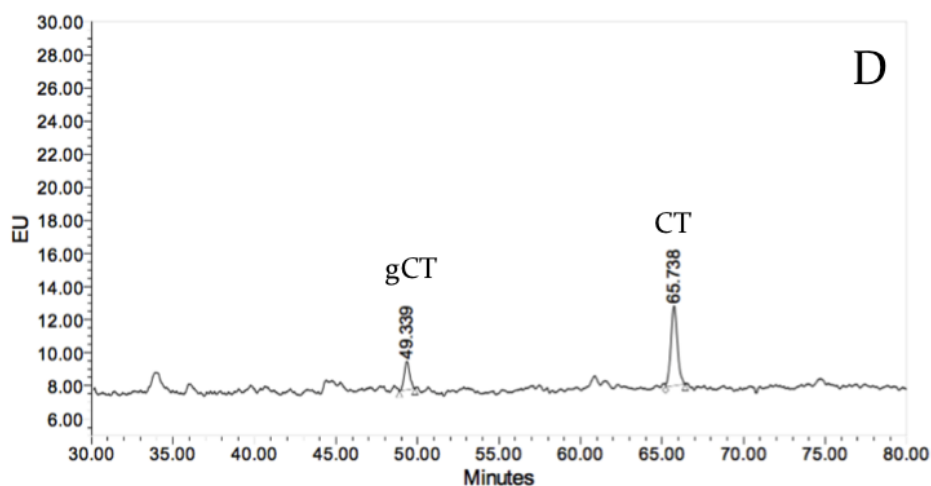
Figure 2.1: *HPLC chromatograms of* **A:** *DMS53 culture medium, after incubation for 24 h in 10 ml of growth medium;* **B:** *DMS53 culture medium, after incubation for 24 h in 30 ml of growth medium;* **C:** *DMS53 culture lysate, after incubation for 24 h in 10 ml of growth medium;* **D:** *DMS53 culture lysate, after incubation for 24 h in 30 ml of growth medium.*

In **Figure 2.1**, representative medium and lysate chromatograms for DMS53 cultures incubated in either 10 ml or 30 ml of growth medium for 24 h are presented. The difference in medium volume of the 10 ml (**A**) and 30 ml (**B**) cultures was 3-fold. Therefore, if the 10 ml and 30 ml cultures secreted equal amounts of CT-related species into the medium, the total peak areas in the 30 ml culture chromatograms would be 3-fold smaller than those in the 10 ml culture chromatograms due to the dilution of the CT-related species in the larger volume. The sum of the CT-related species' peak areas in the 30 ml medium chromatogram is approximately 37% of that of the CT-related species' peak areas in the 10 ml medium chromatogram, indicating that after 24 h both cultures were producing approximately equivalent amounts of CT-related species in the medium.

In the medium of the 10 ml culture, the CT to CT-G ratio was 1.03 and the gCT to gCT-G ratio was 2.90, while in the medium of the 30 ml culture, the CT to CT-G ratio decreased to 0.58 and the gCT to gCT-G ratio to 1.91. The non-glycosylated to glycosylated species ratio was 1.56 in the 10 ml culture medium, and increased to 1.85 in the 30 ml culture

medium. In the lysate chromatograms of the 10 ml (**C**) and 30 ml (**D**) cultures, the levels of gCT-G and CT-G were below the limits of accurate quantification after 24 h. Incubation volume had no discernable effect on intracellular CT and gCT levels in the lysate; the peak area of CT was approximately 4-fold that of gCT in both the 10 ml and 30 ml culture lysate chromatograms. The average cell number in the 10 ml culture was 25 x 10^6 compared with 27 x 10^6 in the 30 ml culture, indicating incubation volume had little effect on cell proliferation over 24 h.
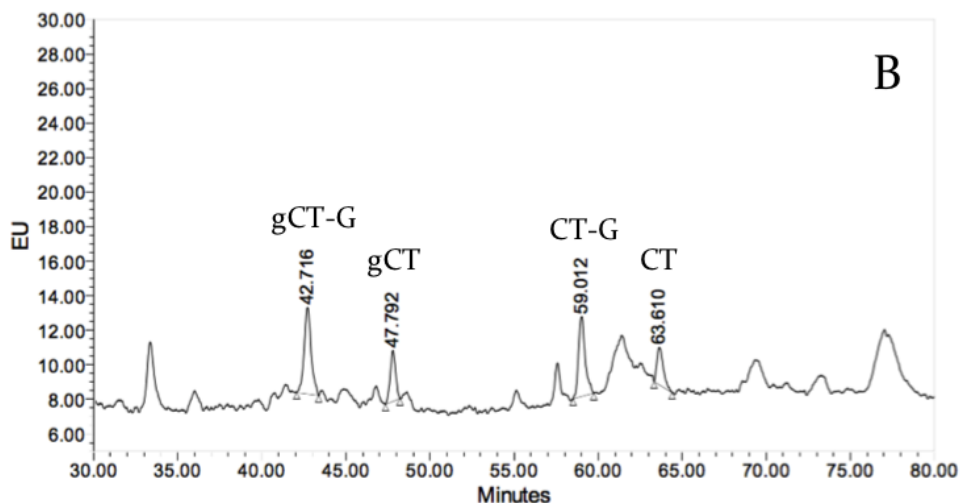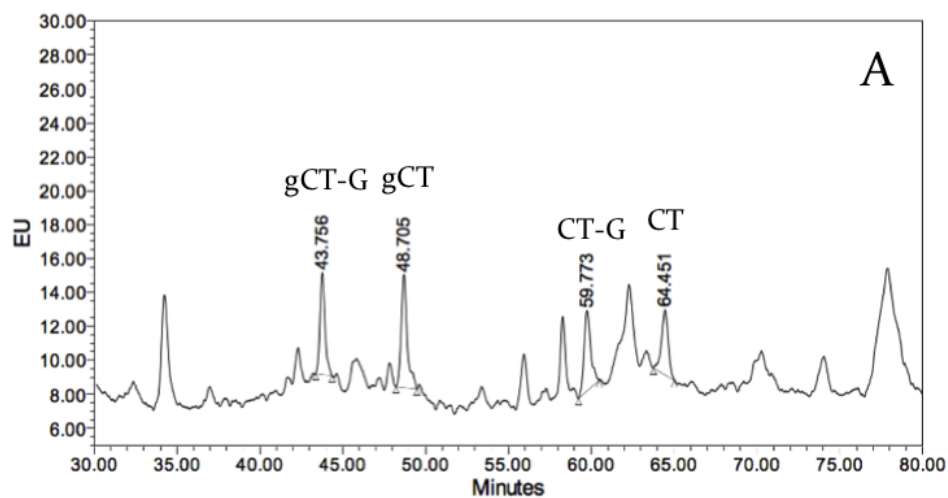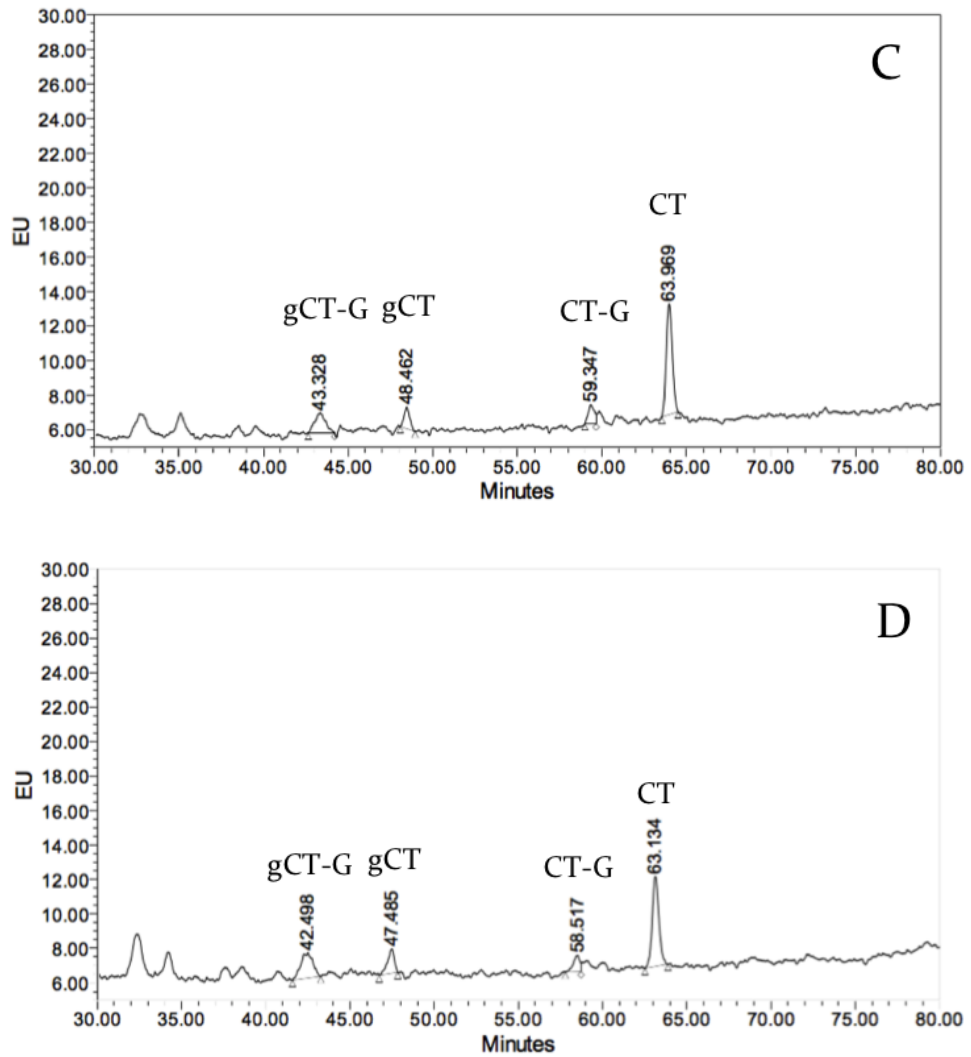
Figure 2.2: HPLC chromatograms of **A:** *DMS53 culture medium, after incubation for 72 h in 10 ml of growth medium;* **B:** *DMS53 culture medium, after incubation for 72 h in 30 ml of growth medium;* **C:** *DMS53 culture lysate, after incubation for 72 h in 10 ml of growth medium;* **D:** *DMS53 culture lysate, after incubation for 72 h in 30 ml of growth medium.*

In **Figure 2.2**, representative medium and lysate chromatograms for DMS53 cultures incubated in either 10 ml or 30 ml of growth medium for 72 h are presented. Comparing the relative levels of CT-related species in the medium and lysate of the 10 ml culture experiments at the 24 h and 72 h time points demonstrates the effect of incubation time on the production of these species. In the 10 ml culture lysate after 72 h (**C**), CT-G and gCT-G were quantifiable. However, the levels of gCT-G, gCT, and CT-G relative to CT did not change greatly when compared to the levels after 24 h. Compared to the 24 h 10 ml

culture experiments, the 72 h 10 ml (**A**) medium chromatogram shows many additional unidentified species. The relative proportions of the CT-related species changed with incubation time as well. After 72 h, the ratio of non-glycosylated to glycosylated species in the 10 ml culture medium was 0.75, compared to 1.56 after 24 h. There was also a decrease in the relative proportion of amidated species. The gCT to gCT-G ratio decreased from 2.90 after 24 h to 1.03 after 72 h. The CT to CT-G ratio decreased from 1.03 after 24h to 0.72 after 72 h. Average cell numbers in the 10 ml culture increased from 25×10^6 after 24 h to 30×10^6 after 72 h.

As with the 24 h experiment, if the 10 ml and 30 ml cultures secreted equal amounts of CT-related species into the medium, the peak areas in the 30 ml culture chromatogram would be 3-fold smaller than those in the 10 ml culture chromatogram. After 72 h, in the 30 ml culture medium chromatogram (**B**), the sum of the CT-related species' peak areas is 72% of that of the CT-related species' peak areas in the 10 ml medium chromatogram. This indicates that more than double the amount of CT-related species was present in the 30 ml culture medium compared to the 10 ml culture medium. After 72 h, the CT to CT-G and gCT to gCT-G ratios in the 10 ml culture medium (0.78 and 1.28, respectively) were higher than those observed in the 30 ml culture medium (0.44 and 0.45, respectively). There was no major difference in the non-glycosylated to glycosylated species ratio between the 10 ml culture and 30 ml culture medium. In the lysate chromatograms of the 10 ml (**C**) and 30 ml (**D**) cultures, little variation in the relative proportions of the CT-related species was observed. There was some variation in cell numbers between the 10 ml and 30 ml cultures after 72 h, with averages of 30×10^6 and 39×10^6 observed, respectively.

The levels of CT-related species in the DMS53 culture medium change with time. After 24 h, it appears that DMS53 cultures prioritise the production and secretion of CT, as the production ratios favour non-glycosylated and C-terminal amidated species. However,

after 72 h, it appears that CT is no longer the biosynthetic priority; production ratios favour glycosylation, and the ratio of glycine-extended precursors to the C-terminally amidated products increases. In the lysate after 72 h, the levels of gCT-G and CT-G are quantifiable, but do not change to any major extent relative to CT.

No changes were observed in the lysate of a larger incubation volume, which is consistent with the incubation time-variable assays. This again demonstrates that intracellular levels of CT-related species, particularly CT, are tightly controlled in DMS53 cultures. The production of CT-related precursors was up-regulated in the 30 ml culture medium in a larger incubation volume. After 24 h, CT-G was the major precursor, but after 72 h, gCT-G and CT-G were produced in more equal amounts. PAM activity limited the conversion of CT-G and gCT-G to their respective amidiated products. However, with up-regulation of the CT-related species' production pathway after 72 h, levels of gCT and CT began to increase in the medium. This suggests that if cultures were incubated for a longer duration, the concentration of gCT and CT in the 30 ml culture medium would become comparable to that observed in the 10 ml culture medium.

There have been reports of CT-producing lung cancer cells maintaining homeostatic control of extracellular CT-related species in the literature. Ellison and coworkers,[160] using a radioimmunoassay which did not distinguish CT from its precursors, observed that in a bronchial carcinoma cell line (BEN) concentrations of immunoreactive CT-related species plateaued over time, and incubation in increased volumes of culture medium stimulated the cells to produce more CT-related species over 72 h until comparable concentrations across all medium volumes were achieved.[158, 160] This suggests that specific concentrations of external CT-related species are desirable for BEN cells.

The experiments performed in this Chapter demonstrate that DMS53 cells respond to larger incubation volumes with increased production of CT-related species in a similar manner to BEN cells. With the ability to discern the relative level of the CT-related species, it was observed that glycine-extended precursors made up the majority of the extracellular species detected after 72 h, rather than CT, as was suggested in the analysis of the BEN culture medium. It was also demonstrated that the changes in the levels of CT-related species had no effect on the intracellular levels of CT-related species, which could not be explored previously. It is not clear yet whether immunoassays detect gCT or gCT-G, but if the glycosylation of CT–related species is generic across CT-producing cell lines, it may be that up to half the CT-related content observed in the BEN cell medium is glycosylated.

2.3 Conclusion

In the work described by Cao and coworkers, it was demonstrated that intracellular CT concentration was tightly controlled, even in the presence of biosynthetic enzyme inhibitors. This conclusion is reinforced by the experiments performed in this Chapter, as it was shown that the levels of CT-related species in the medium of DMS53 cultures vary with changes in incubation duration and medium volume, but the levels in the lysate remain stable. At shorter incubation times, DMS53 cultures favour the production of non-glycosylated species in the medium and after 72 h, production priority shifts towards glycosylated species. In larger volumes of medium, DMS53 cultures up-regulate the production of CT-related precursors, with the conversion to gCT and CT limited by PAM processing. In spite of this limitation, up-regulation leads to increased amounts of all CT-related species present into the medium after 72 h. These observations suggest that DMS53 cultures respond to the external concentration of CT-related species and attempt to maintain a particular range of concentrations through changes in CT biosynthesis.

Cellular mechanisms to maintain both intracellular and extracellular CT-related species suggest it is important to the biology of DMS53 cells. These mechanisms appear to frustrate strategies to reduce CT production, such as targeting biosynthesis with PBA and GEMSA treatment. Thus, an understanding of their function is prerequisite to controlling CT. It was proposed by Hunt and coworkers[158] that the BEN cells' response to extracellular CT concentration might be mediated by the hCTR. To investigate the possibility that the hCTR is responsible for the response to extracellular CT concentration in DMS53 cells, work in Chapter 3 was directed to the treatment of DMS53 cultures with a specific hCTR agonist in order to determine if hCTR activation affects the production of CT-related species.

Chapter Three

Results and Discussion: The Effect of a Human Calcitonin Receptor Agonist on the Production of Calcitonin-Related Species in DMS53 Cells

3.1 Introduction

In the work described in Chapter 2, it was demonstrated that incubating DMS53 cultures in an increased volume of growth medium resulted in the up-regulation of CT precursor biosynthesis, and an eventual increase in the levels of all CT-related species present in the medium. These observations imply a feedback loop is operating in DMS53 cells, which maintains the extracellular concentrations of CT-related species in response to an increase in growth medium volume. Similar responses in other CT-producing cell lines have been reported, by Ellison and coworkers[160] in BEN cells, and by Hunt and coworkers[158] in thyroid C cells. Hunt and coworkers speculated that this feedback mechanism might be initiated by hCTR activation and mediated by cAMP signalling through AC. Subsequently, it has been reported that there is a cAMP responsive element (CRE) modulating the transcription of the CT gene,[170] further linking CT transcription to hCTR activation.

If hCTR acts as a detector for extracellular CT, and its activation causes changes in the levels of CT-related species in the medium, then treatment of DMS53 cultures with a specific hCTR agonist should change these levels as well. These changes could be assessed using the HPLC-fluorescence method reported in Chapter 2. Since this method

involves the post-separation tagging of free primary amino groups with fluorescamine, treatment with sCT or other peptidic hCTR agonists is undesirable as these compounds would be tagged in the analysis and may interfere with the detection of analytes. For this reason, the small molecule hCTR agonist SUNB8155 (**Figure 3.1**) was selected, as it contains no primary amine group. As described by Katayama and coworkers,[94] SUNB8155 activates the hCTR receptor specifically over hPTHr, and stimulates cAMP production at concentrations between 10 and 1000 μM. Therefore, in order to discover if the levels of CT-related species produced by DMS53 cultures in the medium changed in response to SUNB8155 treatment, trials were initiated using concentrations of 200 μM and 100 μM.
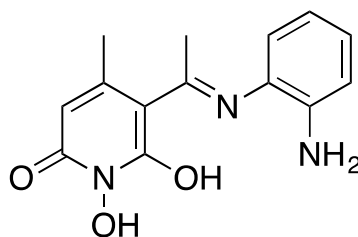
Figure 3.1: *The specific hCTR agonist SUNB8155 reported by Katayama and coworkers.*[94]

3.2 Investigating the Effect of SUNB8155 on the Production of Calcitonin-Related Species in DMS53 Cells Using a First HPLC-Fluorescence Calcitonin Detection Method

Preliminary experiments to evaluate the effect of SUNB8155 on CT production in DMS53 medium were undertaken using the HPLC separation system used for the separation of CT, CT-G, CTGK and CTGKK described in Chapter 2. Outlined in **Figure 3.2**, the CT method 1 (designated CT-M1) begins with online solid phase extraction of the analytes from the injected sample on a reverse phase Oasis® HLB 25 μm cartridge column (2.1 ×

20 mm) with the switching valve open to waste (SW 1 OFF) to pre-clean and pre-concentrate the analytes. The switching valve (SW 1) is then turned on to connect with a C12 Synergi Max-RP column (250 × 4.6 mm) for elution of the analytes and separation. The separation column is followed by a Waters Reagent Manager (SW 2) containing fluorescamine (30 mg/100 ml acetonitrile) and a Waters RXN 1000 coil for online post-column derivatisation of the separated and purified peptides at 25°C, which allows sensitive fluorescence detection at excitation 390 nm and emission 470 nm by a Waters 2475 Fluorescence Detector. The solvent system used is reported in the experimental chapter (section 7.2). This high throughput method of automatic online concentration, separation, derivatisation and detection is rapid, efficient and sensitive.[17]
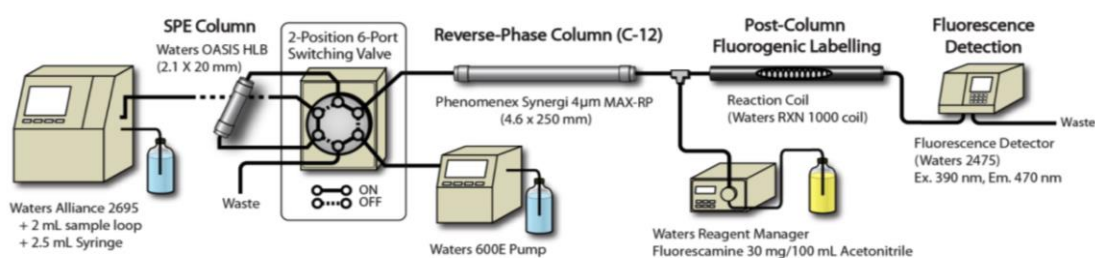
Figure 3.2: *HPLC separation Method 1 for CT species (CT-M1).* Used with permission from Hideki Onagi.

Although SUNB8155 has a primary aromatic amine moiety and it is known that aromatic amines can be labelled by fluorescamine,[171] a control experiment, where a SUNB8155 solution was injected onto the HPLC and analysed using the CT-M1 method, showed no peak on the HPLC trace. This shows that any reaction of SUNB8155 with fluorescamine does not interfere with the assay. The solid phase extraction of the cell culture species is optimised to retain peptides and it is likely that SUNB8155 is not retained during this step and is thus not present during the analysis.In order to obtain detectable levels of CT and its precursors in the cell medium, as well as reproducible HPLC chromatograms with high quality signal to noise ratios, both a high cell density (2-3 million/ml of

medium) and incubation times of at least 24 h were required. The first generation *in vitro* cell assay for testing the effects of SUNB8155 on the levels of CT-related species in the medium involved the incubation of three cultures in 75 cm^2 flasks to confluence in 10 ml of growth medium (3 to 4 days growth from equally seeded cultures). After refreshing the medium, cultures were treated with 200 μM SUNB8155 in DMSO, or 10 μl of DMSO in the control cultures. The cultures were then incubated for a further 24 h. The medium was then harvested and 5 ml was injected directly onto the HPLC and analysed using CT-M1. The areas of the CT and CT-G peaks in the SUNB8155-treated culture were then compared with the peak areas in the control culture to determine if any change in the levels had occurred. A detailed protocol outlined in experimental section 7.4. The expected elution time for the CT peak was approximately 43 min while CT-G eluted at approximately 40 min. The CT and CT-G peaks had been characterised previously through comparison to the elution times of CT and CT-G standards, and confirmation by MS analysis (as described in Chapter 2).[17] The results of this assay are shown in **Figure 3.3**, with experiments repeated twice with concordant results.
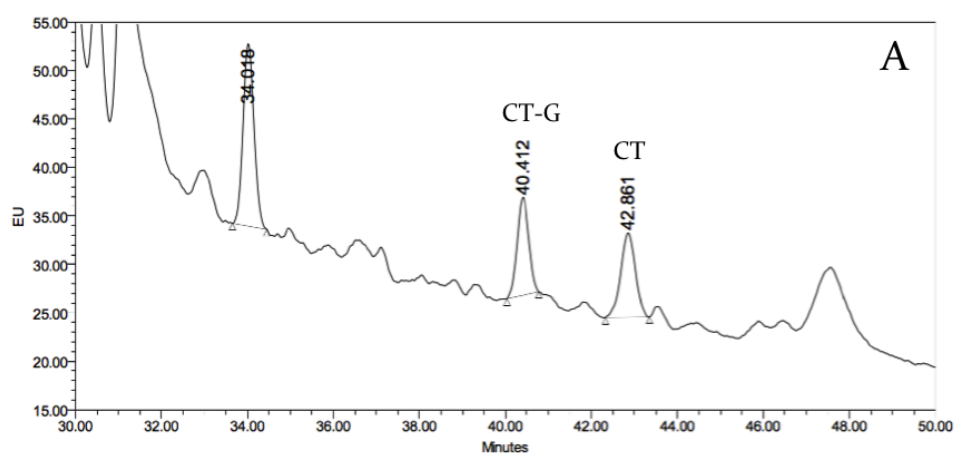
Figure 3.3: *HPLC chromatograms of A: DMS53 culture medium after incubation for 24 h, analysed using CT-MI; B: DMS53 culture medium, after treatment with SUNB8155 (200 μM) and incubation for 24 h, analysed using CT-MI.*

In the control culture (**A**), CT and CT-G were present at similar levels in the medium; the ratio between the two peak areas was 1.05. In contrast, the chromatogram of the DMS53 culture treated with 200 μM SUNB8155 (**B**) showed that the level of CT was higher than CT-G in the medium. The ratio of CT to CT-G was 1.82, a 75% increase compared to the ratio observed in the control culture. To briefly assess the concentration-dependence of the effect of SUNB8155 on DMS53 cultures, the experiment was repeated with 100 μM SUNB8155 treatment (**Figure 3.4**). Again, in the control medium chromatogram (**A**) the CT to CT-G ratio was 1.07, while for cultures treated with 100 μM SUNB8155 (**B**) the ratio in the medium was 2.03, an 89% increase compared to the control.

Figure 3.4: *HPLC chromatograms of* **A:** *DMS53 culture medium after incubation for 24 h, analysed using CT-MI;* **B:** *DMS53 culture medium, after treatment with SUNB8155 (100 μM) and incubation for 24 h, analysed using CT-MI.*

Treatment of DMS53 cultures with SUNB8155 changed the relative proportions of CT-related species present in the medium. In the treated cultures, the ratio of CT to CT-G increased by 75% and 89%, compared to the ratio observed in the control cultures. This suggests that an increase in the activity or expression of PAM may have occurred, as more CT-G appears to have been converted to CT. SUNB8155 is known to activate hCTR, and as both treatment concentrations resulted in similar changes in CT-related species' levels in the medium, this suggests that the binding site of hCTR is saturated at concentrations of 100 μM or lower. These findings support the possibility that hCTR mediates activation of the feedback loop proposed in Chapter 2. As experimental observations suggest that hCTR stimulation increases the proportion of CT in the medium, this implies that a positive feedback loop is operating in DMS53. This raised the question of whether the levels of gCT and gCT-G produced by DMS53 cultures in the medium would respond to SUNB8155 treatment, and if so, whether it would be in the same manner as the levels of CT and CT-G.

3.3 Investigating the Effect of SUNB8155 on the Production of Calcitonin-Related Species by DMS53 Cells Using a Second HPLC-Fluorescence Calcitonin Detection Method

In order to characterise changes in the levels of CT, CT-G, gCT and gCT-G in response to SUNB8155 treatment, the second HPLC method developed in Chapter 2 was used (designated CT-M2). To increase the separation power of CT-M1, the single C12 Synergi Max-RP column was substituted for two columns: a C18 YMC ODS-AQ 3 μm (4.6 x 100 mm) reverse-phase column coupled to a Phenomenex Phenosphere SCX (4.6 x 250 mm) cation-exchange column (**Figure 3.5**). This allowed analytes to be separated on the basis of two properties, hydrophobicity and charge, rather than just hydrophobicity. The solvent system is outlined in section 7.3 of the experimental chapter. In order to take advantage of the additional separating power of the new system, the method was extended to 80 min and the acetonitrile gradient decreased. Additionally, the concentration of AccQ.Tag™ Eluent A acetate buffer was increased from 25 ml/l to 100 ml/l.
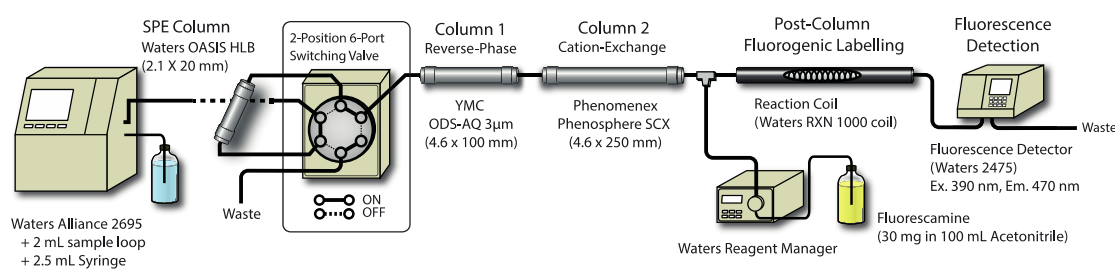
Figure 3.5: *HPLC separation Method 2 for CT species (CT-M2).* Used with permission from Hideki Onagi.

As well as refining the HPLC method, the cell assay was redesigned. The second generation cell assay featured duplicate control and SUNB8155-treated 25 cm^2 cultures that were seeded with equal cell numbers (approximately 3 million cells) at low density

in 5 ml of growth medium and incubated until confluent (2-3 days, approx. 10 million cells). The growth medium was refreshed, and the cultures were treated with either 100 μM of SUNB8155 in DMSO, or 10 μl of DMSO in the control cultures. The cultures were incubated for a further 24 h, and then the medium was removed and placed into 15 ml Falcon™ tubes. The medium was centrifuged (10,000g for 5 min at 4 °C) to remove dead cells and insoluble medium components, then 3 ml was injected onto the HPLC and analysed using CT-M2. A detailed protocol is outlined in experiment section 7.5. Experiments were repeated at least twice with concordant results.
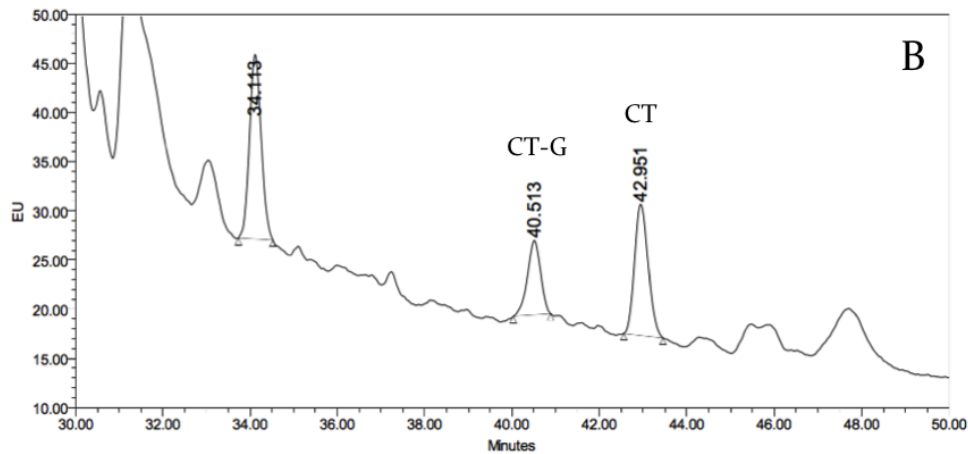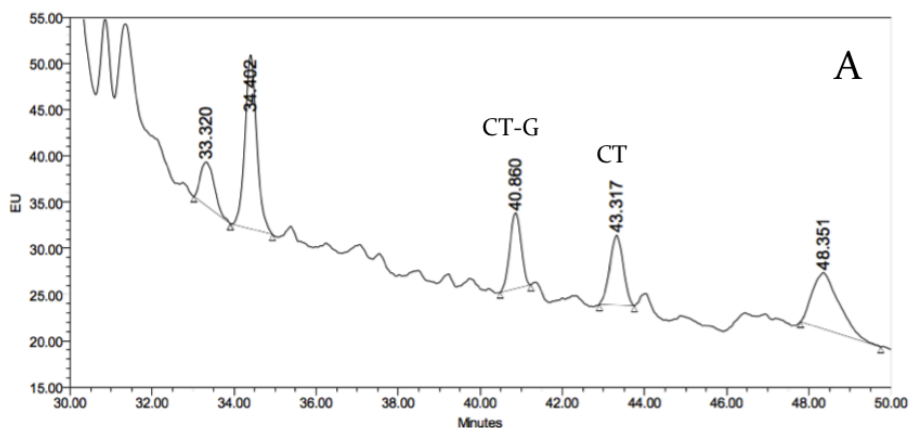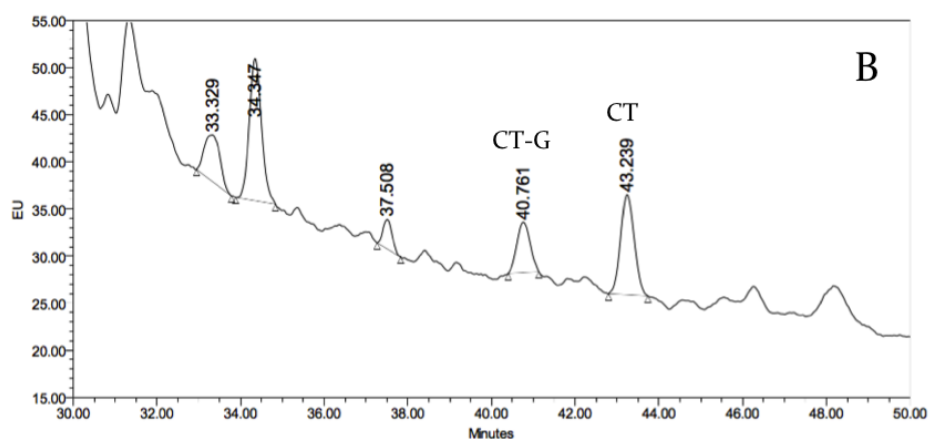

Figure 3.6: *HPLC chromatograms of* **A:** *DMS53 culture medium after incubation for 24 h, analysed using CT-M2;* **B:** *DMS53 culture medium, after treatment with SUNB8155 (100 μM) and incubation for 24 h, analysed using CT-M2.*

Figure 3.6A is a representative chromatogram of DMS53 control medium analysed using CT-M2. The elution time of CT and CT-G increased compared to medium samples analysed using CT-M1, to approximately 65 min and 60 min respectively. In addition, two other peaks were observed at approximately 49 min and 44 min. As described in Chapter 2, these were identified as CT and CT-G glycosylated at the Thr21 position with Neu-Ac(α2-3)Gal-(β1-3)-[NeuAc(α2-6)]GalNAc (gCT and gCT-G), having being characterised through MS and enzymology. The effect of SUNB8155 treatment on the levels of glycosylated and non-glycosylated CT species in the medium is shown in **Figure 3.6B**. The CT to CT-G peak area ratio increased from 0.36 in the control medium to 0.63 in the SUNB8155 treated culture medium, an increase of 75%. In contrast, the gCT to gCT-G ratio increased by only 27%, from 0.29 in the control medium to 0.40 in the treated culture medium. There was a small increase in the ratio of non-glycosylated to glycosylated species, from 1.11 to 1.32 (18%).

Treatment of DMS53 cultures changed the levels of gCT and gCT-G in the medium. The gCT to gCT-G ratio increased, but by less than half the increase observed in the CT to CT-G ratio. This suggests that the putative activation of hCTR increases the proportion of CT in the medium selectively over gCT. Interestingly, little change was observed in the non-glycosylated to glycosylated species ratio. This implies that PAM expression or activity is up-regulated and that the turnover of CT-G is favoured over gCT-G.

In order to have a more comprehensive understanding of SUNB8155 action on CT regulation in DMS53, the concentration-dependence of the effect required quantification, and a comparison of the intracellular and extracellular CT-related species was performed. This would allow the changes in CT biosynthesis and secretion of CT-related species to be distinguished from one another, in turn examining the mechanisms

triggered by putative hCTR activation. To accomplish this, changes in peak area needed to be compared between experimental replicates, and the results averaged across a number of experiments. In turn, this required a more consistent assay with comparable cell numbers between the treated and control cultures, and lysate analysis methodology.

3.4 Investigating the Effect of SUNB8155 on the Production of Calcitonin-Related Species by DMS53 Cells with a More Robust Assay.

The third generation cell assay focused on tight control of cell numbers at the beginning of treatment and at the end of the experiment to allow direct comparison between experimental replicates. Methodology was also developed to analyse cell lysates alongside media, allowing the intracellular levels of CT-related species to be observed. With these tools, the effect of SUNB8155 treatment at three increasing concentrations on the levels of CT-related species in DMS53 culture medium and lysate was assessed.

Stock cultures (in 175 cm^2 flasks) of DMS53 were grown to confluence, lifted and counted. Eight cultures were each seeded with 10 million cells. The cells were grown for 3 days, with a final cell count of 20-25 million cells per culture. After refreshing the medium, 2 cultures were treated with the relevant concentrations of SUNB8155 (1 µM, 10 µM and 100 µM), or 10 µl of DMSO in the control cultures. The cultures were incubated for 24 h, then the medium and cells harvested for analysis. The experiment was repeated three times with concordant results. Both the medium and cell lysates were prepared as described in Chapter 2. Briefly, the cells were lysed by freeze-thawing, where the cell pellet was frozen in liquid nitrogen then heated to 100 °C for 7 min to denature proteases that might otherwise degrade the CT-related species. The lysate was then

subjected to centrifugal filtration using a 50 kDa cut-off filter. The centrifugal filtration was also applied to the medium to remove cell debris as an improvement over the centrifugation methodology described above. A detailed protocol is outlined in section 7.6 of the experimental Chapter.
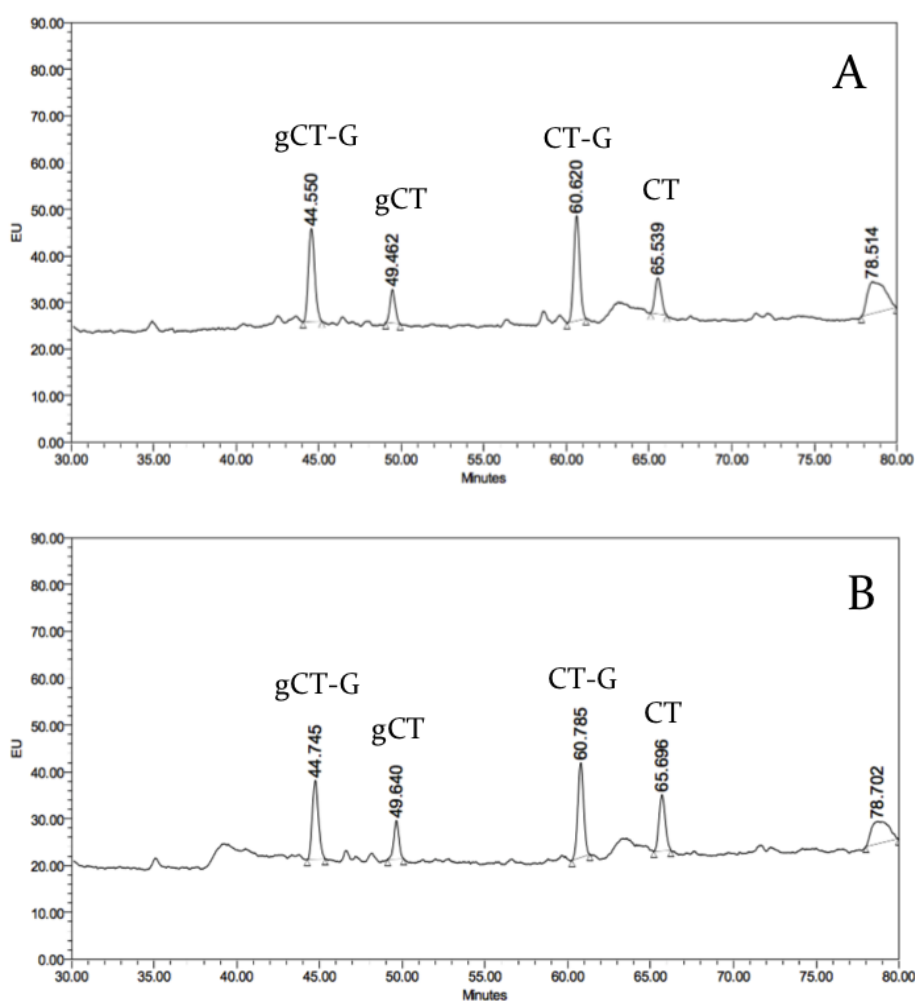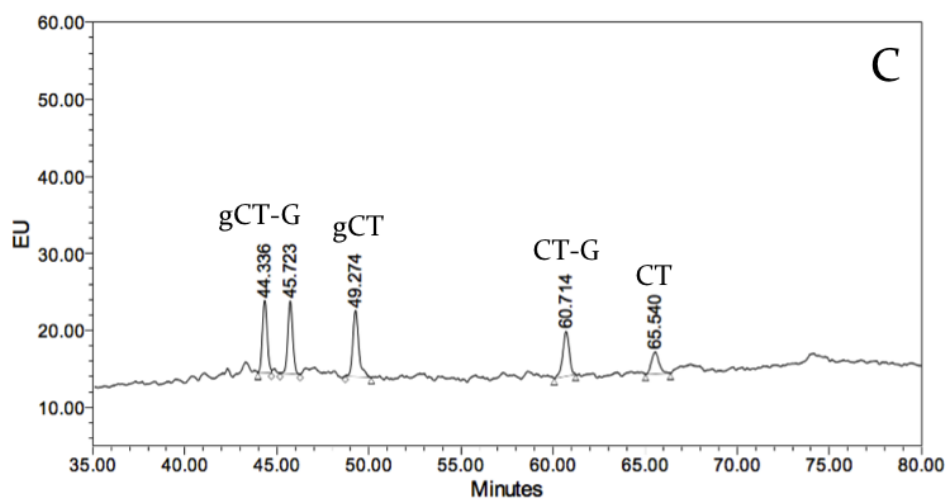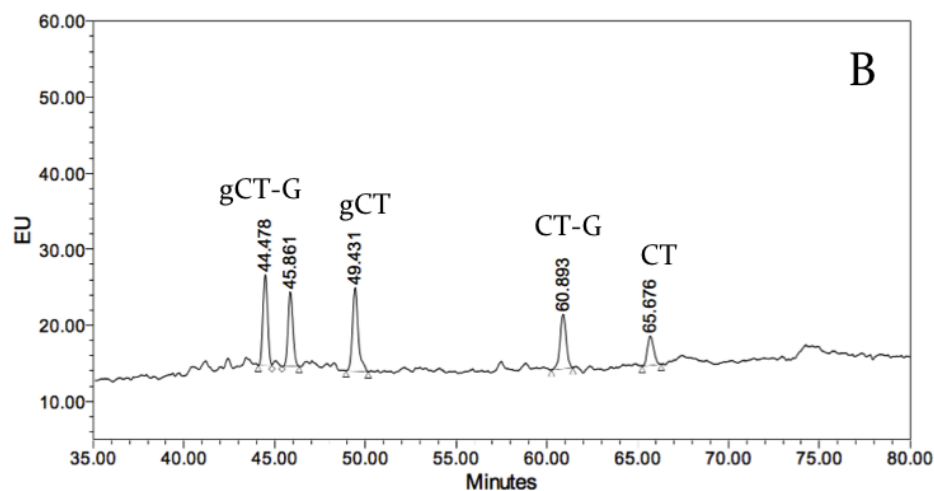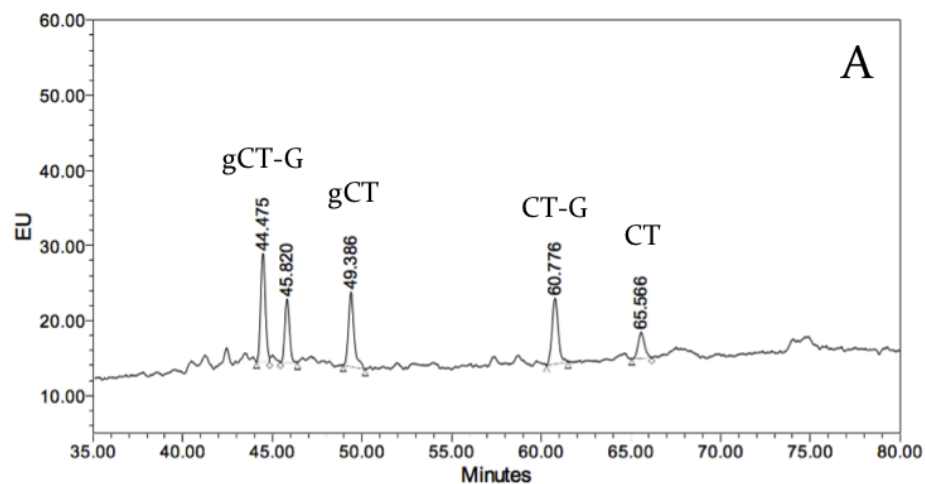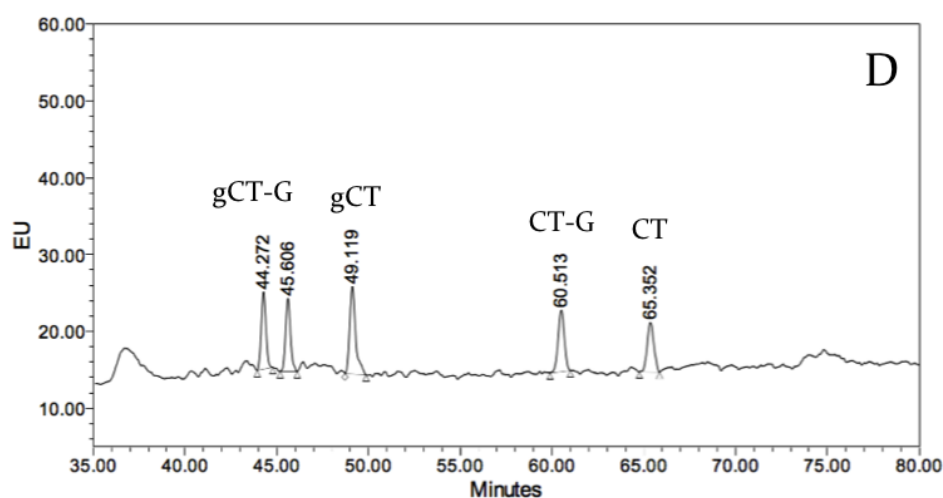
Figure 3.7: *HPLC chromatograms of* **A:** *DMS53 culture medium after incubation for 24 h, analysed using CT-M2;* **B:** *DMS53 culture medium, after treatment with SUNB8155 (1 μM) and incubation for 24 h, analysed using CT-M2;* **C:** *DMS53 culture medium, after treatment with SUNB8155 (10 μM) and incubation for 24 h, analysed using CT-M2;* **D:** *DMS53 culture medium, after treatment with SUNB8155 (100 μM) and incubation for 24 h, analysed using CT-M2.*

Representative medium chromatograms are presented in **Figure 3.7A-D,** with species ratios summarised in **Table 3.1** and **Table 3.2**. In the control medium, the average CT to CT-G ratio was 0.53 ± 0.03. This ratio did not increase significantly in the medium of cultures treated with 1 μM and 10 μM SUNB8155 (0.61 ± 0.06 and 0.58 ± 0.03 respectively), while in the medium of the cultures treated with 100 μM SUNB8155, the average ratio increased by 96% to 1.04 ± 0.07. This trend was mirrored in the gCT to gCT-G ratio with an average of 1.09 ± 0.07 in the control cultures, remaining the same within error at 1.08 ± 0.05 and 1.15 ± 0.07 in the 1 μM and 10 μM treated cultures respectively, before increasing by 36% to 1.49 ± 0.05 in the 100 μM treated cultures. When comparing the proportion of non-glycosylated to glycosylated species in the medium, the ratio increased by 37% from an average of 0.70 ± 0.07 in the control cultures to 0.96 ± 0.06 in the 100 μM treated cultures.

Representative lysate chromatograms are presented in **Figure 3.8A-D**, with the species ratios summarised in **Table 3.3.** The work described in Chapter 2 demonstrated that CT was the major species present in untreated DMS53 lysate, and CT levels relative to the other CT-related species did not significantly change with treatment. The predominance of CT was again observed in the lysate of the control cultures in this experiment. Treatment of cultures with SUNB8155 at a concentration of 100 μM had no significant effect on the CT to CT-G ratio, or the levels of CT relative to the other CT-related species in the lysate.

Changes to the levels of CT-related species in the medium and lysate were further interrogated to determine the level of statistical significance. .As described in Appendix One, the average relative proportions of each CT-related species in a given treatment condition was calculated and normalised. Treatment conditions were then compared to the control using Welch's unequal variances t-test (**Table A1.1**). At 100 μM, SUNB8155 treatment was found to increase the relative proportion of CT in the medium ($p<0.05$, **Table A.12**),consistent with the observations above. Only minor effects were observed in the lysate, and lower concentrations had little effect.
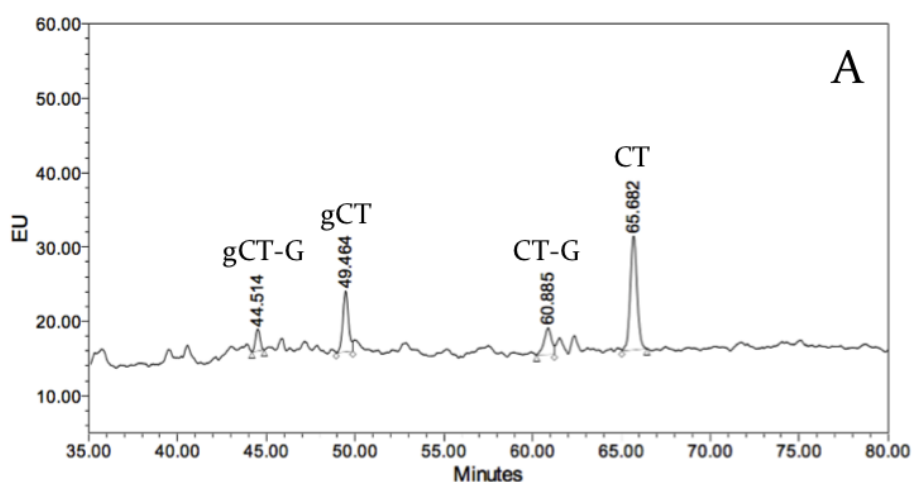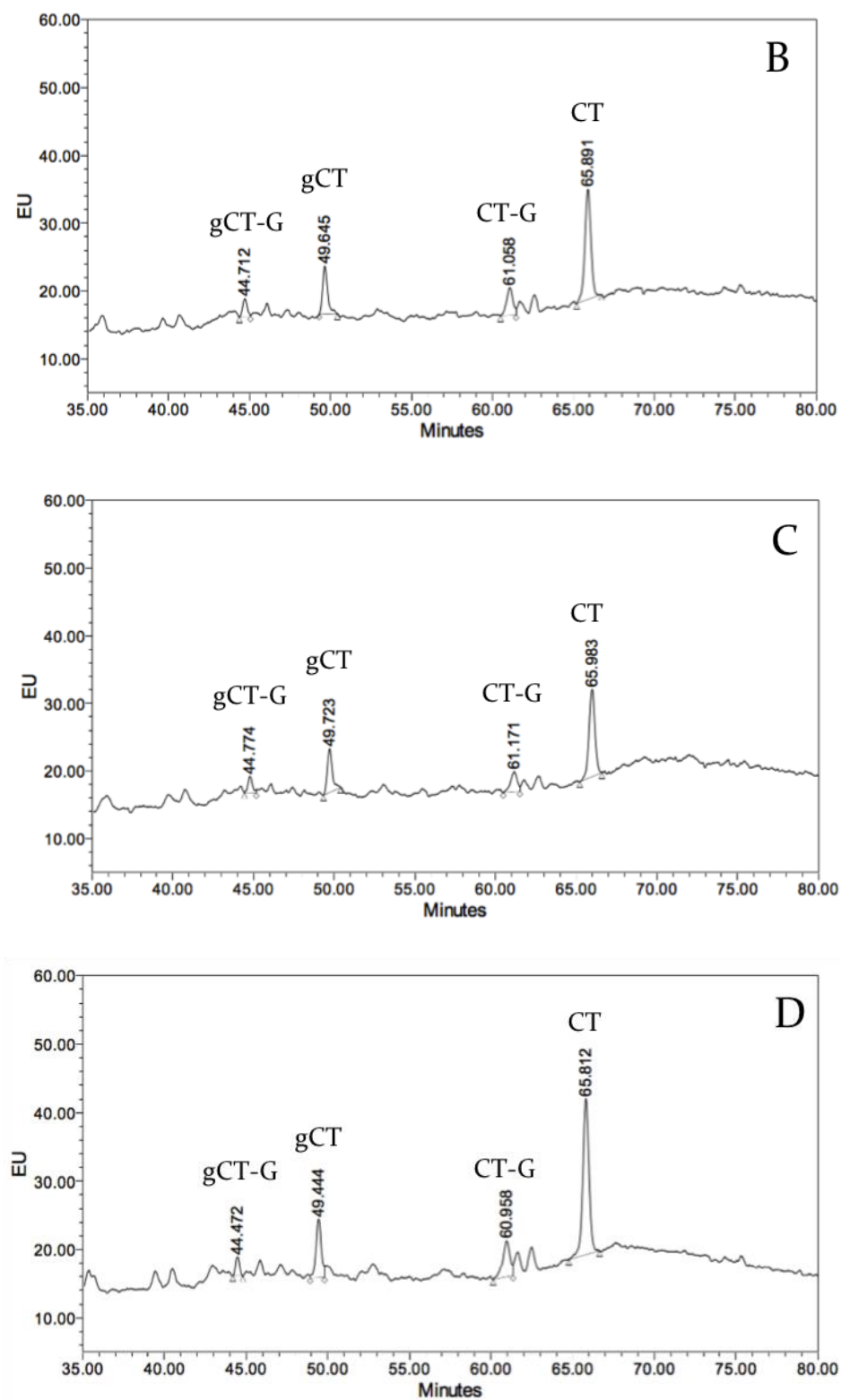
Figure 3.8: *HPLC chromatograms of* **A:** *DMS53 culture lysate after incubation for 24 h, analysed using CT-M2;* **B:** *DMS53 culture lysate, after treatment with SUNB8155 (1 µM) and incubation for 24 h, analysed using CT-M2;* **C:** *DMS53 culture lysate, after treatment with SUNB8155 (10 µM) and incubation for 24 h, analysed using CT-M2;* **D:** *DMS53 culture lysate, after treatment with SUNB8155 (100 µM) and incubation for 24 h, analysed using CT-M2.*

Table 3.1: *CT-related species ratios in the medium of DMS53 cultures treated with increasing concentrations of SUNB8155. Data obtained from triplicate experiments. Standard error of the mean determined from corrected sample standard deviation.*

SUNB8155 Concentration	gCT/gCT-G	SEM (+/-)	CT/CT-G	SEM (+/-)
Control	1.09	*0.07*	0.53	*0.03*
1 μM	1.08	*0.05*	0.61	*0.06*
10 μM	1.15	*0.07*	0.58	*0.03*
100 μM	1.49	*0.05*	1.04	*0.07*

Table 3.2: *Further CT-related species ratios in the medium of DMS53 cultures treated with increasing concentrations of SUNB8155. Data obtained from triplicate experiments. Standard error of the mean determined from corrected sample standard deviation.*

SUNB8155 Concentration	non-glycosylated/ glycosylated	SEM (+/-)	Total Peak Area/ Control Total Peak Area	SEM (+/-)
Control	0.70	*0.07*	1.00	*0.04*
1 μM	0.80	*0.08*	1.10	*0.07*
10 μM	0.81	*0.08*	0.94	*0.06*
100 μM	0.96	*0.06*	0.84	*0.07*

Table 3.3: *CT-related species ratios in the lysate of DMS53 cultures treated with increasing concentrations of SUNB8155.* Data obtained from triplicate experiments. Standard error of the mean determined from corrected sample standard deviation.

SUNB8155 Concentration	CT/CT-G	SEM (+/-)	CT Peak Area/ Total Peak Area	SEM (+/-)
Control	4.80	*0.62*	0.57	*0.02*
1 µM	5.00	*0.60*	0.56	*0.03*
10 µM	4.12	*0.25*	0.60	*0.06*
100 µM	4.72	*0.38*	0.63	*0.09*

These experiments demonstrate that treatment of DMS53 cultures with SUNB8155 at a concentration of 100 µM increased the proportion of CT relative to gCT in the medium. In the medium, the CT to CT-G and gCT to gCT-G ratios increased by 96% and 36% respectively, indicating that the expression or activity of PAM was up-regulated and that processing was biased away from glycosylation. In the lysate, the levels of CT did not change relative to the other CT-related species in the lysate.

3.5 Conclusions

Given that SUNB8155 is a specific hCTR agonist, it is inferred that the increases in intracellular and extracellular CT in response to SUNB8155 treatment are initiated by hCTR activation and are the result of secondary messengers activating transcriptional or biosynthetic mechanisms downstream. hCTR expression in DMS53 cells had yet to be demonstrated. If present though, this would suggest that hCTR has the capability to

regulate the production and secretion of its own ligand in an autocrine manner, previously reported only for the glucagon, insulin and gastrin receptors.[172] One caveat to this conclusion is that because GPCR ligands may trigger biased receptor signalling (the preferential activation of one transduction pathway over another), the cellular response to the activation of hCTR by SUNB8155 may not be the same as the response to CT.[122] However, the experiments performed in this Chapter have demonstrated that putative hCTR activation has the ability to affect the levels of CT-related species in the medium, implicating it as a mediator of CT regulation. The stability of CT levels in the lysate is consistent with the observations made in Chapter 2, which suggested tight intracellular CT regulation. The possibility that off-target activation is responsible for the changes to the levels of CT-related species observed is unlikely, as it has been shown that SUNB8155 is specific to hCTR and does not activate hPTHr (human parathyroid hormone receptor, the target most likely after hCTR to have influence over CT production) in CHO cells at the treatment concentrations.[94]

Treatment of DMS53 cultures with 100 μM SUNB8155 increased the proportion of amidated species in the medium, suggesting an up-regulation of PAM expression or activity had occurred. In the work described in Chapter 2, DMS53 cultures incubated in larger volumes of medium experienced lower effective extracellular concentrations of CT. In the larger volume cultures, greater proportions of CT-G and gCT-G accumulated in the medium, suggesting PAM activity or concentration was limiting the turnover of these species to CT and gCT. Together, these observations provide strong evidence that activation of hCTR increases PAM activity or expression. However, implicating hCTR as the initiator of a positive feedback loop that increases CT production requires that hCTR is expressed in DMS53. Work described in Chapter 4 was directed to determining whether this is the case.

Chapter Four

Results and Discussion: Characterisation of the Human Calcitonin Receptor in DMS53 Cells by Reverse Transcription PCR and Western Blot

4.1 Introduction

In the work described in Chapter 2, evidence was presented demonstrating that proportions of CT-related species produced in DMS53 culture medium changed in response to incubation in larger volumes of medium. This finding suggested that levels of CT-related species are recognised and regulated by DMS53 cultures.   The work described in Chapter 3 implicated hCTR as a component in this regulation mechanism, since the specific hCTR agonist SUNB8155 up-regulated CT relative to gCT in the medium of DMS53 cultures. This implies that hCTR activation regulates the biosynthesis of CT-related species in DMS53 cells; however there was no evidence in the literature to suggest that hCTR is expressed. The presence of hCTR in DMS53 cells was therefore investigated.

The presence of hCTR mRNA and protein in cells has generally been established using reverse transcription PCR and Western blot.[153, 173] If hCTR was positively identified in DMS53, these techniques would also allow the specific isoform to be determined. This is of value because the hCTR isoform is reported to dictate the signalling pathways utilised. [102] For example, hCTR1 and hCTR6, which possess the 48 bp sequence in the putative first intracellular loop excised in hCTR2 and other isoforms, are unable to signal through

the Ca^{2+}-dependent PLC/PKC pathway[102] or MAPK pathway,[174] ostensibly due to the extra loop residues blocking the binding of the relevant G protein(s). Thus identifying any hCTR isoform expressed in DMS53 cells is important in order to understand the receptor signalling.

4.2 Detection and Characterisation of Human Calcitonin Receptor mRNA in DMS53 and PC3 Cell Lysate using Reverse Transcription PCR

To identify the hCTR mRNA transcript expressed in DMS53, previously published primers and reverse transcription PCR conditions were initially used.[175, 176] To aid in interpreting the experimentally amplified cDNA sequences, a hCTR cDNA reference sequence annotated with the reported isoform variations was generated (**Figure 4.1**), based on the longest hCTR transcript (NM_001164737.1) in the NBCI RefSeq database.[177] This sequence is an aggregate of 10 cDNA sequences reported in the literature,[99, 104, 178, 179] and codes for the longest hCTR isoform, hCTR1. The reported sequences of hCTR2-6[97, 101, 104, 105, 107] were then aligned to this reference sequence and the regions of variation noted. With this model in hand, literature primers could then be aligned to the model sequence to identify which regions of the model sequence the primers would amplify, and how amplicon length would change if certain isoform variations were present. In **Figure 4.2**, all the primers used in this work are aligned to the hCTR model sequence.
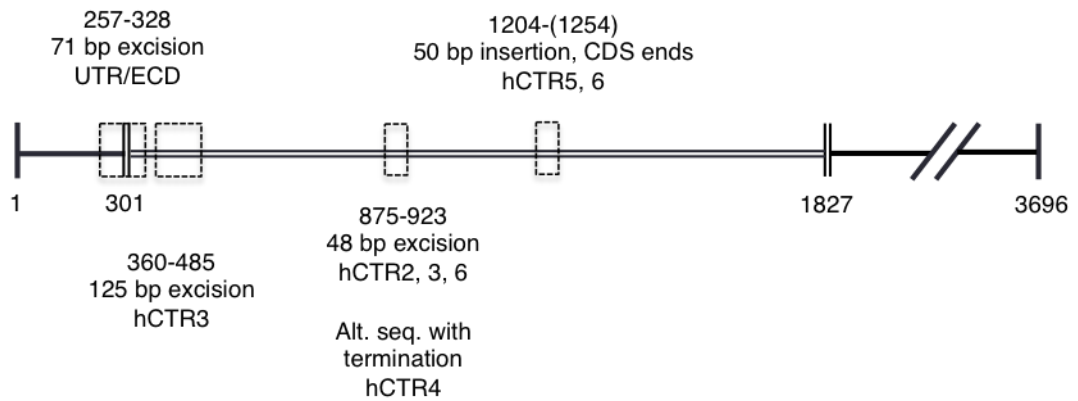
Figure 4.1: *A homology model of hCTR cDNA with reported transcript variants aligned.* The double line represents the CDS region, the solid line represents the UTR regions, and dotted boxes represent regions of variation from the reference sequence (NM_001164737.1). The UTR/ECD excision refers to the cDNA sequence reported by Gorn and coworkers in 1995.[100]

Initially, hCTR mRNA transcripts in DMS53 were evaluated using primer pairs designed by Wu and colleagues,[175] designated P1P2 and P3P4. The primer pair P3P4 is reported to amplify a region common to all the hCTR isoforms (339 bp). Complementarily, the P1P2 pair is reported to amplify the 674 bp region containing the 48 bp excision specific to isoforms 2, 3 and 6 (**Figure 4.2**). In addition, based on the sequence homology analysis, it was determined that the P1P2 pair would generate a larger amplicon for isoform hCTR5 and 6 compared to hCTR2 (98 bp greater). This had not been reported in the original paper as hCTR5 and 6 had not been discovered at the time of publication. In a number of publications the prostate cancer cell line PC3 is used as a negative control for the presence of hCTR,[152, 153] so it was also utilised for these experiments.

RNA was extracted from 1 million or 2 million cells for the analyses of PC3 and DMS53, and 10 million for DMS53 only. An initial screen using these samples evaluated the optimal amplification conditions for the P1P2 and P3P4 primer pairs. After the initial one-step RT-PCR reaction, an additional round of cDNA amplification was performed. It was determined that the RNA derived from 2 million cells resulted in the strongest amplicon bands. A detailed protocol and thermocycler conditions are reported in

experimental section 7.7.
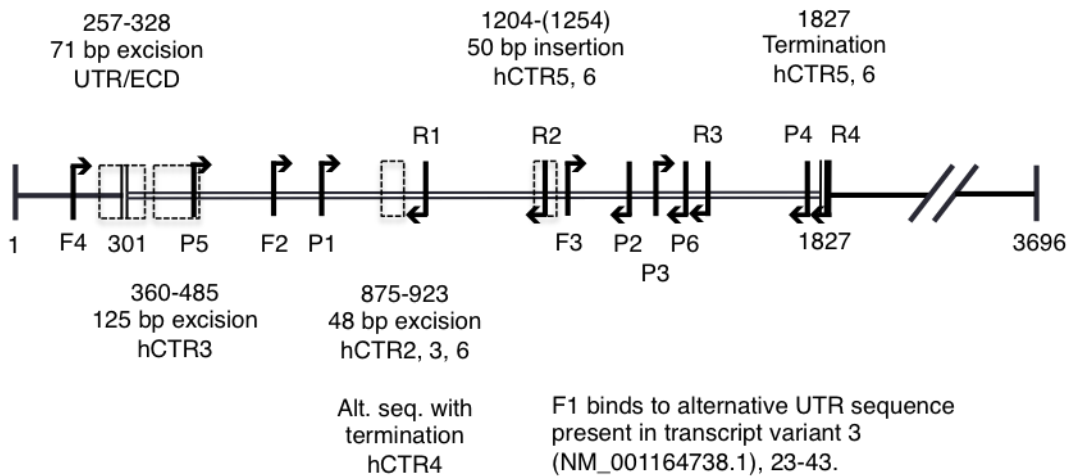
Figure 4.2: *A homology model of hCTR cDNA with all primers discussed in this chapter aligned to the NM_001164737.1 reference sequence (hCTR1).* Vertical black bars represent primer-binding locations, and the arrowheads indicate primer direction. P1-P4 reported by Wu and coworkers,[175] F1-F4 and R1-R4 reported by Silvestris and coworkers,[176] and P5 and P6 designed herein. P1, P3, P5 and F1-F4 are forward primers, while P2, P4, P6 and R1-R4 are reverse primers. Primer binding positions are reported in experimental section 7.7. Base pair positions are in reference to the NM_001164737.1 sequence.

In **Figure 4.3**, DMS53 cDNA amplification with primer pair P1P2 produced a band at a migration consistent with the 674 bp amplicon, or a slightly truncated version of it. No bands were detected in the PC3 lane when amplified with P1P2. DMS53 samples amplified with the P3P4 primers generated a product at a migration consistent with the 339 bp amplicon, as well as a smaller second band. Multiple products were observed in the PC3 sample, however they were smaller that those in the DMS53 sample. Amplification of DMS53 cDNA by the P1P2 and P3P4 primer pairs indicates that hCTR mRNA is transcribed in DMS53 cells. However, the identity of the product generated by P3P4 amplification in the PC3 sample is not clear, as hCTR mRNA transcription and thus amplification was not expected. In order to confirm the identity of the observed bands in both DMS53 and PC3 samples, each sample was sequenced. The results are summarised in **Table 4.1**.

Figure 4.3: *Agarose gel displaying the amplified products from the first RT-PCR approach.* '-' refers to a control experiment with no template mRNA.

Table 4.1: *Sequencing results for DMS53 and PC3 amplified products from the first RT-PCR approach.* Samples were generated through further amplification of the PCR products, using forward and reverse primers separately. Sequenced using Sanger sequencing with 3730xl DNA Analyzer from Applied Biosystems.

Amplicon (Primer)	Length	hCTR1 cDNA match regions: Query (Subject)	Identity	Gaps
DMS53 P1P2 (P1)	601	791-875 (38-122), 941-1399 (123-600)	473/478, 83/85	2/478, 0/85
DMS53 P1P2 (P2)	686	727-875 (596-447), 924-1337(446-33)	414/414, 148/150	0/414, 1/150
DMS53 P3P4 (P3)	307	1499-1795 (12-307)	292/298	3/298
DMS53 P3P4 (P4)	265	1504-1761 (257-6)	235/258	6/258
PC3 P1P2 (P1)	637	No match		

PC3 P1P2 (P2)	463	No match		
PC3 P3P4 (P3)	441	1521-1803 (37-315)	262/285	8/285
PC3 P3P4 (P4)	444	1453-1657 (297-104)	185/206	13/206

The sequences of the DMS53 forward and reverse amplicons generated by the P1P2 and P3P4 primer pairs in **Table 4.1** show an almost complete identify match with the hCTR model sequence (**Figure 4.1**) when aligned. This provides strong evidence that hCTR mRNA is transcribed in DMS53 cells. Surprisingly, the sequences of the PC3 forward and reverse amplicons generated by P3P4 also have regions of sequence homology with the hCTR model sequence, although the identify match was lower than sequences amplified from DMS53. This was not observed in sequences generated by the P1P2 primer pair however. Although the majority of reports in the literature characterise PC3 cells as hCTR-negative,[152, 153] there have been accounts of hCTR mRNA transcription in the cell line.[180] Given the discrepancy between the identity matches of the P1P2 and P3P4 amplicons with the hCTR model sequence, a definitive conclusion regarding the presence of hCTR mRNA in the PC3 cells could not be made. Since this was not relevant to the investigation into DMS53 cells, it was not pursued further.

The P1P2 primer pair amplifies a region of hCTR cDNA containing the 48 bp excision that distinguishes hCTR isoforms 2, 3 and 6. The sequences of the forward and reverse DMS53 P1P2 amplicons show a gap of at least 49 bp from base pair 875 in this region when aligned to the hCTR model sequence. This indicates that in DMS53 cells the 48 bp excision most likely occurs. Conversely, no gap was observed in the amplicon sequence from base pair 1204, indicating that the 50 bp excision associated with hCTR5 and 6 is

not present. Together, this suggests that the most likely isoforms transcribed in DMS53 are hCTR 2 or 3. Compared to hCTR2, hCTR3 is characterised by additional truncation in the ECD, which may affect ligand binding. Therefore, it was desirable to distinguish which of these isoforms is present in DMS53.

4.3 Identification of the Human Calcitonin Receptor mRNA Isoform in DMS53 and TT Cell Lysate using Reverse Transcription PCR

In order to distinguish hCTR2 from hCTR3, a primer pair that amplifies the region encompassing the 125 bp excised (at position 360-485 on hCTR model sequence) from hCTR3 in the putative ECD was designed using the NCBI Primer-BLAST database[177] (P5P6). The P5 binding region overlaps with the 125 bp excised region, while P6 binds to an isoform-generic region near P2 (**Figure 4.2**). Amplification with this primer pair would occur only if isoforms other than hCTR3 are transcribed in DMS53, as P5 would be unable to bind to hCTR3 cDNA. Since it was concluded from the previous approach that either hCTR2 or 3 mRNA is transcribed in DMS53, amplification would indicate that hCTR2 cDNA is present.

The RT-PCR protocol was refined from the first approach. Given the ambiguity of hCTR mRNA transcription in PC3 cells encountered in the previous approach, a positive control was included in this approach. RNA derived from the TT cell line, a medullary thyroid carcinoma reported to express hCTR2,[63] was amplified to allow comparison with DMS53 RNA. Cells were harvested at 60-70% confluence, as hCTR mRNA concentration is likely to be highest when cells are actively dividing. RNA was extracted from 10 million cells, thus the second round of amplification after the initial RT-PCR step used in the first approach was not required. A detailed protocol and thermocycler

conditions are described in experimental section 7.7. Primer pairs P1P2, P5P6, P1P6 and P5P2 were tested against both DMS53 and TT cDNA. The agarose gel displaying the resulting amplicon bands is presented in **Figure 4.4**.

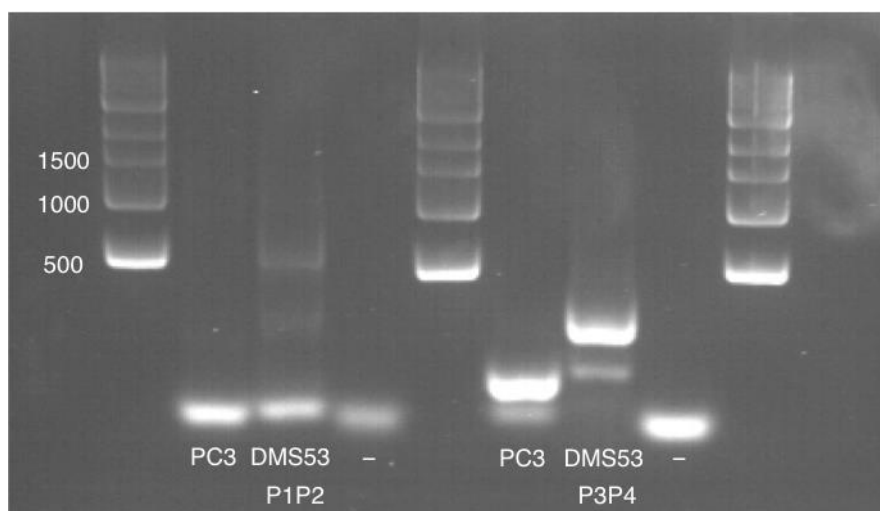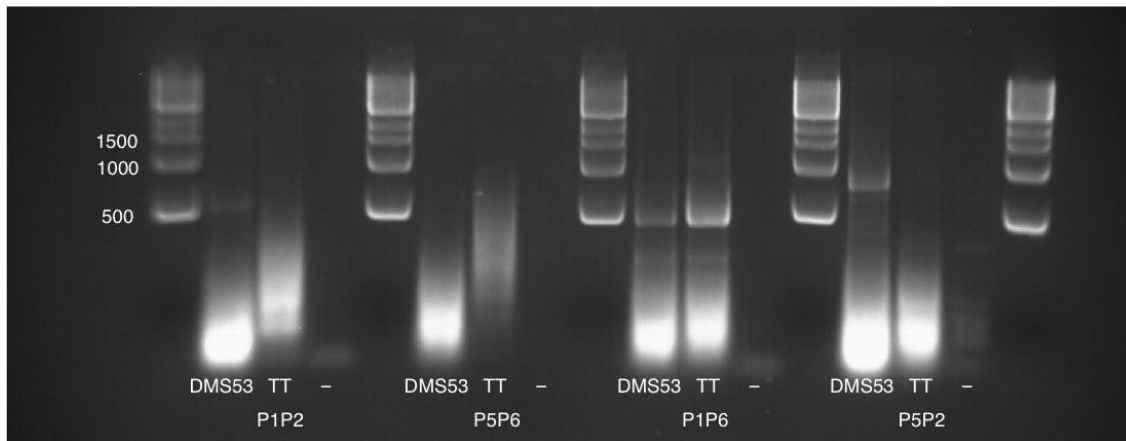**Figure 4.4:** *Agarose gel displaying the amplified products from the second RT-PCR approach.* '-' refers to a control with no template mRNA.

As with the first approach, the amplification of DMS53 cDNA with P1P2 primers produced a faint band at a migration consistent with the 674 bp amplicon. No products were observed when amplified with P5P6. Surprisingly, given TT is reported to express hCTR2 mRNA, no product was detected with P1P2 amplification. A similar result was observed when TT and DMS53 cDNA was amplified using P5P2; a band at a migration consistent with 932 bp amplicon was observed in the DMS53 sample, but no amplification was observed for the TT sample. Although it is not clear why, P2 did not amplify TT cDNA. This could be related to the relative primer affinity of P2 or cDNA concentration in the TT samples. Regardless, products at migrations consistent with 717 bp were identified in both the DMS53 and TT samples when amplified using the primer pair P1P6, confirming the presence of hCTR cDNA in DMS53 and TT samples.

For the P5P2 forward sequence to be amplified, P5 must have bound to the hCTR cDNA, proving the 125 bp excision associated with hCTR2 is not present in at least a proportion

of the hCTR mRNA in DMS53 cells. This means hCTR2 mRNA is transcribed in DMS53. In order to confirm the identity of the amplicons observed, sequencing was undertaken on the RT-PCR products. The results are summarised in **Table 4.2**. The sequences of the forward and reverse P1P6 amplicons from DMS53 and TT are almost identical, with similar amplicon length and the characteristic 48 bp excision at base pair 875, as observed previously. The DMS53 P5P2 forward sequence and the P1P2 forward sequence also display this excision, however neither of the P2 reverse sequences displayed matches with the model sequence.

Table 4.2: *Sequencing results for DMS53 and TT RT-PCR samples from the second RT-PCR approach. Samples were generated through further amplification of the RT-PCR product, using forward and reverse primers separately. Sequenced using Sanger sequencing with 3730xl DNA Analyzer from Applied Biosystems.*

Amplicon (Primer)	Length	hCTR1 cDNA match regions: Query (Subject)	Identity	Gaps
DMS53 P1P2 (P1)	1249	938-1399 (145-604)	416/463	4/463
DMS53 P1P2 (P2)	1256	No match.		
DMS53 P1P6 (P1)	523	792-875 (37-119), 924-1324 (120-519)	387/402, 74/83	3/402, 0/83
DMS53 P1P6 (P6)	535	731-875 (528-385), 924-1294 (384-17)	338/372, 144/145	5/372, 1/145
DMS53 P5P2 (P5)	844	490-875 (49-435), 924-1330 (436-844)	400/409, 361/387	2/409, 1/387
DMS53 P5P2 (P2)	476	No match.		

			398/403,	2/403,
TT P1P6 (P1)	540	768-875 (13-118), 924-1324 (119-521)	105/108	2/108
			376/383,	5/383,
TT P1P6 (P6)	525	738-875 (523-386), 924-1306 (385-8)	138/138	0/138

The forward and reverse sequences of the P1P6 amplicons for the DMS53 and TT samples exhibited the 48 bp excision at base pair 875 characteristic of hCTR2 and 3. Amplification of the forward sequence of P5P2 in DMS53 indicated that P5 had bound to hCTR mRNA not exhibiting the 125 bp excision associated with hCTR3. By the process of elimination, this means that hCTR2 must be transcribed in DMS53, although it does not rule out the possibility of hCTR3 co-transcription. Given this possibility, primer pairs amplifying the entire region of hCTR isoform-defining excisions would be required to determine if multiple isoforms are transcribed in DMS53.

4.4 Assessment of Human Calcitonin Receptor mRNA Variant Co-transcription in DMS53 and TT Cell Lysate using Reverse Transcription PCR

In 2008, Silvestris and coworkers[176] published 8 primers (four forward primers (F1-4) and four reverse primers (R1-4)) designed to bind different regions of an hCTR sequence derived from osteoclasts,[107] but the results from the use of only one of these combinations were displayed. The hCTR model sequence described previously (**Figure 4.1**) was used to identify the binding regions of each primer and find those suitable for distinguishing the 125 bp excision associated with hCTR3 and the 48 bp excision

associated with hCTR2. Further, this would allow the 71 bp excision at the UTR/ECD interface observed by Nishikawa and coworkers,[107] unaccounted for in the analysis of hCTR isoforms by Beaudreuil and coworkers,[97] to also be interrogated.

Several discrepancies were identified between the analysis of primer utility performed in this work and the utility outlined in the publication. For example, the primer pair F2R3 was said to be designed to identify the 48 bp excision associated with hCTR2, and the 125 bp excision in hCTR3. However, based on **Figure 4.2**, primer F2 actually binds 300 bp after this excision, at base pair 619, and thus cannot amplify this region. Primer R2 was designed to bind to the 50 bp insert present in hCTR5 and 6 at position 1204, but did match the sequence in the RefSeq database[177] relating to hCTR cDNA. The F1 primer did match the model hCTR sequence but to an alternative sequence in the UTR of hCTR transcript variant 3 according to the RefSeq database. As a result, the primer pairings proposed by Silvestris and coworkers were adapted.

Instead of F2R3, the primer pair F4R3 was used as it amplifies a region encompassing the 125 bp hCTR3 excision, the 48 bp hCTR2 excision and the 71bp UTR/ECD excision. Amplifying DMS53 cDNA with the F4R3 primer pair was expected to identify the combinations of excisions that occur together, and whether multiple hCTR variants occur. Based on the earlier approaches used, the length of the F4R3 amplicon in DMS53 is 1321 bp, accounting for the presence of the hCTR2 excision and the lack of the hCTR3 and UTR/ECD excisions. If all excisions were present, an amplicon length of 1125 bp would be observed. If multiple amplicons were observed, this would indicate that more than one isoform of hCTR mRNA is transcribed in DSM53.

 TT cells were used again as a control. The primer pair F3R3, which binds to an isoform-generic region of the hCTR mRNA and produces an amplicon of 296 bp, was used as a control for mRNA sample quality. To avoid the variation in TT and DMS53 amplification

with the same primer pair in the previous approach, the cell culture protocol was altered to standardise cell growth between flasks. The cells were then lysed, and RNA was isolated from approximately a quarter of the total lysate. An additional DNase cleanup and purification step was included in the extraction protocol. mRNA concentration and quality was estimated by nanodrop. A detailed protocol and thermocycler conditions are reported in experimental section 7.7. The results of the RT-PCR approach are presented in **Figure 4.5.**
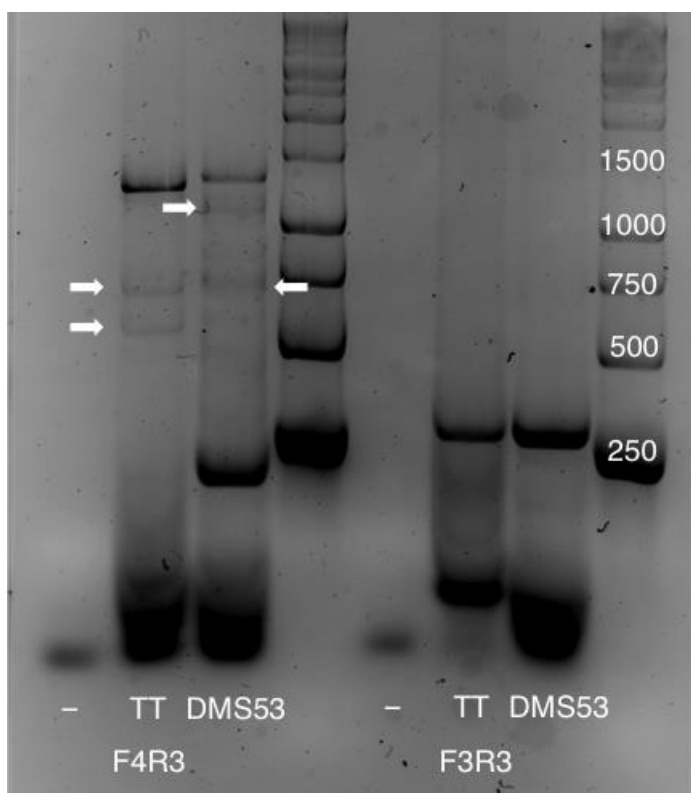
Figure 4.5: *Agarose gel displaying the amplified products from the third RT-PCR approach. '-' refers to a* control with no template mRNA.

In **Figure 4.5**, the amplicons produced in the DMS53 and TT samples for primer pairs F4R3 and F3R3 are compared. Amplification with F3R3 produced a band at a migration consistent with 296 bp, confirming hCTR transcription in both DMS53 and TT cells.

Amplification with F4R3 produced a major band at a migration consistent with 1300 bp in both the TT and DMS53 samples. This amplicon is consistent with the presence of hCTR2 cDNA. In the TT sample, additional minor bands at migrations consistent with 750 bp and 600 bp (marked with white arrows) were observed. In the DMS53 sample, weaker bands at migrations consistent with 1100 bp and 750 bp (marked with white arrows) were observed, as well as an intense band consistent with 250 bp. The larger minor band (1100 bp) may represent another isoform of hCTR with the 48, 71 and 125 bp excisions. The smaller products (600-700 bp) do not correlate with any expected amplicons, and may be the result of the fragmentation of the full-length amplicon. The origin of the 250 bp product in DMS53 cells is also unclear. Due to the mixture of amplified products observed in each sample, sequencing was not pursued. Nevertheless, these observations confirm that hCTR2 mRNA is transcribed in DMS53, even though it may not be the only variant present.

In summary, analysis of extracted RNA using RT-PCR showed that hCTR2 mRNA is present in DMS53. The first approach demonstrated that the 48 bp excision associated with hCTR2 occurred in DMS53 hCTR mRNA, while the second approach showed that this excision did not occur alongside the 125 bp excision associated with hCTR3. The third approach demonstrated that hCTR2 is again present but might not be the only mRNA variant transcribed. The confirmation of not only hCTR transcription but also expression in DMS53 required that the hCTR protein be characterised. This would possibly also allow the isoform of the expressed protein to be determined.

4.5 Detection and Characterisation of Human Calcitonin Receptor Immunoreactivity in DMS53 using Western Blot Analysis

Numerous reports have demonstrated expression of hCTR in various cell types by Western analysis.[153, 173, 178, 181] Wookey and coworkers[178] report a 70 kDa protein corresponding to the fully glycosylated membrane protein hCTR and a smaller protein at 52 kDa, presumably belonging to the non-glycosylated protein, Alternatively Segovia-Silvestre and coworkers,[173] Liu and coworkers,[181] and Aljameeli and coworkers[153] report proteins migrating between 50 kDa and 60 kDa corresponding to an hCTR isoform (predicted MWs of the isoforms according to amino acid analysis are hCTR1: 59 kDa, hCTR2: 55 kDa, hCTR3: 49 kDa, hCTR4: 22 kDa, hCTR5: 34 kDa, hCTR6: 32 kDa).[98] Upon assessing the methodologies used, the latter three reports used a cytosol-targeted lysis with RIPA buffer, while Wookey and coworkers used membrane-targeted lysis with Lamelli buffer. The RIPA lysis buffer was chosen for use in this work in order to try and establish a clearer picture of which hCTR isoform is expressed. Glycosylation typically causes the protein to run as a smear, making detecting various sized proteins complicated, so lysis with Lamelli buffer was avoided. A rabbit polyclonal antibody raised against hCTR2 (RefSeq: NP_001733.1) was obtained from Abcam (ab103422) for the purpose of identifying hCTR in DMS53 cells, with target protein predicted to have a molecular weight of 55 kDa.[182]

DMS53 cells were grown to confluence, lysed, and the protein extract cleared by centrifugation. The protein concentration was determined using a DC BioRad protein assay with BSA as a standard curve. The lysates were denatured at 95 °C in the presence of β-mercaptoethanol and 15 µg, 23 µg and 30 µg of protein lysate was loaded onto a precast 4-20% polyacrylamide gel. The gel was run for approximately 2 hours, after which time the proteins were transferred to a PVDF membrane. The membrane was

blocked and incubated with 15 μg of the primary antibody overnight. The following day the membrane was washed then incubated with the secondary anti-rabbit-HRP antibody (1.5 μg) for 1 hour before final washing. The protein was detected using chemiluminescent imaging with ECL Western blotting reagents. A detailed lysis protocol and Western blot protocols are outlined in experimental section 7.8. The result of this investigation is illustrated in **Figure 4.6**.
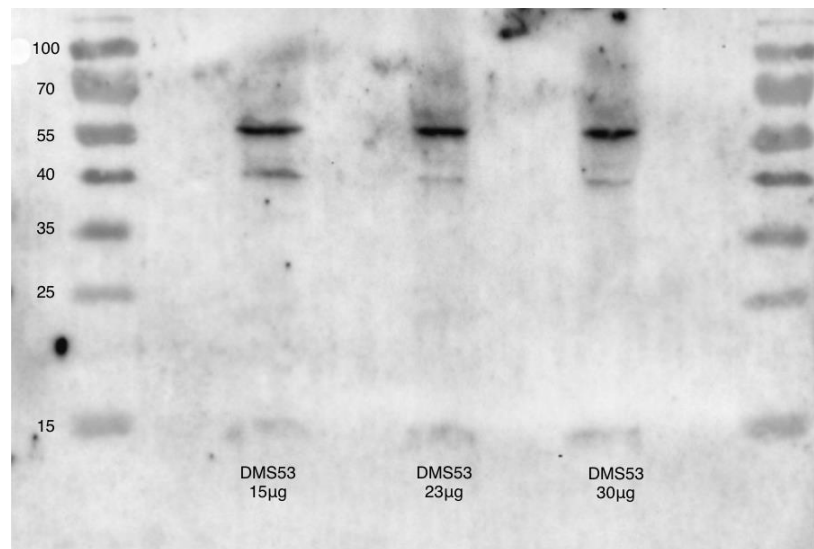
Figure 4.6: *Western blot of DMS53 lysate imaged with an hCTR2-specific antibody comparing different loading amounts of total lysate protein.*

An intense immunoreactive band was observed, independent of protein concentration, at a migration consistent with 55 kDa, the predicted molecular weight of hCTR2. There was also a protein detected at approximately 40 kDa. Since there is no obvious correlation with the predicted molecular weight of any other isoform, it is more likely to be non-specific binding or degradation of hCTR2. It was concluded that 25 μg of protein is an appropriate loading amount for the detection of hCTR, and that hCTR (most likely hCTR2) is expressed in DMS53. In order to validate the hCTR isoform expressed, comparison between the protein observed in DMS53 and the protein observed in a cell line expressing a known hCTR isoform was therefore performed.

4.6 Comparison of Human Calcitonin Receptor Immunoreactivity in DMS53, DU145 and PC3 Cell Lysate using Western Blot

In work described by Aljameeli and coworkers,[153] DU145 and PC3 (prostate cancer cell lines) were used as positive and negative controls respectively for Western blot analysis of hCTR2-transfected cell line protein lysate. Thus protein lysate samples were prepared from these cell lines as well as duplicate samples from DMS53, and were then analysed using Western blot as described previously, except that the protein lysate (25 µg) was separated by SDS-PAGE for a longer time (2½ h) to improve the resolution of the blot. The protocol is described in detail in experimental section 7.8, and the resulting blot is displayed in **Figure 4.7**.
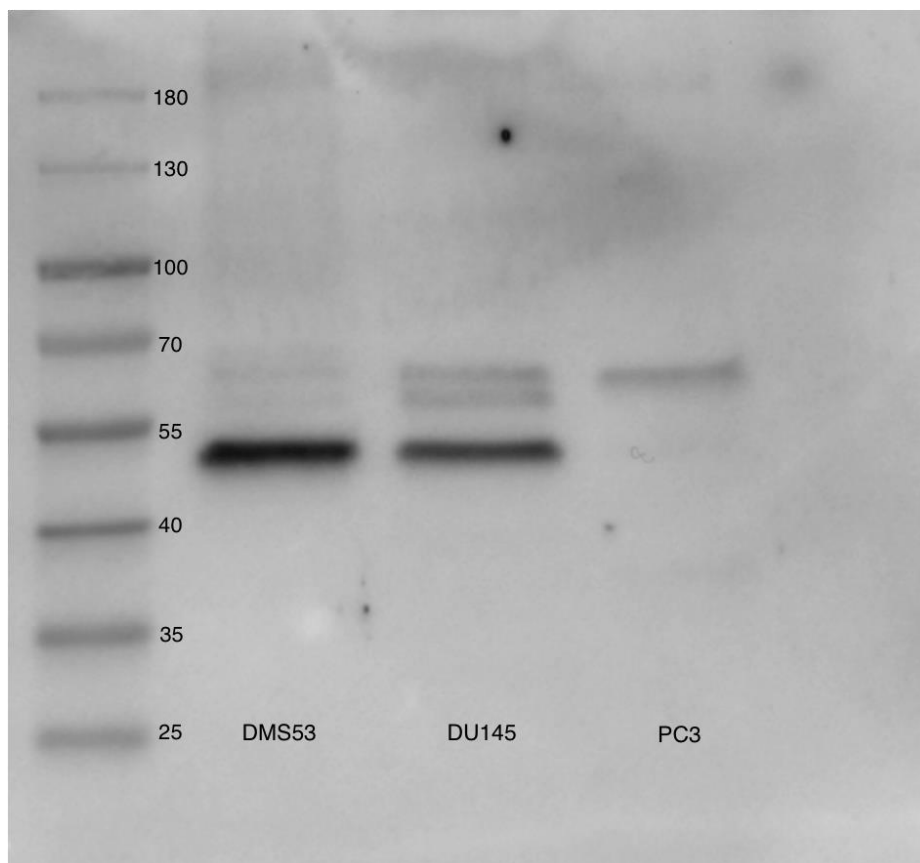
Figure 4.7: *Western blot of DMS53, DU145 and PC3 lysate imaged with an hCTR2-specific antibody.*

In the DMS53 sample, a protein with a migration of approximately 50 kDa was observed. A band with the same migration was also observed in the DU145 sample, and was not observed in the PC3 sample. This appears to be the same major band observed in the first experiment based on the intensity, and therefore corresponds to hCTR. Since hCTR2 is expressed in DU145, the co-migration of the DU145 band with the DMS53 band confirms hCTR2 expression in DMS53. The difference in migration compared to the previous experiment may be due to the increased blot resolution as a result of longer SDS-PAGE separation. Since hCTR is not expressed in PC3 cells, it is likely the bands common to the PC3 sample and the other samples are the result of non-specific binding rather than other hCTR isoforms.

4.7 Conclusions

Using RT-PCR and Western blot analysis, the presence of hCTR mRNA and protein was shown in DMS53 cells. Specifically, hCTR2 mRNA was present in DMS53, as was the protein. Evidence of mRNA transcripts that may correspond to smaller hCTR isoforms was observed in the RT-PCR studies. Since the antibody used in the Western blot experiments was raised against hCTR2, it is not clear if it would identify other hCTR isoforms. Therefore, the co-expression of smaller hCTR isoforms with hCTR2 in DMS53 remains a possibility. Although hCTR mRNA has been identified in lung cancer cells previously,[183] this study represents the first characterisation of an hCTR isoform in a lung cancer cell line. The presence of hCTR2 in DMS53 cells implies that both the Ca^{2+}- and cAMP-dependent signalling pathways could be utilised in this cell line when the receptor is activated.

In the work described in Chapter 3, it was observed that application of the hCTR agonist SUNB8155 to DMS53 cultures increased the proportion of CT relative to gCT in the

medium. This may have occurred through the up-regulation of PAM activity or expression, or an increase in CT precursor transcription. With the discovery of hCTR2 expression in DMS53, it is now reasonable to assume that the changes to the levels of CT-related species are the result of hCTR activation by SUNB8155, and that the cellular mechanisms responsible are most likely mediated by cAMP- or Ca^{2+}-dependent signal transduction. Selectively inhibiting enzymes in the signal transduction pathways would reveal which pathways are involved in the regulation of CT-related species in DMS53, and may help to discern the mechanisms the cell uses to control the production of these species. Work in Chapter 5 was therefore directed toward the treatment of DMS53 cultures with signalling enzyme inhibitors.

Chapter Five

Results and Discussion: Inhibition of Human Calcitonin Receptor Signal Transduction Enzymes and its Effect on the Levels of Calcitonin-Related Species in DMS53

5.1 Introduction

In the work described in Chapter 3, it was observed that treatment of DMS53 cultures with the hCTR agonist SUNB8155 at 100 μM concentration increased the proportion of CT in the medium, while levels in the lysate were unaffected. In the work described in Chapter 4, hCTR transcription and expression was characterised in DMS53 for the first time, and hCTR2 was identified as the isoform expressed. It was concluded that ostensible hCTR activation increased the production of CT and CT-related species in DMS53. Therefore, intramolecular signal transduction originating from hCTR is likely to mediate the biosynthesis of CT-related species within the cell. Understanding which pathways are utilised in the hCTR-dependent regulation of CT production would aid in the identification of the cellular mechanisms involved.

hCTR signal transduction is well characterised in the literature. It has been demonstrated that hCTR2 can bind $G_{\alpha s}$ and $G_{\alpha i}$, which up-regulate and down-regulate production of cAMP, respectively.[120] hCTR2 can also bind $G_{\alpha q}$, which up-regulates production of the secondary messenger Ca^{2+}.[162] As mentioned previously, it has been shown that the CT/CGRP gene (CALCA) has a cAMP responsive element (CRE)[170] as well as a more recently identified Ca^{2+}-dependent downstream regulating element

(DRE)[184] suggesting that gene expression and therefore CT transcription is linked to cAMP and Ca^{2+} flux. To identify whether a given hCTR signalling enzyme is involved in the regulation of CT-related species' production in DMS53 cells, the relative concentrations of the CT-related species could be monitored while hCTR signal transduction is selectively disrupted with inhibitors. The cAMP- and Ca^{2+}-mediated pathways were interrogated in this preliminary study (**Figure 5.1**)
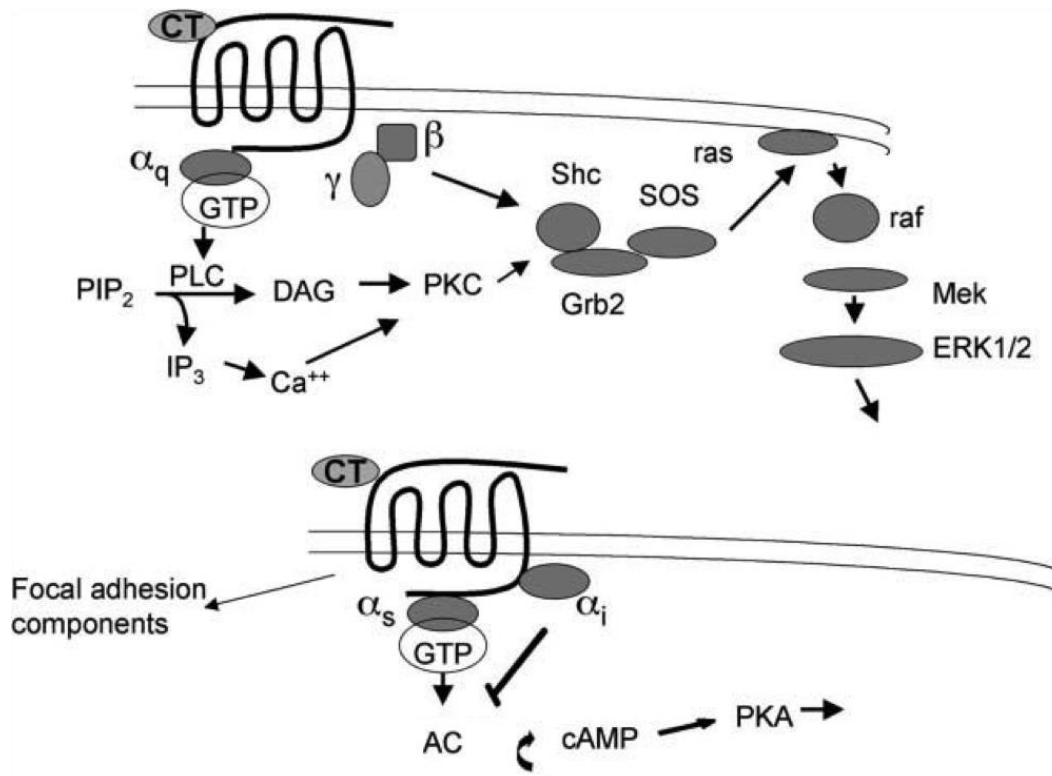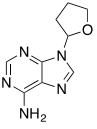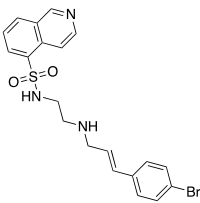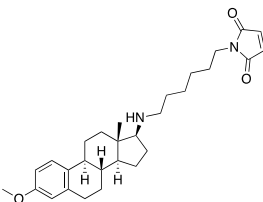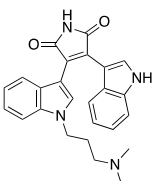
Figure 5.1: *The known Ca^{2+}-dependent (top) and cAMP-dependent (bottom) signal transduction pathways of hCTR.*[8] Used with permission from Elsevier.

Table 5.1: *hCTR signalling pathway inhibitors used in this study.*

Name	Structure	Primary Target	Efficacy (IC$_{50}$)	Mechanism	Specificity
SQ22536		AC	13 μM (human platelets)[185]	Non-competitive [186]	May also inhibit the neuritogenic cAMP sensor downstream of AC[187]
H89		PKA	10-30 μM (PC12D cells)[188]	Competitive with ATP[189]	Inhibits at least three other kinases with IC$_{50}$ comparable to PKA[189, 190]
U73122		PLC	1-13 μM (human platelets)[191]	Unknown, may be covalent through the alkylation of cysteine residues[192]	Interacts with ion channels; effects Ca^{2+} and K^{+} flux[192]
GF109203X (BIM1)		PKC	0.8-0.9 μM (human platelets)[193]	Competitive with ATP[194]	Inhibits all isoforms, low promiscuity[195]

The inhibitors used in the work are summarised in **Table 5.1**. Two enzymes in each of the cAMP- and Ca^{2+}-dependent signalling pathways were targeted with small molecule

inhibitors. In each pathway, the enzyme responsible for the generation of the secondary messenger was targeted; AC in the cAMP-dependent pathway, and PLC in the Ca^{2+}-dependent pathway. Additionally, the kinase responding to the respective secondary messenger was target in each pathway; PKA in the cAMP-dependent pathway, and PKC in the Ca^{2+}-dependent pathway. Small molecule inhibitors for each of the four enzymes were selected based on efficacy *in vitro* and common usage in the literature. Target promiscuity is a problem for many signalling enzyme inhibitors, particularly kinase inhibitors,[189] but the compounds selected are widely used for inhibiting the designated targets, and represent the best candidates available for this role.

5.2 Investigating the Effect of Signalling Pathway Inhibition on the Production of Calcitonin-Related Species by DMS53 Cells Using a First HPLC-Fluorescence Detection Method

Initial experiments to screen whether signalling inhibitors had an effect on the levels of CT-related species in the medium of treated DMS53 cultures used a variation of the second generation *in vitro* assay (described in experimental section 7.5), and were analysed using the first HPLC method, CT-M1 (described in experimental section 7.2). After reaching confluence, cultures were incubated for 24 h, before being treated with the relevant signalling enzyme inhibitor and incubated for a further 24 h. Inhibitors SQ22536 (100 μM) and H89 (1 μM) were tested in parallel, as were inhibitors U73122 (10 μM) and GF109203X (2 μM), as each pair targets enzymes in the same transduction pathway (the cAMP-dependent and Ca^{2+}-dependent pathways, respectively). Treatment concentrations were based on literature reports for specificity *in vitro*,[120, 196, 197, 198] with experiments repeated twice with concordant results. Representative medium chromatograms of cultures treated with SQ22536 and H89 are presented in **Figure 5.2**,

and those treated with U73312 and GF109203X are presented in **Figure 5.3**.

Figure 5.2: *HPLC chromatograms of* **A:** *DMS53 culture medium after incubation for 48 h, analysed using CT-M1;* **B:** *DMS53 culture medium, after incubation for 24 h, treatment with SQ22536 (100 μM) and incubation for a further 24 h, analysed using CT-M1.* **C:** *DMS53 culture medium, after incubation for 24 h, treatment with H89 (1 μM) and incubation for a further 24 h, analysed using CT-M1.*

Figure 5.3: *HPLC chromatograms of* **A:** *DMS53 culture medium after incubation for 48 h, analysed using CT-MI;* **B:** *DMS53 culture medium, after incubation for 24 h, treatment with U73122 (10 μM) and incubation for a further 24 h, analysed using CT-MI.* **C:** *DMS53 culture medium, after incubation for 24 h, treatment with GFI09203X (2 μM) and incubation for a further 24 h, analysed using CT-MI.*

In **Figure 5.2B**, treatment with SQ22536 increased the CT to CT-G ratio from 0.50 in the control culture medium, to 0.61 in the treated culture medium. The ratios of the CT and CT-G peaks to the peak at 34 min (later discovered to be gCT) also increased. The CT to gCT ratio increased from 1.07 in the control medium (**Figure 5.2A**) to 1.66 in the treated culture medium. The CT-G to gCT ratio increased from 2.15 in the control medium to 2.74 in the treated culture medium. The H89 treatment (**Figure 5.2C**) had no affect on CT-related species ratios. H89 concentration was increased to 10 μM and again, no effect was observed (data not shown). In **Figure 5.3B**, treatment of DMS53 cultures with U73122 did not change the CT to CT-G ratio in the medium compared to the control (**Figure 5.3A),** however a new large peak appeared at 50 min. GF109203X treatment of DMS53 cultures (**Figure 5.3C**) increased the CT to CT-G ratio to 0.68, from a ratio of 0.51 in the control culture medium.

These experiments suggest that SQ22536 and GF109203X have an effect on the levels of CT-related species in the medium of treated cultures. U73122 may also have an effect on the species secreted by DMS53 cultures, based on the appearance of a large new peak in the medium. However, given the size of this peak compared to the other species in the medium chromatogram, it may be of exogenous origin. H89 appeared to have no effect on the levels of CT-related species in the medium. With the discovery of the glycosylated CT-related species in the course of this work and the development of an HPLC method to separate and quantify these species (as described in Chapter 2), these preliminary results suggested that subsequent experiments should focus on comparing the effect of GF109203X, SQ22536 and U73122 on the levels of glycosylated and non-glycosylated CT and CT-G in the medium of DMS53 cultures. As H89 had no effect on CT-related species, the target enzyme PKA was not implicated as a potential mediator of hCTR signal transduction. As a result no further experiments with this inhibitor were pursued.

5.3 Investigating the Effect of Signalling Pathway Inhibition on the Production of Calcitonin-Related Species by DMS53 Cells Using a Second HPLC-Fluorescence Detection Method

In order to investigate whether signalling enzyme inhibitors affected the levels of gCT and gCT-G in the same way as CT and CT-G, treatment of DMS53 cultures with SQ22536 and U73122 followed the second generation DMS53 *in vitro* assay methodology (outlined in experimental section 7.5), and were analysed using CT-M2 (outlined in experimental section 7.3). Experiments were repeated twice with concordant results. The treatment concentration of U73122 was increased to 40 µM; treatment at this concentration is still specific to PLC.[197] The effect of GFI09203X treatment was explored in a subsequent experiment.

In **Figure 5.4**, a representative medium chromatogram of a DMS53 culture treated with 100 µM SQ22536 is compared to that of a control culture. In **Figure 5.4A**, the CT to CT-G and gCT to gCT-G ratios in the control culture medium are equivalent, at 0.46, and the non-glycosyated to glycosylated ratio was 1.29. In **Figure 5.4B**, a DMS53 culture treated with SQ22536 showed CT to CT-G and gCT to gCT-G ratios of 0.45 and 0.39 respectively, while the non-glycosylated to glycosylated species ratio was 1.66.

In **Figure 5.5**, a representative medium chromatogram of a DMS53 culture treated with 40 µM U73122 is compared to that of a control culture. In **Figure 5.5B**, the culture treated with U73122 produced a large peak at 61 min. This is presumably the same species that was detected at 50 min in the first experiment. In **Figure 5.5C**, a chromatogram of U73122 in MilliQ showed that no peak was observed at 61 min. Accurate integration of the CT and CT-G peaks could not be obtained due to the overlap with the 61 min peak. The gCT to gCT-G ratio in the control (**Figure 5.5A**) was 0.69, while in the treated culture, a ratio of 0.67 was observed.
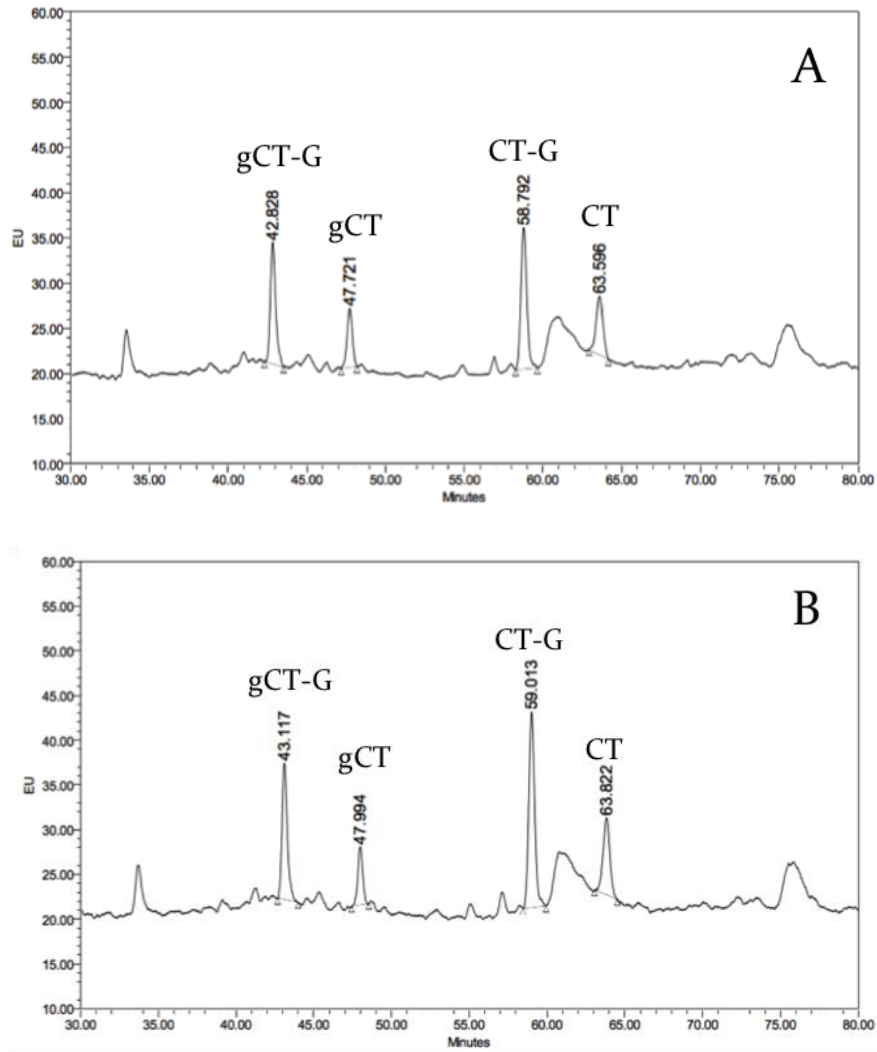
Figure 5.4: *HPLC chromatograms of* **A:** *DMS53 culture medium after incubation for 24 h, analysed using CT-M2;* **B:** *DMS53 culture medium, after treatment with SQ22536 (100 μM) and incubation for 24 h, analysed using CT-M2.*
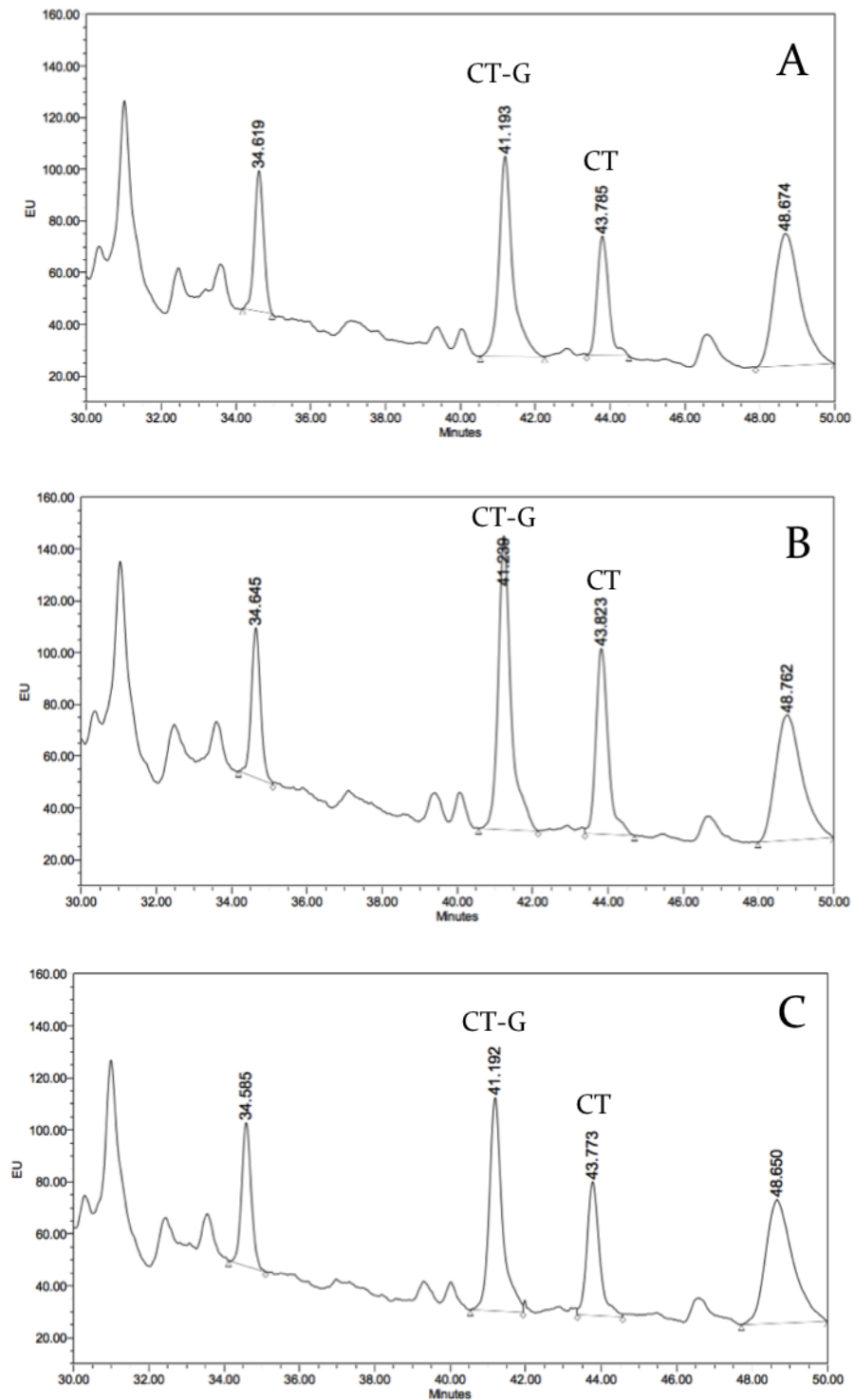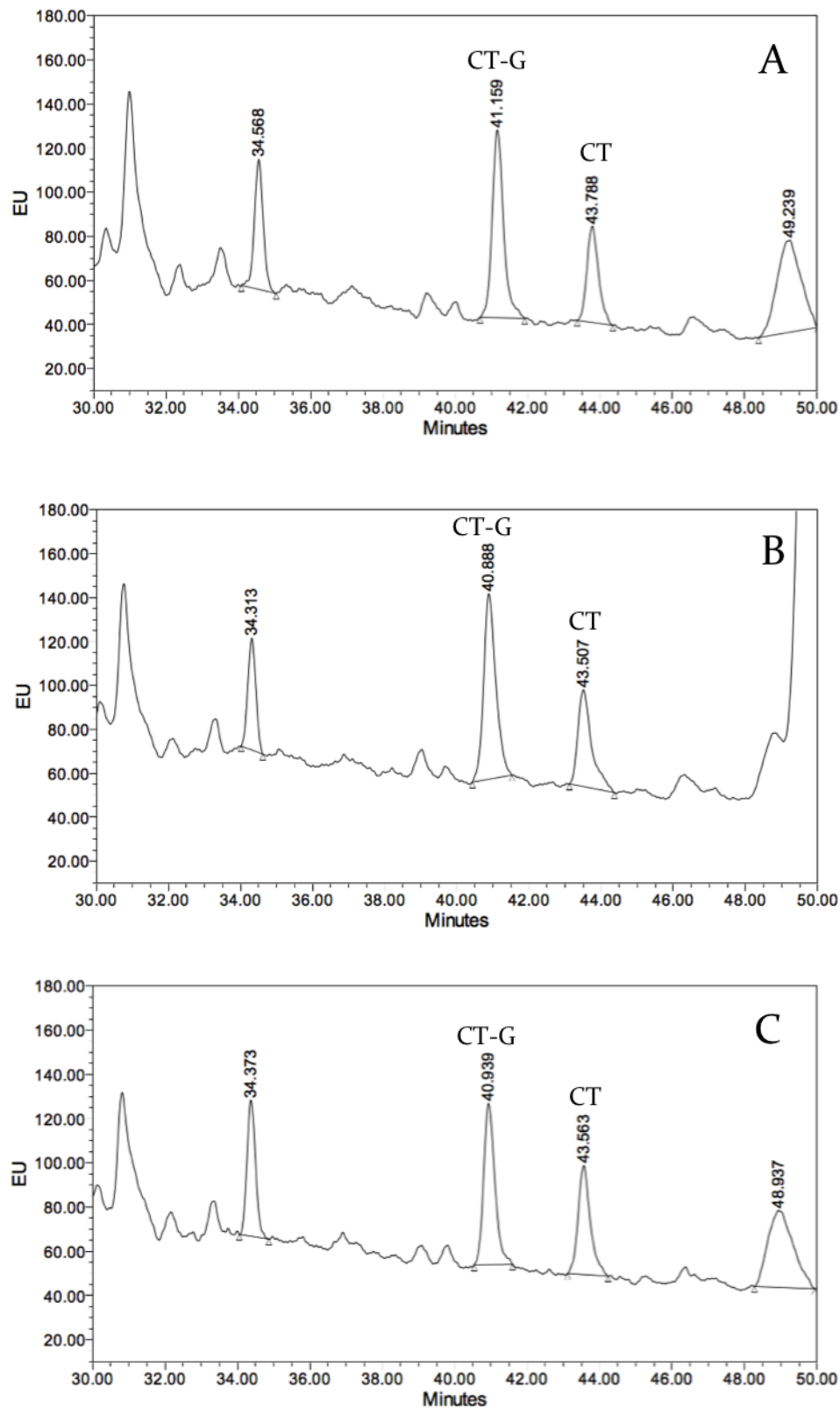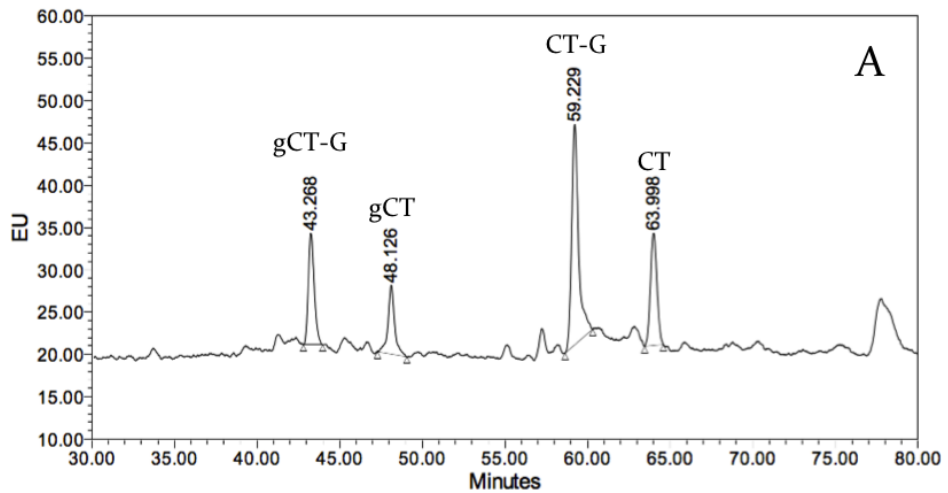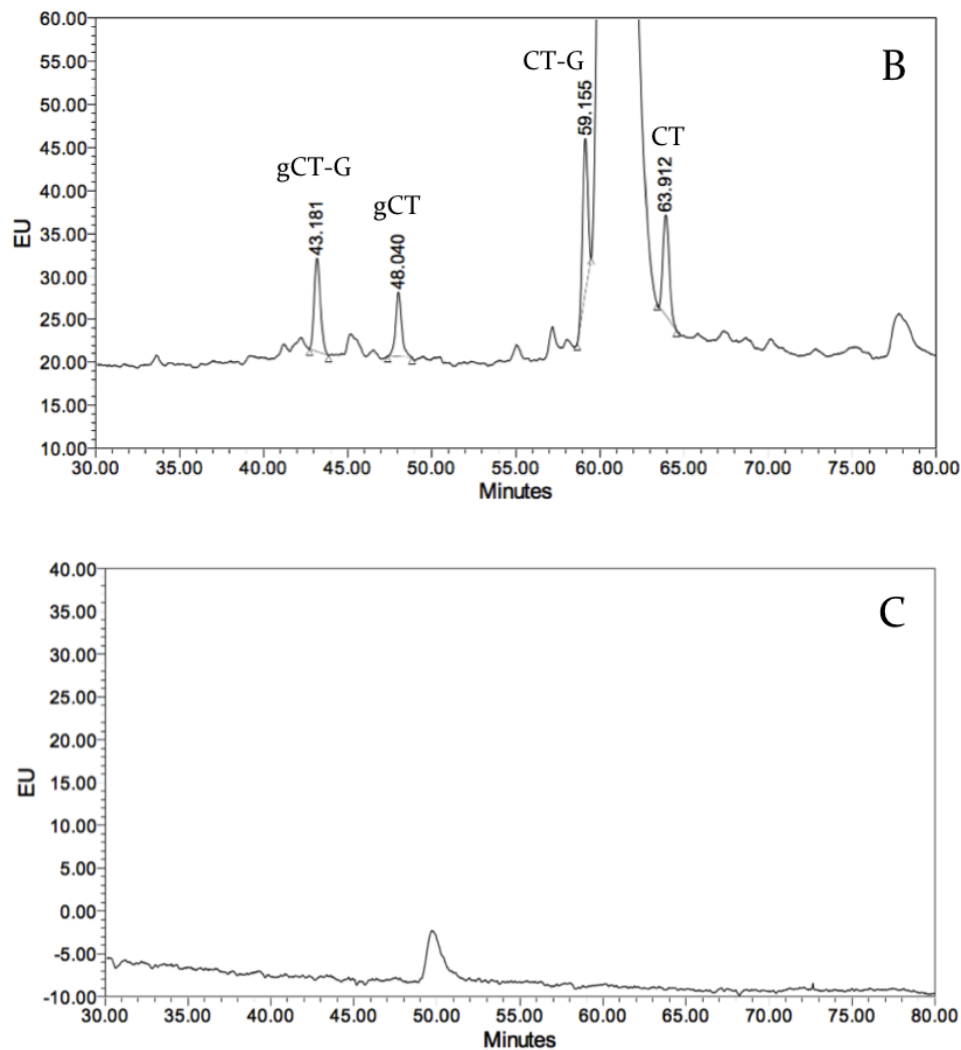
Figure 5.5: *HPLC chromatograms of* **A:** *DMS53 culture medium after incubation for 24 h, analysed using CT-M2;* **B:** *DMS53 culture medium, after treatment with U73122 (40 μM) and incubation for 24 h, analysed using CT-M2;* **C:** *U73122 (5 μM) in MilliQ water, analysed using HPLC CT-M2.*

Treatment of DMS53 cultures with SQ22536 may have had a small effect on the ratio of non-glycosylated species to glycosylated. U73122 treatment caused a large peak to be observed at 61 min, interfering with the integration of CT and CT-G. As the mechanism of action is thought to proceed via the alkylation of cysteine residues,[192] it may be that this peak originated from an alkylated peptide or protein. Alternatively, the inhibitor may degrade and generate a fluorescently active species. In any event, due to incompatibility with the assay, U73122 was abandoned as a signalling pathway probe.

In the work described in Chapter 3, a more robust assay was designed which allowed changes in the levels of CT-related species in the medium and lysate of DMS53 cultures to be averaged across experimental replicates. This meant that the effect of SUNB8155 could be quantified, and distinguished from experimental variation. Because the possible effects of SQ22536 in the previous experiment appeared to be small, this methodology was employed to provide evidence of whether levels of CT-related species change significantly in response to SQ22536 treatment. It would also allow the effects on CT-related species in the lysate to be assessed. As the effects of GFI09203X on the levels of gCT and gCT-G had not been assessed by the time this methodology was developed, GFI09203X was also be tested using the new methodology.

5.4 Investigating the Effect of Signalling Pathway Inhibition on the Production of Calcitonin-Related Species by DMS53 Cells with a More Robust Assay.

Using the third generation *in vitro* assay (outlined in experimental section 7.6) and the HPLC method CT-M2, the effect of SQ22536 (100 µM) and GFI09203X (10 µM) on the levels of CT-related species in DMS53 medium and lysate was interrogated. The treatment concentration of GFI09203X was increased from 2 µM to 10 µM (GFI09203X is still selective for PKC at this concentration).[198] The experiment was repeated three times with concordant results. Representative medium chromatograms are presented in **Figure 5.6**, while lysate chromatograms are shown in **Figure 5.7**. Summaries of the ratio changes between CT-related species are presented in **Table 5.2** to **Table 5.4**.
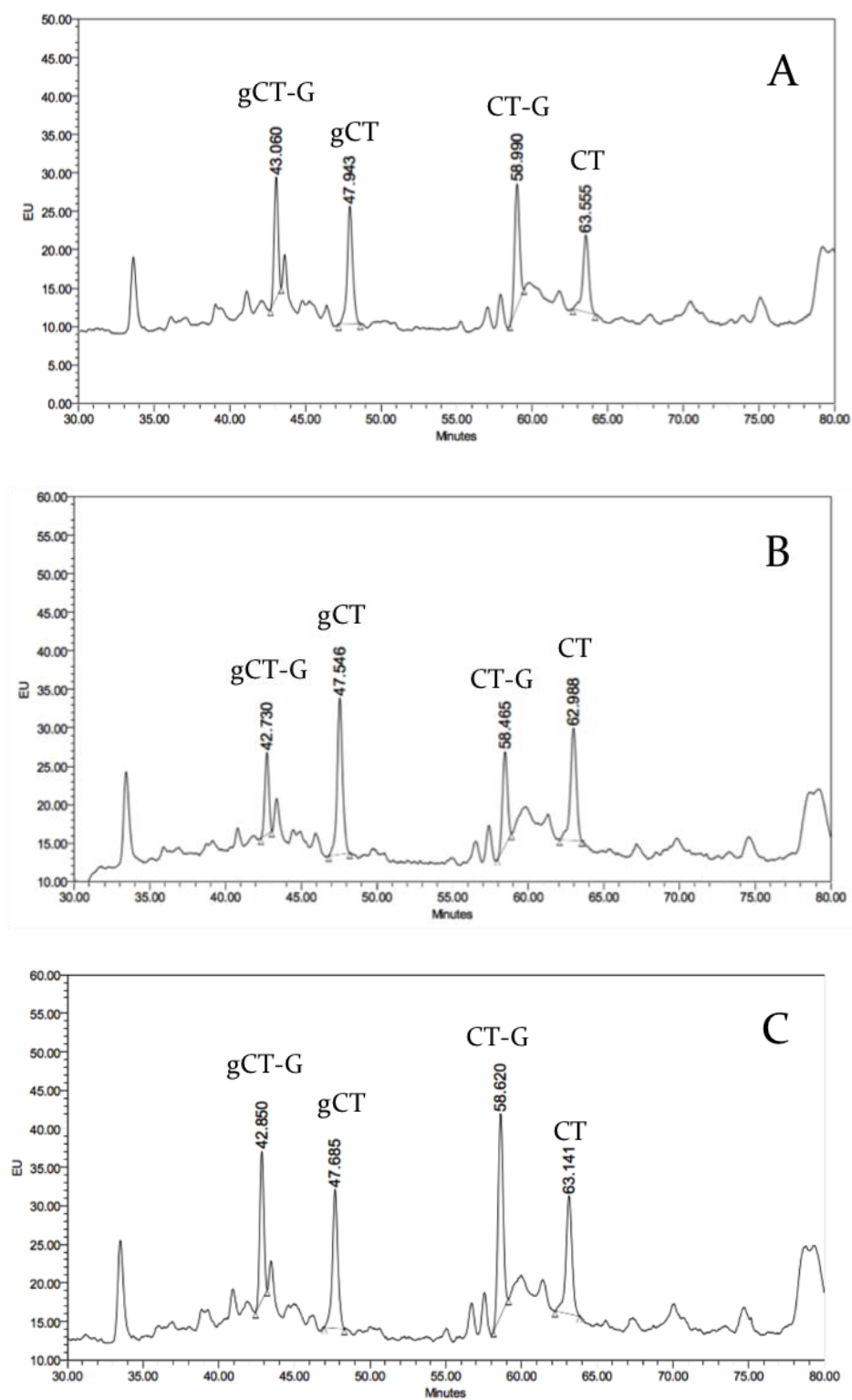
Figure 5.6: *HPLC chromatograms of* **A:** *DMS53 culture medium after incubation for 24 h, analysed using CT-M2;* **B:** *DMS53 culture medium, after treatment with GFI0920X (10 μM) and incubation for 24 h, analysed using CT-M2;* **C:** *DMS53 culture medium, after treatment with SQ22536 (100 μM) and incubation for 24 h, analysed using CT-M2.*
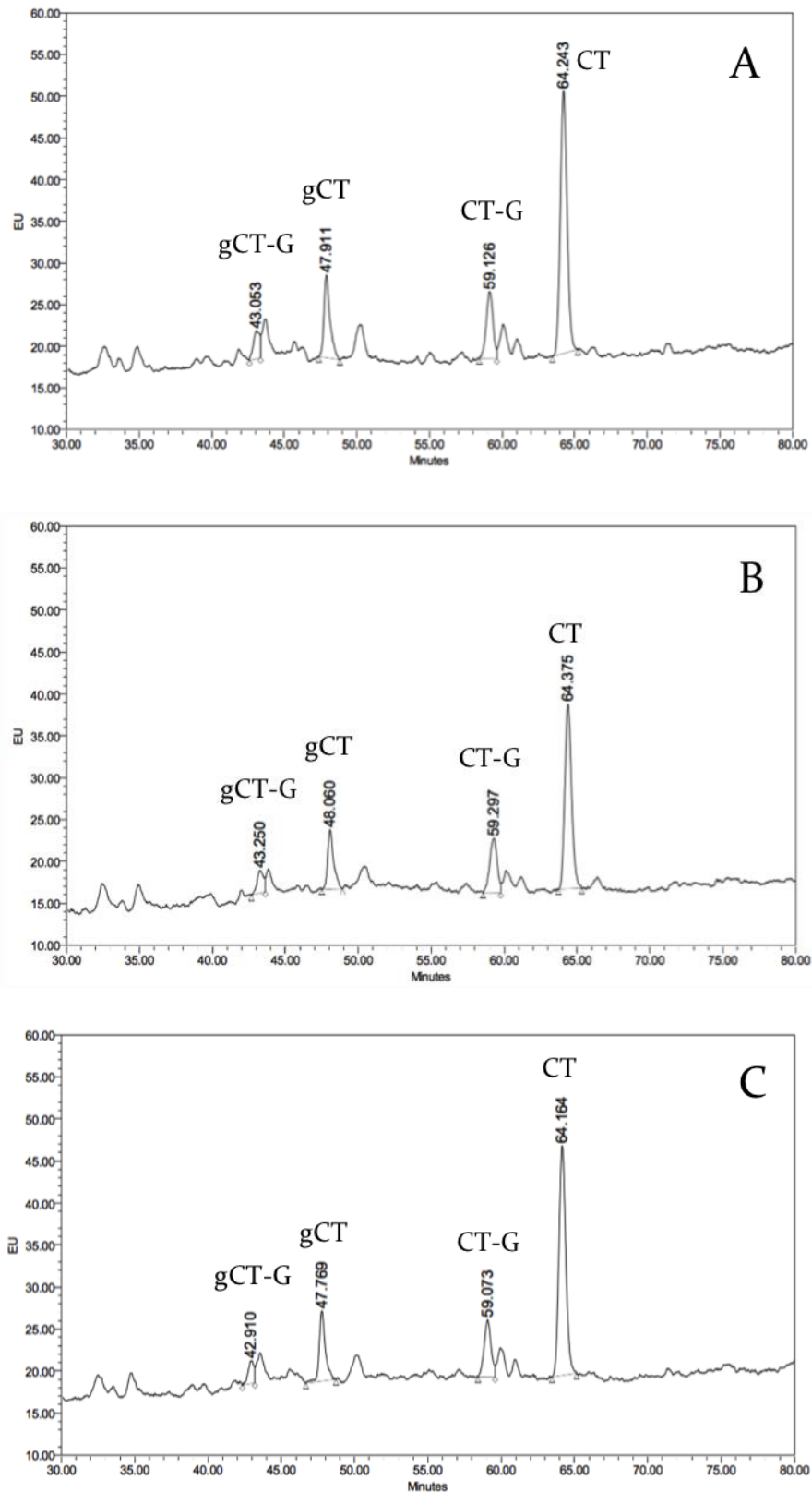
Figure 5.7: *HPLC chromatograms of* **A:** *DMS53 culture lysate after incubation for 24 h, analysed using CT-M2;* **B:** *DMS53 culture lysate, after treatment with GFI0920X (10 μM) and incubation for 24 h, analysed using CT-M2;* **C:** *DMS53 culture lysate, after treatment with SQ22536 (100 μM) and incubation for 24 h, analysed using CT-M2.*

Table 5.2: *CT-related species ratios in the medium of DMS53 cultures treated with inhibitors SQ22536 and GFI09203X.* Data obtained from triplicate experiments. Standard error of the mean determined from corrected sample standard deviation.

Treatment (medium)	gCT/gCT-G	SEM (+/-)	CT/CT-G	SEM (+/-)
Control	1.09	*0.13*	0.52	*0.09*
GFI09203X (10 µM)	2.17	*0.16*	1.02	*0.14*
SQ22536 (100 µM)	1.04	*0.12*	0.57	*0.07*

Table 5.3: *Further CT-related species ratios in the medium of DMS53 cultures treated with inhibitors SQ22536 and GFI09203X.* Data obtained from triplicate experiments. Standard error of the mean determined from corrected sample standard deviation.

Treatment (medium)	non-glycosylated/ glycosylated	SEM (+/-)	Total Peak Area/ Control Total Peak Area	SEM (+/-)
Control	0.81	*0.05*	1	*0.03*
GFI09203X (10 µM)	0.91	*0.09*	0.93	*0.06*
SQ22536 (100 µM)	1.18	*0.17*	1.31	*0.11*

Table 5.4: *CT-related species ratios in the lysate of DMS53 cultures treated with inhibitors SQ22536 and GFI09203X.* Data obtained from triplicate experiments. Standard error of the mean determined from corrected sample standard deviation.

Treatment (lysate)	CT/CT-G	SEM (+/-)	CT Peak Area/ Total Peak Area	SEM (+/-)
Control	4.55	*0.64*	0.63	*0.01*
GFI09203X (10 μM)	4.13	*0.91*	0.63	*0.03*
SQ22536 (100 μM)	4.27	*0.33*	0.63	*0.01*

In **Table 5.2,** the medium of the GFI09203X treated cultures showed changes in the CT to CT-G and gCT to gCT-G ratios compared to the control cultures. The CT to CT-G ratio increased from 0.52 ± 0.09 in the control to 1.02 ± 0.14 in the treated cultures; the gCT to gCT-G ratio increased from 1.09 ± 0.13 in the control to 2.17 ± 0.16 in the treated cultures. In **Table 5.3**, with cultures treated with SQ22635, the ratio of non-glycosylated to glycosylated CT species (1.18 ± 0.17) was slightly higher than in the control culture (0.81 ± 0.05). In **Table 5.4**, treatment of cultures with GFI09203X and SQ22536 had no significant effect on the levels of CT relative to the other CT-related species in the lysate, or on the CT to CT-G ratio.

Changes to the levels of CT-related species in the medium and lysate were further interrogated to determine the level of statistical significance. .As described in Appendix One, the average relative proportions of each CT-related species in a given treatment condition were calculated and normalised. Treatment conditions were then compared to the control using Welch's unequal variances t-test (**Table A1.3**). GFI09203X (40 μM) treatment was found have a significant effect on the levels of CT-related species in the

medium (p<0.05, **Table A1.4**), while the effect of SQ22536 was not significant due to uncertainty, again consistent with the observations above. Minor changes to the levels of CT-related species in the lysate were observed with GF190203X treatment.

GF109203X treatment of DMS53 cultures resulted in significant changes to CT to CT-G and gCT to gCT-G ratios in the medium. However, the relative proportions of the CT-related species in the lysate remained remarkably unchanged. The effect of GF109203X on CT-related species suggests that PKC, the target of GF109203X, is involved in hCTR signal transduction. As the ratios of CT to CT-G and gCT to gCT-G in the medium increased by almost 100%, this in turn suggests that PKC activity has some control over the activity or expression of PAM. SQ22536 treatment of DMS53 cultures may have slightly increased levels of non-glycosylated species in the medium. However changes were smaller compared to those observed with GF109203X treatment, and the proportional error was larger. For this reason it was concluded that AC, the target of SQ22536, might be involved in hCTR signal transduction, but the evidence is much less convincing than for the involvement of PKC.

5.5 Conclusion

The experiments performed in this Chapter have demonstrated that the levels of CT and its related species in DMS53 medium changed significantly with GF109203X treatment, and possibly with SQ22536 treatment. This suggests that PKC is involved in the hCTR signal transduction pathway, and that AC could be involved. The relative levels of the CT-related species in the lysate were again unchanged by treatment with these inhibitors, consistent with the observations in Chapters 2 and 3. This further reinforces the tight regulation intracellular CT is under. Treatment of DMS53 cultures with U73122 generated a large peak that disrupted the analysis of the CT-related species levels, leading to experiments with the inhibitor being abandoned. This meant that the effect of

PLC inhibition on the levels of CT-related species was not accurately assessed. Therefore, the possibility remains that the Ca^{2+}-dependent pathway as a whole may be involved in hCTR signal transduction. Treatment with H89 had no significant effect on the levels of CT-related species in the medium, suggesting that PKA is not involved in hCTR signal transduction. As PKA is downstream of AC, this indicates that the cAMP-dependent pathway as a whole is not involved in hCTR signal transduction. cAMP may activate other signalling pathways such as the MAPK pathway however,[148] so this observation does exclude AC involvement in hCTR signal transduction.

In the work described in Chapter 2, it was observed that DMS53 cultures grown in larger volumes of medium showed decreased CT to CT-G and gCT to gCT-G ratios due to the accumulation of CT-G and gCT-G in the medium. In contrast, experiments described in Chapter 3 showed DMS53 cultures treated with the hCTR agonist SUNB8155 exhibited increased CT to CT-G and gCT to gCT-G ratios in the medium, as a response to putative hCTR activation. As it appears that treatment with GF190203X alters PAM activity or expression, this observation suggests that the apparent changes in PAM processing observed previously were mediated by PKC signalling.

Chapter Six

Conclusions and Future Directions

Peptide hormones are essential in physiology and heavily involved in a range of pathological conditions, notably neuroendocrine cancers. In particular, CT is used as a diagnostic marker for MTC, and drives growth and proliferation of prostate cancer, among others. Understanding the oncogenic mechanisms activated by CT and how they differ from system to system, and cognately, the biosynthesis of CT and how it can be perturbed, is limited by the ability to detect and quantify CT and its biosynthetic precursors *in vitro*. This thesis presents the development of an HPLC-fluorescence method to measure CT and its related species in the DMS53 SCLC cell line, and the characterisation of mechanisms that regulate the production of these species.

The development of an HPLC method capable of separating CT from CT-G, CTGK and CTGKK in DMS53 cell medium and lysate was described in Chapter 2. The method featured on-line concentration, separation of analytes with a two-column system and post-separation fluorescent labeling. With this system, CT precursors were detected and quantified of the first time, novel glycosylated versions of each species forming a parallel biosynthetic pathway were detected and characterised, and the effect of biosynthesis inhibitors, time, and medium volume on the regulation of CT species characterised. It was demonstrated that DMS53 cells tightly regulated intracellular CT concentration, which could not be perturbed through treatment with biosynthesis inhibitors. Moreover, the results suggest that the glycosylation pathway might play a role in regulating the intracellular CT concentration by removing excess precursors from the system. DMS53

cultures incubated in larger volumes of medium showed altered distributions and up-regulated production of CT-related species, suggesting that the cells sought to maintain specific external levels of CT-related species, although these levels were controlled less tightly than intracellular levels.

Understanding the effect of the glycosylation on the functionality of CT-related species is the first step in determining its importance. If glycosylation is simply a means to mediate export of CT-related species, targeting glycosylation enzymes in tandem with PAM inhibitors may upset the homeostasis of intracellular CT. However, if glycosylation plays a role in the oncogenicity of CT, then reducing production of the glycosylated species is also desirable. Tagashira and coworkers[199] examined the effect of O-glycosylation on the structure of eel CT, based on an interest of improving treatments for osteoporosis. It was found that glycosylation at the Thr21 position decreased the α-helicity of the peptide. This suggests that glycosylation may change the receptor binding properties of CT-related species. Future work to investigate the effect of glycosylation of CT would begin with the synthesis of gCT and comparing gCT and CT hCTR binding properties.

The detection of glycosylated CT-related species in DMS53 raises the question of whether these species are unique to DMS53, or whether they are present in other cancer cell lines or in other tissue types. The generality of these species may also provide information regarding the function of the glycosylation. To this end, a preliminary attempt to identify any CT-related species produced in the TT cell line was carried out. TT cells were first isolated from a MTC biopsy in 1981,[200] and are reported to secrete CT and express hCTR2.[63, 201] Initial investigations began by culturing cells in a similar manner to DMS53 and analysing the medium using the HPLC methodology. It was found that CT and CT-G could be detected in the medium, with the identity confirmed by MS, but that cultures had to reach higher cell numbers and be grown for longer in order for detection to be possible. Even then, levels of CT and CT-G were lower in TT

medium than in DMS53 culture medium grown under the conditions of the third generation *in vitro* assays. For this reason, method development became focused on the detection of CT-related species in the TT lysate.

The preliminary investigation into the intracellular CT-related species in TT cells was undertaken using a modified version of the third generation *in* vitro assay (outlined in experimental section 7.6). TT cultures were seeded with 20 million cells in a 75 cm^2 flask and incubated for 13 days with medium changes every two days, except for the final 96 h. Cell lysate was then harvested. Briefly, the cells were lysed by freeze-thawing, where the cell pellet was frozen in liquid nitrogen then heated to 100 °C for 7 min to denature proteases that might otherwise degrade the CT-related species. The lysate was then purified via centrifugal filtration using a 50 kDa cut-off filter. The lysate (1 ml) was analysed using CT-M2, with the resulting chromatogram shown in **Figure 6.1**.
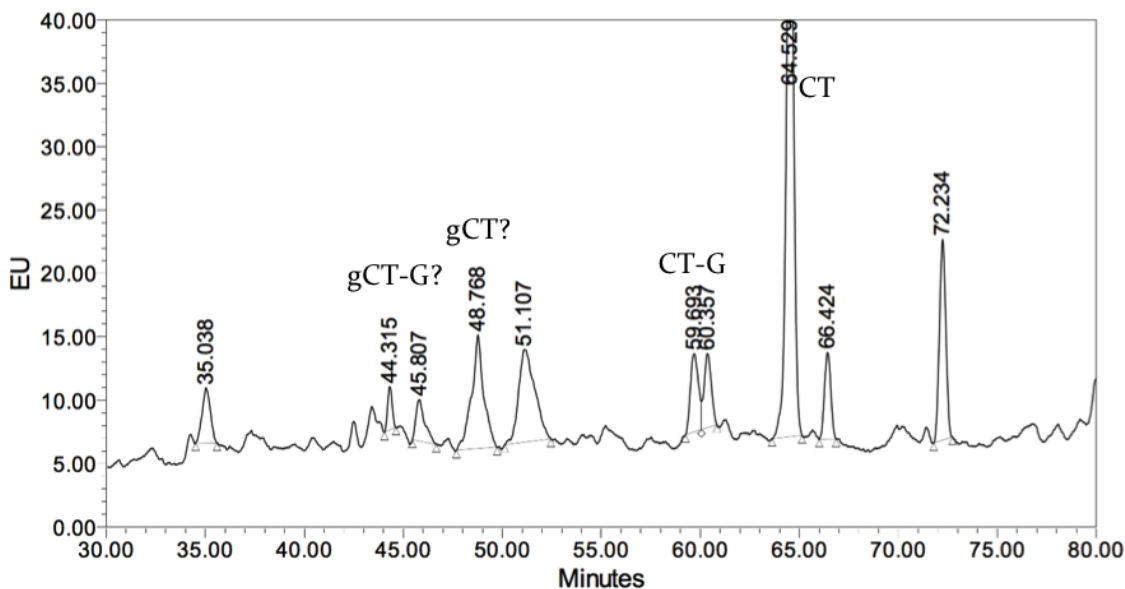
Figure 6.1: *HPLC chromatogram of TT culture lysate after 13 days of culture growth, analysed using CT-M2.*

In the TT lysate HPLC chromatogram (**Figure 6.1**), a large CT peak was observed along with a much smaller CT-G peak, with a CT to CT-G ratio of 7.4. These peaks co-eluted with the CT and CT-G standards, and MS confirmed the presence of CT and CT-G in TT lysate. However, the presence of gCT and gCT-G could not be confirmed with this technique. The relative proportions of CT and CT-G are very similar to those observed in the lysate of DMS53 cultures, indicating that the preferred intracellular levels of CT-related species may be the same in both cell lines. Four peaks were detected between 43 and 51 min, the region in which elution of gCT and gCT-G is observed in DMS53. Without standards of the gCT and gCT-G species however, identification of these species in TT samples was difficult.

For this reason, LCMS MRM was selected as the primary analysis tool to identify gCT and gCT-G in TT lysate. TT cells were seeded in a 175 cm^2 flask and cultured in 50 ml of medium until confluent, then incubated for a further 5 days (approx. 200 million cells). The new culture procedure was designed to maximise cell number and therefore, the levels of gCT and gCT-G levels in the lysate. Lysate was harvested and analysed using LCMS MRM (shown in **Figure 6.2**). LCMS MRM conditions are described in detail in experimental section 7.9.
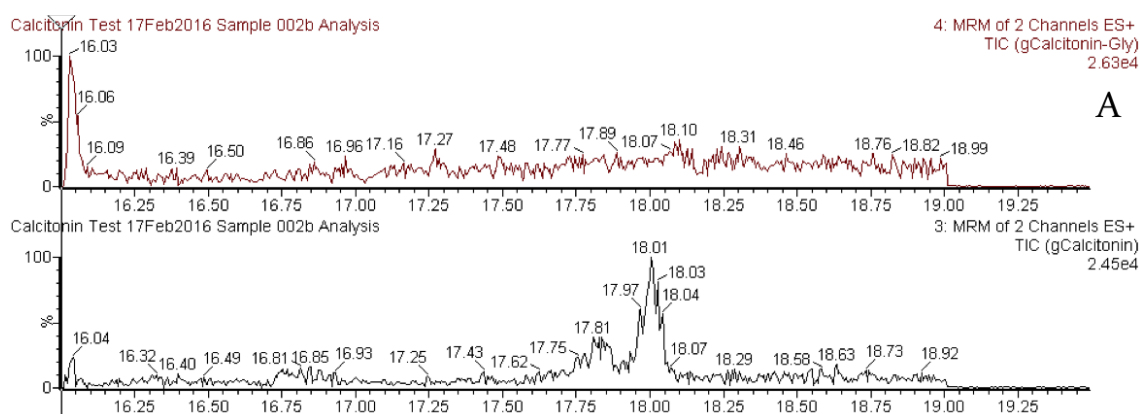
Figure 6.2: *LCMS MRM analyses for gCT and gCT-G in TT lysate.*

In the MRM analysis for gCT-G and gCT in the TT lysate, there was a clear peak at 18 min corresponding to the MRM signature of gCT. This indicates that the gCT parent ion in the 4+ charge state (1092.65) and two specific daughter ions (70.07 and 115.15) generated by fragmentation of the parent ion in the MS were simultaneously detected at the elution time equivalent to that of gCT in DMS53. This is strong evidence that gCT is present in TT lysate. The presence of gCT in TT cultures requires the production of gCT-G, based on the biosynthetic pathway established with DMS53. As gCT-G was not observed in the lysate, it was postulated that it might be present in the medium. To overcome the lower production of CT-related species in the medium of TT cultures, which hindered efforts at detecting gCT and gCT-G, a method to concentrate TT culture medium through lyophilisation was developed. This resulted in a 15-fold increase in concentration of the TT medium (sample preparation protocol described in detail in experimental section 7.9).

A lyophilised concentrated medium sample was generated from cultures grown under the same assay conditions as for the lysate analysis, and was then fractionated using the LCMS. From 17 min 30 s until 20 min, 8 second fractions were collected in HPLC vials and then reinjected and analysed by MS (sample preparation protocol to detect gCT-G in the medium and LCMS MRM conditions are described in detail in experimental section 7.9). **Figure 6.3A** shows the structure, exact mass and the molecular mass of gCT-G. In **Figure 6.3B,** the MS spectrum for fraction 10 of the lyophilised medium concentrate is presented, which was found to contain 4 charge states corresponding to gCT-G (1474.6 (+3), 1106.2 (4+), 885.1 (5+) and 632.5 (7+)). Ions corresponding to gCT-G were also detected in fractions 11-13. This provides strong evidence that gCT-G is produced by TT cells and is found in the medium.

Chemical Formula: $C_{189}H_{285}N_{43}O_{73}S_3$
Exact Mass: 4420.91
Molecular Weight: 4423.77

A

H−CysGlyAsnLeuSerThrCysMetLeuGly−ThrTyrThrGlnAspPheAsnLysPheHis−ThrPheProGlnThrAla·IleGlyValGly−AlaPro−N−OH

B
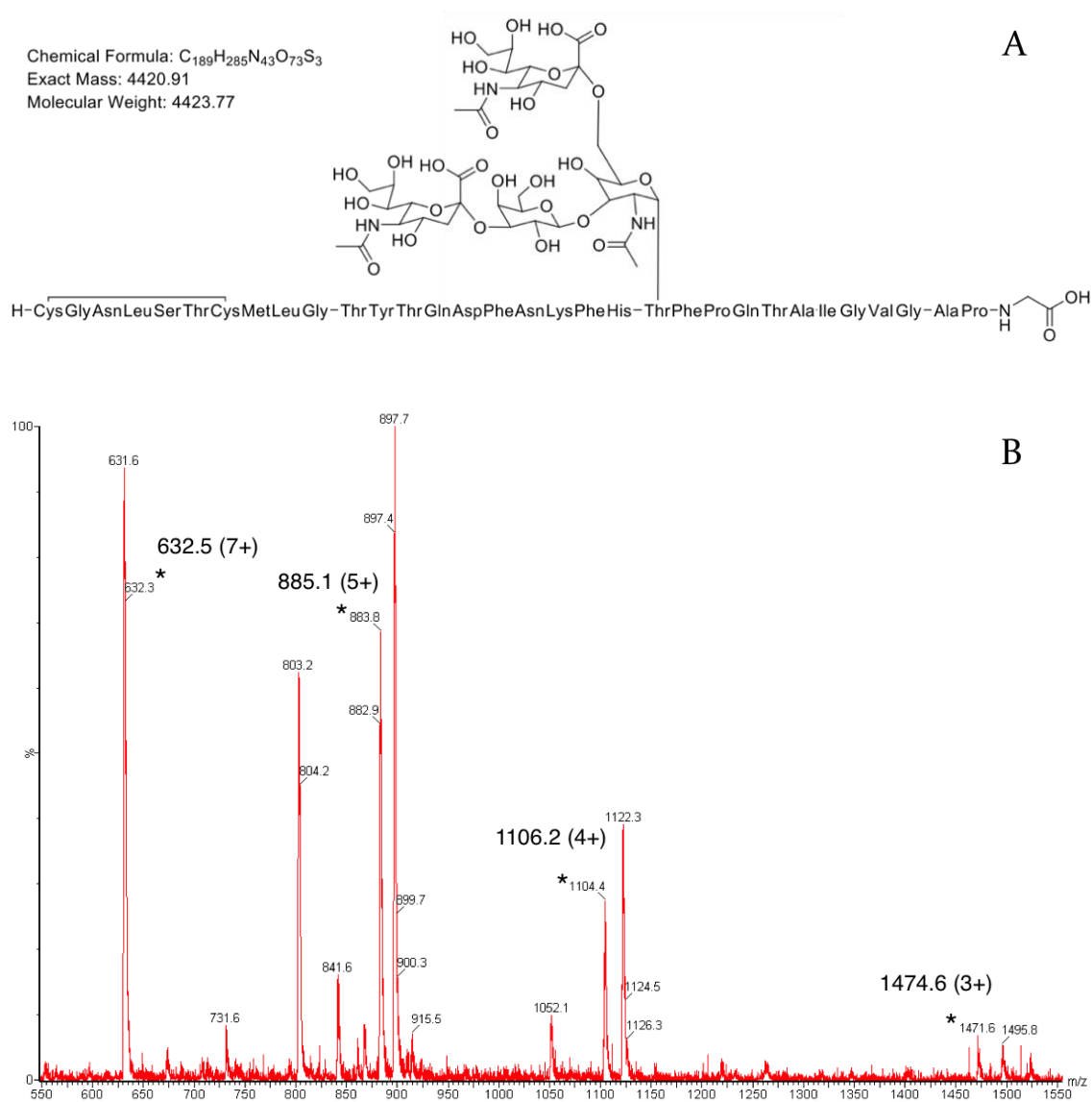
Figure 6.3A: *Structure and mass characteristics of gCT-G;* **B:** *MS spectrum of gCT-G in fractionated TT medium.* Fractions 10-13 showed evidence of gCT-G, with 4 charge states present in fraction 10 (3+, 4+, 5+, 7+).

With these preliminary experiments, it has been demonstrated that the HPLC-fluorescence methodology developed in Chapter 2 can be applied to the detection of CT-related species in multiple cell lines. The TT lysate chromatogram shows ratios of CT-related species that are very similar to DMS53 lysate, despite the fact that the levels of CT-related species in the medium are very different between the two cell lines. This implies that intracellular CT levels are important to CT-producing cell lines in general,

and that intracellular levels in TT may be under similar control to those in DMS53. It has also been demonstrated that the production gCT and gCT-G is not unique to DMS53, also indicating that is not unique to SCLC or lung tissue. In Chapter 2, it was proposed that in DMS53 cells, CT precursor flux through the glycosylation pathway allowed excess precursor to be produced and selectively secreted when not required. This pathway could be diverted to maintain intracellular CT levels when required. Given the lower levels of CT-related species in the TT culture medium relative to the lysate, this mechanism may not be operating in TT cultures. Future experiments would begin which the development of a stable cell culture protocol, presumably over longer time periods than DMS53, to allow for the measurement of CT, CT-G. gCT and gCT-G in the medium and lysate. With this in hand, the experiments performed on DMS53 cultures in chapter 2 could be repeated on TT cultures, such as treatment with PBA and GEMSA, as well as varying assay time, and incubating in larger volumes.

The observation that levels of CT-related species produced by DMS53 cultures changed when incubated in larger volumes of medium prompted experiments to determine the mechanism of this response. It was hypothesised that hCTR might initiate a cellular response to changes in extracellular CT, and mediate increases in CT biosynthesis and secretion. In the work described in Chapter 3, it was demonstrated that treatment of DMS53 with a specific small molecule hCTR agonist, SUNB8155 (100 μM), increased the CT to CT-G and gCT to gCT-G ratios, and the proportion of CT to gCT in the medium. SUNB8155 treatment had no significant effect on the relative levels of CT-related species in the lysate. This suggested that hCTR was expressed in DMS53, and that activation of this receptor selectively increased extracellular CT. In the work described in Chapter 4, the transcription and expression of hCTR in DMS53, as well as the identity of the isoform, was interrogated using RT-PCR and Western blot analyses. RT-PCR confirmed that mRNA corresponding to hCTR2 was transcribed in DMS53 samples. Western blot

using an antibody raised against hCTR2 compared DMS53 protein lysate to that of the hCTR2-positive DU145 cell line. The blot showed co-migrating immunoresponsive bands, indicating hCTR2 was expressed in DMS53.

Treatment of DMS53 cultures with SUNB8155 demonstrated that hCTR2 activation increases CT in the medium, which strongly suggests that an autocrine positive feedback loop is active in DMS53. This conclusion could be further interrogated by treating cultures with an hCTR antagonist (such as sCT8-32) and SUNB8155 in concert to confirm that the effect observed is due to activation of hCTR, rather than off-target effects. The possibly that hCTR activation is ligand-dependent, and therefore that activation by SUNB8155 may have a different effect on the levels of CT-related species to activation by CT, could be probed using an alternative agonist such as sCT, and observing whether changes in the levels of CT-related species are different to those observed with SUNB8155 treatment.

There are few examples of peptide hormone receptors behaving in this manner in the literature,[172] and none of those identified are in the CT family of peptide hormones. With that said, hCTR acts as the base for the RAMP-functionalised AMY receptor, and CGRP is generated from a splice variant of CALCA mRNA (the same gene CT is transcribed from). This may indicate that AMY and CGRP are also mediated by positive feedback loops, given the close relationship with the CT-hCTR signalling axis. Future work could involve investigating whether these receptors and their ligands are also regulated through positive feedback loops.

In the work described in Chapter 5, enzymes in two of the canonical signalling pathways of hCTR were investigated using inhibitors, in order to determine their involvement in the regulation of CT-related species. Two enzymes in each pathway were selected for inhibition: AC and PKA in the cAMP-dependent pathway, and PLC and PKC in the Ca^{2+}-

dependent pathway. It was discovered that PKA inhibition with H89 (1 and 10 μM) had no effect on the levels CT-related species in the medium, and the PLC inhibitor U73122 (10 and 40 μM) was unsuitable in assay conditions. It was concluded that treatment with SQ22536 (100 μM) may have had a small effect on CT and CT-G production in the medium, either by influencing transcription or by diverting precursors away from the glycosylation pathway. Treatment with GF109203X (10 μM) increased the levels of CT and gCT, presumably by increasing PAM turnover. The relative proportions of CT-related species in the lysate were not significantly affected by treatment with either inhibitor.

These experiments suggest that PKC, and possibly AC signalling is involved in regulation of CT-related species, and that together these enzymes have influence over the flux of CT precursors and PAM expression or activity. These are the same mechanisms that appear to be controlled under putative hCTR activation by SUNB8155. However, this activity is mainly confined to the CT-related species in the medium, while the CT-related species in the lysate remain relatively unchanged. This is consistent with the observations made in Chapters 2 and 3, where the levels of the CT-related species in the lysate stayed constant despite treatment with biosynthesis inhibitors and an hCTR agonist, longer incubation times, and incubation in larger volumes of medium.

The enzyme inhibitor treatments provided a basis to screen for the association of individual signalling enzymes in the regulation of CT-related species, but did not conclusively prove their involvement. Experiments investigating the concentration-dependence of the inhibitors on the levels of CT-related species would confirm the observations made. One caveat is that at higher concentrations, the inhibitors would lose specificity, so the interpretation of changes to CT-related species at high inhibitor concentrations would have to be conservative. Additional experiments to strengthen the link between signalling enzymes and the regulation of CT-related species could involve

the treatment of DMS53 cultures with alternative inhibitors for each of the enzymes tested, or treatment with secondary messengers such as cAMP. More in-depth approaches could include G protein α-subunit knockdowns to isolate signalling pathways, and partial mRNA silencing of signalling enzymes to mute their effects. These experiments are required to ultimately prove the involvement of specific signalling enzymes in the regulation of CT-related species.

The work described in this thesis has demonstrated that CT and its related species are carefully regulated in the intracellular and extracellular environment, and has interrogated the mechanisms that direct this regulation. The presence of this cellular infrastructure suggests that the levels of CT are important to the DMS53 cells, and may play some role in the development of the cancer. Experiments involving the treatment of DMS53 cultures with biosynthesis and signaling enzyme inhibitors, as well as an hCTR agonist have demonstrated that while extracellular levels of CT-related species show some response to treatment, intracellular levels are resistant to disruption. It was not possible to effectively reduce the production of CT-related species with any of these approaches. This suggests new approaches are required to control the production of CT and its related species, and perhaps, peptide hormones in general. With these conclusions reached, it became of interest to investigate the regulation of another hormone implicated in cancer development, in order to compare the regulation with that of CT. The first step in this investigation is the development of a method to detect and quantify the hormone, first from a standard, and then *in vitro*.

For these preliminary detection experiments, OT was selected as the candidate hormone because it is physiologically and clinically relevant; it has received much attention for its physiological actions in pair bonding, trust and relationships,[202] as well as more classical roles in pregnancy and lactation.[203] Unsurprisingly, OT dysregulation has been associated with autism and other social disorders.[204] It is also associated with

neuroendocrine cancers, but its role is complex, as it has been reported as both a positive[40, 205] and negative[206] growth modulator. In a small cell lung cancer cell line, DMS79, OT has been shown to act as an autocrine growth factor.[207] OT is similar in structure to CT as it has a disulphide-bonded 5 membered ring, and is C-terminally amidated (**Figure 6.4**). Its biosynthesis is thought to follow a pathway similar to that derived for CT, and as antibody detection of OT is more advanced than that of CT, immunoassays can distinguish between OT, OT-G, OT-GK and OT-GKR.[208] This has allowed biological impact of OT precursors to be assessed, such as observations of an increased OT/OT-X ratio in autism patients[209] and the characterisation of the cardiomyogenic effect of OT-GKR.[210] With that said, doubts have been raised regarding the specificity of antibodies to OT, as inflated concentrations have been reported in plasma samples, particularly in unextracted samples.[211, 212] OT is reported to have a half-life of approximately 5 min,[213] which is shorter than the 10-30 min half-lives reported for CT-related peptides[214] and may affect detection. Direct detection of OT and its biosynthetic precursors with the HPLC-fluorescence method would verify the generality of the approach and provide a tool to confirm conclusions drawn from immunoassays.

Cys-Tyr-Ile-Gln-Asn-Cys-Pro-Leu-Gly-NH$_2$
 1 2 3 4 5 6 7 8 9
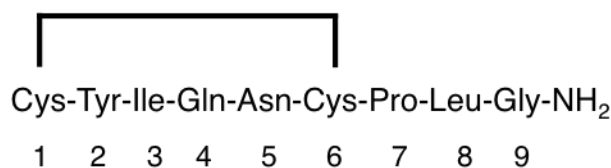
Figure 6.4: *Amino acid sequence of human OT.* A disulphide bridge is formed between Cys1 and Cys5, with Gly9 C-terminally amidated.

OT production has been quantified in the SCLC cell line DMS79 medium and lysate, with a maximum of 30 pg/ml per 1 x 10^6 cells after 96 h, and a maximum of 120 pg/ml per 1 x 10^6 cells after 96h, respectively.[215] As DMS79 cells are a suspension cell line, the ability to control the ratio between cell number and medium volume is more limited

than with adherent cultures such as DMS53. Based on the reported levels of OT in the medium, it was not possible to design a culture protocol to produce OT at levels above the detection limit of approximately 1 ng/ml. For this reason, assay development focused on detection of OT and OT-G in the lysate of DMS79 cultures. As DMS79 cells are reported to produce 120 pg/ml of OT per 1×10^6 cells after 96 h in the lysate, a culture of 50 million cells is expected to produce approximately 6 ng/ml of OT, well above the limit of detection.
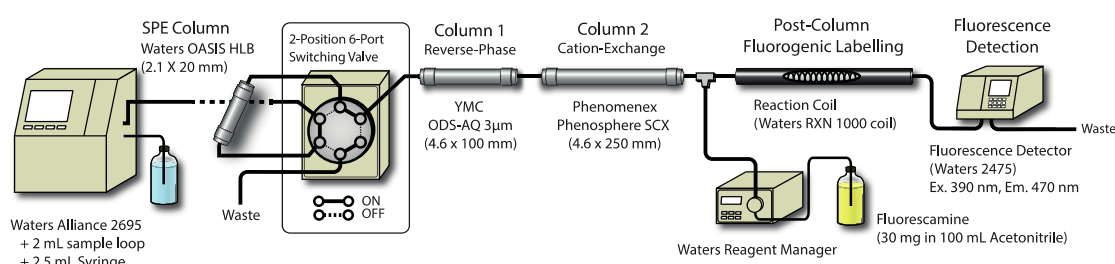
Figure 6.5: *HPLC system for OT detection and quantification.* Used with permission from Hideki Onagi.

An HPLC separation method for OT and OT-G in DMS79 lysate was developed. In **Figure 6.5,** the two-column system used to separate OT and OT-G is shown, the same system as described in Chapters 2 and 3. Several iterations of separation methodologies were designed and tested, and the final method was denoted OT-M3, with the solvent system outlined in **Table 6.1**. Separation occurred from 7 to 70 min, due to an increasing acetonitrile gradient (from 15:85 acetonitrile to AccQ.tag Eluent A buffer (100 ml concentrate in 1000ml) at 7 min, to 20:80 at 70 min).

Two DMS79 cultures were grown to a density of approx. 65 million cells over at least 96 h. Cultures were then lysed. Briefly, the cells were lysed by freeze-thawing, where the cell pellet was frozen in liquid nitrogen then heated to 100 °C for 7 min to denature proteases that might otherwise degrade the CT-related species. The lysate was then purified via centrifugal filtration using a 50 kDa cut-off filter. To minimise the loss of OT

and OT-G due to degradation, one sample was treated with P3840 and EDTA (1 mM), while the other was used as a control (detailed protocol outlined in experimental section 7.10). Both samples were analysed using OT-M3 (**Figure 6.6**)

Table 6.1: *Solvent system for the first generation OT separation method (OT-M3).*

Time (min)	Flow (ml/min)	Water (%)	Acetonitrile (%)	0.1% TFA in 2-Propanol (%)	Waters AccQ.Tag™ Eluent A (100 ml in 1000 ml water) (%)	Gradient Curve
0.00	3.00	0.0	0.0	0.0	100.0	0
1.00	1.00	0.0	0.0	0.0	100.0	6
3.00	1.00	0.0	3.0	0.0	97.0	6
3.50	1.00	0.0	3.0	0.0	97.0	6
4.00	1.00	0.0	10.0	0.0	90.0	6
7.00	1.00	0.0	15.0	0.0	85.0	6
70.00	1.00	0.0	20.0	0.0	80.0	6

Figure 6.6: *HPLC chromatograms of* **A:** *OT standard (0.1 μg/ml, 50 μl injection) in MilliQ, analysed using OT-M3;* **B:** *OT-G standard (0.1 μg/ml, 50 μl injection) in MilliQ, analysed using OT-M3;* **C:** *DMS79 culture lysate after 24 h incubation, treated with P8340 protease inhibitor cocktail solution (1:20 by volume), and EDTA (1 mM), analysed using OT-M3;* **D:** *DMS79 culture lysate after 24 incubation, analysed using OT-M3.*

The experiment was repeated with LCMS MRM analysis of the DMS79 lysate, as a check of the observations of the HPLC-fluorescence experiment. For the generation of the lysate samples, EDTA treatment was omitted and instead both samples were treated with P3840. Additionally, one sample was spiked with OT-d_{10} to act as an internal standard for LCMS detection (detailed protocol outlined in experimental section 7.9). LCMS chromatograms are displayed in **Figure 6.7**.
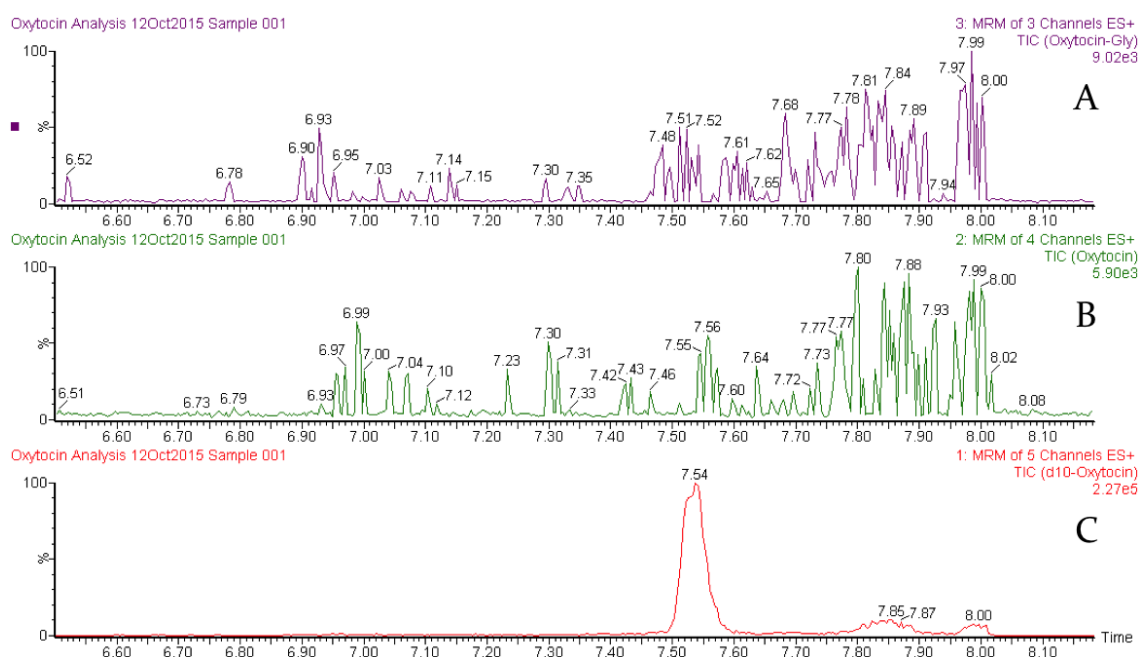
Figure 6.7A: *LCMS MRM analysis for OT-G in DMS79 lysate.* **B:** *LCMS MRM analysis for OT in DMS79 lysate.* **C:** *LCMS MRM analysis for OT-d$_{10}$ spike (50 µg/ml) in DMS79 lysate.*

Figure 6.6A and **B** shows the elution times of OT (33.4 min) and OT-G (28.4 min) standards respectively using the OT-M3 separation method. **Figure 6.6C** shows the lysate sample treated with protease inhibitors. Major peaks were observed at 24.6, 30.6 and 32.4 min, but none of these corresponded to the OT or OT-G elution times. The absence of protease inhibitor (**Figure 6.6D**) led to the appearance of two new peaks at 20.7 and 23.0 min, suggesting that these may be breakdown products. Again, no peaks corresponding to OT or OT-G were observed. In **Figure 6.7**, the LCMS MRM analyses are presented. **Figure 6.7C** shows the MRM analysis of the OT spike in the lysate, with an elution time of 7.54 min. In **Figure 6.7B**, no corresponding peak above the background is observed in OT MRM analysis of the unspiked lysate. This is reflected in **Figure 6.7A**, where no peak above noise is observed for OT-G.

These experiments demonstrate that OT and OT-G were not present in DMS79 lysate above the limit of detection. Based on literature reports of OT quantification in

DMS79,[215] OT should have been detectable in the DMS79 lysate given the culture conditions used. A second cell line, N38 (a mouse hypothalamus cell line) was also investigated using the same methodology. The structure of mouse OT is the same as human, and OT expression in N38 had been confirmed through Western blot, but not been quantified.[216] However, no evidence of OT or OT-G was observed in the medium or lysate using both HPLC-fluorescence detection and LCMS.

One possibility is that the half-life of OT is too short for the assays used, and that sample concentrations decrease below the limit of detection before they can be analysed. Another possibly is that OT and OT-G are not present as monomers. A study reporting HPLC separation of OT from synthetic impurities for use in pharmaceutical preparations reported multiple dimer species stemming from intermolecular disulphide bonds forming between cysteine residues.[217] If these species account for the majority of OT *in vitro,* these detection methods would not have observed them. Alternatively, it may be that the quantity of OT in DMS79 was overestimated by the immunoassay used to detect it due to non-specific recognition. Szeto and coworkers[212] reported that in plasma samples, even after HPLC fractionation, multiple immunoreactive peaks were detected by EIA and RIA, suggesting OT antibody cross-reactivity confounded quantification. It is possible that this may have occurred in the literature characterisation[215] of OT production in DMS79, and that the cell line does not produce OT above the limits of detection of the HPLC-fluorescence method.

The application of this technique to the detection of other peptide hormones is still a priority, and candidate hormones such as CGRP and AM have been identified as potential targets. These hormones are of comparable size to CT, are C-terminally amidated, have half-lives greater than 10 min[218] and are reportedly overproduced in

DMS53 and other SCLC cell lines.[157] Method development for each species needs to be undertaken, and then screening DMS53 medium and lysate for these species can follow.

Many pharmaceutical purifications and assays, as well as general biochemistry experiments, rely on the quantification of peptides. An ultra-sensitive analytical method would remove the need for pre-separation tagging or the use of hazardous reagents such as radioactive labels. Possible applications for the HPLC-fluorescence method described in this work include assessing the degradation of therapeutic peptides and characterising the fragments, measuring the turnover of substrate peptides in the characterisation of enzyme activity, and separating wild type and engineered peptides from biological expression sources. The ability to separate large species with minor differences at such low concentrations is very powerful, and the possible applications of this method have only begun to be explored.

Chapter Seven

Experimental

7.1 General

The experimental related to the work described in Chapter 2 of this thesis has been published as part of the manuscript derived from that work, and is incorporated in this thesis at pages 44-70

Materials and Reagents

SUNB8155, SQ22536, H89 and GFI09203X were obtained from Tocris Bioscience. Fluorescamine, tris HCl, SDS, triton X-100, tween 20, bromophenol blue, β-mercaptoethanol, NaF, deocycholic acid and the P3840 mammalian protease inhibitor cocktail were obtained from Sigma Aldrich. NaCl and EDTA were obtained from Univar. GelRed™ was obtained from Biotium. CT, CT-G, CT-GK, CT-GKK, OT and OT-G standards (99% purity) were obtained from GL Biochem. RNasin was obtained from Promega. 4-20% mini-PROTEAN® precast polyacrylamide gels, secondary HRP anti-rabbit antibody and Clarity™ Western ECL blotting reagents were obtained from BioRad. Primers for RT-PCR analysis were obtained from IDT. UltraPure agarose was obtained from Invitrogen. AccQ.Tag™ Eluent A concentrate was obtained from Waters. Primary anti-hCTR2 antibody ab103422 obtained from Abcam.

Kits

Onestep RT-PCR and RNeasy Mini kits were obtained from QIAGEN. cOmplete™ lysis-M

(EDTA free) kit was obtained from Roche. RQ1 DNase kit was obtained from Promega. Bradford protein assay and Bio-Rad Trans-Blot® Turbo™ semi-dry transfer kits were obtained from BioRad.

Cell Culture

DMS53, DMS79, PC3, TT, and DU145 cells were obtained from the American Type Culture Collection. N38 cells were obtained from CELLutions Biosystems. DMS53, DMS79, PC3, TT and DU145 cells were cultured in GIBCO© RPMI-1640 supplemented with 10% fetal bovine serum obtained from Sigma Aldrich, and penicillin-streptomycin (55,000 U Penicillin, 55mg Streptomycin) from Invitrogen. N38 cells were cultured in Dubecco's Modified Eagle's Medium (DMEM) supplemented with 10% fetal bovine serum obtained from Sigma Aldrich, and penicillin-streptomycin (55,000 U Penicillin, 55 mg Streptomycin) from Invitrogen. Cell lines were cultured in 95% humidity under a 5% CO_2/ 95% air atmosphere at 37 °C, in growth medium refreshed every two days unless otherwise stated. Cell lines were passaged weekly; cells were washed twice with Dubeccos's Phosphate-Buffered Saline (DPBS) from ThermoFisher Scientific and lifted with 0.05% Trypsin-EDTA from Invitrogen. Cells were counted using the BioRad TC20 automated cell counter and Trypan Blue stain from Invitrogen.

7.2 HPLC Method 1 for the Detection of CT and its Prohormones

HPLC separation and quantification of CT and its prohormones (*i.e.*, CT-G, CTGK and CTGKK) from DMS53 and TT cell medium and lysate used a Waters Alliance 2695 separation module and a Waters 600E Pump connected to a two position, six port switching valve (Switch 1), a Waters Reagent Manager (Switch 2) containing fluorescamine (30 mg/100 ml acetonitrile) and a Waters 2475 Fluorescence Detector (**Figure 7.1**).
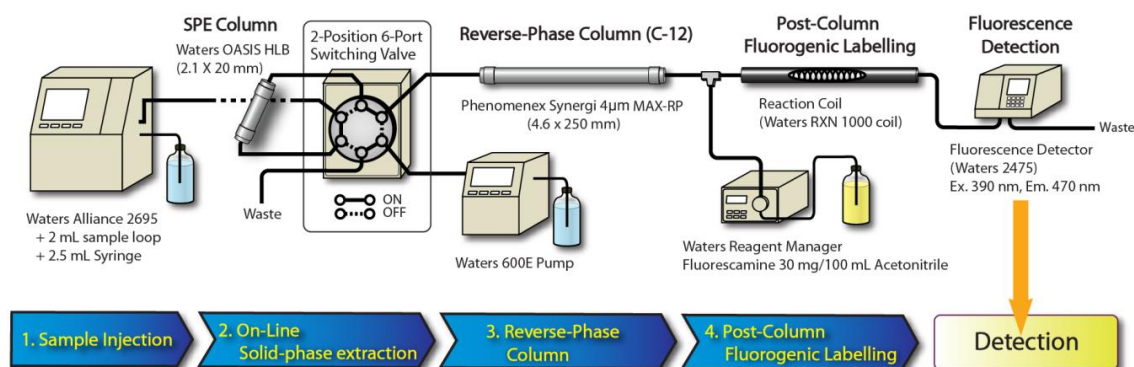
Figure 7.1: *First generation HPLC setup for peptide hormone detection and quantification.*

Injected samples underwent an online solid phase extraction on a reverse phase Oasis®
HLB 25 µm cartridge column (2.1 × 20 mm) with the switching valve open to waste
(Switch 1 OFF). After 6 min switch 1 was turned ON allowing separation of CT, CTG,
CTGK, CTGKK with a C12 Synergi 4u Max-RP column (250 × 4.6 mm) over 50 min. After
30 min switch 2 was turned ON, allowing fluorescent labelling of the *N*-terminus of
substrate and product by reaction with fluorescamine (30 mg fluorescamine in 100 ml
acetonitrile) in a post-column Waters 1000 RXN coil at 25 °C and detection with a
Waters 2475 Fluorescence Detector (Ex. 390 nm, Em. 470 nm). The solvent and gradient
system for the separation is shown in **Table 7.1**. Data were collected and processed with
Empower Pro-Empower 2 software using an IBM data station. Between each sample
injection a cleaning routine was applied (20 min total) using the solvent and gradient
system in **Table 7.2.**

Table 7.1: *Solvent and gradient system for Waters 2695 separations module used for separation of CT, CTG, CTGK and CTGKK over 50 min.* Events: 6 min Switch 1 is ON; 30 min Switch 2 is ON.

Time (min)	Flow (ml/min)	Water (%)	Acetonitrile (%)	Waters AccQ.Tag™ Eluent A (25 ml in 1000 ml water) (%)	Gradient Curve
0.00	3.00	100.0	0.0	0.0	0
2.00	3.00	100.0	0.0	0.0	6
4.00	3.00	0.0	20.0	80.0	6
5.00	1.20	0.0	20.0	80.0	6
40.00	1.20	0.0	30.0	70.0	6

Table 7.2: *Solvent and gradient system for Waters 2695 separations module used for cleaning routine.* Events: 8.70 min Switch 1 is ON; 17.0 min Switch 1 is OFF.

Time (min)	Flow (ml/min)	Water (%)	Acetonitrile (%)	0.1% TFA in 2-Propanol (%)	Waters AccQ.Tag™ Eluent A (25 ml in 1000 ml water) (%)	Gradient Curve
0.00	2.00	0.0	0.0	100.0	0.0	0
4.50	2.00	0.0	0.0	100.0	0.0	6
5.50	2.00	50.0	50.0	0.0	0.0	6
8.00	2.00	50.0	50.0	0.0	0.0	6
8.50	0.30	50.0	50.0	0.0	0.0	6
8.80	0.30	0.0	50.0	0.0	50.0	6
9.00	1.20	0.0	50.0	0.0	50.0	6
12.00	1.20	0.0	10.0	0.0	90.0	6
17.00	1.20	0.0	10.0	0.0	90.0	6
18.50	3.00	100.0	0.0	0.0	0.0	6
20.00	3.00	100.0	0.0	0.0	0.0	6

7.3 HPLC Method 2 for the Detection of CT and its Prohormones

HPLC separation and quantification of CT and its prohormones (*i.e.*, CT-G, CTGK and CTGKK) from DMS53 and TT cell medium and lysate used a Waters Alliance 2695 separation module and a Waters 600E Pump connected to a two position, six port switching valve (Switch 1), a Waters Reagent Manager (Switch 2) containing fluorescamine (30 mg/100 ml acetonitrile) and a Waters 2475 Fluorescence Detector (**Figure 7.2**).
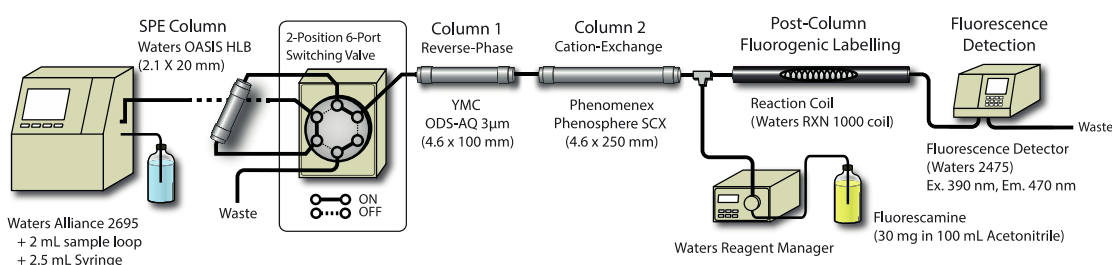
Figure 7.2: *Second generation HPLC setup for peptide hormone detection and quantification.*

Injected samples underwent an online solid phase extraction on a reverse phase Oasis® HLB 25 µm cartridge column (2.1 × 20 mm) with the switching valve open to waste (Switch 1 OFF). After 6 min switch 1 was turned ON allowing separation of CT, CTG, CTGK, CTGKK with a C18 YMC ODS-AQ 3µm (4.6 x 100 mm) reverse-phase column coupled to a Phenomenex Phenosphere SCX (4.6 x 250 mm) cation-exchange column over 80 min. After 10 min switch 2 was turned ON, allowing fluorescent labelling of the *N*-terminus of substrate and product by reaction with fluorescamine (30 mg fluorescamine in 100 ml acetonitrile) in a post-column Waters 1000 RXN coil at 25 °C and detection with a Waters 2475 Fluorescence Detector (Ex. 390 nm, Em. 470 nm). The solvent and gradient system for the separation is shown in **Table 7.3.** Data were collected and processed with Empower Pro-Empower 2 software using an IBM data station. Between each sample injection a cleaning routine was applied (52 min total)

using the solvent and gradient system in **Table 7.4 and Table 7.5,** with the second method directly following the first.

Table 7.3: *Solvent and gradient system for Waters 2695 separations module used for separation of CT, CTG, CTGK and CTGKK over 50 min.* Events: 6 min Switch 1 is ON; 10 min Switch 2 is ON.

Time (min)	Flow (ml/min)	Water (%)	Acetonitrile (%)	Waters AccQ.Tag™ Eluent A (100 ml in 1000 ml water) (%)	Gradient Curve
0.00	3.00	100.0	0.0	0.0	0
2.00	3.00	100.0	0.0	0.0	6
4.00	3.00	0.0	20.0	80.0	6
5.00	1.20	0.0	20.0	80.0	6
70.00	1.20	0.0	30.0	70.0	6

Table 7.4: *Solvent and gradient system for Waters 2695 separations module used for cleaning routine.* Events: 8.70 min Switch 1 is ON.

Time (min)	Flow (ml/min)	Water (%)	Acetonitrile (%)	0.1% TFA in 2-Propanol (%)	Waters AccQ.Tag™ Eluent A (100 ml in 1000 ml water) (%)	Gradient Curve
0.00	2.00	0.0	0.0	100.0	0.0	0
1.00	2.00	100.0	0.0	0.0	0.0	6
2.00	2.00	0.0	0.0	100.0	0.0	6
3.00	2.00	100.0	0.0	0.0	0.0	6
4.00	2.00	0.0	0.0	100.0	0.0	6
5.50	2.00	50.0	50.0	0.0	0.0	6
8.00	2.00	50.0	50.0	0.0	0.0	6
8.50	0.30	50.0	50.0	0.0	0.0	6
9.00	1.20	50.0	50.0	0.0	0.0	6
16.00	1.20	0.0	100.0	0.0	0.0	6
22.00	1.20	50.0	50.0	0.0	0.0	6

27.00	1.20	0.0	100.0	0.0	0.0	6
32.00	1.20	50.0	50.0	0.0	0.0	6
33.00	1.20	0.0	0.0	0.0	100.0	6
42.00	1.20	0.0	0.0	0.0	100.0	6

Table 7.5: *Solvent and gradient system for Waters 2695 separations module used for conditioning routine.* Events: 6.50 min Switch 1 is OFF.

Time (min)	Flow (ml/min)	Water (%)	Acetonitrile (%)	0.1% TFA in 2-Propanol	Waters AccQ.Tag™ Eluent A (100 ml in 1000 ml water) (%)	Gradient Curve
0.00	0.50	0.0	0.0	0.0	100.0	0
1.00	1.20	0.0	20.0	0.0	80.0	6
6.00	1.20	0.0	20.0	0.0	80.0	6
7.00	0.30	0.0	20.0	0.0	80.0	6
8.00	2.00	100.0	0.0	0.0	0.0	6
10.00	2.00	100.0	0.0	0.0	0.0	6

7.4 Procedure for First Generation In Vitro Assays

General Procedure

DMS53 cells were counted and seeded equally into 75 cm^2 flasks at low density in 10 ml of growth medium, with two duplicate control cultures and as many additional cultures as required for the compounds of interest to be tested in duplicate. The cultures were incubated until confluent (approximately 3 days of growth, 40 million cells). Growth medium was then replaced, and the compound of interest was added in 10 μl of DMSO to treated cultures. 10 μl of DMSO only was added to the control cultures. All cultures were then incubated for 24 h. After incubation, 10 ml of medium from each culture was collected in a 15 ml Falcon™ tube. 5 ml of this sample was injected onto the HPLC (5 x 1 ml aliquots) and analysed using CT-M1. The remainder was frozen at -80 °C for further analysis. The cells remaining in the cultures were washed twice with DPBS, and lifted with Trypsin-EDTA before being counted.

Experimental Specifics

In section 3.2, DMS53 cultures were treated with 100 and 200 μM SUNB8155 in successive experiments. Each concentration treatment was compared to duplicate controls, and at least two replicates were performed. Treatment had no significant effect on cell numbers relative to the control cultures.

7.5 Procedure for Second Generation In Vitro Assays

General Procedure

DMS53 cells were counted and cultures seeded equally into 25 cm^2 flasks at low density in 5 ml of growth medium, with two duplicate control cultures and as many additional cultures as required for the compounds of interest to be tested in duplicate. The cultures

were incubated until confluent (approximately 3 days of growth, 10 million cells). Growth medium was then replaced, and the compound of interest was added at the desired concentration in 10 µl of DMSO to the relevant cultures. 10 µl of DMSO was then added to the control cultures. All cultures were then incubated for 24 h. After incubation, 5 ml of medium from each culture was collected in a 15 ml Falcon™ tube. The medium was then centrifuged at 10,000g for 5 min to pellet any insoluble components. 3 ml of this sample was injected onto the HPLC (3 x 1 ml aliquots) and analysed using CT-M2. The remainder was frozen at -80 °C for further analysis. The cells remaining in the cultures were washed twice with DPBS, and lifted with Trypsin-EDTA-EDTA before being counted. Cell counts averaged 10-15 million cells per flask.

Experimental Specifics

In section 3.3, DMS53 cultures were treated with 100 µM SUNB8155. Treatment was performed in duplicate and compared to duplicate controls, with two replicates were performed. Treatment had no significant effect on cell numbers relative to the control cultures.

In section 5.2, DMS53 cultures were incubated for 24 h before treatment, and an additional 24 h with treatment. Cultures were treated with 100 µM SQ22536, 1 µM and 10 µM H89, 20 µM U73122 and 2µM GF109203X. Each treatment was compared to duplicate controls, and two replicates were performed. Treatment had no significant effect on cell numbers relative to the control cultures.

In section 5.3, DMS53 cultures were treated with 100 µM SQ22536 and 40 µM U73122. 5 µM U73122 in MilliQ was also analysed to determine signal response under assay conditions. Each treatment was performed in duplicate and compared to duplicate controls, and two replicates were performed. Treatment had no significant effect on cell numbers relative to the control cultures.

7.6 Procedure for Third Generation In Vitro Assays

General Procedure

DMS53 cells were grown to high density in 175 cm^2 flasks before being lifted, combined and counted. 10 million cells were then seeded into 75 cm^2 flasks with 10ml of growth medium. Two duplicate control cultures, and duplicate pairs for each compound of interest or compound concentration were established. The cultures were then incubated over 72 h, to achieve a cell count of approximately 20-25 million cells. The growth medium was refreshed and each of the duplicate pairs was dosed with the compound of interest in 10 μl of DMSO. The control cultures were then dosed with 10 μl of DMSO. All cultures were then incubated for 24 h.

After incubation, 3.5 ml of medium was transferred directly into Amicon® 4 ml Ultra-4 50 kDa size-exclusion centrifuge filters (Millipore, presoaked for a minimum of 48 h in 50% fetal bovine serum to reduce non-specific adsorption), and the remainder stored in 15 ml Falcon™ tubes at -80 °C for further analysis. The 50 kDa filters were then centrifuged at 7000g for 15 min to remove insoluble components from solution. 3 ml of the filtered medium (3 x 1 ml aliquots) was injected onto the HPLC and analysed using the second-generation separation method.

The cells remaining in each culture were lifted and counted, then pelleted (2500g, 5 min) in 15 ml Falcon™ tubes before being washed with DPBS and repelleted. The cell pellets were resuspended in 400 μl RPMI/10% FCS and frozen in liquid nitrogen. After at least 10 min, the frozen tubes were transferred directly to a 100 °C water bath and heated for 7 minutes. The rapid freeze-thawing process resulted in the lysis of the cells. The lysate was then transferred to Amicon® 0.5 ml Ultra-4 50 kDa centrifuge filters (Millipore, presoaked for a minimum of 48 h in 50% fetal bovine serum) and was centrifuged at 12000g for 30 min. 200 μl RPMI/10% FCS was used to wash each Falcon™

tube and was then transferred to the corresponding 50 kDa filter. The filters were then centrifuged for 10 min. The washing step was repeated again, and after centrifugation, the filtrate was transferred to HPLC vials. A third washing step was performed, and the filters centrifuged for 30 min or until the solution had passed through, and the remaining filtrate was transferred to the corresponding HPLC vials. The filtered lysate (~1 ml) was injected onto the HPLC and analysed using the second-generation separation method.

Experimental Specifics

In section 2.2, DMS53 cultures were grown for either 24 or 72 h with either 10 ml or 30 ml of growth medium. Each growth condition was performed in duplicate. Cell numbers did not significantly differ between cultures incubated for 24 h in 10 h and 30 ml of medium. After 72 h, 10 ml cultures comprised, on average, 30 million cells, while 30 ml cultures comprised, on average, 39 million cells.

In section 3.4, DMS53 cultures were treated with 1 μM, 10 μM and 100 μM SUNB8155. Each concentration treatment was performed in duplicate and compared to duplicate controls, and three replicates were performed and averaged. Treatment had no significant effect on cell numbers relative to the control cultures.

In section 5.4, DMS53 cultures were treated with 10 μM GF109203X and 100 μM SUNB8155. Medium samples were frozen at -80 °C, then for analysis were thawed and centrifuged at 10000g, 5 min, 4 °C. Centrifuged medium (3 x 1 ml aliquots) was injected onto the HPLC and analysed using CT-M2. Each concentration treatment was performed in duplicate and compared to duplicate controls, and three replicates were performed and averaged. Treatment had no significant effect on cell numbers relative to the control cultures.

In Chapter 6, for the detection of gCT and gCT-G, two TT cultures were seeded with 20 million cells and cultured for 13 days (approx. 100 million cells). Medium was changed every two days except for the final 96 h. Lysate was prepared as above and analysed using CT-M2.

7.7 Reverse Transcription PCR Procedures

mRNA extraction from mammalian cell cultures

General Procedure

mRNA was obtained from cell lysates using the QIAGEN RNeasy mini kit following the manufacturer's instructions. Cultures of the cell line of interest were grown until the desired confluence had been reached and then lifted with 0.05% trypsin-EDTA and counted. The cells were aliquoted into Eppendorf tubes (less than 10 million per sample) and were pelleted by centrifugation at 1200g for 5 min, washed with DPBS, and then re-pelleted. The appropriate volume of RLT buffer (350-600 µl with 1% β-mercaptoethanol added) was added to lyse each pellet, which was then mixed thoroughly by pipetting. The same volume of 70% ethanol was added to the lysate and mixed thoroughly. Each lysate sample (700 µl) was loaded onto separate RNeasy spin columns, which were centrifuged at 10000g for 30 s and the run through discarded, before being loaded with another 700 µl of lysate and centrifuged again. The columns were then washed with subsequent aliquots of 1 x 700 µl of RW1 buffer and 2 x 500 µl of RPE buffer (with ethanol added), with the columns spun at 10000g for 30 s and the run through discarded after each loading. The columns were placed in clean collection tubes and spun for 2 min at 10000g to dry the column. RNase–free water (30 µl) was then added to each column, and they were placed in 1.5 ml Eppendorf tubes and centrifuged for 1 min to elute the mRNA from the columns. The extracted mRNA samples were then stored at -20 °C.

Experimental Specifics

In the first RT-PCR approach (Section 4.2), cultures in 75 cm^2 flasks were grown for mRNA analysis. A PC3 culture and a DMS53 culture were both grown to confluence and lifted with 2 ml of 0.05% trypsin-EDTA. After counting, these were divided into 1 and 2 million cell aliquots for the PC3 cells, and 1, 2 and 10 million aliquots for the DMS53 cells for lysis. RLT buffer and ethanol (600 µl of each) were used to lyse each sample.

In the second RT-PCR approach (Section 4.3), cultures in 175 cm^2 flasks were grown for mRNA analysis. A TT culture was incubated until it reached approximately 80% confluence while a DMS53 culture was incubated until it reached approximately 50% confluence. Both were lifted with 5 ml of 0.05% trypsin-EDTA and counted. A sample of 10 million cells was aliquoted for each cell line, and these were lysed with 1 ml of RLT and 1 ml of 70% ethanol. mRNA was eluted with 45 µl of RNase-free water.

In the third RT-PCR approach (Section 4.4), two cultures of TT and DMS53 cells were grown in 175 cm^2 flasks until 80% confluent (approx. 60-80 million cells). The adhered cells were washed twice on ice with DPBS before 6 ml of RLT buffer was added to lyse the cells in-flask, followed by scrapping. Ethanol (6 ml, 70%) was then added and the lysate mixed thoroughly. For the TT cell lysate, two duplicate columns were loaded and washed as described in the general procedure, then eluted with 50 µl RNase-free water. For the DMS53 lysate, one column was loaded and washed as described above, while one was loaded with only one 700 µl aliquot of lysate and then washed as described above. Each column was eluted with 2 x 30 µl RNase-free water, and these were not combined. The six resulting samples then underwent DNase treatment with the Promega RQ1 DNase kit. DNase (30 units, 1 u/µl) was added to each sample with 10 µl of reaction buffer and incubated for 30 min at 37 °C. The DNase activity was then quenched with 10 µl STOP solution and incubated at 65 °C for 10 min. RNasin RNase-inhibitor (2 µl) was

added to each sample before freezing at -20 °C.

Before use, these samples underwent an additional purification step, where 350 μl of RLT buffer and 250 μl of 100% ethanol were added to each sample, followed by loading onto RNeasy spin columns and undergoing the washing process outlined in the general procedure, before elution with 30 μl RNase-free water. Samples were then analysed using nanodrop. 260:280 ratios were all greater than 1.98, most 260:230 ratios were greater 1.93 (the second elution of the 2 x 700 μl loaded DMS53 sample was 1.39). mRNA quantifications were as follows: DMS53 1 x 700 μl elution 1: 778 ng/μl, DMS53 1 x 700 μl elution 2: 189 ng/μl, DMS53 2 x 700 μl elution 1: 1849 ng/μl, DMS53 2x 700 μl elution 2: 256 ng/μl, TT1 2 x 700 μl: 363 ng/μl, TT2 2 x 700 μl: 321 ng/μl.

One step cDNA synthesis and hCTR cDNA Amplification

General Procedure

All RT-PCR reactions were undertaken using QIAGEN OneStep RT-PCR kits. For each primer pair used in a given analysis, a master mix of the primers along with the required deoxynucleotide triphosphates (dNTPs), enzymes and buffers was made up according to the number of reactions required, and then aliquoted into PCR tubes along with the template. The general composition of this mix is listed in **Table 7.6**. This composition was scaled up according to the number of templates to analysed with a particular primer pair, with a new master mix made for each primer pair used. Primer sequences and binding regions are listed in **Table 7.7**.

Thermocycler conditions were obtained from the OneStep RT-PCR kit protocol and adapted based the reports published by Wu and coworkers[175] (Primers P1-6, **Table 7.8**) and by Silvestris and coworkers[173] (Primers F1-4 and R1-4, **Table 7.9**). After

amplification was complete, samples were stored at -20 °C.

Amplification for sequencing was undertaken with the Taq polymerase protocol (**Table 7.10** and **Table 7.11**), but using only one primer of the pair used in the amplification of the sample (i.e. primer A but not B added to a sample transcribing the AB amplicon, and vice versa for the reverse reaction). Sequencing performed using the Sanger method with with a 3730xl DNA Analyzer from Applied Biosystems.

Table 7.6: *General composition of RT-PCR master mix.*

PCR Reaction Component	Vol. Required per Reaction (μl)
RNase-Free Water	24.5 (+ 5 μl (10% total vol.) to account for loss)
5x PCR Buffer	10
Primer A (10 μM)	3
Primer B (10 μM)	3
dNTPs 10 mM (dATP, dCTP, dGTP, dTTP)	2
Enzyme Mix (reverse transcriptases + DNA polymerase)	2
RNasin	0.5
Template	5 (if less, made up with RNAse-free water)

Table 7.7: *Primers used for RT-PCR, Taq PCR and PCR for sequencing.*

Primer (Direction)	Length	Sequence	hCTR transcript variant 1 (NM_001164737.1) binding region
P1 (F)[175]	20	CAATCGAACCTGGTCCAACT	726-745
P2 (R)[175]	20	CCTCATGGGTTTCCCTCATT	1399-1380
P3 (F)[175]	20	TGGGAATCCAGTTTGTCGTC	1457-1476
P4 (R)[175]	20	AAGGGATGATCTCAGCACTC	1795-1776
P5 (F)	20	CCAACAATAGAGCCCAAGCC	448-467
P6 (R)	20	AGGTCTCCAGGGAAAGACGA	1491-1472
F1 (F)[176]	23	CCAGTGAGAAGTATGAGAGAGTG	Binds to alternative sequence (NM_001742.3) 21-44
F2 (F)[176]	22	GTATTGTCCTATCAGTTCTGCC	619-640
F3 (F)[176]	21	ACTGCTGGCTGAGTGTGGAAA	1265-1285
F4 (F)[176]	21	TTGCTTCTATTGAGCTGTGCC	212-232
R1 (R)[176]	21	ATGTTCTTGTGCAGGGTTACC	962-942

R2 (R)[176]	20	GAG AAG GCC AGG GAA AGG AA	No binding against any hCTR transcript in ReqSeq database.
R3 (R)[176]	21	GAAGCAGTAGATGGTCGCA **C**(A?)C C should be A based on binding.	1581-1561
R4 (R)[176]	24	ACATTCAAGCAGATGACTCTTGCT	1831-1808

Table 7.8: *Thermocycler conditions for RT-PCR with primers P1-6.* Adapted from Wu.[175]

Temperature (°C)	Duration	Purpose
50	30 min	Reverse transcription
95	15 min	Initial PCR activation
94	45 s	*3 step cycling:* Denaturation
50	45 s	Annealing
72	1 min	Extension *40 cycles*
72	10 min	Final extension
Final	∞	Stasis

Table 7.9: *Thermocycler conditions for RT-PCR with primers F1-4 and R1-4.* Adapted from Silvestris.[176]

Temperature (°C)	Duration	Purpose
50	30 min	Reverse transcription
95	15 min	Initial PCR activation
94	45 s	*3 step cycling:* Denaturation
60	60 s	Annealing
72	90 s	Extension *35 cycles*
72	10 min	Final extension
Final	∞	Stasis

Experimental Specifics

In the first RT-PCR approach (Section 4.2), DMS53 and PC3 cDNA was amplified with two primer pairs, P12 and P34. Since three concentrations of DMS53 mRNA (from 1, 2 and 10 million cells, 2 and 10 million samples in duplicate) and two of PC3 mRNA (from 1 and 2 million cells) were obtained, 16 RT-PCR reactions were run (including controls) following the general procedure above, except that 10 μl of template was used rather than 5 μl. No RNasin was used. These samples were run on an agarose gel to determine which conditions produced the best amplification. However, band intensity was low so an additional Taq PCR reaction was undertaken with each RT-PCR product. Master mix

composition is outlined in **Table 7.10**, and thermocycler conditions are outlined in **Table 7.11**. These samples were rerun on an agarose gel, and it was determined that mRNA from the DMS53 and PC3 2 million cell samples was the most effective. These samples were rerun in isolation. The agarose gel composition was 2% agarose, with 1.5 µl of 10000x GelRed™ stain in 60 ml total volume. Samples were loaded in a solution comprising 10 µl of PCR product, 6 µl of RNase-free water and 4 µl Bromophenol Blue solution. A 500bp ladder (5 µl) was loaded, and the gel was run at 200 V for approx. 20 min (**Figure 4.3**).

Table 7.10: *Master mix composition for Taq PCR reaction.*

PCR Reaction Component	Vol. Required per Reaction (µl)
RNase-Free Water	36.5 (+ 5µl (10% total vol.) to account for loss)
10x Taq Buffer	5
Primer A (10 µM)	1
Primer B (10 µM)	1
dNTPs 10 mM (dATP, dCTP, dGTP, dTTP)	1
Taq polymerase	0.5
Template	5

Table 7.11: *Thermocycler conditions for secondary Taq PCR and for sequencing.*

Temperature (°C)	Duration	Purpose
94	2 min	Initial PCR activation
50	30 sec	*3 step cycling:* Denaturation
72	2 min	Annealing
94	10 sec	Extension *40 cycles*
50	2 min	Final annealing
72	5 min	Final extension
4	∞	Stasis

In the second RT-PCR approach (Section 4.3), DMS53 and TT cDNA was amplified with four primer pairs, P12, P56, P16 and P52. Primers P5 and P6 were designed using the NCBI Primer-BLAST tool, with T_m of 58.8 °C and 59.8 °C, GC% of 55 and 55, self-complementarities of 2 and 4, and self-3′ complementarities of 1 and 0. Twelve PCR reactions were performed in total. The master mix solution comprised 10 μl of Q-solution (provided in OneStep RT-PCR kit to improve amplification of GC-rich regions) and 10 μl (+5 μl to account for loss) of water, allowing 10 μl of template to be used. No RNasin was used. The annealing and extension steps were altered, with annealing occurring at 52 °C for 45 s, and extension occurring at 72 °C for 1 min. The agarose gel

composition was 2% agarose, with 1.5 μl of 10000x GelRed™ stain in 60 ml total volume. Samples were loaded in a solution comprising 5 μl of PCR product, 3 μl of RNase-free water and 2 μl Bromophenol Blue solution. A 500bp ladder (5 μl) was loaded, and the gel was run at 200 V for approx. 20 min (**Figure 4.4**).

In the third RT-PCR approach (Section 4.4), DMS53 and TT mRNA samples were amplified. DMS53 2 x 700 μl elution one and TT1 2 x 700 μl samples were used. These samples were amplified with primer pairs F4R3 and F3R3, resulting in a total of 6 PCR reactions (including controls). Based on nanodrop analysis, 1.5 μg mRNA was aliquoted for each sample and made up to 5 μl for use as the template. The agarose gel composition was 2% agarose, with 4 μl of 10000x GelRed™ stain in 60 ml total volume. Samples were loaded in a solution comprising 16 μl of PCR product and 4 μl bromophenol blue solution. A 1000bp ladder (3 μl) was loaded, and the gel was run at 100 V for approx. 1 ½ h (**Figure 4.5**).

7.8 Western Blot Procedures

Cell Lysis and Protein Quantification Procedures

General Procedure

RIPA buffer was prepared from the components listed in **Table 7.12**. Flasks containing the cell lines of interest were placed on ice, the medium aspirated and the cells washed twice with DPBS followed by aspiration. RIPA buffer (10 ml in 175 cm^2 flasks, 5 ml in 75 cm^2 flasks) was added each flasks, which were then rocked for 2 min and scrapped. The lysate was transferred to 15 ml Falcon™ tubes and centrifuged at 750g for 10 min. The supernatant was removed and aliquoted into 1.5ml Eppendorf tubes, then frozen at -20 °C.

Protein quantification was undertaken using the Bio-Rad Bradford protein assay kit. Cell lysate was aliquoted into a 96 well plate alongside known concentrations of bovine serum albumin (BSA) ranging from 0.2 mg/ml to 2 mg/ml as per the manufacturer's instructions. The colourmetric reagents provided in the kit were then added and the relative absorbance intensities for each well were recorded using a plate reader. The absorbance of the BSA samples was plotted and a linear relationship between concentration and absorbance derived. Absorbance measurements from cell lysate samples could then be used to determine protein concentration based on this relationship.

Table 7.12: *Components of RIPA buffer.*

Component	Volume (ml)
MilliQ water	85.6
2 M Tris.HCl solution	2.5
5 M NaCl solution	2
0.54 M EDTA solution	0.4
10% SDS (v/v) solution	1
20% Deocycholic acid (w/v) solution	2.5
1M NaF solution	5
Triton x100	1
P8340 protease inhibitor cocktail	0.1 per 10 ml of complete buffer

Experimental Specifics

In Western blot experiment 1 (Section 4.5), a 175 cm^2 flask of DMS53 cells was cultured to confluence and lysed as described in the general procedure. The protein concentration was found to be 1.5 µg/µl.

In Western blot experiment 2 (Section 4.6), DMS53 cultures were grown in 75 cm^2 flasks. Growth was controlled by seeding flasks with 10 million cells and culturing for 3 days before lysing. Lysis was carried out as described in the general procedure. In addition, PC3 and DU145 cultures in 75 cm^2 flasks were grown and lysed using the same method. The protein concentrations found are as follows: DMS53: 0.65 µg/µl, PC3: 0.82 µg/µl, DU145: 0.98 µg/µl.

Western Blot Procedures

General Procedure

A volume of cell lysate corresponding to the desired total protein concentration was transferred into an Eppendorf tube for each sample, along with 6x SDS-PAGE loading buffer containing β-mercaptoethanol, and was made up to 24 µl with milliQ water. The samples were heated at 95 °C for 10 min. Each sample (24 µl) was loaded onto a 4-20% mini-PROTEAN® 10 well precast polyacrylamide gel assembled in a Bio-Rad mini-PROTEAN 3 assembly with running buffer. PageRuler™ prestained protein ladder (15-180 kDA, 10 µl) was loaded. The gel was then run at 100 V for approximately 2 hours or until the 70 kDa marker was in the middle of the gel. The gel was then removed from the cassette and transferred using the Bio-Rad Trans-Blot® Turbo™ semi-dry transfer kit onto a PVDF membrane, according to the manufacturers instructions (Mixed MW setting; 2.5 A constant, 7 min).

The PVDF membrane was blocked with 5% (w/v) skim milk powder in TBST (Tris

buffered saline – Tween 20, comprising 50 mM Tris, 150 mM NaCl, 0.05% Tween 20) buffer for an hour. The specific hCTR2 rabbit polyclonal antibody ab103422 from Abcam (15 µg) was added to 3 ml of 5% (w/v) skim milk powder in TBST in a 50 ml Falcon™ tube, and the PVDF membrane was placed in the tube and incubated with rotation overnight at 4 °C. The membrane was then washed three times with TBST for 5 min while rocking. The membrane was then incubated with secondary antibody (rabbit with horseradish peroxidase, 1:2000 or 1.5 µg) in 3 ml 5% (w/v) skim milk powder in TBST for an hour. The membrane was again washed three times with TBST for 5 min while rocking. Finally, Bio-Rad Clarity™ Western ECL blotting reagents (50:50 reagents A and B, 1 ml) pipetted onto the membrane, and the chemiluminescence was measured using the Chemidoc imager from Bio-Rad.

Experimental Specifics

In Western blot experiment 1 (Section 4.5), three different total protein concentration samples were loaded onto the gel; 15 µg, 23 µg and 30 µg.

In Western blot experiment 2 (Section 4.6) one sample of DMS53 lysate, one sample of PC3 lysate, and one sample of DU145 lysate were loaded onto the gel in volumes corresponding to 20 µg. The loading solution volume was doubled to 48 µl and the entirety loaded, to account for lower total protein concentration in the lysate. After primary antibody incubation, three washes were undertaken with 5% (w/v) skim milk powder in TBST instead of TBST.

7.9 LCMS Methodology for the Detection of CT and OT species

Detection

LCMS separation and detection of CT and its related species, as well as OT and its precursor from cell lysate used a Waters Alliance 2695 separation module connected to a

Waters Flow Splitter, a Waters TQD Mass Detector (ESI) and a Waters Fraction Collector. For separation of CT species, injected samples underwent separation with a Waters Symmetry C8 (4.6 x 150 mm) reverse phase column. The solvent and gradient system is shown in **Table 7.13**. For separation of OT species, injected samples underwent separation with a Synergi 4u MAX-RP 80A (2 x 250 mm) reverse phase column. The solvent and gradient system is shown in **Table 7.14**. For analysis, the flow splitter was set to a single output and analytes were directed to the TQD Mass Detector for MS or MRM analysis. The parameters for MRM detection of CT and OT species including parent and daughter ions, cone voltage and collision energy are listed in **Table 7.15**. For fractionation, the flow splitter was set to dual output and analytes were directed to the Waters Fraction Collector and TQD Mass Detector in a 15:1 ratio. Fractions of relevant chromatogram regions were then reinjected onto the LCMS for analysis.
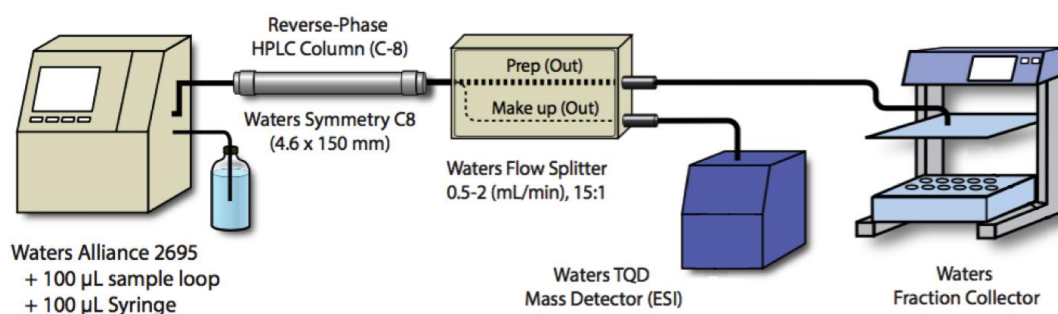
Figure 7.3: *LCMS system used in the separation and detection of peptide hormones and their related species.*

Table 7.13: *LCMS solvent system used for separating CT species.*

Time (min)	Flow (ml/min)	Water + 0.1% Formic Acid (%)	Acetonitrile + 0.1% Formic Acid (%)	Gradient Curve
0.00	0.30	95.0	5.0	1
1.00	0.30	95.0	5.0	1
10.00	0.30	70.0	30.0	6
24.00	0.30	70.0	30.0	6
25.00	0.30	95.0	5.0	6

Table 7.14: *LCMS solvent system used for separating OT species.*

Time (min)	Flow (ml/min)	Water + 0.1% Formic Acid (%)	Acetonitrile + 0.1% Formic Acid (%)	Gradient Curve
0.00	0.30	95.0	5.0	1
1.00	0.30	95.0	5.0	1
5.00	0.30	60.0	40.0	6
9.00	0.30	60.0	40.0	6
10.00	0.30	95.0	5.0	6

Table 7.15: *MRM conditions for the detection of CT and OT species using LCMS.*

Compound	Parent (m/z)	Daughter (m/z)	Cone (V)	Collision (V)
Calcitonin	1140.09	70.07	34	50
	1140.09	115.15	34	46
	1140.09	1102.16	34	24
Calcitonin-Glycine	1159.47	70.07	42	60
	1159.47	173.15	42	44
	1159.47	1102.16	42	14
Glycosylated Calcitonin	1092.65	70.07	34	50
	1092.65	115.15	34	46
Glycosylated Calcitonin- Glycine	1106.0	70.07	42	60
	1106.0	173.15	42	44
Oxytocin	1007.40	86.11	52	76
	1007.40	136.06	52	66
	1007.40	285.18	52	48
	1007.40	323.06	52	66
Oxytocin-Glycine	1048.34	70.07	84	80

Oxytocin-Glycine	1048.34	86.11	84	80
Oxytocin-Glycine	1048.34	86.51	84	58

Sample Preparation and Analysis

For the detection of gCT and gCT-G from TT lysate, TT cells were seeded in a 175 cm^2 flask and cultured until confluent, then incubated for a further 5 days (approx. 200 million cells). Cultures were lysed as outlined in experimental section 7.6, and analysed by LCMS.

For the detection of gCT and gCT-G in TT medium, concentrated TT medium samples were prepared for fractionation studies by lyophilisation. The medium was harvested from cultures and frozen, then 15 ml was thawed and filtered as outlined in section 7.6. The filtered medium was frozen in liquid nitrogen in a 50 ml Falcon™ tube, lyophilised overnight at -20 °C, 160 mBar and reconstituted in 1 ml of MilliQ. This was centrifuged at 10000g (5 min, 4 °C) and the supernatant transferred to an HPLC vial for LCMS analysis. The fraction collector was set to collect fractions from 17 min 30 sec to 20 min, with each fraction accounting for 8 s of elution. These fractions were reinjected onto the LCMS for analysis.

For detection of OT, OT-d$_{10}$ and OT-G in DMS79 lysate, cells were cultured in a 175 cm^2 flask in 50 ml of RPMI for at least 96 h until large clumps of suspended cells were present (approx. 60-70 million cells). Cells were lifted and counted, then pelleted (2500g, 5 min) in a 15 ml Falcon™ tube before being washed with DPBS and repelleted. The cell pellet was resuspended in 400 μl RPMI/10% FCS and frozen in liquid nitrogen. After at least 10 min, the frozen tube was transferred directly to a 100 °C water bath and

heated for 7 minutes. The rapid freeze-thawing process resulted in the lysis of the cells. The lysate was then transferred to an Amicon® 0.5 ml Ultra-4 50 kDa centrifuge filter (Millipore, presoaked for a minimum of 48 h in 50% fetal bovine serum) and was centrifuged at 12000g for 30 min. 200 μl RPMI/10% FCS was used to wash the Falcon™ tube and was then transferred to the corresponding 50 kDa filter. The filter and contents were then centrifuged for 10 min. The washing step was repeated again, and after centrifugation, the filtrate was transferred to HPLC vials. A third washing step was performed, and the filter centrifuged for 30 min or until the solution had passed through, and the remaining filtrate was transferred to the corresponding HPLC vial (1 ml). OT-d_{10} (100 μl, 0.5 ng/ml) was spiked into one lysate sample while the other acted as a control.

7.10 HPLC Method for Detection OT and OT-G (OT-M3)

HPLC separation and quantification of OT from N38 cell medium and lysate used the same HPLC system as outlined in section 7.3 (**Figure 7.2**). The solvent and gradient system for the separation is shown in **Table 7.16.** Data were collected and processed with Empower Pro-Empower 2 software using an IBM data station. Between each sample injection a cleaning routine was applied (52 min total) using the solvent and gradient system in **Table 7.4 and Table 7.5,** with the second method directly following the first.

Table 7.16: *Solvent system for the third generation OT separation method.*

Time (min)	Flow (ml/min)	Water (%)	Acetonitrile (%)	0.1% TFA in 2-Propanol (%)	Waters AccQ.Tag™ Eluent A (100 ml in 1000 ml water) (%)	Gradient Curve
0.00	3.00	0.0	0.0	0.0	100.0	0
1.00	1.00	0.0	0.0	0.0	100.0	6
3.00	1.00	0.0	3.0	0.0	97.0	6
3.50	1.00	0.0	3.0	0.0	97.0	6
4.00	1.00	0.0	10.0	0.0	90.0	6
7.00	1.00	0.0	15.0	0.0	85.0	6
70.00	1.00	0.0	20.0	0.0	80.0	6

Sample Preparation

For DMS79 lysate preparation, cells were cultured in a 175 cm^2 flask in 50 ml of RPMI for at least 96 h until large clumps of suspended cells were present (approx. 60-70 million cells). Cells were lifted and counted, then pelleted (2500g, 5 min) in a Falcon™ tube before being washed with DPBS and repelleted. P3840 mammalian protease inhibitor solution (20 μl) was added to the pellet. The cell pellet was resuspended in 400 μl RPMI/10% FCS and frozen in liquid nitrogen. After at least 10 min, the frozen tube was transferred directly to a 100 °C water bath and heated for 7 minutes. The rapid freeze-thawing process resulted in the lysis of the cells. The lysate was then transferred to an Amicon® 0.5 ml Ultra-4 50 kDa centrifuge filter (Millipore, presoaked for a minimum of 48 h in 50% fetal bovine serum) and was centrifuged at 12000g for 30 min. RPMI/10% FCS (200 μl) was used to wash the Falcon™ tube and was then transferred to the corresponding 50 kDa filter. The filter and contents were then centrifuged for 10 min. The washing step was repeated again, and after centrifugation, the filtrate was transferred to HPLC vials. A third washing step was performed, and the filter centrifuged for 30 min or until the solution had passed through, and the remaining filtrate (1 ml) was transferred to the corresponding HPLC vial for analysis.

References

[1] J. E. Griffin and S. R. Ojeda, *Textbook of Endocrine Physiology*, Oxford University Press, **2004**, p. 1.

[2] R. I. G. Holt and N. A. Hanley, *Essential Endocrinology and Diabetes*, John Wiley and Sons, **2012**, p. 14.

[3] D. L. Nelson and C. Lehninger, *Principles of Biochemistry*, W. H. Freeman, England, **2004**, p. 881.

[4] W. M. Bayliss and E. H. Starling, *J. Physiol.* **1902**, *28*, 325-353.

[5] E. H. Starling, *Lancet* **1905**, *2*, 339-341.

[6] U. Renner, U. Pagotto, E. Arzt and G. K. Stalla, *Eur. J. Endocrinol.* **1996**, *135*, 515-532.

[7] S. Melmed, K. S. Polosky, P. R. Larsen and H. M. Kronenberg, *Williams Textbook of Endocrinology*, Elsevier, USA, **2011**, p. 21-43.

[8] D. M. Findlay and P. M. Sexton in *Calcitonin A2 - H. L. Henry, Vol. 1* (Ed. A. W. Norman), Academic Press, New York, **2003**, p. 220.

[9] A. D. McNaught and A. Wilkinson, *IUPAC. Compendium of Chemical Terminology, 2nd ed. (the "Gold Book")*, Blackwell Scientific Publications, Oxford, **1997**, p. 1194.

[10] A. Ferrand and T. C. Wang, *Cancer Lett.* **2006**, *238*, 15-29.

[11] G. Wilcox, *Clin. Biochem. Rev.* **2005**, *26*, 19-39.

[12] R. A. Davey and D. M. Findlay, *J. Bone Miner. Res.* **2013**, *28*, 973-979.

[13] T. R. Insel, *Am. J. Psychiatry* **1997**, *154*, 726-735.

[14] K.-H. Kim and B. L. Seong, *Biotechnol. Bioprocess Eng.* **2001**, *6*, 244-251.

[15] S. T. Prigge, R. E. Mains, B. A. Eipper and L. M. Amzel, *Cell. Mol. Life Sci.* **2000**, *57*, 1236-1259.

[16] R. E. Mains, B. T. Bloomquist and B. A. Eipper, *Mol. Endocrinol.* **1991**, *5*, 187-193.

[17] F. Cao, *PhD Thesis - Australian National University* **2012**.

[18] R. C. Cuneo, F. Saiomon, O. A. McGauiey and P. H. Sönksen, *Clin. Endocrinol. (Oxf)*

1992, *37*, 387-397.

[19] M. T. Barakat, K. Meeran and S. R. Bloom, *Endocr.-Relat. Cancer* **2004**, *11*, 1-18.

[20] S. Kovac, A. Shulkes and G. S. Baldwin, *Curr. Opin. Endocrinol. Diabetes Obes.* **2009**, *16*, 79-85.

[21] P. M. Sexton, D. M. Findlay and T. J. Martin, *Curr. Med. Chem.* **1999**, *6*, 1067-1093.

[22] A. J. Felsenfeld and B. S. Levine, *Clin. Kidney J.* **2015**, *8*, 180-187.

[23] E. Zudaire, A. Martínez and F. Cuttitta, *Regul. Pept.* **2003**, *112*, 175-183; L. L. Nikitenko, S. B. Fox, S. Kehoe, M. C. P. Rees and R. Bicknell, *Br. J. Cancer* **2005**, *94*, 1-7; V. A. Siclari, K. S. Mohammad, D. R. Tompkins, H. Davis, C. R. McKenna, X. Peng, L. L. Wessner, M. Niewolna, T. A. Guise, A. Suvannasankha and J. M. Chirgwin, *Breast Cancer Res.* **2014**, *16*, 458.

[24] F. Wang, M. Herrington, J. Larsson and J. Permert, *Mol. Cancer* **2003**, *2*, 1-5; J. T. Magruder, D. Elahi and D. K. Andersen, *Pancreas* **2011**, *40*, 339-351.

[25] L. Levine, J. A. Lucci, B. Pazdrak, J.-Z. Cheng, Y.-S. Guo, J. Courtney M. Townsend and M. R. Hellmich, *Cancer Res.* **2003**, *63*, 3495-3502; S. R. Preston, G. V. Miller and J. N. Primrose, *Crit. Rev. Oncol. Hematol.* **1996**, *23*, 225-238.

[26] T. J. Martin, D. M. Findlay, I. MacIntyre, J. A. Eisman, V. P. Michelangeli, J. M. Moseley and N. C. Partiridge, *Biochem. Biophys. Res. Commun.* **1980**, *96*, 150-156; D. M. Findlay, M. deLuise, V. P. Michelangeli, M. Ellison and T. J. Martin, *Cancer Res.* **1980**, *40*, 1311-1317.

[27] S. Thomas, A. Muralidharan and G. V. Shah, *Int. J. Oncol.* **2007**, *31*, 1425-1437.

[28] P. Trimboli, L. Giovanella, A. Crescenzi, F. Romanelli, S. Valabrega, G. Spriano, N. Cremonini, R. Guglielmi and E. Papini, *Head Neck* **2014**, *36*, 1216-1223.

[29] H. Zhao, L. L. Ning, Z. Y. Wang, H. T. Li, D. Qiao, Y. Yao and H. L. Qin, *Cell Biochem. Biophys.* **2014**, *70*, 1097-1104; V. Papantoniou, S. Tsiouris, M. Sotiropoulou, P. Valsamaki, J. Koutsikos, N. Ptohis, C. Dimitrakakis, E. Sotiropoulou, M. Melissinou, L. Nakopoulou, A. Antsaklis and C. Zerva, *Am. J. Clin. Oncol.* **2007**, *30*, 420-427; O. Nagakawa, M. Ogasawara, H. Fujii, K. Murakami, J. Murata, H. Fuse and I. Saiki, *Cancer Lett.* **1998**, *133*, 27-33.

[30] R. T. Dorsam and J. S. Gutkind, *Nat. Rev. Cancer* **2007**, *7*, 79-94.

[31] H.-G. Yu, S.-L. Tong, Y.-M. Ding, J. Ding, X.-M. Fang, X.-F. Zhang, Z.-J. Liu, Y.-H. Zhou, Q.-S. Liu, H.-S. Luo and J.-P. Yu, *Int. J. Cancer* **2006**, *119*, 2724-2732; J. P. Smith and T. E. Solomon, *Am. J. Physiol. Gastrointest. Liver Physiol.* **2014**, *306*, G91-G101.

[32] P. Mishra, S. Senthivinayagam, V. Rangasamy, G. Sondarva and B. Rana, *Mol. Endocrinol.* **2010**, *24*, 598-607; O. O. Ogunwobi and I. L. P. Beales, *Regul. Pept.* **2006**, *134*, 1-8.

[33] O. Patel, A. Shulkes and G. S. Baldwin, *BBA-Rev. Cancer* **2006**, *1766*, 23-41.

[34] H. Ligumsky, I. Wolf, S. Israeli, M. Haimsohn, S. Ferber, A. Karasik, B. Kaufman and T. Rubinek, *Breast Cancer Res. Treat.* **2011**, *132*, 449-461; J. A. Koehler, T. Kain and D. J.

Drucker, *Endocrinology* **2011**, *152*, 3362-3372; M. A. Nauck and N. Friedrich, *Diabetes Care* **2013**, *36*, S245-S252.

[35] S. Fister, A. R. Günthert, G. Emons and C. Gründker, *Cancer Res.* **2007**, *67*, 1750-1756; K.-Y. Kim, K.-C. Choi, N. Auersperg and P. C. K. Leung, *Endocr.-Relat. Cancer* **2006**, *13*, 211-220; S. Kraus, Z. Naor and R. Seger, *Cancer Lett.* **2006**, *234*, 109-123.

[36] A. V. Schally, J. L. Varga and J. B. Engel, *Nat. Clin. Pract. End. Met.* **2008**, *4*, 33-43; G. Siriwardana, A. Bradford, D. Coy and P. Zeitler, *Mol. Endocrinol.* **2006**, *20*, 2010-2019; Z. Kahán, J. M. Arencibia, V. J. Csernus, K. Groot, R. D. Kineman, W. R. Robinson and A. V. Schally, *J. Clin. Endocrinol. Metab.* **1999**, *84*, 582-589.

[37] Y. Wu, K. McRoberts, S. S. Berr, H. F. Frierson, Jr., M. Conaway and D. Theodorescu, *Oncogene* **2006**, *26*, 765-773; K. Ketterer, B. Kong, D. Frank, N. A. Giese, A. Bauer, J. Hoheisel, M. Korc, J. Kleeff, C. W. Michalski and H. Friess, *Cancer Lett.* **2009**, *277*, 72-81.

[38] M. Körner and J. C. Reubi, *Peptides* **2007**, *28*, 419-425; M. Ruscica, E. Dozio, M. Motta and P. Magni, *Peptides* **2007**, *28*, 426-434.

[39] C. Pequeux, B. P. Keegan, M. T. Hagelstein, V. Geenen, J. J. Legros and W. G. North, *Endocr.-Relat. Cancer* **2004**, *11*, 871-885; M. Petersson, *Regul. Pept.* **2008**, *150*, 50-54; M. Zhong, M. L. Boseman, A. C. Millena and S. A. Khan, *Mol. Cancer Res.* **2010**, *8*, 1164-1172.

[40] M.-C. Déry, P. Chaudhry, V. Leblanc, S. Parent, A.-M. Fortier and E. Asselin, *Biol. Reprod.* **2011**, *85*, 1133-1142.

[41] P. Onori, C. Wise, E. Gaudio, A. Franchitto, H. Francis, G. Carpino, V. Lee, I. Lam, T. Miller, D. E. Dostal and S. S. Glaser, *Int. J. Cancer* **2010**, *127*, 43-54.

[42] M. Rosso, M. J. Robles-Frías, R. Coveñas, M. V. Salinas-Martín and M. Muñoz, *Tumor Biology* **2008**, *29*, 245-254; L. Raffaghello, P. Chiozzi, S. Falzoni, F. Di Virgilio and V. Pistoia, *Cancer Res.* **2006**, *66*, 907-914; S. Garcia-Recio, G. Fuster, P. Fernandez-Nogueira, E. M. Pastor-Arroyo, S. Y. Park, C. Mayordomo, E. Ametller, M. Mancino, X. Gonzalez-Farre, H. G. Russnes, P. Engel, D. Costamagna, P. L. Fernandez, P. Gascón and V. Almendro, *Cancer Res.* **2013**, *73*, 6424-6434.

[43] B. Collado, M. J. Carmena, C. Clemente, J. C. Prieto and A. M. Bajo, *Peptides* **2007**, *28*, 1896-1901; A. Valdehita, M. J. Carmena, B. Collado, J. C. Prieto and A. M. Bajo, *Regul. Pept.* **2007**, *144*, 101-108.

[44] D. H. Copp, E. C. Cameron, B. A. Cheney, A. G. F. Davidson and K. G. Henze, *Endocrinology* **1962**, *70*, 638-649.

[45] M. Azria, *The Calcitonins: Physiology and Pharmacology*, Karger, Basel, **1989**, p. 20-25; G. Andreotti, B. L. Mendez, P. Amodeo, M. A. Morelli, H. Nakamuta and A. Motta, *J. Biol. Chem.* **2006**, *281*, 24193-24203.

[46] S. Houssami, D. M. Findlay, C. L. Brady, T. J. Martin, R. M. Epand, E. E. Moore, E. Murayama, T. Tamura, R. C. Orlowski and P. M. Sexton, *Mol. Pharmacol.* **1995**, *47*, 798-809.

[47] S. R. J. Hoare, *Drug Discovery Today* **2005**, *10*, 417-427.

[48] M. Dong, D. I. Pinon, R. F. Cox and L. J. Miller, *J. Biol. Chem.* **2004**, *279*, 1167-1175.

[49] S. D. Stroop, H. Nakamuta, R. E. Kuestner, E. E. Moore and R. M. Epand, *Endocrinology* **1996**, *137*, 4752-4756.

[50] D. J. Merkler, *Enzyme Microb. Technol.* **1994**, *16*, 450-456.

[51] C. Bergwitz, T. J. Gardella, M. R. Flannery, J. T. Potts, H. M. Kronenberg, S. R. Goldring and H. Jüppner, *J. Biol. Chem.* **1996**, *271*, 26469-26472.

[52] S. Deshayes, M. C. Morris, G. Divita and F. Heitz, *Cell. Mol. Life Sci.* **2005**, *62*, 1839-1849.

[53] M. C. Schmidt, B. Rothen-Rutishauser, B. Rist, A. Beck-Sickinger, H. Wunderli-Allenspach, W. Rubas, W. Sadée and H. P. Merkle, *Biochemistry* **1998**, *37*, 16582-16590.

[54] Z. Machova, C. Mühle, U. Krauss, R. Tréhin, A. Koch, H. P. Merkle and A. G. Beck-Sickinger, *ChemBioChem* **2002**, *3*, 672-677.

[55] U. Krauss, F. Kratz and A. G. Beck-Sickinger, *J. Mol. Recogn.* **2003**, *16*, 280-287.

[56] M. Kamihira, H. Saitô and A. Naito in *Kinetics of Amyloid Fibril Formation of Human Calcitonin*, (Ed. G. A. Webb), Springer Netherlands, Dordrecht, **2006**, p. 11.

[57] T. Arvinte, A. Cudd and A. F. Drake, *J. Biol. Chem.* **1993**, *268*, 6415-6422.

[58] N. S. Davis, P. A. DiSant'Agnese, J. F. Ewing and R. A. Mooney, *J. Urol.* **1989**, *142*, 884-888.

[59] A. R. Tabassian, E. S. Nylen, A. E. Giron, R. H. Snider, M. M. Cassidy and K. L. Becker, *Life Sci.* **1988**, *42*, 2323-2329.

[60] H. E. Sjoberg, S. Arver and E. Bucht, *Acta Physiol. Scand.* **1980**, *110*, 101-102.

[61] J. A. Fischer, P. H. Tobler, M. Kaufmann, W. Born, H. Henke, P. E. Cooper, S. M. Sagar and J. B. Martin, *Proc. Natl. Acad. Sci. U.S.A.* **1981**, *78*, 7801-7805.

[62] M. Zaidi, L. H. Breimer and I. Macintyre, *Exp. Physiol.* **1987**, *72*, 371-408.

[63] J. L. Frendo, F. Pichaud, R. D. Mourroux, Z. Bouizar, N. Segond, M. S. Moukhtar and A. Jullienne, *FEBS Lett.* **1994**, *342*, 214-216.

[64] S. G. Amara, V. Jonas, M. G. Rosenfeld, E. S. Ong and R. M. Evans, *Nature* **1982**, *298*, 240-244.

[65] I. MacIntyre, C. J. Hillyard, P. K. Murphy, J. J. Reynolds, R. E. Gaines Das and R. K. Craig, *Nature* **1982**, *300*, 460-462.

[66] B. A. Roos, J. A. Fischer, W. Pignat, C. B. Alander and L. G. Raisz, *Endocrinology* **1986**, *118*, 46-51.

[67] J. W. Jacobs, P. K. Lund, J. T. Potts, N. H. Bell and J. F. Habener, *J. Biol. Chem.* **1981**, *256*, 2803-2807.

[68] V. Y. Hook, A. V. Azaryan, S. R. Hwang and N. Tezapsidis, *FASEB J.* **1994**, *8*, 1269-1278.

[69] J. J. Park and Y. P. Loh, *Mol. Endocrinol.* **2008**, *22*, 2583-2595.

[70] L. Masi and M. L. Brandi, *Clin. Cases Miner. Bone Metab.* **2007**, *4*, 117-122.

[71] B. A. Eipper, D. A. Stoffers and R. E. Mains, *Annu. Rev. Neurosci.* **1992**, *15*, 57-85.

[72] L. Deftos, M. Lee and J. Potts, *Proc. Natl. Acad. Sci. U.S.A.* **1968**, *60*, 293-299.

[73] P. Motté, P. Vauzelle, P. Gardet, P. Ghillani, B. Caillou, C. Parmentier, C. Bohuon and D. Bellet, *Clin. Chim. Acta* **1988**, *174*, 35-54.

[74] O. Gulbahar, C. Konca Degertekin, M. Akturk, M. M. Yalcin, I. Kalan, G. F. Atikeler, A. E. Altinova, I. Yetkin, M. Arslan and F. Toruner, *J. Clin. Endocrinol. Metab.* **2015**, *100*, 2147-2153.

[75] P. H. Tobler, A. Jöhl, W. Born, R. Maier and J. A. Fishcer, *BBA-Protein Struct. M.* **1982**, *707*, 59-65.

[76] R. H. Buck and F. Maxl, *J. Pharm. Biomed. Anal.* **1990**, *8*, 761-769.

[77] H. S. Lee, S. J. Choi, H. M. Lee, C. K. Jeong, S. B. Kim, J. T. Lee, S. D. Yoo, P. P. DeLuca and K. C. Lee, *Chromatographia* **1999**, *50*, 701-704.

[78] K. C. Lee, J. Y. Yoon, B. Ho Woo, C.-K. Kim and P. P. Deluca, *Int. J. Pharm.* **1995**, *114*, 215-220; T. Fukuda, K. Ishikawa and K. Imai, *Biomed. Chrom.* **1995**, *9*, 52-55.

[79] K.-H. Song, H.-M. An, H.-J. Kim, S.-H. Ahn, S.-J. Chung and C.-K. Shim, *J. Chromatogr. B* **2002**, *775*, 247-255.

[80] S. J. Marx, C. J. Woodard and G. D. Aurbach, *Science* **1972**, *178*, 999-1001.

[81] J. Bockaert and J. Philippe Pin, *EMBO J.* **1999**, *18*, 1723-1729.

[82] K. J. Culhane, Y. Liu, Y. Cai and E. C. Yan, *Front. Pharmacol.* **2015**, *6*, 264.

[83] S. G. Rasmussen, B. T. DeVree, Y. Zou, A. C. Kruse, K. Y. Chung, T. S. Kobilka, F. S. Thian, P. S. Chae, E. Pardon, D. Calinski, J. M. Mathiesen, S. T. Shah, J. A. Lyons, M. Caffrey, S. H. Gellman, J. Steyaert, G. Skiniotis, W. I. Weis, R. K. Sunahara and B. K. Kobilka, *Nature* **2011**, *477*, 549-555.

[84] N. Media in *"The Nobel Prize in Chemistry 2012"*, *Vol. 2016,* Nobelprize.org, Web, **2014**.

[85] G. V. Segre and S. R. Goldring, *Trends Endocrinol. Metab.* **1993**, *4*, 309-314; H. Lin, T. Harris, M. Flannery, A. Aruffo, E. Kaji, A. Gorn, L. Kolakowski, H. Lodish and Goldring, *Science* **1991**, *254*, 1022-1024.

[86] K. Pal, K. Melcher and H. E. Xu, *Acta Pharmacol. Sin.* **2012**, *33*, 300-311.

[87] L.-H. Zhao, Y. Yin, D. Yang, B. Liu, L. Hou, X. Wang, K. Pal, Y. Jiang, Y. Feng, X. Cai, A. Dai, M. Liu, M.-W. Wang, K. Melcher and H. E. Xu, *J. Biol. Chem.* **2016**, *291*, 15119-15130; J. M. Booe, C. S. Walker, J. Barwell, G. Kuteyi, J. Simms, M. A. Jamaluddin, M. L. Warner, R. M. Bill, P. W. Harris, M. A. Brimble, D. R. Poyner, D. L. Hay and A. A. Pioszak, *Mol. Cell.* **2015**, *58*, 1040-1052.

[88] J. Barwell, J. J. Gingell, H. A. Watkins, J. K. Archbold, D. A. Poyner and D. H. Hay, *Br. J. Pharmacol.* **2012**, *166*, 51-65.

[89] D. L. Hay, G. Christopoulos, A. Christopoulos, D. R. Poyner and P. M. Sexton, *Mol. Pharmacol.* **2005**, *67*, 1655-1665.

[90] M. Morfis, N. Tilakaratne, S. G. Furness, G. Christopoulos, T. D. Werry, A. Christopoulos and P. M. Sexton, *Endocrinology* **2008**, *149*, 5423-5431.

[91] J.-N. Ma, E. A. Currier, A. Essex, M. Feddock, T. A. Spalding, N. R. Nash, M. R. Brann and E. S. Burstein, *Biochem. Pharmacol.* **2004**, *67*, 1279-1284.

[92] J. H. M. Feyenx, F. Cardinaux, R. Gamse, C. Bruns, M. Azria and U. Trechsel, *Biochem. Biophys. Res. Commun.* **1992**, *187*, 8-13.

[93] G. Pozvek, J. M. Hilton, M. Quiza, S. Houssami and P. M. Sexton, *Mol. Pharmacol.* **1997**, *51*, 658-665.

[94] T. Katayama, M. Furuya, K. Yamaichi, K. Konishi, N. Sugiura, H. Murafuji, K. Magota, M. Saito, S. Tanaka and S. Oikawa, *Biochim. Biophys. Acta* **2001**, *1526*, 183-190.

[95] D. Wootten, L. J. Miller, C. Koole, A. Christopoulos and P. M. Sexton, *Chem. Rev.* **2016**, DOI: 10.1021/acs.chemrev.1026b00049.

[96] M. Dong, R. F. Cox and L. J. Miller, *J. Biol. Chem.* **2009**, *284*, 21839-21847.

[97] J. Beaudreuil, S. Balasubramanian, J. Chenais, J. Taboulet, M. Frenkian, P. Orcel, A. Jullienne, W. C. Horne, M. C. de Vernejoul and M. Cressent, *Gene* **2004**, *343*, 143-151.

[98] U. Consortium, *Nucleic Acids Res.* **2014**, *42*, D191-198.

[99] A. H. Gorn, H. Y. Lin, M. Yamin, P. E. Auron, M. R. Flannery, D. R. Tapp, C. A. Manning, H. F. Lodish, S. M. Krane and S. R. Goldring, *J. Clin. Invest.* **1992**, *90*, 1726-1735.

[100] A. H. Gorn, S. M. Rudolph, M. R. Flannery, C. C. Morton, S. Weremowicz, T. Z. Wang, S. M. Krane and S. R. Goldring, *J. Clin. Invest.* **1995**, *95*, 2680-2691.

[101] R. E. Kuestner, R. D. Elrod, F. J. Grant, F. S. Hagen, J. L. Kuijper, S. L. Matthewes, P. J. O'Hara, P. O. Sheppard, S. D. Stroop and D. L. Thompson, *Mol. Pharmacol.* **1994**, *46*, 246-255.

[102] D. R. Nussenzveig, C. N.Thaw and M. C. Gershengorn, *J. Biol. Chem.* **1994**, *269*, 28123-28129.

[103] M. Pondel, *Int. J. Clin. Exp. Pathol.* **2000**, *81*, 405-422.

[104] K. Albrandt, E. M. Brady, C. X. Moore, E. Mull, M. E. Sierzega and K. Beaumont, *Endocrinology* **1995**, *136*, 5377-5384.

[105] E. E. Moore, R. E. Kuestner, S. D. Stroop, F. J. Grant, S. L. Matthewes, C. L. Brady, P. M. Sexton and D. M. Findlay, *Mol. Endocrinol.* **1995**, *9*, 959-968.

[106] P. N. Graves, Y. Tomer and T. F. Davies, *Biochem. Biophys. Res. Commun.* **1992**, *187*, 1135-1143; A. Takeshita, Y. Nagayama, K. Fujiyama, N. Yokoyama, H. Namba, S. Yamashita, M. Izumi and S. Nagataki, *Biochem. Biophys. Res. Commun.* **1992**, *188*, 1214-

1219.

[107] T. Nishikawa, H. Ishikawa, S. Yamamoto and Y. Koshihara, *FEBS Lett.* **1999**, *458*, 409-414.

[108] M. Nakamura, Z. Q. Zhang, L. Shan, T. Hisa, M. Sasaki, R. Tsukino, T. Yokoi, A. Kaname and K. Kakudo, *Hum. Genet.* **1997**, *99*, 38-41.

[109] K. A. McCuaig, H. S. Lee, J. C. Clarke, H. Assar, J. Horsford and J. H. White, *Nucleic Acids Res.* **1995**, *23*, 1948-1955.

[110] L. Masi, L. Becherini, L. Gennari, E. Colli, R. Mansani, A. Falchetti, C. Cepollaro, S. Gonnelli, A. Tanini and M. L. Brandi, *Biochem. Biophys. Res. Commun.* **1998**, *245*, 622-626.

[111] L. A. Austin, H. Heath and V. L. W. Go, *J. Clin. Invest.* **1979**, *64*, 1721-1724.

[112] O. Chabre, B. R. Conklin, H. Y. Lin, H. F. Lodish, E. Wilson, H. E. Ives, L. Catanzariti, B. A. Hemmings and H. R. Bourne, *Mol. Endocrinol.* **1992**, *6*, 551-556.

[113] A. deBustros, S. B. Baylin, M. A. Levine and B. D. Nelkin, *J. Biol. Chem.* **1986**, *261*, 8036-8041.

[114] J. K. Northup, P. C. Sternweis, M. D. Smigel, L. S. Schleifer, E. M. Ross and A. G. Gilman, *Proc. Natl. Acad. Sci. U.S.A.* **1980**, *77*, 6516-6520; D. R. Manning and A. G. Gilman, *J. Biol. Chem.* **1983**, *258*, 7059-7063.

[115] W. M. Oldham and H. E. Hamm, *Nat. Rev. Mol. Cell Biol.* **2008**, *9*, 60-71.

[116] M. Simon, M. Strathmann and N. Gautam, *Science* **1991**, *252*, 802-808.

[117] S. L. Ritter and R. A. Hall, *Nat. Rev. Mol. Cell. Biol.* **2009**, *10*, 819-830.

[118] P. Orcel, H. Tajima, Y. Murayama, T. Fujita, S. M. Krane, E. Ogata, S. R. Goldring and I. Nishimoto, *Mol. Endocrinol.* **2000**, *14*, 170-182.

[119] T. Force, J. V. Bonventre, M. R. Flannery, A. H. Gorn, M. Yamin and S. R. Goldring, *Am. J. Physiol.* **1992**, *262*, F1110-1115; J.-F. Shyu, D. Inoue, R. Baron and W. C. Horne, *J. Biol. Chem.* **1996**, *271*, 31127-31134.

[120] Y. Chen, J.-F. Shyu, A. Santhanagopal, D. Inoue, J.-P. David, S. J. Dixon, W. C. Horne and R. Baron, *J. Biol. Chem.* **1998**, *273*, 19809-19816.

[121] M. Chakraborty, D. Chatterjee, S. Kellokumpu, H. Rasmussen and R. Baron, *Science* **1991**, *251*, 1078-1082.

[122] K. V. Andreassen, S. T. Hjuler, S. G. Furness, P. M. Sexton, A. Christopoulos, O. Nosjean, M. A. Karsdal and K. Henriksen, *PLoS One* **2014**, *9*, e92042.

[123] X. Gao, P. Dwivedi, J. Omdahl, H. Morris and B. May, *J. Mol. Endocrinol.* **2004**, *32*, 87-98.

[124] D. P. Cohen, C. N. Thaw, A. Varma, M. C. Gershengorn and D. R. Nussenzveig, *Endocrinology* **1997**, *138*, 1400-1405.

[125] M. A. Aliapoulios, P. Goldhaber and P. L. Munson, *Science* **1966**, *151*, 330-331; T. J. Chambers, P. M. McSheehy, B. M. Thomson and K. Fuller, *Endocrinology* **1985**, *116*, 234-239.

[126] A. Del Fattore, A. Teti and N. Rucci, *Arch. Biochem. Biophys.* **2008**, *473*, 147-160.

[127] N. Takahashi, H. Yamana, S. Yoshiki, G. D. Roodman, G. R. Mundy, S. J. Jones, A. Boyde and T. Suda, *Endocrinology* **1988**, *122*, 1373-1382.

[128] C. S. Kovacs, *J. Mammary Gland Biol. Neoplasia* **2005**, *10*, 105-118.

[129] C. W. Cooper, P. F. Hirsch, S. U. Toverud and P. L. Munson, *Endocrinology* **1967**, *81*, 610-616.

[130] M. Zaidi, B. S. Moonga and E. Abe, *J. Clin. Invest.* **2002**, *110*, 1769-1771.

[131] D. L. Hurley , R. D. Tiegs , H. W. Wahner and H. I. Heath *N. Engl. J. Med.* **1987**, *317*, 537-541.

[132] J. Keller, P. Catala-Lehnen, A. K. Huebner, A. Jeschke, T. Heckt, A. Lueth, M. Krause, T. Koehne, J. Albers, J. Schulze, S. Schilling, M. Haberland, H. Denninger, M. Neven, I. Hermans-Borgmeyer, T. Streichert, S. Breer, F. Barvencik, B. Levkau, B. Rathkolb, E. Wolf, J. Calzada-Wack, F. Neff, V. Gailus-Durner, H. Fuchs, M. H. de Angelis, S. Klutmann, E. Tsourdi, L. C. Hofbauer, B. Kleuser, J. Chun, T. Schinke and M. Amling, *Nat. Commun.* **2014**, *5*, 5215.

[133] M. Cochran, M. Peacock, G. Sachs and B. E. Nordin, *Br. Med. J.* **1970**, *1*, 135-137; O. L. Bijvoet, J. van der Sluys Veer and A. P. Jansen, *Lancet* **1968**, *1*, 876-881.

[134] P. M. Sexton, W. R. Adam, J. M. Moseley, T. J. Martin and F. A. Mendelsohn, *Kidney Int.* **1987**, *32*, 862-868; A. G. Turner, F. Tjahyono, W. S. Chiu, J. Skinner, R. Sawyer, A. J. Moore, H. A. Morris, D. M. Findlay, J. D. Zajac and R. A. Davey, *Bone* **2011**, *48*, 354-361.

[135] D. Meleleo and V. Picciarelli, *Biometals* **2016**, *29*, 61-79.

[136] R. Dacquin, R. A. Davey, C. Laplace, R. Levasseur, H. A. Morris, S. R. Goldring, S. Gebre-Medhin, D. L. Galson, J. D. Zajac and G. Karsenty, *J. Cell Biol.* **2004**, *164*, 509-514.

[137] L. J. Zhu, M. K. Bagchi and I. C. Bagchi, *Endocrinology* **1998**, *139*, 330-339.

[138] T. Xiong, Y. Zhao, D. Hu, J. Meng, R. Wang, X. Yang, J. Ai, K. Qian and H. Zhang, *Hum. Reprod* **2012**, *27*, 3540-3551.

[139] J. Wang, U. K. Rout, I. C. Bagchi and D. R. Armant, *Development* **1998**, *125*, 4293-4302.

[140] A. Pecile, S. Ferri, P. C. Braga and V. R. Olgiati, *Experientia* **1975**, *31*, 332-333.

[141] H. Nakamoto, Y. Soeda, S. Takami, M. Minami and M. Satoh, *Brain Res. Mol. Brain Res.* **2000**, *76*, 93-102.

[142] M. I. Colado, M. J. Ormazabal, C. Goicoechea, F. Lopez, M. J. Alfaro and M. I. Martin, *Eur. J. Pharmacol.* **1994**, *252*, 291-297.

[143] E. J. Visser, *Acute Pain* **2005**, *7*, 185-189.

[144] L. A. Blau and J. D. Hoehns, *Ann. Pharmacother.* **2003**, *37*, 564-570.

[145] R. Cohen, J.-M. Campos, C. Salaün, H. M. Heshmati, J.-L. Kraimps, C. Proye, É. Sarfati, J.-F. Henry, P. Niccoli-Sire and E. Modigliani, *J. Clin. Endocrinol. Metab.* **2000**, *85*, 919-919.

[146] D. Molè, E. Gentilin, T. Gagliano, F. Tagliati, M. Bondanelli, M. R. Pelizzo, M. Rossi, C. Filieri, G. Pansini, E. C. d. Uberti and M. C. Zatelli, *Endocrinology* **2012**, *153*, 2088-2098.

[147] G. V. Shah, W. Rayford, M. J. Noble, M. Austenfeld, J. Weigel, S. Vamos and W. K. Mebust, *Endocrinology* **1994**, *134*, 596-602.

[148] T. Chen, R. W. Cho, P. J. S. Stork and M. J. Weber, *Cancer Res.* **1999**, *59*, 213-218.

[149] J. Chien and G. V. Shah, *Int. J. Cancer* **2001**, *91*, 46-54.

[150] V. S. Sabbisetti, S. Chirugupati, S. Thomas, K. S. Vaidya, D. Reardon, M. Chiriva-Internati, K. A. Iczkowski and G. V. Shah, *Int. J. Cancer* **2005**, *117*, 551-560.

[151] S. Thomas, S. Chigurupati, M. Anbalagan and G. Shah, *Mol. Endocrinol.* **2006**, *20*, 1894-1911.

[152] G. V. Shah, S. Thomas, A. Muralidharan, Y. Liu, P. L. Hermonat, J. Williams and J. Chaudhary, *Endocr.-Relat. Cancer* **2008**, *15*, 953-964.

[153] A. Aljameeli, A. Thakkar, S. Thomas, V. Lakshmikanthan, K. A. Iczkowski and G. V. Shah, *PLoS One* **2016**, *11*, e0150090.

[154] C. J. Hillyard, R. C. Coombes, P. B. Greenberg, L. S. Galante and I. MacIntyre, *Clin. Endocrinol. (Oxf)* **1976**, *5*, 1-8.

[155] C. Gropp, K. Havemann and A. Scheuer, *Cancer* **1980**, *46*, 347-354.

[156] C. G. W. Luster, H.F. Kern & K. Havemann, *Br. J. Cancer* **1985**, *51*, 865-875.

[157] G. D. Sorenson, O. S. Pettengill, T. Brinck-Johnsen, C. C. Cate and L. H. Maurer, *Cancer* **1981**, *47*, 1289-1296.

[158] N. H. Hunt, M. Ellison, J. C. Underwood and T. J. Martin, *Br. J. Cancer* **1977**, *35*, 777-784.

[159] J. D. Zajac, S. A. Livesey and T. J. Martin, *Biochem. Biophys. Res. Commun.* **1984**, *122*, 1040-1046.

[160] M. L. Ellison, C. J. Hillyard, G. A. Bloomfield, L. H. Rees, R. C. Coombes and A. M. Neville, *Clin. Endocrinol. (Oxf)* **1976**, *5 Suppl*, 397s-406s.

[161] M. d'Herbomez, P. Caron, C. Bauters, C. Do Cao, J. L. Schlienger, R. Sapin, L. Baldet, B. Carnaille and J. L. Wemeau, *Eur. J. Endocrinol.* **2007**, *157*, 749-755.

[162] D. M. Findlay, V. P. Michelangeli and P. J. Robinson, *Endocrinology* **1989**, *125*, 2656-2663.

[163] Y. Iwasaki, J. Iwasaki and H. C. Freake, *Biochem. Biophys. Res. Commun.* **1983**, *110*,

235-242.

[164] F. N. Bolkenius and A. J. Ganzhorn, *Vascul. Pharmacol.* **1998**, *31*, 655-659.

[165] N. Iwai, A. Martínez, M.-J. Miller, M. Vos, J. L. Mulshine and A. M. Treston, *Lung Cancer* **1999**, *23*, 209-222.

[166] S. R. K. Murthy, E. Dupart, N. Al-Sweel, A. Chen, N. X. Cawley and Y. P. Loh, *Cancer Lett.* **2013**, *341*, 204-213.

[167] J. Douglass, O. Civelli and E. Herbert, *Annu. Rev. Biochem.* **1984**, *53*, 665-715.

[168] A. M. Treston, J. L. Mulshine and F. Cuttitta, *J. Natl. Cancer Inst. Monogr.* **1992**, 169-175.

[169] F. Cao, A. B. Gamble, H. Onagi, J. Howes, J. E. Hennessy, C. Gu, J. A. M. Morgan and C. J. Easton, *Analytical Chemistry* **2017**, *89*, 6992-6999.

[170] A. deBustros, D. W. Ball, R. Peters, D. Compton and B. D. Nelkin, *Biochem. Biophys. Res. Commun.* **1992**, *189*, 1157-1164.

[171] E. Rinde and W. Troll, *Analytical Chemistry* **1976**, *48*, 542-544.

[172] B. Leibiger, T. Moede, T. P. Muhandiramlage, D. Kaiser, P. V. Sanchez, I. B. Leibiger and P.-O. Berggren, *Proc. Natl. Acad. Sci. U.S.A.* **2012**, *109*, 20925-20930; I. B. Leibiger, B. Leibiger, T. Moede and P.-O. Berggren, *Mol. Cell* **1998**, *1*, 933-938; S. Kovac, L. Xiao, A. Shulkes, O. Patel and G. S. Baldwin, *FEBS Lett.* **2010**, *584*, 4413-4418.

[173] T. Segovia-Silvestre, C. Bonnefond, B. C. Sondergaard, T. Christensen, M. A. Karsdal and A. C. Bay-Jensen, *BMC Res. Notes* **2011**, *4*, 407-414.

[174] L. Raggatt, A. Evdokiou and D. Findlay, *J. Endocrinol.* **2000**, *167*, 93-105.

[175] G. Wu, D. T. Burzon, P. A. D. Santagnese, S. Schoen, L. J. Deftos, S. Gershagen and A. T. K. Cockett, *Urology* **1996**, *47*, 376-381.

[176] F. Silvestris, P. Cafforio, M. De Matteo, C. Quatraro and F. Dammacco, *Leuk Res* **2008**, *32*, 611-623.

[177] K. D. Pruitt, G. R. Brown, S. M. Hiatt, F. Thibaud-Nissen, A. Astashyn, O. Ermolaeva, C. M. Farrell, J. Hart, M. J. Landrum, K. M. McGarvey, M. R. Murphy, N. A. O'Leary, S. Pujar, B. Rajput, S. H. Rangwala, L. D. Riddick, A. Shkeda, H. Sun, P. Tamez, R. E. Tully, C. Wallin, D. Webb, J. Weber, W. Wu, M. DiCuccio, P. Kitts, D. R. Maglott, T. D. Murphy and J. M. Ostell, *Nucleic Acids Res.* **2014**, *42*, D756-763.

[178] P. J. Wookey, C. A. McLean, P. Hwang, S. G. Furness, S. Nguyen, A. Kourakis, D. L. Hare and J. V. Rosenfeld, *Histopathology* **2012**, *60*, 895-910.

[179] A. Norek, D. Sands, A. Sobczynska-Tomaszewska, D. Chmielewski, K. Szamotulska, K. Czerska and J. Bal, *Med. Wieku. Rozwoj.* **2010**, *14*, 334-343; V. S. Oganov, V. S. Baranov, O. E. Kabitskaia, V. E. Novikov, A. V. Bakulin, M. V. Moskalenko, M. V. Aseev and L. V. Voitulevich, *Aviakosm. Ekolog. Med.* **2010**, *44*, 18-23; D. R. Nussenzveig, S. Mathew and M. C. Gershengorn, *Endocrinology* **1995**, *136*, 2047-2051; M. Egerton, M. Needham, S. Evans, A. Millest, G. Cerillo, J. McPheat, M. Popplewell, D. Johnstone and M. Hollis, *J. Mol. Endocrinol.* **1995**, *14*, 179-189; R. J. Blattner, *J. Pediatr.* **1967**, *71*, 284-287;

M. Horikoshi, H. Yaghootkar, D. O. Mook-Kanamori, U. Sovio, H. R. Taal, B. J. Hennig, J. P. Bradfield, B. St Pourcain, D. M. Evans, P. Charoen, M. Kaakinen, D. L. Cousminer, T. Lehtimaki, E. Kreiner-Moller, N. M. Warrington, M. Bustamante, B. Feenstra, D. J. Berry, E. Thiering, T. Pfab, S. J. Barton, B. M. Shields, M. Kerkhof, E. M. van Leeuwen, A. J. Fulford, Z. Kutalik, J. H. Zhao, M. den Hoed, A. Mahajan, V. Lindi, L. K. Goh, J. J. Hottenga, Y. Wu, O. T. Raitakari, M. N. Harder, A. Meirhaeghe, I. Ntalla, R. M. Salem, K. A. Jameson, K. Zhou, D. M. Monies, V. Lagou, M. Kirin, J. Heikkinen, L. S. Adair, F. S. Alkuraya, A. Al-Odaib, P. Amouyel, E. A. Andersson, A. J. Bennett, A. I. Blakemore, J. L. Buxton, J. Dallongeville, S. Das, E. J. de Geus, X. Estivill, C. Flexeder, P. Froguel, F. Geller, K. M. Godfrey, F. Gottrand, C. J. Groves, T. Hansen, J. N. Hirschhorn, A. Hofman, M. V. Hollegaard, D. M. Hougaard, E. Hypponen, H. M. Inskip, A. Isaacs, T. Jorgensen, C. Kanaka-Gantenbein, J. P. Kemp, W. Kiess, T. O. Kilpelainen, N. Klopp, B. A. Knight, C. W. Kuzawa, G. McMahon, J. P. Newnham, H. Niinikoski, B. A. Oostra, L. Pedersen, D. S. Postma, S. M. Ring, F. Rivadeneira, N. R. Robertson, S. Sebert, O. Simell, T. Slowinski, C. M. Tiesler, A. Tonjes, A. Vaag, J. S. Viikari, J. M. Vink, N. H. Vissing, N. J. Wareham, G. Willemsen, D. R. Witte, H. Zhang, J. Zhao, J. F. Wilson, M. Stumvoll, A. M. Prentice, B. F. Meyer, E. R. Pearson, C. A. Boreham, C. Cooper, M. W. Gillman, G. V. Dedoussis, L. A. Moreno, O. Pedersen, M. Saarinen, K. L. Mohlke, D. I. Boomsma, S. M. Saw, T. A. Lakka, A. Korner, R. J. Loos, K. K. Ong, P. Vollenweider, C. M. van Duijn, G. H. Koppelman, A. T. Hattersley, J. W. Holloway, B. Hocher, J. Heinrich, C. Power, M. Melbye, M. Guxens, C. E. Pennell, K. Bonnelykke, H. Bisgaard, J. G. Eriksson, E. Widen, H. Hakonarson, A. G. Uitterlinden, A. Pouta, D. A. Lawlor, G. D. Smith, T. M. Frayling, M. I. McCarthy, S. F. Grant, V. W. Jaddoe, M. R. Jarvelin, N. J. Timpson, I. Prokopenko and R. M. Freathy, *Nat. Genet.* **2013**, *45*, 76-82.

[180] N. Segawa, M. Nakamura, Y. Nakamura, I. Mori, Y. Katsuoka and K. Kakudo, *Cancer Res.* **2001**, *61*, 6060-6063.

[181] H. Liu, A. Singla, M. Ao, R. K. Gill, J. Venkatasubramanian, M. C. Rao, W. A. Alrefai and P. K. Dudeja, *J. Cell Mol. Med.* **2011**, *15*, 2697-2705.

[182] S. Kamano, S. Ikeda, M. Sugimoto and S. Kume, *J. Reprod. Dev.* **2014**, *60*, 317-323.

[183] D. M. Findlay, M. deLuise, V. P. Michelangeli, M. Ellison and T. J. Martin, *Cancer Res.* **1980**, *40*, 1311-1317.

[184] M. Matsuda, T. A. Yamamoto and M. Hirata, *Endocrinology* **2006**, *147*, 4608-4617.

[185] R. Seifert, G. H. Lushington, T. C. Mou, A. Gille and S. R. Sprang, *Trends Pharmacol. Sci.* **2012**, *33*, 64-78.

[186] R. J. Haslam, M. M. L. Davidson and J. V. Desjardins, *Biochem. J.* **1978**, *176*, 83-95.

[187] A. C. Emery, M. V. Eiden and L. E. Eiden, *Mol. Pharmacol.* **2013**, *83*, 95-105.

[188] T. Chijiwa, A. Mishima, M. Hagiwara, M. Sano, K. Hayashi, T. Inoue, K. Naito, T. Toshioka and H. Hidaka, *J. Biol. Chem.* **1990**, *265*, 5267-5272.

[189] S. P. Davies, H. Reddy, M. Caivano and P. Cohen, *Biochem. J.* **2000**, *351*, 95-105.

[190] Y. Li, T. J. Dillon, M. Takahashi, K. T. Earley and P. J. S. Stork, *J. Biol. Chem.* **2016**, *291*, 21584-21595.

[191] J. E. Bleasdale, N. R. Thakur, R. S. Gremban, G. L. Bundy, F. A. Fitzpatrick, R. J. Smith and S. Bunting, *J. Pharm. Exp. Ther.* **1990**, *255*, 756-768.

[192] M. G. Leitner, N. Michel, M. Behrendt, M. Dierich, S. Dembla, B. U. Wilke, M. Konrad, M. Lindner, J. Oberwinkler and D. Oliver, *Br. J. Pharmacol.* **2016**, *173*, 2555-2569.

[193] D. Toullec, P. Pianetti, H. Coste, P. Bellevergue, T. Grand-Perret, M. Ajakane, V. Baudet, P. Boissin, E. Boursier, F. Loriolle, L. Duhamelll, D. Charon and J. Kirilovsky, *J. Biol. Chem.* **1991**, *266*, 15771-15781.

[194] I. M. Smith and N. Hoshi, *PLoS ONE* **2011**, *6*, e26338.

[195] A. X. Wu-Zhang and A C. Newton, *Biochem. J.* **2013**, *452*, 195-209.

[196] N. Flacco, V. Segura, M. Perez-Aso, S. Estrada, J. F. Seller, F. Jimenez-Altayo, M. A. Noguera, P. D'Ocon, E. Vila and M. D. Ivorra, *Br. J. Pharmacol.* **2013**, *169*, 413-425; F. M. Pulcinelli, P. Gresele, M. Bonuglia and P. P. Gazzaniga, *Biochem. Pharmacol.* **1998**, *56*, 1481-1484.

[197] A. Thompson and V. Kanamarlapudi, *Biochem. Pharmacol.* **2015**, *93*, 72-84.

[198] J. Yao, J. Li, L. Zhou, J. Cheng, S. M. Chim, G. Zhang, J. M. Quinn, J. Tickner, J. Zhao and J. Xu, *J. Cell Physiol.* **2015**, *230*, 1235-1242.

[199] M. Tagashira, H. Iijima, Y. Isogai, M. Hori, S. Takamatsu, Y. Fujibayashi, K. Yoshizawa-Kumagaye, S. Isaka, K. Nakajima, T. Yamamoto, T. Teshima and K. Toma, *Biochemistry* **2001**, *40*, 11090-11095.

[200] M. Andreoli and F. Monaco, *Advances in Thyroid Neoplasia 1981*, Field Educational Italia, Rome, **1981**, p. 1.

[201] M. Zabel and J. Grzeszkowiak, *Histol. Histopathol.* **1997**, *12*, 283-289; P. J. Gkonos, W. Born, B. N. Jones, J. B. Petermann, H. T. Keutmann, R. S. Birnbaum, J. A. Fischer and B. A. Roos, *J. Biol. Chem.* **1986**, *261*, 14386-14391.

[202] M. Kosfeld, M. Heinrichs, P. J. Zak, U. Fischbacher and E. Fehr, *Nature* **2005**, *435*, 673-676; P. Kirsch, C. Esslinger, Q. Chen, D. Mier, S. Lis, S. Siddhanti, H. Gruppe, V. S. Mattay, B. Gallhofer and A. Meyer-Lindenberg, *J. Neurosci.* **2005**, *25*, 11489-11493.

[203] M. Soloff, M. Alexandrova and M. Fernstrom, *Science* **1979**, *204*, 1313-1315.

[204] E. Hollander, J. Bartz, W. Chaplin, A. Phillips, J. Sumner, L. Soorya, E. Anagnostou and S. Wasserman, *Biol. Psychiatry* **2007**, *61*, 498-503.

[205] M. Busnelli, V. Rimoldi, P. Vigano, L. Persani, A. M. Di Blasio and B. Chini, *Fertil. Steril.* **2010**, *94*, 1869-1874.

[206] T. Morita, K. Shibata, F. Kikkawa, H. Kajiyama, K. Ino and S. Mizutani, *Int. J. Cancer* **2004**, *109*, 525-532.

[207] C. Péqueux, C. Breton, J.-C. Hendrick, M.-T. Hagelstein, H. Martens, R. Winkler, V. Geenen and J.-J. Legros, *Cancer Res.* **2002**, *62*, 4623-4629.

[208] N. Gassanov, D. Devost, B. Danalache, N. Noiseux, M. Jankowski, H. H. Zingg and J. Gutkowska, *STEM CELLS* **2008**, *26*, 45-54.

[209] L. Green, D. Fein, C. Modahl, C. Feinstein, L. Waterhouse and M. Morris, *Biol. Psychiatry* **2001**, *50*, 609-613.

[210] B. A. Danalache, J. Gutkowska, M. J. Ślusarz, I. Berezowska and M. Jankowski, *PLoS ONE* **2010**, *5*, e13643.

[211] M. E. McCullough, P. S. Churchland and A. J. Mendez, *Neurosci. Biobehav. Rev.* **2013**, *37*, 1485-1492.

[212] A. Szeto, P. M. McCabe, D. A. Nation, B. A. Tabak, M. A. Rossetti, M. E. McCullough, N. Schneiderman and A. J. Mendez, *Psychosom. Med.* **2011**, *73*, 393-400.

[213] T. Chard, N. R. H. Boyd, M. L. Forsling, A. S. Mcneilly and J. Landon, *J. Endocrinol.* **1970**, *48*, 223-234.

[214] T. Buclin, M. C. Rochat, P. Burckhardt, M. Azria and M. Attinger, *J. Bone Miner. Res.* **2002**, *17*, 1478-1485; K. Antonin, V. Saano, P. Bieck, J. Hastewell, R. Fox, P. Lowe and M. Mackay, *Clin. Sci.* **1992**, *83*, 627-627.

[215] C. Pequeux, J. C. Hendrick, M. T. Hagelstein, V. Geenen and J. J. Legros, *Scand. J. Clin. Lab. Invest.* **2001**, *61*, 407-415.

[216] D. Sharma, R. J. Handa and R. M. Uht, *Endocrinology* **2012**, *153*, 2353-2361.

[217] D. Ashenafi, E. Van Hemelrijck, S. Chopra, J. Hoogmartens and E. Adams, *J. Pharm. Biomed. Anal.* **2010**, *51*, 24-29.

[218] K. Meeran, D. O'Shea, P. D. Upton, C. J. Small, M. A. Ghatei, P. H. Byfield and S. R. Bloom, *J. Clin. Endocrinol. Metab.* **1997**, *82*, 95-100; J. R. McEwan, N. Benjamin, S. Larkin, R. W. Fuller, C. T. Dollery and I. MacIntyre, *Circulation* **1988**, *77*, 1072-1080.

Appendix One

Statistical Analyses

A1.1 Statistical Analysis of Data Presented in Section 3.4.

To further interrogate the effect of SUNB8155 treatment on the relative levels of CT-related species in DMS53 lysate and medium, additional data analysis was performed. As described in **Equation A1.1**, in a given treatment condition the relative proportion of each CT-related species was determined by comparing the peak area of the species of interest to the total peak area of the four species. Each relative proportion was then normalised that of the control replicate. The relative proportions in each treatment replicate were then averaged and compared to the control cultures using a two-sided Welch's unequal variances t-test. The normalised relative proportions are presented in **Table A1.1** and the associated p-values presented in **Table A1.2**. This data indicates that treatment of DMS53 cultures with 100 μM SUNB8155 significantly increases CT ($p<0.05$), and amidated species in general ($p<0.01$) in the medium, along with minor decreases in glycosylated species in the lysate. Lower concentrations had little significant effect on CT-related species in the medium or lysate. These observations are consistent with the conclusions drawn in Section 3.4.

$$\frac{\left(\frac{P_t(x)}{P_t(CT+CTG+gCT+gCTG)}\right)}{\left(\frac{P_c(x)}{P_c(CT+CTG+gCT+gCTG)}\right)} = x'$$

Equation A1.1: *Normalised relative proportions of CT-related species*; where x is the HPLC peak area of interest, x′ is the normalised proportion, P_t is the peak area of the given peak in the treated culture and P_c is the peak area of the given peak in the control chromatogram.

Table A1.1: *Summary of average proportional changes of the CT-related species determined by HPLC peak area, normalised to the replicate control, in response to SUNB8155 treatment at concentrations of 1, 10 and 100 μM.* Data are reported as mean ± standard deviation (SD), and are based on n=3 biological replicates for each condition, with two technical replicates performed. Significance was determined by comparing normalised proportion averages obtained from treated cultures with those obtained from control cultures using an unpaired, two-sided Welch's t-test. A p-value of <0.05 was considered to be significant. * = p<0.05, ** = p<0.01

	gCTG ± S.D.	gCT ± S.D.	CTG ± S.D.	CT ± S.D.	Amidated ± S.D.	Glycosylated ± S.D.
Medium						
Control	1.00 ± 0.18	1.00 ± 0.07	1.00 ± 0.12	1.00 ± 0.24	1.00 ± 0.06	1.00 ± 0.11
SUNB8155 1 μM	0.95 ± 0.06	0.95 ± 0.06	1.02 ± 0.02	1.18 ± 0.13	1.02 ± 0.03	0.95 ± 0.04
SUNB8155 10 μM	0.92 ± 0.06	0.97 ± 0.05	1.05 ± 0.02	1.15 ± 0.05*	1.03 ± 0.04	0.94 ± 0.01**
SUNB8155 100 μM	0.73 ± 0.05*	1.00 ± 0.03	1.01 ± 0.09	1.79 ± 0.22*	1.24 ± 0.03**	0.86 ± 0.03*
Lysate						
Control	1.00 ± 0.22	1.00 ± 0.11	1.00 ± 0.22	1.00 ± 0.11	1.00 ± 0.05	1.00 ± 0.12
SUNB8155 1 μM	1.40 ± 0.41	1.01 ± 0.07	0.95 ± 0.15	0.98 ± 0.04	0.98 ± 0.04	1.09 ± 0.09
SUNB8155 10 μM	0.82 ± 0.06*	0.85 ± 0.05*	1.19 ± 0.19	1.05 ± 0.06	0.99 ± 0.02	0.84 ± 0.05*
SUNB8155 100 μM	0.82 ± 0.12	0.77 ± 0.09*	1.11 ± 0.11	1.11 ± 0.09	1.01 ± 0.02	0.76 ± 0.09

Table A1.2: *P-values corresponding to treatment data presented in Table A1.1.* Normalised proportion averages obtained from treated cultures were compared with those obtained from control cultures using an unpaired, two-sided Welch's t-test. A p-value of <0.05 was considered to be significant (underlined).

	gCTG ± S.D.	gCT ± S.D.	CTG ± S.D.	CT ± S.D.	Amidated ± S.D.	Glycosylated ± S.D.
Medium						
Control	-	-	-	-	-	-
SUNB8155 1 µM	0.253	0.269	0.154	0.138	0.300	0.139
SUNB8155 10 µM	0.141	0.465	0.053	<u>0.039</u>	0.400	<u>0.001</u>
SUNB8155 100 µM	<u>0.013</u>	0.891	0.227	<u>0.026</u>	<u>0.007</u>	<u>0.017</u>
Lysate						
Control	-	-	-	-	-	-
SUNB8155 1 µM	0.233	0.829	0.601	0.398	0.497	0.240
SUNB8155 10 µM	<u>0.031</u>	<u>0.036</u>	0.221	0.274	0.566	<u>0.036</u>
SUNB8155 100 µM	<u>0.074</u>	<u>0.041</u>	0.235	0.166	0.639	<u>0.047</u>

A1.2 Statistical Analysis of Data Presented in Section 5.4.

The data concerning the effect of inhibitors SQ22536 and GFI90203X on CT-related species in DMS53 medium and lysate presented in Section 5.4 were subjected to the same statistical analysis as described above for Section 3.4. The normalised relative proportions derived from this analysis are presented in **Table A1.3,** with associated p-values presented in **Table A1.4**. This analysis indicates that treatment with GFI09203X has a statistically significant effect on the levels of CT-related species in the medium, while the effect of SQ22536 on CT-related species in the medium and lysate is not evident. Only minor changes are observed to the relative proportions of species in the lysate with GFI09203X treatment. These observations are consistent with the conclusions drawn in Section 5.4.

Table A1.3: *Summary of average proportional changes of the CT-related species as determined by HPLC peak area, normalised to the replicate control, in response to SQ22536 (100 μM) and GF109203X (40 μM) treatment.* Data are reported as mean ± standard deviation (SD), and are based on n=3 biological replicates for each condition, with two technical replicates performed. Significance was determined by comparing normalised proportion averages obtained from treated cultures with those obtained from control cultures using an unpaired, two-sided Welch's t-test. A p-value of <0.05 was considered to be significant. * = p<0.05, ** = p<0.01.

	gCTG ± S.D.	gCT ± S.D.	CTG ± S.D.	CT ± S.D.	Amidated ± S.D.	Glycosylated ± S.D.
Medium						
Control	1.00 ± 0.22	1.00 ± 0.17	1.00 ± 0.12	1.00 ± 0.38	1.00 ± 0.21	1.00 ± 0.08
SQ22536 100 μM	0.87 ± 0.11	0.83 ± 0.07	1.14 ± 0.10	1.34 ± 0.29	0.99 ± 0.03	0.85 ± 0.09
GF109203X 40 μM	0.63 ± 0.08*	1.28 ± 0.05*	0.79 ± 0.06*	1.66 ± 0.57	1.40 ± 0.18	0.96 ± 0.09
Lysate						
Control	1.00 ± 0.10	1.00 ± 0.07	1.00 ± 0.14	1.00 ± 0.01	1.00 ± 0.02	1.00 ± 0.07
SQ22536 100 μM	0.96 ± 0.03	0.95 ± 0.07	1.07 ± 0.07	1.01 ± 0.01	0.99 ± 0.01	0.95 ± 0.05
GF109203X 40 μM	0.90 ± 0.26	0.90 ± 0.01**	1.13 ± 0.05	1.01 ± 0.04	0.98 ± 0.03	0.90 ± 0.06

Table A1.4: *P-values corresponding to treatment data presented in Table A1.3.* Normalised proportion averages obtained from treated cultures were compared with those obtained from control cultures using an unpaired, two-sided Welch's t-test. A p-value of <0.05 was considered to be significant (underlined).

	gCTG ± S.D.	gCT ± S.D.	CTG ± S.D.	CT ± S.D.	Amidated ± S.D.	Glycosylated ± S.D.
Medium						
Control	-	-	-	-	-	-
SQ22536 100 μM	0.174	0.058	0.126	0.185	0.690	0.098
GF109203X 40 μM	0.018	0.012	0.033	0.188	0.064	0.506
Lysate						
Control	-	-	-	-	-	-
SQ22536 100 μM	0.190	0.343	0.247	0.365	0.418	0.223
GF109203X 40 μM	0.562	0.001	0.063	0.746	0.441	0.118